RET-altered Induced Pluripotent Stem Cells (iPSCs) for modeling Hematopoiesis and Non-Small Cell Lung Cancer (NSCLC)

Paul Marcoux

▶ **To cite this version:**

Paul Marcoux. RET-altered Induced Pluripotent Stem Cells (iPSCs) for modeling Hematopoiesis and Non-Small Cell Lung Cancer (NSCLC). Cancer. Université Paris-Saclay, 2023. English. NNT : 2023UPASQ062 . tel-04415412

HAL Id: tel-04415412
https://theses.hal.science/tel-04415412

Submitted on 24 Jan 2024

HAL is a multi-disciplinary open access archive for the deposit and dissemination of scientific research documents, whether they are published or not. The documents may come from teaching and research institutions in France or abroad, or from public or private research centers.

L'archive ouverte pluridisciplinaire **HAL**, est destinée au dépôt et à la diffusion de documents scientifiques de niveau recherche, publiés ou non, émanant des établissements d'enseignement et de recherche français ou étrangers, des laboratoires publics ou privés.

université PARIS-SACLAY

RET-altered Induced Pluripotent Stem Cells (iPSCs) for modeling Hematopoiesis and Non-Small Cell Lung Cancer (NSCLC)

Cellules souches pluripotentes induites (CSPi) exprimant RET pour la modélisation de l'hématopoïèse et du cancer du poumon non-à petites cellules

Thèse de doctorat de l'université Paris-Saclay

École doctorale n°569 : Innovation Thérapeutique : du Fondamental à l'Appliqué (ITFA)
Spécialité de doctorat : Immunologie
Graduate School : Santé et médicaments
Référent : Faculté de Pharmacie

Thèse préparée dans l'unité de recherche **Modèles de cellules souches malignes et thérapeutiques (Université Paris-Saclay, INSERM)** sous la direction de **Ali TURHAN**, PU-PH

Thèse soutenue à Paris-Saclay, le 1er décembre 2023, par

Paul MARCOUX

Composition du Jury

Membres du jury avec voix délibérative

Eric DEUTSCH PU-PH, Institut Gustave Roussy / Paris Saclay	Président
Evelyne LAURET CR CNRS, HDR, Université Paris-Descartes / Institut Cochin	Rapporteur
Stéphane VINCENT MCU, HDR, ENS de Lyon	Rapporteur
Jamila FAIVRE PU-PH, Université Paris-Saclay	Examinatrice

THÈSE DE DOCTORAT

NNT : 2023UPASQ062

université PARIS-SACLAY

ÉCOLE DOCTORALE
Innovation thérapeutique
du fondamental à l'appliqué
(ITFA)

Title: RET-altered Induced Pluripotent Stem Cells (iPSCs) for modeling Hematopoiesis and Non-Small Cell Lung Cancer (NSCLC)

Keywords: iPSCs ; NSCLC ; Hematopoiesis ; RET ; Models

Abstract: Induced pluripotent stem cells (iPSCs) are generated by reprogramming adult cells back into an embryonic-like state. iPSCs can be differentiated into various cell types, making them a valuable tool for regenerative medicine, disease modeling and drug discovery.

In case of monogenic or malignant diseases where a driver gene has been identified, it is possible to use both patient-derived iPSCs and their CRISPR-corrected isogenic control iPSCs to identify the distinct characteristics linked to the mutation. We have used this strategy to unravel the effect of REarranged during Transfection (RET), a tyrosine kinase receptor, during iPSC differentiation within two different contexts. We first studied the potential role of RET in the induction of hematopoietic cells. In the second part, the objective was to replicate a malignant lung carcinoma *in vitro* by generating lung organoids and lung progenitor cells (LPC) from these iPSCs. For these purposes we have used an iPSC derived from a patient carrying the *RET*^{C634Y} somatic mutation (iRET^{C634Y}) which is responsible for the autophosphorylation of the protein RET and therefore the constitutive activation of its signaling pathway. We have completed our studies with the generation of a RET^{C634Y} knock-in iPSC (PB68-RET^{C634Y}).

In the first part of this manuscript, these iPSCs were differentiated into hematopoietic cells to investigate the role of RET in iPSC-derived hematopoiesis. Indeed, previous studies have shown that RET plays a role in mice hematopoiesis as demonstrated by *RET* knock-out mice exhibiting significant deficiencies in hematopoiesis. In the context of cord blood (CB) cells, RET activation led to a significant amplification of hematopoietic stem cell (HSCs). These published results prompted us to analyze the potential role of RET in iPSC-derived hematopoiesis. We have studied this potential by using *in vitro* hematopoietic induction strategies allowing reproducible generation of hematopoietic cells with HSC markers using control versus RET-activated or overexpressed iPSCs. As opposed to the reports in mice and adult CB cells, we report an inhibitory effect of RET activation in the context of iPSCs. Transcriptomic analyses revealed a specific activated expression profile in iRET^{C634Y}, including overexpression of genes associated with the MAPK network and negative hematopoietic regulator activities. These findings suggest that RET activation might be associated with inhibitory effects on iPSC-derived hematopoiesis, potentially through MAPK activation.

In the second part of this work, we have asked whether we could reproducibly generate LPCs from patient-derived iPSCs carrying the *RET*^{C634Y} somatic mutation using a 16-day protocol with the purpose to generate a model of RET-driven non-small cell lung cancer (NSCLC). Indeed, *RET* oncogenic rearrangements can occur in 1-2% of lung adenocarcinomas and only a few models for studying this disease are available. We have shown the successful generation of LPCs expressing expected lung progenitor markers. LPCs generated from RET^{C634Y} iPSCs displayed an overexpression of cancer-associated markers as compared to control iPSCs. Transcriptomic analysis revealed distinct signatures indicating lung multilineage dedifferentiation in NSCLC tumors, along with an upregulated signature associated with the *RET*^{C634Y} mutation, potentially linked to worse NSCLC prognosis. The findings were further validated using the RET^{C634Y} knock-in iPSC model, highlighting key cancerous targets *PROM2* and *C1QTNF6,* known for their association with poor prognostic outcomes. Moreover, LPCs derived from RET^{C634Y} iPSCs showed a positive response to the RET inhibitor Pralsetinib, evidenced by the downregulation of cancer markers. This study establishes the first model of RET-driven NSCLC LPCs generated from patient-derived iPSCs.

Due to their theoretically unlimited differentiation potential under the appropriate cues, iPSCs represent a major tool to study different diseases starting from the same oncogene-bearing clone. This work also demonstrates the versatility of iPSCs, as a single iPSC line can be utilized to investigate various mechanisms and serve as model for different tissues.

université PARIS-SACLAY

ÉCOLE DOCTORALE
Innovation thérapeutique
du fondamental à l'appliqué
(ITFA)

Titre : *Cellules souches pluripotentes induites (CSPi) exprimant RET pour la modélisation de l'hématopoïèse et du cancer du poumon non-à petites cellules*

Mots clés : CSPi ; CPNPC ; Hématopoïèse ; RET ; Modélisation

Résumé : Les cellules souches pluripotentes induites (CSPi) sont générées en reprogrammant des cellules adultes pour les ramener à un état semblable à l'état embryonnaire. Les CSPi ont la capacité de se différencier en divers types de cellules, ce qui en fait des outils précieux pour la médecine régénératrice, la modélisation des maladies et la découverte de médicaments.

Lorsqu'un gène « driver » a été identifié dans le cas d'une maladie monogénique ou maligne, il est possible d'utiliser à la fois une CSPi dérivée d'un patient et de générer une CSPi isogénique contrôle pour identifier les caractéristiques spécifiques liées à la mutation. Nous avons utilisé cette stratégie pour étudier l'effet du gène REarranged during Transfection (RET), un récepteur de tyrosine kinase, au cours de la différenciation des CSPi dans deux contextes. Nous avons d'abord étudié le rôle potentiel de RET dans l'induction des cellules hématopoïétiques. Dans la deuxième partie, l'objectif était de reproduire un carcinome pulmonaire malin *in vitro* en générant des cellules progénitrices pulmonaires (CPP) et des organoïdes à partir de ces CSPi. Pour répondre à ces deux objectifs, nous avons utilisé des CSPi dérivées d'un patient porteur de la mutation somatique RET^{C634Y} (iRET^{C634Y}), causant l'autophosphorylation de la protéine RET et donc l'activation constitutive de sa voie de signalisation. Nous avons complété nos études avec la génération d'une CSPi RET^{C634Y} knock-in (PB68-RET^{C634Y}).

Dans la première partie de ce manuscrit, ces CSPi ont été différenciées en cellules hématopoïétiques pour étudier le rôle de RET dans l'hématopoïèse dérivée des CSPi. En effet, des études antérieures ont montré que RET joue un rôle dans l'hématopoïèse murine, comme en témoigne l'importante dérégulation de l'hématopoïèse chez les souris *RET* knock-out. Dans le contexte des cellules hématopoïétiques du cordon ombilical (CO), l'activation de RET conduit à une amplification significative des cellules souches hématopoïétiques (CSH). Ces résultats nous ont incités à analyser le rôle potentiel de RET dans l'hématopoïèse dérivée des CSPi. Nous avons étudié le rôle de RET en utilisant des stratégies d'induction hématopoïétique *in vitro* permettant de générer de manière reproductible des cellules hématopoïétiques avec les marqueurs de CSH. Les CSPi témoins ont été comparées aux CSPi exprimant la version mutée de *RET* ou surexprimant RET. Contrairement aux données sur les souris et les cellules de CO adultes, nous montrons un effet inhibiteur de l'activation de RET dans le contexte des CSPi. Les analyses transcriptomiques ont révélé un profil d'expression spécifique dans les cellules hématopoïétiques dérivées de la CSPi iRET^{C634Y}, comprenant la surexpression de gènes associés à la voie des MAPKs et de protéines régulant négativement l'hématopoïèse. Ces résultats suggèrent que l'activation de RET pourrait être associée à un effet inhibiteur sur l'hématopoïèse dérivée des CSPi, potentiellement par l'activation de la voie des MAPKs.

Dans la deuxième partie de ce travail, nous nous sommes demandé si nous pouvions générer de manière reproductible des CPP à partir de CSPi dérivées de patients porteurs de la mutation somatique RET^{C634Y}. Nous avons utilisé un protocole de 16 jours dans le but de générer un des progéniteurs pulmonaires pouvant reproduire un modèle de carcinome pulmonaire non à petites cellules (CPNPC) lié à l'activation de la protéine RET. En effet, les réarrangements oncogéniques de RET peuvent survenir dans 1 à 2% des adénocarcinomes pulmonaires et seuls quelques modèles d'études pour cette maladie sont disponibles. Nous avons généré des CPP exprimant les marqueurs caractéristiques des progéniteurs pulmonaires. Les CPP dérivées de CSPi porteur de la mutation RET^{C634Y} ont montré une surexpression de marqueurs associés au cancer par rapport aux CSPi témoins. L'analyse transcriptomique a révélé des signatures distinctes indiquant une dédifférenciation pulmonaire dans les tumeurs CPNPC, ainsi qu'une signature suractivée associée à la mutation RET^{C634Y}, potentiellement liée à des mauvais pronostics de CPNPC. Les résultats ont été validés ultérieurement en utilisant le modèle de CSPi où la mutation RET^{C634Y} avait été knock-in, mettant en évidence les marqueurs de cancer *PROM2* et *C1QTNF6*, connus pour leur association avec des pronostics défavorables. De plus, les CPP dérivées de CSPi porteur de la mutation RET^{C634Y} ont montré une réponse positive à l'inhibiteur de RET, le Pralsetinib, comme en témoigne la régulation à la baisse des marqueurs de cancer. Cette étude établit le premier modèle de CPNPC lié à l'activation de l'oncogène RET généré à partir de CSPi dérivées de patients.

En raison de leur potentiel de différenciation théoriquement illimité en présence de facteurs appropriés, les CSPi représentent un outil majeur pour étudier différentes maladies à partir du même clone porteur d'une mutation. Ce travail démontre également la polyvalence des CSPi, car une seule lignée de CSPi peut être utilisée pour étudier divers mécanismes et servir de modèles pour différents tissus.

ACKNOWLEDGEMENT

I would like to start this manuscript by thanking all the people who have contributed directly and indirectly to my PhD project.

First and foremost, I extend my gratitude to my thesis advisor, Professor Ali Turhan, for welcoming me into the lab and allowing me to work on this subject. Thank you once again for your advice and for your work on the papers and the manuscript. My thanks also go to Pr. Annelise Bennaceur for welcoming me into her INSERM unit.

I would also like to express my appreciation to the members of my thesis jury. I am very grateful to Dr. Stéphane Vincent and Dr. Evelyne Lauret for agreeing to be my rapporteurs, to Pr. Jamila Faivre, and Pr. Eric Deutsch for agreeing to examine this thesis.

I would like to give special thanks to Dr. Jusuf Imeri for everything he has provided me with over the last few years. Thank you for your help in the lab, for your work on the papers and the manuscript, for the scientific discussions, and the casual times after the lab. I could not have done it without you.

I would like to thank all the members of INSERM 1310 for the knowledge they have shared, their support, and friendly conversations. Particularly, I want to thank Dr. Jinwook Hwang for his significant contribution to the organoid project; Matthias Huygue for his participation in all my projects; Patricia Hugues for her assistance with the hematological assays; Dr. Christophe Desterke for the bioinformatic analysis; Dr. Diana Chaker for sharing her knowledge of FACS and in vivo experiments; Dr. Yucel Erbilgin for working on the CRISPR project and teaching me a lot about molecular biology; Théodoros Latsis for his help and expertise in cell culture; Dr. Jérôme Artus for his advice and discussions regarding this project.

I would also like to express my gratitude to Pr. Eric Delabesse for agreeing to be part of my CST. Thank you for your advice and remarks that have allowed me to put this thesis on the right track.

I am grateful to my family and friends for their unwavering support. I particularly want to thank Dr. Alexandre Eeckhoutte and Dr. Baptiste Tesson for their intensive reading of this manuscript and all their suggestions to improve it.

Finally, I want to express my sincere gratitude to Chloé for her constant support during this journey. I am looking forward to share many more life adventures together in the future.

TABLE OF CONTENT

TABLE OF FIGURES

ABBREVIATIONS

AGM – Aorta-Gonad-Mesonephros
ALK – Anaplastic Lymphoma Kinase
ANGPT1 – Angiopoietin-1
ARTN – Artemin
AT1/2 – Alveolar Type 1/2
BCP – B-Cell precursor
bFGF – Basic Fibroblast Growth Factor
bHLH – Basic Helix-Loop-Helix
BM – Bone Marrow
BMP – Bone Morphogenetic Protein
BRAF – RAF homolog B
BSA – Bovine Serum Albumin
C1QTNF6 – Complement C1q Tumor Necrosis Factor-related protein 6
CD – Cluster of Differentiation
CDK – Cyclin-Dependent Kinase
CFU – Colony-Forming Unit
CFU-S – Colony-Forming Unit Spleen
CGH – Comparative Genomic Hybridization
CKI – Cyclin-dependent Kinase Inhibitor
CLD – Cadherin-Like Domain
CLP – Common Lymphoid Progenitor
CMP – Common Myeloid Progenitor
CPM – Carboxypeptidase M
CRD – Cysteine-Rich Domain
CXCL12 / SDF-1 – CXC motif chemokine 12 / Stromal cell-Derived Factor 1
DAPI – 4',6-Diamidino-2-Phenylindole
DC – Dendritic Cell
EB – Embryoid Body
ECM – Extracellular Matrix
EGFR – Epithelial Growth Factor Receptor
EHT – Endothelial-to-Hematopoietic Transition
EMA – European Medicines Agency
EMP – Erythro-Myeloid Progenitor
ERK – Extracellular signal-Regulated Kinase
ESC – Embryonic Stem Cell
FACS – Fluorescence Activated Cell Sorting
FAK – Focal Adhesion Kinase
FCS – Fetal Calf Serum
FDA – Food and Drugs Administration
FMTC – Familial Medullary Thyroid Carcinoma
GDNF - Glial cell line Derived Neurotrophic Factor
GEM – Genetically Engineered Mouse
GFL – GDNF family ligand
GFRα – GDNF family receptor alpha
GM – Granulocytes and Macrophages
GM-CSF – Granulocyte-Macrophage Colony-Stimulating Factor
GPI – Glycosyl-Phosphatidylinositol
GvHD – Graft-versus-Host Disease
HE – Hemogenic Endothelium
HER2 – Human Epidermal growth factor Receptor-2
hESC – Human Embryonic Stem Cell
HPCS – High-Plasticity Cell State
HLA – Human Leukocyte Antigen
HMG-box – High Mobility Groupe box
HSC – Hematopoietic Stem Cell
HSCR – Hirschsprung's disease
HSCT – Hematopoietic Stem Cell Transplantation
IARC – International Agency for Research on Cancer
IL – Interleukin
iPSC – Induced Pluripotent Stem Cell
ITAG6 – Integrin Subunit Alpha 6
ITS-X – Insulin Transferrin Selenium and Ethanolamine
JAK – Janus Kinase
KRAS – Kirsten Rat Sarcoma Virus
LCC – Large Cell Carcinoma
LIF – Leukemia Inhibitory Factor
LMP – Lympho-Myeloid Progenitor
LT-HSC – Long-Term Hematopoietic Stem Cell
LTC-IC – Long Term Culture-Initiating Cell
MAPK – Mitogen-Activated Protein Kinase
MEFs – Murine Embryonic Fibroblasts
MEN2 – Multiple Endocrine Neoplasia type 2
MEPs – Megakaryocyte–Erythroid Progenitor
mESC – Murine Embryonic Stem Cell
MET – Mesenchymal-Epithelial Transition
MKI – Multi-Kinase Inhibitor

MPP – Multi-Potent Progenitor
MSC – Mesenchymal Stromal Cell
MTC – Medullary Thyroid Carcinoma
NOD/SCID – Non-Obese-Diabetic/Severe Combined Immunodeficiency
NK – Natural Killer
NRTN – Neurturin
NSCLC – Non-Small Cell Lung Cancer
OKSM – OCT4 SOX2 KLF4 c-MYC
OPN – Osteopontin
ORR – Overall Response Rate
OS – Overall survival
PAX6 – Paired Box protein 6
PCW – Post Conception Weeks
PDX – Patient-Derived Xenograft
PFS – Progression-Free Survival
PI3K – Phosphoinositide 3-Kinase
PLCγ – Phospholipase C-γ
PROM2 – Prominin 2
PSPN – Persephin
PTC – Papillary Thyroid Carcinoma
PVA – Polyvinyl Alcohol
RAF – Rapidly Accelerated Fibrosarcoma
RAS – Rat Sarcoma Virus
RET – REarranged during Transcription
ROS – Reactive Oxygen Species
ROS1 – ROS proto-oncogene 1
RTK – Receptor Tyrosine Kinase
SC-islet – Stem Cell-derived pancreatic Islet
SpCC – Spermatogonial Stem Cells
SCC – Squamous Cell Carcinoma
SCF – Stem Cell Factor
SCLC – Small Cell Lung Cancer
scRNA-Seq – Single-cell RNA sequencing
αSMA – Smooth Muscle Actin
SOX – SRY-Box transcription factor
SR1 – StemRegenin-1
SSEA-3/4 – Stage-Specific Embryonic Antigen ¾
STAT – Signal Transducers and Activators of Transcription
ST-HSC – Short-Term Hematopoietic Stem Cell
TBXT – T-Box transcription factor T
TGF-β – Transforming Growth Factor-β
TK – Tyrosine Kinase domain
TKI – Tyrosine Kinase Inhibitor
TMD – Transmembrane Domain
TNK – T/NK progenitor
TPO – Thrombopoietin
TRA-1-60 – T cell Receptor Alpha locus-1-60
TTF-1 – Thyroid Transcription Factor 1
UCB – Umbilical Cord Blood
VE-cadherin – Vascular-Endothelial Cadherin
VEGF – Vascular Endothelial Growth Factor
YS – Yolk Sac

SUMMARY

Les cellules souches pluripotentes induites (CSPi) sont générées en reprogrammant des cellules adultes pour les ramener à un état semblable à l'état embryonnaire. Les CSPi ont la capacité de se différencier en divers types de cellules, ce qui en fait des outils précieux pour la médecine régénératrice, la modélisation des maladies et la découverte de médicaments.

Lorsqu'un gène « driver » a été identifié dans le cas d'une maladie monogénique ou maligne, il est possible d'utiliser à la fois une CSPi dérivée d'un patient et de générer une CSPi isogénique contrôle pour identifier les caractéristiques spécifiques liées à la mutation. Nous avons utilisé cette stratégie pour étudier l'effet du gène REarranged during Transfection (RET), un récepteur de tyrosine kinase, au cours de la différenciation des CSPi dans deux contextes. Nous avons d'abord étudié le rôle potentiel de RET dans l'induction des cellules hématopoïétiques. Dans la deuxième partie, l'objectif était de reproduire un carcinome pulmonaire malin *in vitro* en générant des cellules progénitrices pulmonaires (CPP) et des organoïdes à partir de ces CSPi. Pour répondre à ces deux objectifs, nous avons utilisé des CSPi dérivées d'un patient porteur de la mutation somatique *RET*^{C634Y} (iRET^{C634Y}), causant l'autophosphorylation de la protéine RET et donc l'activation constitutive de sa voie de signalisation. Nous avons complété nos études avec la génération d'une CSPi RET^{C634Y} knock-in (PB68-RET^{C634Y}).

Dans la première partie de ce manuscrit, ces CSPi ont été différenciées en cellules hématopoïétiques pour étudier le rôle de RET dans l'hématopoïèse dérivée des CSPi. En effet, des études antérieures ont montré que RET joue un rôle dans l'hématopoïèse murine, comme en témoigne l'importante dérégulation de l'hématopoïèse chez les souris *RET* knock-out. Dans le contexte des cellules hématopoïétiques du cordon ombilical (CO), l'activation de RET conduit à une amplification significative des cellules souches hématopoïétiques (CSH). Ces résultats nous ont incités à analyser le rôle potentiel de RET dans l'hématopoïèse dérivée des CSPi. Nous avons étudié le rôle de RET en utilisant des stratégies d'induction hématopoïétique *in vitro* permettant de générer de manière reproductible des cellules hématopoïétiques avec les marqueurs de CSH. Les CSPi témoins ont été comparées aux CSPi exprimant la version mutée de *RET* ou surexprimant RET. Contrairement aux données sur les souris et les cellules de CO adultes, nous montrons un effet inhibiteur de l'activation de RET dans le contexte des CSPi. Les analyses transcriptomiques ont révélé un profil d'expression spécifique dans les cellules hématopoïétiques dérivées de la CSPi iRET^{C634Y}, comprenant la surexpression de gènes associés à la voie des MAPKs et de protéines régulant négativement l'hématopoïèse. Ces résultats suggèrent que l'activation de RET pourrait être associée à un effet inhibiteur sur l'hématopoïèse dérivée des CSPi, potentiellement par l'activation de la voie des MAPKs.

Dans la deuxième partie de ce travail, nous nous sommes demandé si nous pouvions générer de manière reproductible des CPP à partir de CSPi dérivées de patients porteurs de la mutation somatique *RET*^{C634Y}. Nous avons utilisé un protocole de 16 jours dans le but de générer un des progéniteurs pulmonaires pouvant reproduire un modèle de carcinome pulmonaire non à petites cellules (CPNPC) lié à l'activation de la protéine RET. En effet, les réarrangements oncogéniques de RET peuvent survenir dans 1 à 2% des adénocarcinomes pulmonaires et seuls quelques modèles d'études pour cette maladie sont disponibles. Nous avons généré des CPP exprimant les marqueurs caractéristiques des progéniteurs pulmonaires. Les CPP dérivées de CSPi porteur de la mutation *RET*^{C634Y} ont montré une surexpression de marqueurs associés au cancer par rapport aux CSPi témoins. L'analyse transcriptomique a révélé des signatures distinctes indiquant une dédifférenciation pulmonaire dans les tumeurs CPNPC, ainsi qu'une signature suractivée associée à la mutation *RET*^{C634Y}, potentiellement liée à des mauvais pronostics de CPNPC. Les résultats ont été validés ultérieurement en utilisant le modèle de CSPi où la mutation *RET*^{C634Y} avait été knock-in, mettant en évidence les marqueurs de cancer *PROM2* et *C1QTNF6*, connus pour leur association avec des pronostics défavorables. De plus, les CPP dérivées de CSPi porteur de la mutation *RET*^{C634Y} ont montré une réponse positive à l'inhibiteur de RET, le Pralsetinib, comme en témoigne la régulation à la baisse des marqueurs de cancer. Cette étude établit le premier modèle de CPNPC lié à l'activation de l'oncogène RET généré à partir de CSPi dérivées de patients.

En raison de leur potentiel de différenciation théoriquement illimité en présence de facteurs appropriés, les CSPi représentent un outil majeur pour étudier différentes maladies à partir du même clone porteur d'une mutation. Ce travail démontre également la polyvalence des CSPi, car une seule lignée de CSPi peut être utilisée pour étudier divers mécanismes et servir de modèles pour différents tissus.

ABSTRACT

Induced pluripotent stem cells (iPSCs) are generated by reprogramming adult cells back into an embryonic-like state. iPSCs can be differentiated into various cell types, making them a valuable tool for regenerative medicine, disease modeling and drug discovery.

In case of monogenic or malignant diseases where a driver gene has been identified, it is possible to use both patient-derived iPSCs and their CRISPR-corrected isogenic control iPSCs to identify the distinct characteristics linked to the mutation. We have used this strategy to unravel the effect of REarranged during Transfection (RET), a tyrosine kinase receptor, during iPSC differentiation within two different contexts. We first studied the potential role of RET in the induction of hematopoietic cells. In the second part, the objective was to replicate a malignant lung carcinoma *in vitro* by generating lung organoids and lung progenitor cells (LPC) from these iPSCs. For these purposes we have used an iPSC derived from a patient carrying the *RET*^{C634Y} somatic mutation (iRET^{C634Y}) which is responsible for the autophosphorylation of the protein RET and therefore the constitutive activation of its signaling pathway. We have completed our studies with the generation of a RET^{C634Y} knock-in iPSC (PB68-RET^{C634Y}).

In the first part of this manuscript, these iPSCs were differentiated into hematopoietic cells to investigate the role of RET in iPSC-derived hematopoiesis. Indeed, previous studies have shown that RET plays a role in mice hematopoiesis as demonstrated by *RET* knock-out mice exhibiting significant deficiencies in hematopoiesis. In the context of cord blood (CB) cells, RET activation led to a significant amplification of hematopoietic stem cell (HSCs). These published results prompted us to analyze the potential role of RET in iPSC-derived hematopoiesis. We have studied this potential by using *in vitro* hematopoietic induction strategies allowing reproducible generation of hematopoietic cells with HSC markers using control versus RET-activated or overexpressed iPSCs. As opposed to the reports in mice and adult CB cells, we report an inhibitory effect of RET activation in the context of iPSCs. Transcriptomic analyses revealed a specific activated expression profile in iRET^{C634Y}, including overexpression of genes associated with the MAPK network and negative hematopoietic regulator activities. These findings suggest that RET activation might be associated with inhibitory effects on iPSC-derived hematopoiesis, potentially through MAPK activation.

In the second part of this work, we have asked whether we could reproducibly generate LPCs from patient-derived iPSCs carrying the *RET*^{C634Y} somatic mutation using a 16-day protocol with the purpose to generate a model of RET-driven non-small cell lung cancer (NSCLC). Indeed, *RET* oncogenic rearrangements can occur in 1-2% of lung adenocarcinomas and only a few models for studying this disease are available. We have shown the successful generation of LPCs expressing expected lung

progenitor markers. LPCs generated from RET^{C634Y} iPSCs displayed an overexpression of cancer-associated markers as compared to control iPSCs. Transcriptomic analysis revealed distinct signatures indicating lung multilineage dedifferentiation in NSCLC tumors, along with an upregulated signature associated with the *RET^{C634Y}* mutation, potentially linked to worse NSCLC prognosis. The findings were further validated using the RET^{C634Y} knock-in iPSC model, highlighting key cancerous targets *PROM2* and *C1QTNF6,* known for their association with poor prognostic outcomes. Moreover, LPCs derived from RET^{C634Y} iPSCs showed a positive response to the RET inhibitor Pralsetinib, evidenced by the downregulation of cancer markers. This study establishes the first model of RET-driven NSCLC LPCs generated from patient-derived iPSCs.

Due to their theoretically unlimited differentiation potential under the appropriate cues, iPSCs represent a major tool to study different diseases starting from the same oncogene-bearing clone. This work also demonstrates the versatility of iPSCs, as a single iPSC line can be utilized to investigate various mechanisms and serve as model for different tissues.

INTRODUCTION

INTRODUCTION

1. Induced Pluripotent Stem Cells and Embryonic Stem Cells

1.1. Stem cells: Definition

Stem cells are undifferentiated cells that have the unique ability to both self-renew and differentiate into various specialized cell types. Self-renewal is a process where stem cells can proliferate indefinitely without modifications, essentially maintaining a population of undifferentiated cells. Differentiation is the process by which stem cells give rise to specialized cell types, according to their tissues of origin, making up the various tissues and organs of the body during embryogenesis. Stem cells exist both at the embryonic and adult stages. There are several types of stem cells that are classified based on their developmental potential and the types of specialized cells they can differentiate into.

- **Totipotent stem cells** are the most versatile type of stem cells and can differentiate into any type of cell, including both embryonic and extra-embryonic tissues. Totipotent stem cells are only found in the earliest stages of development, such as in the zygote (the fertilized egg) and in the first few cell divisions of the embryo.
- **Pluripotent stem cells** can differentiate into any cell type of the three germ layers (ectoderm, mesoderm, and endoderm) found in embryos, including the germinal lineage, but not into extra-embryonic tissues (e.g., placenta).
- **Multipotent stem cells** can differentiate into a limited range of cell types within a particular tissue or organ. For example, hematopoietic stem cells (HSCs) found in bone marrow can differentiate into distinct types of blood cells, but not into other types of cells. Multipotent stem cells represent the most abundant type of stem cells.
- **Oligopotent cells** can differentiate into only a few closely related cell types. They are typically found in tissues that require constant replenishment or repair, such as the blood circulation system.

With their self-renewal capacity, stem cells can indefinitely divide while maintaining their phenotypic, genotypic, and epigenetic properties. It is made possible by the combination of two processes: asymmetric cell division and stochastic differentiation (Morrison & Kimble 2006). When a mother stem cell undergoes an asymmetric division, it divides into two daughter cells that have different fates. One daughter cell remains a stem cell and retains the ability to divide and differentiate into different cell types, while the other one differentiates into a specialized cell type. Asymmetric

division is thought to be regulated by internal and external cues. It is important for maintaining a balance between stem cells and differentiated cells. On the other hand, stochastic differentiation produces two identical daughter stem cells from the mitosis of a mother stem cell. This type of division plays a crucial role in generating more stem cells. Together, these mechanisms ensure the stability of the stem cell population.

The cell stemness potential decreases during embryonic development. After the fusion of an egg and sperm cell, totipotent stem cells will constitute the first stages of embryonic development. Pluripotent stem cells originate from inside the blastocyte, and they will be at the origin of the three germ layers. Multipotent stem cells will then give rise to the different cells of the body, while unipotent stem cells will differentiate into a single specialized cell type.

While stem cells are crucial for embryonic development, they are also present in adult tissues and organs, where they play a role in tissue regeneration and repair. However, adult stem cells are more limited in their differentiation potential than embryonic stem cells.

1.2. Embryonic stem cells (ESCs)

Embryonic stem cell (ESC) research in mice has been ongoing since the early 1970s when the first stem cell of a tumor was generated and successfully transplanted (Stevens 1970). In 1981, the first mouse embryonic stem cell (mESC) lines were established from cells isolated from the inner mass of the blastocyst (Evans & Kaufman 1981). The cells were cultured in medium conditioned by teratocarcinoma cells with fetal calf serum (FCS), on mitotically inactivated murine embryonic fibroblasts (MEFs), still used today for providing critical factors that could promote self-renewal while inhibiting differentiation (Martin 1981). The pluripotency of mESCs was demonstrated *in vivo* by a now gold standard assay called chimera-forming ability. Mouse ESCs were injected into pre-implanted embryos and showed contribution to the three cell lineages including the germ line of the live-born animals (Bradley et al. 1984). The preservation of pluripotency in these cells was improved by the discovery of specific factors, such as leukemia inhibitory factor (LIF) (Smith et al. 1988).

Another type of mESC can be derived from embryos at 5.5-6.5 days post-conception (Brons et al. 2007). They are called epiblast stem cells. Although they are pluripotent, they cannot generate chimeras when transplanted into mouse blastocysts. Additionally, one of their X chromosomes is inactivated, making it challenging to maintain them as a clonal population. These cells express both pluripotency and differentiation genes at higher levels than pluripotent stem cells from the inner cell mass. As a result, the term "naive" pluripotent stem cells has been used to describe mouse ESCs derived from the blastocyst, whereas epiblast stem cells are called "primed".

In 1998, the first human ESC lines were derived by Thomson et al, including the H1 and H9 lines, which became the most widely used human ESC (hESC) lines for research purposes (Thomson et al. 1998). This breakthrough was significant because it provided a new source of pluripotent cells for research and potential therapeutic applications. Prior to this, the only source was from fetal tissue, which raised ethical concerns and was limited in supply.

Murine ESCs have been extensively utilized to study the signaling pathways involved in ESC differentiation into different tissue lineages and have been crucial for disease modeling. Similarly, human ESCs have also been used for disease modeling and more recently, for therapeutic purposes.

Human and murine ESCs share some common characteristics, such as their pluripotency. However, there are also significant differences between the two. Mouse ESCs are easier to culture and maintain *in vitro* contrary to hESCs that need basic fibroblast growth factor (bFGF) and serum-free medium where LIF is insufficient to inhibit their differentiation (Amit et al. 2000a; Dahéron et al. 2004). Mouse ESCs are also more genetically stable whereas hESCs tend to accumulate more genetic abnormalities during long-term culture (Lamm et al. 2016). Moreover, hESCs have a "primed" pluripotent state closer to the mouse epiblast stem cells than to the one of "naive" mESCs. Specific culture conditions are required to obtain naive hESCs comparable to mESCs (Hanna et al. 2010). Therefore, epiblast stem cells serve as a useful experimental model to investigate whether the differences observed between mouse and human embryonic stem cells reflect species differences or diverse temporal origins.

Since the derivation of the first hESC line, researchers have continued to study and refine the process of growing and differentiating these cells, with the aim of using them to treat a range of diseases. However, the use of hESCs, raises many ethical and practical challenges which creates the need for alternative sources of pluripotent cells, such as induced pluripotent stem cells (iPSCs).

1.3. Induced pluripotent stem cells (iPSCs)

1.3.1. History of iPSCs

The research for reprogramming adult somatic cells into pluripotent cells started in 1962 with the work of John Gurdon in Cambridge (UK). In his experiment, the nucleus from a differentiated intestinal cell taken at the tadpole stage was transplanted into an enucleated Xenopus oocyte (Gurdon 1962). The egg developed into a tadpole, indicating that the transplanted nucleus had been reprogrammed to a pluripotent state by the factors contained in the cytoplasm of the oocyte. This experiment also demonstrated that the embryonic genetic information in a differentiated cell is not irreversibly lost and can be reactivated to generate pluripotent cells. This groundbreaking revolutionary experiment represented the first milestone in this field (Gurdon 2006).

In 1976, cellular fusion was developed as another reprogramming method for generating pluripotent cells (Miller & Ruddle 1976). Cellular fusion between pluripotent embryonic stem cells and somatic cells can result in hybrid tetraploid cells where the pluripotency state is maintained. These hybrid synkaryons acquire properties of pluripotent cells such as self-renewal and the capacity of differentiation in the three germ layers (Cowan et al. 2005; Piccolo et al. 2011).

In 2006, Yamanaka and Takahashi made a groundbreaking discovery by showing that adult mouse fibroblasts could be reprogrammed to an embryonic-like state by the overexpression of the 4 pluripotency factors OCT4, SOX2, KLF4, and c-MYC (known as OKSM) (Takahashi & Yamanaka 2006). Soon after, they showed that this method could also be used to reprogram human adult cells into pluripotent stem cells (Takahashi et al. 2007). Their initial hypothesis was based on previous experiments of reprogramming by nuclear transfer or fusion suggesting that the pluripotency factors of stem cells could confer pluripotency to differentiated somatic cells. They selected 24 pluripotency genes identified in transcriptomic analyses of ESCs and with retroviral transduction they showed that only 4 of them were necessary and sufficient for inducing pluripotency and reprogramming adult differentiated cells. Therefore, cells generated by this technique are called induced pluripotent stem cells (iPSCs).

It overturned the central dogma that adult cells are irreversibly committed to their fate and that their differentiation is irreversible. For this major discovery, Shinya Yamanaka, alongside with John Gurdon, was awarded the Nobel Prize in Medicine in 2012.

iPSCs have emerged as a crucial tool for modeling diseases and exploring the cellular and molecular mechanisms that contribute to their development. They offer the ability to generate patient-specific cells and tissues that are histocompatible for cell replacement therapy. Additionally, iPSCs can be utilized in drug discovery and development, enabling large-scale screening of molecules in a more physiologically relevant context. Consequently, the development of iPSC reprogramming protocols paves the way for making iPSC technology more accessible.

1.3.2. Reprogramming of adult cell into iPSCs

For a cell to become pluripotent, it must overcome various obstacles such as apoptosis, senescence, metabolic and mesenchymal-to-epithelial transition, acquisition of early pluripotency genes, and activation of the complete epigenetic and transcriptional network of pluripotency. Consequently, the reprogramming process is not very effective as less than 1% of somatic cells expressing the necessary OKSM factors are able to become iPSCs after 30 days (Rao & Malik 2012).

The first step is the introduction of the reprogramming factors (OKSM) into the somatic cell. There are several techniques of introduction that can be classified in two categories: integrative and non-integrative techniques:

- **Integrative retroviruses** were the first tools used to induce the expression of the OKSM factors. The transgenes are randomly and permanently integrated into the genome leading to potential risks such as insertional mutations and altered differentiation potentials of the iPSCs. This can lead to pathologies like tumorigenesis due to the reactivation of *c-MYC* oncogene (Okita et al. 2007). Therefore, new non-integrative techniques have been developed.
- **Non-integrative vectors** regroup Sendai virus (Fusaki et al. 2009), episomal vectors (Yu et al. 2011), RNA transfection (Warren et al. 2010; Yakubov et al. 2010) or protein injection (Zhou et al. 2009). The Sendai virus is the most common technique for cell reprogramming and the one we are using in our laboratory. It is a non-integrating RNA virus capable of delivering the OKSM factors inside the cell. Since it cannot replicate itself at 37°C, the expression of the exogenous factors will decrease over time (Ban et al. 2011).

After their introduction, the reprogramming factors will initiate the activation of genes associated with pluripotency and the inhibition of the genes defining the somatic cell identity. These transcriptional changes are mediated by the remodeling of the chromatin and epigenetic modifications (Maherali et al. 2007). The first changes related to these modifications are a metabolic shift from oxidative phosphorylation to glycolysis, helping to increase the glucose uptake and reducing the quantity of reactive oxygen species (ROS) (Varum et al. 2011). Moreover, it has been shown that hypoxia is beneficial for the maintenance of hESC and for increasing the reprogramming efficiency of iPSCs (Yoshida et al. 2009; Forristal et al. 2010). The discontinuation of the somatic program is also associated with major morphologic changes. Reprogrammed cells will undergo mesenchymal-epithelial transition (MET) mediated by the OKSM factors (**Figure 1**). Indeed, SOX2/OCT4 and c-MYC inhibit Snail, a repressor of adhesion molecules, whereas KLF4 induces epithelial protein such as E-cadherin (Li et al. 2010). This transition is essential to produce epithelial stem cells.

Finally, as the iPSCs become more pluripotent, the expression of the viral reprogramming factors is replaced by the expression of the endogenous OKSM, leading to the stable maintenance of the pluripotency (**Figure 1**). For example, endogenous OCT4 expression regulates the Wnt/β-catenin signaling and therefore the balance between pluripotency and differentiation (Abu-Remaileh et al. 2010). Moreover, the expression of LIN28 in TRA-1-60 positive cells (one of the most specific markers of hESCs) inhibits the reversion of the reprogramming by the upregulation of pluripotency-associated microRNAs (Qiu et al. 2010; Zhang et al. 2016). This step is critical because it is the shift from an

exogenous induced pluripotency to an ES-like pluripotency resulting in colonies of iPSCs cells after reseeding (Tanabe et al. 2013).

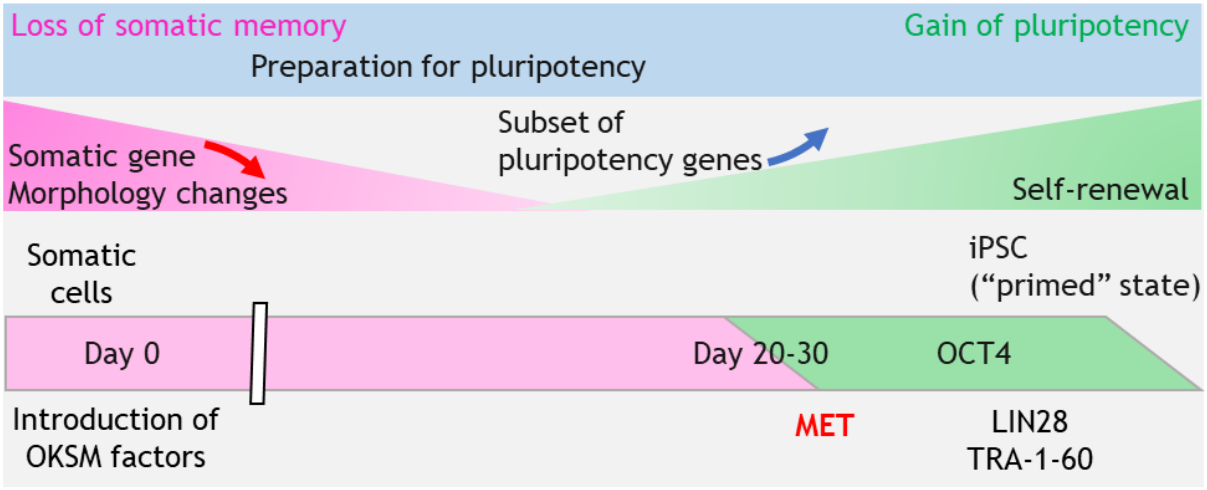

***Figure 1: Sequential events and changes of gene expression during the reprogramming of somatic cells into iPSCs**. (Adapted from Teshigawara et al. 2017).*

To this day, iPSC reprogramming remains a complex and challenging process with relatively small chance of success. The effects of the induced pluripotent factors are heavily correlated with the chromatin state. Indeed, in somatic cells the chromatin is usually condensed making it difficult for the reprogramming factors to bind to their target genes (Li et al. 2017). Cells in division are much easier to reprogram because the chromatin is partially decondensed during mitosis (Hanna et al. 2009). The addition of chromatin-modifier molecules has been shown to improve the efficiency of iPSCs generation (Onder et al. 2012; Federation et al. 2014). Moreover, the expression of p53, a protein described as the guardian of the genome, is also problematic for reprogramming as it inhibits the cellular cycle and the MET (Marión et al. 2009; Brosh et al. 2013).

It is worth noting that in the past few years new chemical reprogramming techniques have been developed and seem to be more efficient than the conventional OKSM factors induction. The chemical stimulation by the exposition of somatic cells to small molecules can create an intermediate plastic state exhibiting key features of ESC (Guan et al. 2022). This protocol enabled a more direct reprogramming process and can shorten the reprogramming time to a minimum of 16 days (Liuyang et al. 2023).

Once iPSCs are generated, it is necessary to evaluate their morphology and their stemness potential. This evaluation encompasses an analysis of their cellular characteristics, including their ability to maintain their pluripotency and to differentiate into various cell lineages.

1.3.3. Characterization and maintenance of iPSCs

iPSCs morphology is similar to that of hESCs. They are small-round cells with a high nuclear-to-cytoplasmic ratio and prominent nucleoli. They form tightly packed colonies and have a distinct flattened shape with a well-defined border (**Figure 2A**). They exhibit a short cell cycle, related with a shortened G1 cell cycle phase, with a doubling time of approximately 16-20h which supports their pluripotency and makes them easy to expand at large scale (Becker et al. 2006; Hanna et al. 2010).

To maintain their pluripotency, iPSCs need to be cultivated in defined conditions. Initial methods for cultivating hESC were modeled on techniques originally developed to culture mESCs. As previously described, it involved a culture on a layer of MEFs feeder cells, in medium supplemented with 20% of FCS (Martin 1981). Refinement of cultivation techniques has permitted the removal of serum and non-human components in favor of the addition of growth factors and small molecules such as FGF-2, TGF-β, and CHIR99021 in a defined medium (Ludwig et al. 2006; Yao et al. 2006). MEFs feeder were also replaced by MEF-conditioned medium, human feeders and more recently by extracellular matrix surface coating (Amit et al. 2000b; Hovatta et al. 2003; Amit et al. 2004). Today in the laboratory, iPSCs are cultivated in true feeder/serum-free conditions with Essential 8™ Medium (Gibco; A1517001) and Geltrex™ (Gibco; A1413302) as extracellular matrix. Essential 8™ Medium is xeno-free and contains only the 8 essential components needed for stem cell culture (Chen et al. 2011). iPSCs are prone to spontaneous differentiation if their environment is altered, therefore they must be carefully monitored every day.

iPSCs express intra and extracellular makers of pluripotency. Immunostaining can be used to assess the expression of extracellular markers such as glycolipids SSEA-3 and SSEA-4 or the keratan sulfate antigen TRA-1-60 (International Stem Cell Initiative et al. 2007) (**Figure 2B-C**). It is also possible to detect their intracellular counterparts such as Nanog, SOX2 or OCT4 by immunofluorescence or to quantify their expression with qRT-PCR (**Figure 2B-D**). Furthermore, iPSCs are characterized by their potential of differentiation. The “gold standard” test for evaluating this ability is the teratoma forming assay where iPSCs are injected into immune-compromised mice in which they form teratoma. Their pluripotency is confirmed after the pathological identification of tissues from the 3 embryonic germ-layers (endoderm, mesoderm, and ectoderm) (Wesselschmidt 2011). However, this technique has been debated due to animal welfare and ethical concerns and candidate alternatives have been proposed such as differentiation of iPSCs into organotypic cells with trilineage differentiation kits or embryonic bodies (**Figure 2E-G**) (Buta et al. 2013).

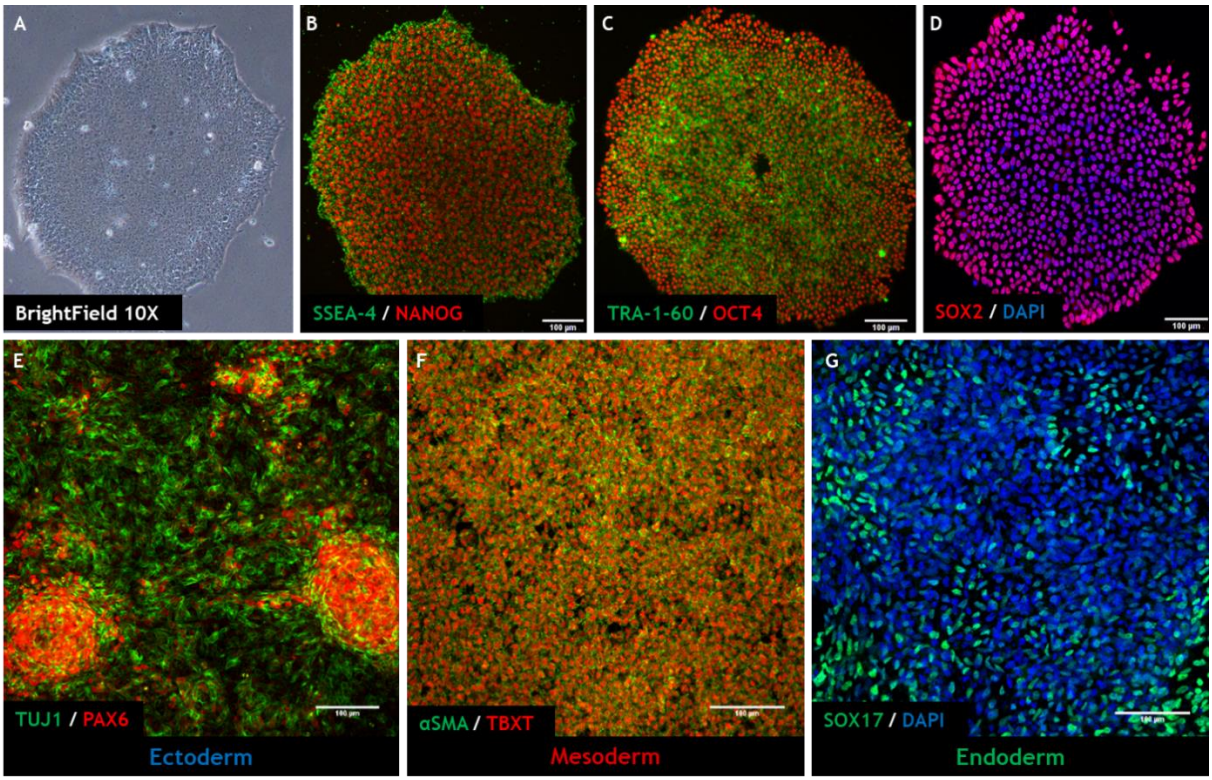

Figure 2: Characterization of iPSCs pluripotency by immunofluorescence. (A) *Morphology of an iPSC colony in brightfield with highly packed cells and well-defined borders.* ***(B-D)*** *Immunofluorescence staining of pluripotency markers:* ***(B)*** *SSEA-4 (green) and Nanog (red),* ***(C)*** *TRA-1-60 (green) and OCT4 (red),* ***(D)*** *SOX2 (red) and DAPI (blue).* ***(E-G)*** *Immunofluorescent staining of markers from each germ layer after the differentiation of iPSCs into the three germ layers.* ***(E)*** *Ectoderm: PAX6 is transcription factor expressed in the early human fetal neuroectoderm, which remains strongly expressed in certain regions of the adult brain and Tuj1 antibody reacts with the neuronal form of tubulin (Beta-III).* ***(F)*** *Mesoderm: Smooth muscle actin (αSMA) is expressed in skeletal myoblastic cells, smooth muscle cell precursors, and pericytes. TBXT is a key transcription factor involved in the early development and specification of the posterior mesoderm.* ***(G)*** *Endoderm: SOX17 is an HMG-box transcription factor necessary for definitive endoderm development. Personal communication from Dr. Imeri (Inserm U1310).*

The characterization of iPSCs is also complemented by safety tests if they are intended for therapeutic purposes. These tests include checking for the absence of mycoplasma infection, the absence of viral infection and the disappearance of reprograming factors, especially c-MYC. It is also important to check for the genomic stability with a karyotype and comparative genomic hybridization (CGH) because iPSCs can accumulate genetic abnormalities during the reprogramming or the cell culture (Tosca et al. 2015; Liu et al. 2020).

Finally, iPSCs must be evaluated for their capacity to differentiate into the desired cell types and to perform their intended functions *in vitro* and *in vivo.* The mechanisms and protocols of iPSC differentiation are described in the chapters dedicated to the specific tissues discussed in this manuscript (see section **2.3. HSCs generation from iPSCs** and section **4.4.4.3. iPSC-derived lung organoid models**).

1.4. Utilization of iPSCs for disease modeling and therapy

iPSCs have revolutionized the field of disease modeling and regenerative medicine by providing a potentially limitless source of patient-specific cells for studying disease mechanisms, drug discovery, and personalized cell-based therapies (**Figure 3**)

1.4.1. iPSC-based disease modeling

Disease derived-iPSCs provide a unique opportunity to study diseases from tissues and cells that have limited lifespan in culture or are difficult to obtain from patients, such as brain tissue or pancreatic cells. Additionally, they can be used to model gene activity associated with diseases that are too complex to model with classical gene editing techniques. Cells differentiated from patient-derived-iPSCs exhibit the features inherent to the disease and demonstrate a strong reproducibility (Robinton & Daley 2012). For example, Ebert and her colleagues generated iPSCs from a patient suffering from spinal muscular atrophy and were able to generate motor neurons that maintained the disease genotype and showed selective deficits (Ebert et al. 2009). Another study shows iPSCs derived from individuals with FGFR3 skeletal dysplasia could be differentiated into degraded cartilage. Interestingly, statin treatment, a commonly used medication for hypertension, was effective in repairing this deteriorated cartilage (Yamashita et al. 2014). Therefore, in addition to being an efficient disease modeling tool, this study shows iPSCs disease derived-iPSCs can be used in drug screening including drug repositioning (Avior et al. 2016).

However, iPSCs present an unpredictable variability in their potential to differentiate into functional cells of a given lineage because of their genetic background. It can be problematic to compare cells differentiated from a patient and control iPSCs when studying subtle phenotypic variations of a given disease (Soldner & Jaenisch 2012). Therefore, isogenic pairs of disease-specific and control iPSCs have been generated to address this variability and isolate the impact of the disease-causing mutation (Soldner et al. 2011). The generalization of genome editing tools such as CRISPR/Cas9 system has helped to overcome the resilience of pluripotent stem cells to conventional gene targeting approaches and allows for the generation of control iPSCs whose mutation is corrected by exploiting homologous recombination (Byrne & Church 2015; Johnson & Hockemeyer 2015; Li, Zhou, et al. 2019). For example, Li and colleagues have corrected an iPSC derived from a Duchenne muscular dystrophy patient and showed that the muscle cells differentiated from these corrected iPSCs express the full-length dystrophin protein (Li, Fujimoto, et al. 2015). Another example is the correction of a *MYO15A* mutation which is responsible for abnormal morphology and dysfunction of the derived hair cell-like cells, resulting in deafness. Derived hair cell-like cells from corrected iPSCs had a normal morphology and function demonstrating the potential therapy of genetic correction on this disease (Chen et al. 2016). Finally, this genome editing approach in iPSCs is promising for studying polygenic diseases and

demonstrating the involvement of alleles or allele associations in pathophysiology (Hockemeyer & Jaenisch 2016).

The concept of "personalized medicine" in which each patient receives a tailored treatment, is becoming increasingly important to minimize adverse side effects and to identify potential non-responders to conventional therapies. Adverse side effects of drugs have resulted in millions of hospitalizations and hundreds of thousands of deaths annually, highlighting the critical need for precision medicine (Doss & Sachinidis 2019). Therefore, iPSC-based disease models are promising candidates due to their unlimited supply of clinically relevant cells of human origin, and their easy accessibility.

In the specific context of cancer research, iPSCs present several advantages. They are specific to a patient thus oncogenic mutations can be studied within a specific genomic context. Furthermore, their unlimited proliferation and self-renewal capacities make them very attractive for high-throughput screening of anti-tumor agents or for toxicological studies. Moreover, the use of genome editing tools allows the introduction of known and/or suspected oncogenes in iPSCs, thus the creation of custom oncogenesis models.

1.4.2. Limits of iPSC disease modeling

Although progress has been made in comprehending diseases, 2D iPSC models are still highly restrictive as they do not consider the intricacy of the tissue where diseases arise. Researchers are actively working on the development of whole organ models that aim to recreate the intricate interactions between different tissues involved in oncogenesis, precisely imitating human tissue and organ dysfunction. This approach involves the *in vitro* generation of "mini organs" known as organoids. For example, organoids replicating organs such as the brain or digestive tract have already been successfully generated (Spence et al. 2011; Lancaster et al. 2013). This will be described further in the section **4.4.4. Organoid models**.

Moreover, many protocols developed for differentiating iPSCs into functional tissues result in embryonic rather than adult human cell types (Spence et al. 2011; Hrvatin et al. 2014). This can be problematic for studies aiming to understand human disease and pathologies in the context of the adult. Indeed, iPSC differentiation experiments suffer from a lack of cellular maturity and a relatively short time lifespan limited by culture conditions. Progress has been made in developing co-culture experiments and protocols for differentiating iPSCs into tissue stem cells or organoid cultures to investigate cell non-autonomous biological problems.

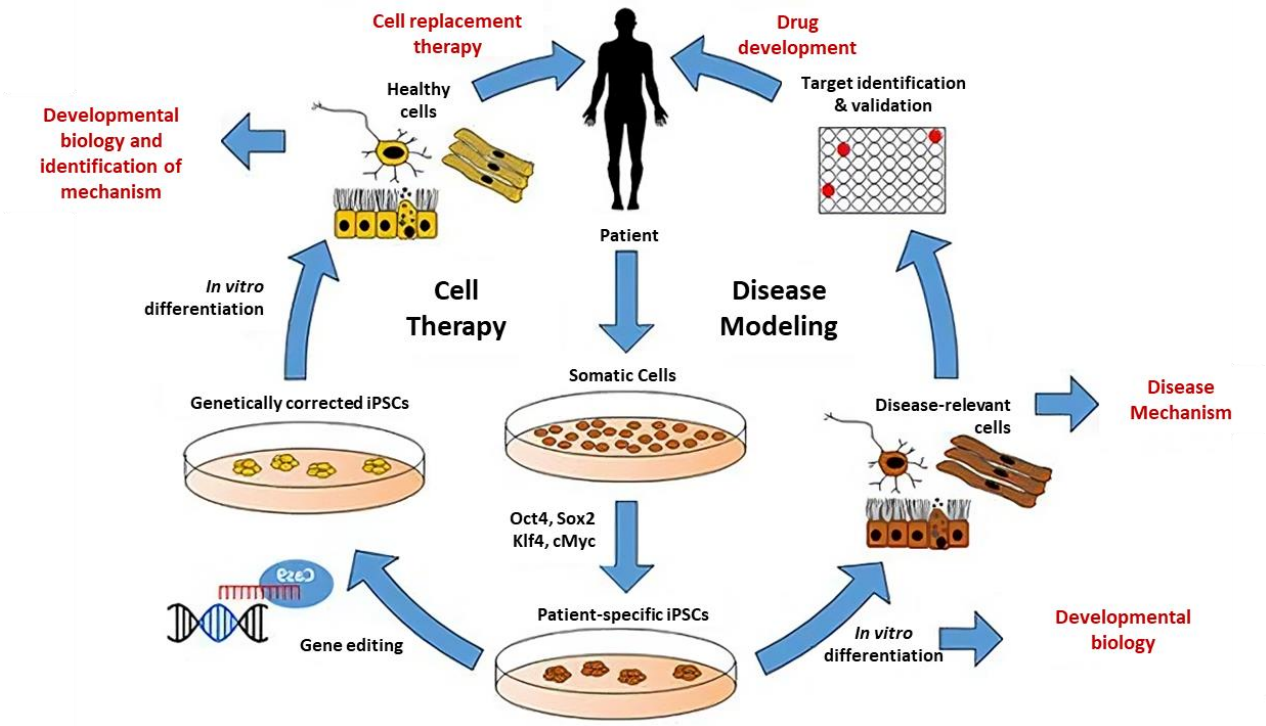

Figure 3: Potential application of iPSCs in cell therapy and disease modeling. *Adapted from Stadtfeld & Hochedlinger 2010)*

1.4.3. iPSC-based therapies

A proof of concept regarding the potential therapeutic application of iPSCs was published in 2007. The study utilized a mouse model of sickle-cell anemia, which is a genetic blood disorder resulting from a β-globin gene mutation. In this study based on a humanized mouse model of sickle cell anemia, the authors have shown that mice can be rescued after transplantation with hematopoietic progenitors obtained from gene-corrected autologous iPSCs (Hanna et al. 2007). The utilization of iPSC-based autologous method has several advantages over allografts from donors, as it eliminates the risk of immunological rejection and infection from unknown viruses or pathogens (Araki et al. 2013; Guha et al. 2013). It has however now been established that even autologous iPSCs can generate immune rejection in the host due to the genetic and epigenetic modifications appearing during the iPSC generation and culture (Scheiner et al. 2014). More recently, several groups have established several protocols for mice *in vivo* transplantation of stem cell-derived pancreatic islet (SC-islet) capable of producing insulin-secreting β cells (Maxwell & Millman 2021). They reported a successful glucose homeostasis in diabetic immunocompetent mice after transplantation opening the way for potential SC-islets graft treatment in diabetic patients, overcoming the current limitations of donor islets. Moreover, with CRISPR/Cas9, it is possible to edit a gene in a patient specific iPSCs and use it for autologous transplant providing an ideal therapeutic solution for genetic diseases such as β-thalassemia and recessive dystrophic epidermolysis bullosa (Xie et al. 2014; Jacków et al. 2019). Overall, this shows the potential of iPSCs for cell replacement therapy.

However, there are several challenges that must be overcome before making iPSCs applicable for therapy. The two other major issues are tumorigenicity and heterogeneity (Yamanaka 2020). Tumorigenicity is a concern as undifferentiated iPSCs can generate benign tumors, and residual PSCs can result in teratoma formation. Heterogeneity represents a typical characteristic of pluripotent stem cell lines and makes it difficult to predict which cell line will be more prone to exhibit efficiency in generating specific cell lineages. There are several approaches to address these challenges, such as the generation of HLA haplotype banks of iPSCs, the HLA cloaking approach or the “priming” of PSCs (Yamanaka 2020). Moreover, it is expensive to generate and use iPSCs which may limit their accessibility for patients who could not afford such therapies (Doss & Sachinidis 2019).

In conclusion, iPSC-based therapies hold great promise for the treatment of a wide range of diseases and disorders, and ongoing research in this field is expected to lead to the development of new and innovative treatments in the years to come.

2. Hematopoiesis and Hematopoietic Stem Cells

2.1. Definitions

In mammals, 100 to 1000 billion new blood cells are generated each day in the bone marrow (BM) to replace the senescent cells and maintain the number of circulating cells constant throughout the life of the individual (Ogawa 1993). This constant and tightly regulated process is ensured by the activity of a very rare subset of stem cells called hematopoietic stem cells (HSCs). HSCs are multipotent cells therefore they have the capacity of self-renewal and generate offspring of increasingly differentiated cells with specific functional activities. This mechanism of differentiation is called hematopoiesis and it can generate all the cellular constituents of the blood. This represents more than ten distinct mature cell types including red blood cells (erythrocytes), megakaryocytes, myeloid cells (monocytes/macrophages and granulocytes), dendritic cells (DCs), B and T lymphocytes as well as natural killer cells (NKs) cells (Weissman 2000). Cell surface marker phenotype analysis by flow-cytometry has been used to identify and isolate discrete sub-populations of developing blood cells, suggesting a hierarchical structure in hematopoietic development in which multi-potency is progressively restricted (**Figure 4**). Four compartments can be described:

- **Multipotent stem cells** are capable of self-renewal and differentiation in all hematopoietic lineages (e.g., HSC).
- **Primitive progenitor cells** are mostly committed to a hematopoietic lineage. They are capable of proliferation and differentiation without the possibility of self-renewal. For example, the Common Myeloid Progenitor (CMP) or the Common Lymphoid Progenitor (CLP).
- **Committed precursor cells** represent the end of differentiation with limited proliferative capacity. For instance, megakaryocyte–erythroid progenitor (MEPs), granulocytes and macrophages progenitor (GM), bipotent T/NK progenitor (TNK) and B-Cell precursor (BCP).
- **Lineage committed cells** are mature, differentiated, and functional cells with a limited life span (NK, DCs, monocytes/macrophages, erythrocytes, …).

a

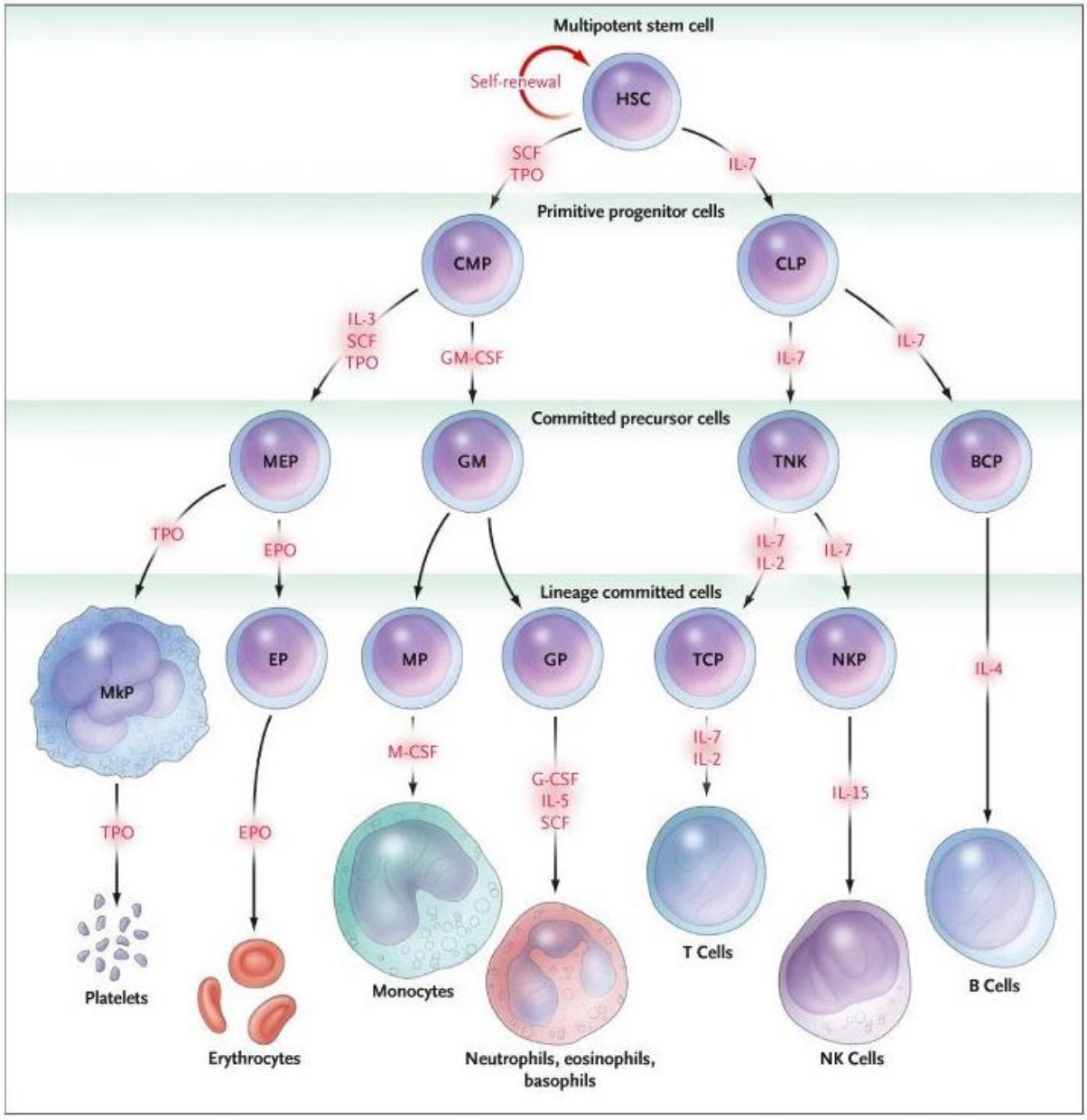

Figure 4: Classical model of hematopoiesis*. Hematopoietic stem cells (HSCs) are multipotent stem cells, which differentiate towards primitive progenitors such as the common myeloid progenitor (CMP) and the common lymphoid progenitor (CLP). These oligopotent progenitors give rise committed precursor cells including megakaryocyte–erythroid progenitor (MEPs), granulocytes and macrophages progenitor (GM), bipotent T/NK progenitor (TNK) and B-Cell precursor (BCP). Collectively, these progenitors give rise to all the lineage-committed cells of the hematopoietic system: Progenitors for megakaryocytes (MkP), erythrocytes (EP), monocytes (MP), granulocytes (GP), T cells (TCP), NK cells (NKP) and B cells (BCP) (Kaushansky 2006).*

2.2. Hematopoietic Stem Cells (HSCs)

Beside their major characteristics of long-term and lifelong self-renewal, HSCs can undergo terminal differentiation towards all blood cell types, including red blood cells, white blood cells, and platelets. In adult, they are found exclusively in the BM. Additionally, they can be obtained from umbilical cord blood (UCB) and peripheral blood for the purpose of transplantation, following mobilization through the administration of growth factors. HSCs are unique in that they can self-renew,

meaning they can divide and produce more HSCs, or differentiate into progenitor cells that can further differentiate into diverse types of blood cells. HSCs play a crucial role in maintaining the body's immune system and are therefore important in treating a wide range of diseases, such as leukemia, lymphoma, and other blood disorders.

2.2.1. Historical discovery of the HSC

The existence of HSCs was initially demonstrated by Till and McCulloch in 1963 through their groundbreaking experiment conducted in mice (Becker et al. 1963). In this study, they transplanted mouse BM cells into irradiated recipient mice and, instead of waiting for long-term reconstitution, mice were sacrificed at day +10. This approach allowed them to identify distinct individual spleen colonies. They dissected and analyzed these individual spleen colonies cytologically, and revealed the presence of various cell lineages, including erythroid, granulocytic, and megakaryocytic cells. These findings provided evidence that a single stem cell can give rise to these differentiated hematopoietic cells within the context of clonogenic growth. Some spleen colonies were capable of being transferred to secondary hosts and subsequently reconstituting all blood cell lineages (Siminovitch et al. 1963). These specific stem cells were named colony-forming unit-spleen (CFU-S). These experiments introduced the two defining criteria of stem cells: self-renewal and multipotency (Wu et al. 1968). In 1988, with the combination of monoclonal antibodies and multi-color Fluorescence Activated Cell Sorting (FACS), the purification of hematopoietic stem cells from mouse BM became possible. The mouse HSCs had a Thy-1^{low} Lin^{-} (Lineage-markers) Sca-1^{+} c-Kit^{+} phenotype (LSK) and account for 0.05% of the total BM cells (Muller-Sieburg et al. 1986; Spangrude et al. 1988). In 1994, the HSC population was separated into at least 3 multipotent populations: Long-Term (LT)-HSCs, Short-Term (ST)-HSCs, and Multi-Potent Progenitors (MPP, progenitors without the self-renewal capacity of HSCs) (Morrison & Weissman 1994). The LT subset keeps its self-renewal capacity throughout the life of the mouse while the ST subset self-renews for only 8 weeks. In 1996, HSC transplants from adult mouse BM to a previously irradiated host have shown that a single HSC can reconstitute an individual's hematopoietic system (Osawa et al. 1996).

The first clues to the existence of HSC in humans have been obtained by the analysis of leukemic hematopoiesis using X-linked clonality markers in chronic myeloid leukemia (Fialkow et al. 1967). With the development of FACS technology, similar techniques to those used for mouse HSCs have been employed to isolate human HSCs i.e., isolation of cells according to their cell-surface marker and subsequent functional assays. Their capacity for long-term reconstitution was evaluated using xenotransplantation models (McCune et al. 1988). Human hematopoiesis is very close to the mouse model although the surface markers used to characterize the progenitors are significantly different. Historically, the surface marker used to study human HSCs was CD34 (cluster of differentiation), a

ligand for L-selectin. $CD34^+$ population is heterogenous but contains all the stem cell activity in the BM (DiGiusto et al. 1994). Most of the $CD34^+$ cells co-express CD38 but only the $CD38^-$ fraction can generate multi-lineage colonies in immune-deficient mice (Huang & Terstappen 1994; Bhatia et al. 1997). Baum et al showed that the presence of the surface marker CD90 (Thy-1) as well as the absence of surface marker of hematopoietic commitment (Lin^-) in $CD34^+$ cells can generate colonies both *in vitro* and *in vivo* (Baum et al. 1992; Miller et al. 1999). Moreover, all $CD34^+$ $CD90^+$ Lin^- cells reside in the $CD38^-$ fraction. These studies show the human HSCs population is enriched in Lin^- $CD34^+$ $CD38^-$ $CD90^+$. Markers of human HSCs will be described in detail in the upcoming section **2.2.3.1 Markers of HSCs.**

2.2.2. Ontogeny of HSCs

HSCs are generated during embryonic development as indicated by their presence in UCB within three successive waves of hematopoiesis. The primitive wave of hematopoiesis appears in the yolk sac (YS) and produces transitory primitive blood cells. A second wave from the YS generates lympho-myeloid progenitors (LMPs) and erythro-myeloid progenitors (EMPs). Then, the definitive waves of hematopoiesis, occurring in the aorta-gonad-mesonephros (AGM) region, progressively colonize the fetal liver, the spleen, and finally the bone marrow which is the site of adult hematopoiesis (Demirci et al. 2020).

2.2.2.1. The primitive wave of hematopoiesis

The primitive wave of hematopoiesis in mammals is the earliest stage of blood cell production in developing animals. It occurs in the YS from the blood islands during the earliest stages of development, at embryonic day E7.25 in the mouse and at 3-4 weeks in humans (Haar & Ackerman 1971). During this stage, a group of cells called hemangioblasts give rise to two types of cells: HSCs and endothelial cells, which form the lining of blood vessels (Choi 2002; Kennedy et al. 2007). The HSCs produced during the primitive wave of hematopoiesis are called primitive HSCs. Primitive HSCs differentiate into primitive erythroblasts which are larger and expressing embryonic hemoglobin (Ferkowicz et al. 2003), primitive megakaryocytes, and primitive macrophages (**Figure 5**). At E8.5, with the establishment of the blood circulation system, primitive cells start to circulate into the embryo to distribute nutrients and oxygen to the developing organs. They also assure the first irrigation and immune defense of the embryo (Palis et al. 2010). Primitive cells of the three-blood lineage rapidly mature, losing their ability to proliferate and remain in the neonatal blood for only a few days after birth (Kingsley et al. 2004).

2.2.2.2. The transient second wave of hematopoiesis

The transient second wave of hematopoiesis also occurs in the YS. It originates from another subset of endothelial cells called hemogenic endothelium (HE) after their conversion into hematopoietic cells. During this process, erythro-myeloid progenitors (EMP) are generated and

expanded in number. Afterward, they seed the fetal liver and generate definitive erythroid, macrophages, megakaryocytes, neutrophils, and mastocytes (**Figure 5**) (Frame et al. 2013). The second wave generates the first mature blood cells and committed progenitors within an HSC-independent process. It also provides long-lasting self-renewing population of macrophages in multiple adult organs (microglia in the brain, Langerhans cells in the skin, Kupffer cells in the liver, and alveolar macrophages in the lungs) (Hoeffel & Ginhoux 2015). The first and second waves are essential to sustain the survival of the embryo until AGM-derived HSC emergence, engraftment, and expansion during the third wave (McGrath et al. 2015).

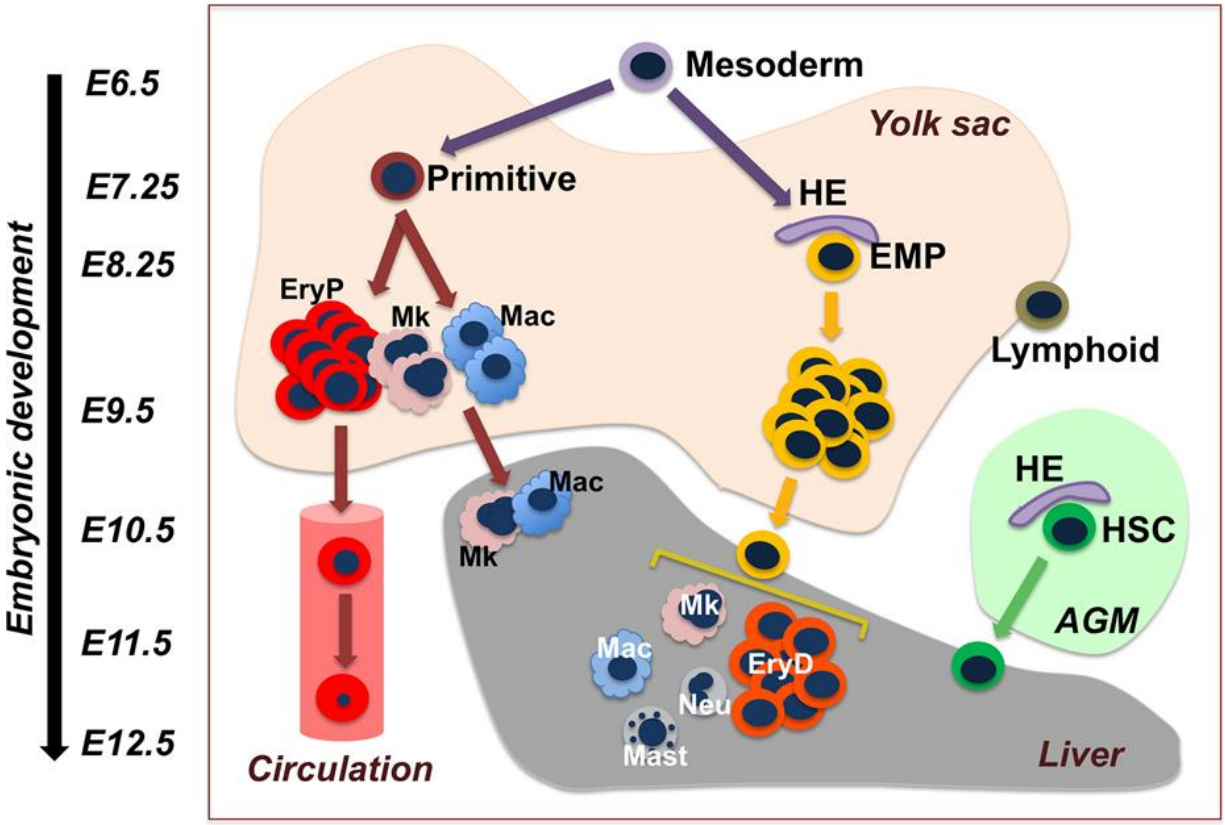

Figure 5: Model of hematopoietic ontogeny during mouse embryonic development*. The process begins with HSC-independent hematopoiesis involving two waves of hematopoietic progenitors originating in the yolk sac. The first wave, or "primitive" wave, gives rise to primitive erythroid (EryP), megakaryocyte (Mk), and macrophage lineages (Mac). The second wave, referred to as the "erythro-myeloid progenitor" (EMP) wave, generates definitive erythroid (EryD), megakaryocyte, macrophage, neutrophil (Neu), and mast cell lineages (Mast). Finally, during the third wave, HSCs emerge from the aorta in the aorta-gonad-mesonephros (AGM) region. Both EMP and HSC arise from hemogenic endothelium (HE). (Palis 2016).*

2.2.2.3. The third and definitive wave of hematopoiesis

The third and last wave of hematopoiesis originates from specialized embryonic vascular cells also called HE cells but in the aorta-gonad-mesonephros (AGM) region at E11, or 5-week human embryo (Tavian et al. 1996). These cells will undergo a trans-differentiation process called endothelial-to-hematopoietic transition (EHT) where they give rise to a bulging structure and emerge from the ventral domain of the human dorsal aorta in the AGM region (Ivanovs et al. 2014). At this stage, HSCs have

robust long-term multilineage reconstitution potential and extreme proliferation capacity. These HSCs then migrate via circulation to the fetal liver, where they continue to differentiate and give rise to the various blood cell lineages necessary to support the growing embryo (Christensen et al. 2004). It makes the fetal liver the main hematopoietic organ during the sixth and seventh post-conception week in humans. Finally, HSCs will initiate a migration and seed the BM via an active recruitment mechanism involving the CXCL12 (SDF-1) chemokine receptor CXCR4 (Ma et al. 1998). The BM will become the primary site of hematopoiesis after birth (Crisan & Dzierzak 2016).

2.2.2.4. Regulation of HSCs ontology

HSCs ontology is controlled by a variety of intrinsic mechanisms, including transcription factors and signaling pathways. Transcription factors such as RUNX1 or GATA-2 and signaling pathways such as Notch are critical for regulating the emergence, proliferation, differentiation, and survival of hematopoietic stem progenitor cells (HSPCs) during embryonic hematopoiesis.

The role of RUNX1 in hematopoietic development has been studied extensively, and it has been shown to be essential for definitive hematopoiesis (Yzaguirre et al. 2017). Its expression in HE is necessary for the generation of HSCs during EHT (Chen et al. 2009). Indeed, *RUNX1* deletion with endothelial-specific Cre-recombinase resulted in complete loss of definitive hematopoiesis and the embryonic death by E13.5. In the endothelial cells, RUNX1 is activated by Notch signaling (Burns et al. 2005) and interacts with other transcription factors such as GATA2 for inducing the expression of key hematopoietic genes such as TAL-1/SCL, and LMO2 (Nottingham et al. 2007; Lichtinger et al. 2012).

TAL-1/SCL protein is a transcription factor belonging to the basic helix-loop-helix (bHLH) family which regulates the blood formation and the multipotency of HSC (Shivdasani et al. 1995; Vagapova et al. 2018). The TAL-1/SCL complex needs LMO2 during the HE stage to locate regulatory elements that are crucial for the establishment of the hematopoietic developmental program. When LMO2 is absent, TAL-1/SCL encounters difficulties to recognize its target sites resulting in impaired gene expression (Stanulović et al. 2017).

GATA2 is initially expressed in the HE after being activated by both RUNX1 and Notch signaling (Robert-Moreno et al. 2005). GATA2 is required for HSC generation because specific deletion results in deficiency of long-term repopulating HSCs (de Pater et al. 2013). It has been shown that RUNX1 and GATA2 could serve redundant roles for HSC production ensuring this critical function in case of failure of one or the other (Bresciani et al. 2021).

At a cellular level, the HE cells express vascular-endothelial cadherin (VE-cadherin) (Taoudi et al. 2008). The Notch induction of the transcription factor RUNX1 and the subsequent proteins described

above will lead to the conversion of endothelial cells to hematopoietic cells expressing hematopoietic markers such as CD41, CD43, and CD45 during EHT (**Figure 6**) (Rybtsov et al. 2011).

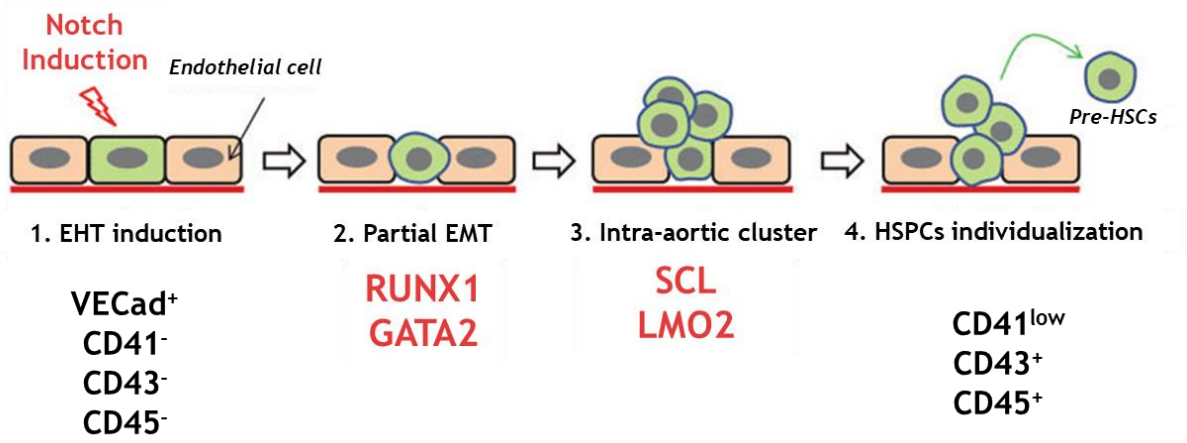

Figure 6: A simplified scheme of the sequential step of HSC ontogeny. *HSCs originate from a precursor that expresses genes associated with endothelial cells, known as hemogenic endothelium (HE). HE undergoes a transition from an endothelial to a hematopoietic state, called endothelial hematopoietic transition (EHT). During this process, there is a precise regulation of genes initiated by Notch induction. The expression of key players during EHT, including RUNX1 and GATA2, is responsible for the epithelial-mesenchymal transition (EMT). During this process, hematopoietic markers such as CD41, CD43, and CD45 are upregulated. (Adapted from Kim et al. 2013; Hamidi & Sheng 2018).*

HSCs ontology can be summarized by three main steps: first the generation of HSCs from the HE, then the expansion inside the fetal liver and finally the maturation and differentiation of HSCs inside the adult BM.

2.2.3. Adult HSCs

Adult HSCs must be capable of self-renewal to maintain the existing pool of HSCs generated at birth, as well as to maintain the appropriate amount of functional mature blood cells throughout life.

2.2.3.1. Markers of HSCs

Adult human HSCs are characterized by the expression of specific cellular markers that distinguish them from other cell types. As described previously, the identification and isolation of HSCs rely on the detection of these markers. The selection of specific markers may vary depending on the research protocol, the source of HSCs (BM, UCB, peripheral blood), and the intended application.

NB: In the context of HSCs, "Lin^-" refers to a population of cells lacking lineage-specific markers (mature blood cell markers) which is used as a criteria to enrich for HSCs.

- **CD34,** the marker historically associated with human HSCs, was initially reported in 1984 (Civin et al. 1984). It is a cell surface glycoprotein involved in cell-cell adhesion and acting as a ligand for the L-selectin (Baumheter et al. 1993). CD34 may facilitate the attachment of hematopoietic stem cells to the extracellular matrix of the BM or directly to stromal cells. It is

expressed by all the stem cells in the BM as well as other progenitor cells in peripheral blood, and UCB (DiGiusto et al. 1994). In clinical settings, CD34 is closely associated with the selection and enrichment of HSCs for BM transplantation. CD34 is not exclusive to HSCs and is expressed by various other cell types such as endothelial cells, epithelial progenitors, fibrocytes, keratocytes, and muscle satellite cells (Sidney et al. 2014). Therefore, additional markers are required to fully characterize HSCs.

- **CD38,** also known as cyclic ADP-ribose hydrolase, is a transmembrane protein expressed on various lymphoid cells, including $CD4^+$, $CD8^+$, B lymphocytes, and NK cells (Kung et al. 1979). In the context of HSCs, low or negative levels of CD38 expression are often associated with the most primitive and undifferentiated HSCs population. Indeed, it has been observed that only the fraction lacking CD38 ($CD38^-$) can generate multi-lineage colonies in immune-deficient mice (Huang & Terstappen 1994; Bhatia et al. 1997). Therefore, CD38 is frequently employed as a marker to identify LT-HSCs with high self-renewal potential (Hao et al. 1995).
- **CD90,** also known as Thy-1, is a glycosylphosphatidylinositol (GPI) anchored protein found on the surface of various cell types, including human HSCs. It is a positive marker used for the enrichment and identification of HSC populations. CD90 expression has been associated with primitive hematopoietic stem and progenitor cells, including those with high repopulating potential. (Baum et al. 1992; Miller et al. 1999). Previous studies suggested that CD90 plays a role in maintaining quiescence in stem cells, thereby improving their functionality (Mayani & Lansdorp 1994).
- **CD45RA** is a specific isoform of the CD45 protein, which is a tyrosine phosphatase found on the surface of leukocytes. The $CD90^+$ $CD45RA^-$ subpopulation was found to contain HSCs capable of long-term engraftment and successful secondary transplantation whereas the $CD90^-$ $CD45RA^-$ subpopulation was identified as candidate for MPPs, exhibiting reduced and incomplete self-renewal capacity (Majeti et al. 2007). The study also revealed a hierarchical relationship among the subpopulations, with $CD90^+CD45RA^-$ cells positioned upstream of $CD90^-CD45RA^-$ cells.
- **CD49f** is an integrin subunit (Integrin Subunit Alpha 6, ITAG6) expressed on the surface of human HSCs and it is involved in cell adhesion and signaling. It has been suggested to mark a subpopulation of HSCs with enhanced long-term multilineage grafts potential and self-renewal capacity (Notta et al. 2011). Combination of CD49f with other markers such as $CD34^+CD38^-CD45RA^-CD90^+$ enhances the enrichment of HSC isolation in terms of purity. Contrariwise, low CD49f expression characterizes a subtype of hematopoietic progenitor cells

with transient engrafting activity. Gene expression analysis confirmed that CD49f^{high} cells represent HSCs, while CD49f^{low} cells are erythroid-biased HPCs (Xu et al. 2019).

These markers allow for the separation of the HSC pool into three subsets based on their pluripotency capacity (**Figure 7**):

- **LT-HSCs** (Long Term HSCs) are identified by the marker profile including Lin$^-$ CD34$^+$ CD38$^-$ CD90+ CD45RA$^-$ CD49f$^+$. They possess self-renewal and differentiation capabilities for all mature blood cell types over an extended period. LT-HSCs are quiescent and contribute to the replenishment of the ST-HSC pool.
- **ST-HSCs** (Short-Term HSCs) are characterized by Lin$^-$ CD34$^+$ CD38$^-$ CD90$^+$ CD45RA$^-$ CD49f$^-$, exhibiting a more limited capacity for self-renewal and differentiation compared to LT-HSCs. They represent an intermediate state between LT-HSCs and committed progenitor cells, playing a crucial role in replenishing progenitor cells, and maintaining hematopoietic system balance.
- **MPPs** (Multipotent Progenitor Cells) are downstream of HSCs and have a more restricted differentiation potential. Their marker profile is Lin$^-$ CD34$^+$ CD38$^-$ CD90$^-$ CD45RA$^-$ CD49f$^-$. MPPs serve as an intermediate stage between HSCs and committed progenitor cells in terms of lineage commitment. While MPPs have lost some self-renewal capacity, they are more committed to specific hematopoietic lineages.

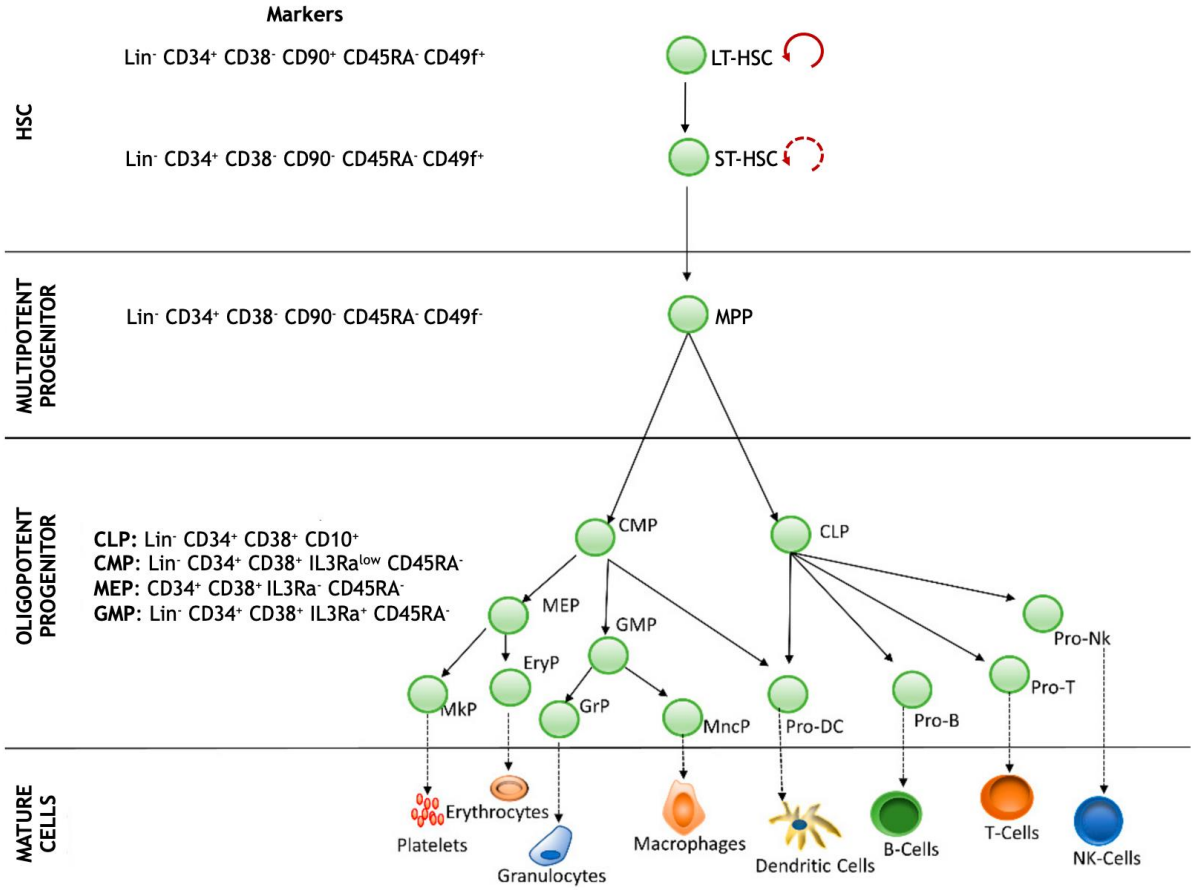

Figure 7: Cellular markers of the human hematopoiesis hierarchy. *LT-HSC: Long Term-HSCs; ST-HSC: Short Term-HSC; MPP: Multipotent Progenitor; OPP: Oligopotent Progenitor; Common Lymphoid Progenitor (CLP); Common Myeloid Progenitor (CMP); Megakaryocyte-Erythrocyte Progenitor (MEP); Granulocyte-Macrophage Progenitor (GMP). Restricted lineage progenitor cells: Megakaryocyte Progenitor (MkP); Erythrocytic Progenitor (EryP); Granulocytic Progenitor (GrP); Monocyte Progenitor (MncP); Dendritic Progenitor Cell (Pro DC); Progenitor Cell-T (Pro-T); Progenitor Cell-B (Pro-B); Progenitor Cell-Nk (Pro-Nk). (Adapted from Ribeiro-Filho et al. 2019).*

More recently, several other markers of HSCs have been identified. For example, the transmembrane protein CD201, also called Endothelial Protein C Receptor (EPCR). Studies have indicated that EPCR$^+$ HSCs occupy a top position in the hematopoietic hierarchy and can give rise to all the HSC populations observed upon transplantation (Anjos-Afonso et al. 2022; Vanuytsel et al. 2022).

2.2.3.2. Functional assessment methods for HSCs

As discussed previously, HSCs are characterized by their unique properties of self-renewal and multilineage differentiation potential. After their isolation and characterization based on their specific cellular markers, their functional capabilities must be evaluated by various assays.

The transplantation assay serves as the gold standard test for evaluating HSC function. By transplanting HSCs isolated from a donor into an irradiated recipient mouse, it is possible to assess their capacity for long-term engraftment and hematopoietic reconstitution (Weissman & Shizuru 2008). Indeed, only multipotent HSCs possess the capacity to restore the entire hematopoietic system in irradiated recipients and sustain long-term survival. Transplantation assays are often associated with

limiting dilution assay which involves diluting HSCs to different concentrations before transplantation (Szilvassy et al. 1990). This protocol allows the estimation of the frequency of functional HSCs from the donor and provides a precise quantification.

A version of this assay has been developed for human HSCs by the group of John Dick in Toronto using NOD/SCID mice (non-obese diabetic/ severe combined immunodeficiency) (Bhatia et al. 1998). NOD/SCID mice are used as recipient strains due to their immunodeficient nature, which allows successful engraftment of human HSCs without rejection. In this assay, purified HSCs obtained from the BM or PBMC of human donors are transplanted into the BM or the bloodstream of the SCID/NOD mice. This allows the HSCs to establish and regenerate a fully functional human hematopoietic system. The objective of the SCID/NOD repopulating assay is to assess the self-renewal and differentiation capabilities of HSCs into various blood cell lineages (e.g., T cells, B cells, myeloid cells, etc.). The engraftment and repopulation process are closely monitored over a period of weeks to months using techniques like flow cytometry, immunohistochemistry, and other molecular and cellular analyses. In certain cases, the assay may extend for several months or more to evaluate the long-term repopulating potential of the transplanted HSCs.

LT-HSCs are typically defined by stable multilineage reconstitution that persists for more than 4 months post-transplantation. The method for identifying LT-HSCs is serial transplantation, where donor cells from a primary recipient are transplanted into a secondary irradiated recipient (Iscove & Nawa 1997). Only LT-HSCs can reconstitute both primary and secondary recipients whereas ST-HSCs can only sustain primary reconstitution for approximately 4 months and fail to reconstitute secondary recipients, indicating limited self-renewal potential.

There are also *in vitro* assays for evaluating the multilineage potential of HSCs. In the Colony-forming unit (CFU) assays, hematopoietic cells originating from BM or blood are cultured in semisolid media that support the growth and differentiation of hematopoietic progenitor cells (Siminovitch et al. 1963). The proliferation and differentiation ability of individual cells can be evaluated by observing the colonies formed by each progenitor cell. The colonies, consisting of differentiated cells such as erythroid, myeloid, and lymphoid, are counted and analyzed after a culture period of about 14 days. The long-term culture-initiating cell (LTC-IC) assay consists in culturing HSCs in conditions that mimic the BM microenvironment. The first experiment demonstrating the requirement of stromal cells were provided by the experiments of Suda and Dexter both in mouse and humans (Suda & Dexter 1981). A quantitative version of this assay was first developed at the Terry Fox Laboratory by the team of Connie Eaves and represents the only *in vitro* test to detect and quantify primitive HSC in humans (Sutherland et al. 1989). This assay has been later extensively used to analyze hematopoietic potential of single

cells (Verfaillie & Miller 1995). The culture conditions include the presence of horse serum, hydrocortisone and supportive stromal cells such as MS-5 providing signals necessary for HSCs maintenance and differentiation. After 5 weeks of culture with weekly half-medium changes, the most clonogenic and differentiated cells are discarded from the culture and the remaining clonogenic cells are evaluated by performing CFC assays in both adherent and non-adherent fractions. The colonies observed in CFUs are therefore the progeny of long-term persisting HSCs, as ST-HSCs present initially would have already completed their differentiation process and eliminated by half-medium changes and would no longer form colonies.

2.2.3.1. Challenges of the classical hierarchical model

The traditional model of hematopoiesis, characterized by discrete bifurcating cell-fate decisions and relatively homogeneous progenitor stages, has been a guiding framework in hematopoietic research.

However, recent research has revealed that this model does not fully capture the complexity of hematopoietic stem and progenitor populations (Müller-Sieburg et al. 2002; Morita et al. 2010; Yamamoto et al. 2013). These studies have shown that HSCs and progenitors are in fact heterogeneous. Most HSCs exhibit a lineage-biased output rather than producing balanced lineages. Lineage tracing experiments using different strategies have demonstrated the extent of this heterogeneity (Naik et al. 2013; Sun et al. 2014). For example, these experiments have shown that megakaryocytes can be directly generated from HSCs (Rodriguez-Fraticelli et al. 2018).

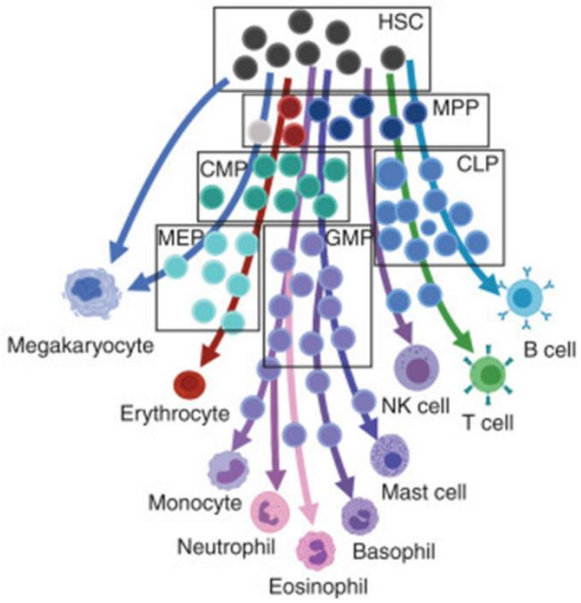

Figure 8: The model of continuous differentiation. *The boxes represent various progenitor states identifiable through phenotypic markers, highlighting the diversity within each of these populations. These include MPP (multipotent progenitor), CMP (common myeloid progenitor), CLP (common lymphoid progenitor), MEP (megakaryocyte-erythroid progenitor), and GMP (granulocyte-macrophage progenitor) (From Olson et al. 2020).*

Single-cell technologies have further illuminated these findings by showing that hematopoietic cells acquire lineage-specific characteristics along a continuous spectrum (Nestorowa et al. 2016; Velten et al. 2017). This challenges the traditional tree-like model of hematopoiesis, suggesting that differentiation trajectories may be established early in development (**Figure 8**). In summary, the traditional hematopoietic model, characterized by discrete cell-fate decisions and uniform progenitor stages, is evolving into a more intricate comprehension of hematopoietic differentiation. This emerging perspective portrays hematopoiesis as a continuous process shaped by initial lineage preferences (Laurenti & Göttgens 2018).

2.2.4. Control of self-renewal and differentiation of adult HSCs

2.2.4.1. Regulatory factors influencing HSCs quiescence and activation

HSCs are mostly quiescent or dormant, meaning they are in a state of low metabolic activity and are not actively dividing (Rumman et al. 2015). By remaining in a quiescent state, HSCs are able to preserve their genomic integrity and avoid accumulating DNA damage. Moreover, HSCs in the G0 phase of the cell cycle have a very slow metabolism and a greater capacity for long-term reconstitution than HSCs in the cycle (Passegué et al. 2005). Quiescent HSCs can also respond to environmental cues and signals. According to the need of the organism (blood loss, infection, injury...), HSCs can be activated to proliferate and differentiate into the necessary cell types. This process is tightly regulated and involves the interaction of various signaling molecules and factors that influence HSCs behavior (**Figure 9**). Several examples are presented below:

- **Cell cycle regulators** such as cyclin-dependent kinase inhibitors (CKIs) suppress the activity of cyclin-dependent kinases (CDKs) and prevent HSCs from progressing through the cell cycle (Sherr & Roberts 1999). For example, absence of $p21^{Cip1}$ (CDK2 and CDK4 inhibitor) increases cell cycling thus HSCs proliferation but it leads to stem cell exhaustion and compromised stemness. (Cheng et al. 2000). Moreover, combined deficiency of $p27^{Kip1}$ and $p57^{Kip2}$ in HSCs reduces bone marrow reconstitution ability by increasing their proliferation (Zou et al. 2011).
- **Transcription factors** play a key role in regulating the self-renewal and differentiation capacity of HSCs. One example is GATA3, which is required for the maintenance of HSCs in a quiescent state (Ku et al. 2012). Another transcription factor, FOXO3A, has been shown, in a *Foxo3a*$^{-/-}$ mouse model, to promote HSC quiescence by inhibiting cell cycle progression and inducing the expression of cell cycle inhibitors such as $p27^{Kip1}$ and $p21^{Cip1}$ (Miyamoto et al. 2007; Du et al. 2016). The last example is C/EBPα, a transcription factor that regulates the differentiation of HSCs into more mature blood cell types. It promotes myeloid differentiation and suppresses HSC self-renewal. Loss of C/EBPα leads to the expansion of HSCs and the depletion of more mature blood cell types (Ye et al. 2013; Ohlsson et al. 2016).

- **Signaling pathways** are involved in regulating HSC quiescence, including the Notch, Wnt, and PI3K/AKT pathways. Notch signaling promotes HSC quiescence by upregulating the expression of CKIs such as $p21^{Cip1}$ and $p57^{Kip2}$, which prevent HSCs from entering the cell cycle. Loss of Notch signaling increases HSCs differentiation and depletion *in vivo* (Duncan et al. 2005). The inhibition of Wnt pathway results in a loss of HSC quiescence while its activation by Wnt ligands promotes HSC self-renewal. Wnt signaling could be mediated by the regulation of p21 (Reya et al. 2003; Fleming et al. 2008). Finally, the PI3K/AKT pathway is involved in regulating cell growth and survival. Activation of this pathway can induce HSC proliferation and differentiation. When the PI3K/AKT pathway is activated, FOXO proteins (like FOXOA3) are phosphorylated and excluded from the nucleus, leading to a decrease in CDKi expression and an increase in HSC proliferation (Tothova et al. 2007).
- **The metabolic state** of HSCs plays an important role in regulating their quiescent state. HSCs have low metabolic activity and rely on oxidative phosphorylation and anaerobic glycolysis for energy production (Morganti et al. 2022). Alterations in metabolism, such as the switch to glycolysis, can lead to the activation and proliferation of HSCs. For example, activation of the PI3K/AKT pathway can promote aerobic glycolysis and increase HSC metabolism, which in turn can stimulate HSC proliferation and differentiation. Conversely, inhibition of the PI3K/AKT pathway can promote oxidative phosphorylation and decrease HSC metabolism, leading to enhanced HSC quiescence and self-renewal (Juntilla et al. 2010).
- **Epigenetic regulators** control gene expression by modifying DNA and histone proteins. One example of an epigenetic regulator involved in regulating HSC quiescence is Polycomb group proteins, which suppress the expression of genes involved in cell cycle progression and promote HSC quiescence (Lu et al. 2018).
- **Growth factors and cytokines** are produced by other cells in the BM microenvironment and act on HSCs to promote their survival, proliferation, and differentiation. For instance, stem cell factor (SCF) and thrombopoietin (TPO) are growth factors that promote the survival and proliferation of HSCs (Carver-Moore et al. 1996; Broudy 1997), while interleukin-6 (IL-6) and granulocyte-macrophage colony-stimulating factor (GM-CSF) promote the differentiation of HSCs into the myeloid lineage (Liu et al. 1997). Another key chemokine is CXCL12 (SDF-1) which is required for HSC maintenance and HSC retention in the BM (Ara et al. 2003; Sugiyama et al. 2006). Other cytokines, such as vascular endothelial growth factor (VEGF), promote the expansion and differentiation of HSCs and progenitor cells by regulating the proliferation and survival of endothelial cells (Gerber et al. 2002). Bone morphogenetic protein (BMP) signaling is necessary to maintain functional adult HSCs *in vivo* as its absence is linked with a significant

reduction in the number of HSCs. Moreover, serial transplantation experiments demonstrated that BMP4-deficient recipients had a defect in their microenvironment (Goldman et al. 2009).

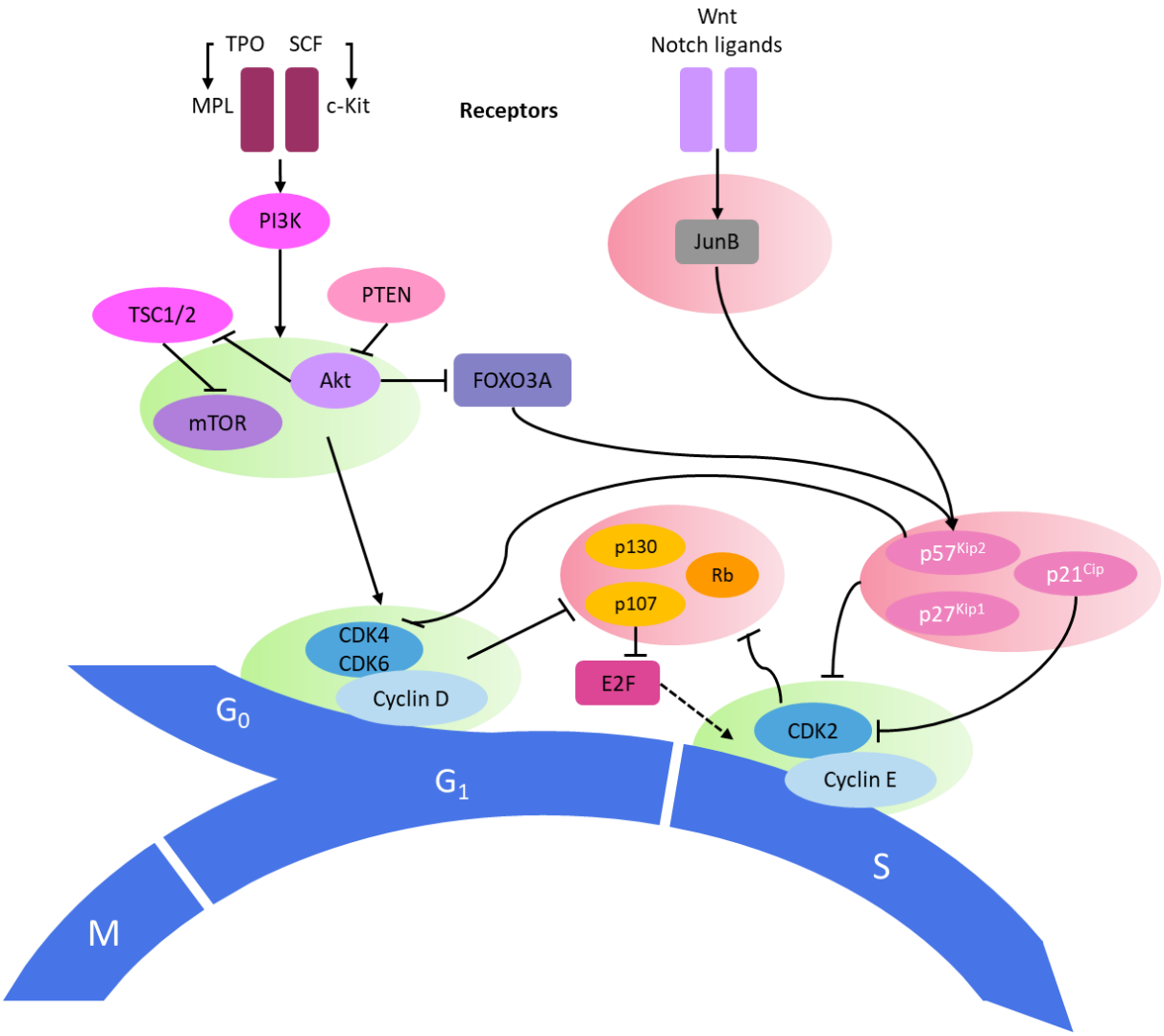

***Figure 9: Cell cycle regulation of HSCs**. The entry of quiescent HSCs from the G0 phase into the G1 phase of the cell cycle is regulated by a complex network of factors. This regulation involves a balance between activating and inhibitory mechanisms that control the activity of cyclin–CDK complexes. Activation of the PI3K/AKT/mTOR pathway a central role in promoting HSC cell cycle activity by activating the cyclin D–CDK4/6 complex. Transition from the G1 to the S phase of the cell cycle is regulated by the Cyclin E–CDK2 complex. Its activity is modulated by the CIP/KIP family of CDK inhibitors and the Rb family. The expression of CIP/KIP family members is regulated by transcription factors like JunB, and FOXO3A, which are activated by external signals that repress cell growth. Functionally related groups of cell cycle activators are shaded in green, while functionally related groups of cell cycle inhibitors are shaded in pink. (adapted from Pietras et al. 2011).*

2.2.4.2. Regulation of hematopoiesis by receptor tyrosine kinases (RTKs)

Receptor tyrosine kinases (RTKs) are known to play a crucial role in the regulation of hematopoiesis. RTKs are a family of cell surface receptors that transmit signals from extracellular growth factors and cytokines to intracellular signaling pathways. RTKs participate in the maintenance, proliferation, differentiation, and survival of HSCs and progenitor cells (Reilly 2003; Fares et al. 2022).

2.2.4.2.1. Importance of RTKs for hematopoietic regulation

One prominent RTK involved in hematopoiesis is the receptor for SCF, known as c-Kit or CD117 (Yarden et al. 1987). Binding of SCF to c-Kit activates downstream signaling pathways such as RAS/MAPK, PI3K/AKT, and JAK/STAT, which regulate the self-renewal and survival of HSCs, as well as the differentiation of hematopoietic progenitors into various blood cell lineages (**Figure 9**) (Linnekin 1999). Disruptions in c-Kit signaling can lead to hematopoietic disorders, including impaired HSCs function and abnormal blood cell development (Gari et al. 1999; Cairoli et al. 2003).

Another essential RTK in hematopoiesis is the receptor for TPO, known as MPL. In addition to its role in HSC regulation, TPO-MPL signaling is crucial for the maintenance and expansion of megakaryocyte-erythroid progenitors and the production of platelets and red blood cells (**Figure 9**) (Besancenot et al. 2014). Activation of MPL triggers signaling pathways such as JAK/STAT and PI3K/AKT, which regulate cell survival, proliferation, and differentiation in the megakaryocytic and erythroid lineages (Miyakawa et al. 2001).

Other RTKs, such as FLT3 and Flt3-like receptor, also contribute to hematopoiesis by modulating the development of specific blood cell lineages and regulating the balance between self-renewal and differentiation of hematopoietic progenitor cells (Rosnet et al. 1993).

2.2.4.2.2. Role of the RET RTK during hematopoiesis

RET (REarranged during Transfection) is an RTK that transmits a proliferative signal in the presence of its co-receptor GFR-alpha (GFRα1) and in response to GDNF family ligands (GFLs). As a RTKs, RET regulates various downstream signaling pathways, including JAK/STAT, PI3K/AKT and ERK (Mulligan 2014). Its roles and function will be described in detail in the chapter dedicated to the RET protein (see **3. The RET proto-oncogene**).

RET is expressed by human HSCs derived from UCB, with a notable enrichment in the $CD49f^{+}$ population (Grey et al. 2020). It is also known to be expressed in intermediate mature myeloid cells and in acute myeloid leukemia (Gattei et al. 1997; Nakayama et al. 1999).

Previous investigations have provided evidence suggesting the importance of RET in the generation and expansion of HSCs. Notably, RET has been identified as a critical factor in the development of hematopoietic potential in mice, emphasizing its role in HSC development (Fonseca-Pereira et al. 2014). The neurotrophic GFLs that partner with RET are produced within the HSCs environment and contribute to the stimulation of HSCs survival, expansion, and functionality. Disruption of RET through null mutation results in the loss of important survival cues provided by Bcl2 and Bcl2l1.

Another study shows that the provision of GDNF/GFRα1 plays a crucial role in maintaining UCB-derived HSC potential *in vitro* (Grey et al. 2020). The activation of RET signaling pathway in these cells reveals an anti-apoptotic and anti-inflammatory program, leading to enhanced survival and expansion of UCB-derived HSCs. Moreover, the stimulation of RET signaling has been shown to reduce the accumulation of ROS in HSCs, preserving their potency, and promoting further expansion *in vitro.* These findings suggest that by augmenting RET activation, the signaling cascades involved in HSCs function can be strengthened and diversified, resulting in improved HSC performance.

Overall, RTKs play diverse roles in hematopoiesis, acting as critical regulators of HSCs maintenance, proliferation, and differentiation, as well as lineage-specific hematopoietic cell development. Understanding the intricate signaling networks mediated by RTKs is crucial for unraveling the molecular mechanisms underlying normal hematopoiesis and may provide insights for the development of novel therapeutic strategies for hematopoietic disorders.

2.2.4.3. The hematopoietic niche

The hematopoietic niche, a concept proposed by Schofield in 1978, is a specialized microenvironment within the BM that provides essential support and regulatory cues for the maintenance and function of HSCs (Schofield 1978). The niche consists of various cellular components, extracellular matrix (ECM), and soluble factors that collectively maintain HSCs (**Figure 10**).

The cellular components provide structural support and secrete regulatory factors. They consist of osteoblasts, endothelial cells, mesenchymal stromal cells (MSCs), and macrophages that collectively create a microenvironment for HSC maintenance. Osteoblasts provide physical support to HSCs and secrete factors such as angiopoietin-1 (ANGPT1), osteopontin (OPN), and TPO, which promote HSC quiescence (Arai et al. 2004; Stier et al. 2005; Yoshihara et al. 2007). Blood vessel endothelial cells within the niche produce factors like SCF, Notch ligands (such as Jagged-1) and CXCL12, which regulate HSC quiescence, self-renewal, and homing (Butler et al. 2010; Ding et al. 2012; Greenbaum et al. 2013; Poulos et al. 2013). MSCs interact with HCS and contribute to the niche by secreting factors like CXCL12 and SCF (Méndez-Ferrer et al. 2010). Tissue-resident macrophages also produce CXCL12 and therefore promote the retention of HSC in the niche (Chow et al. 2011; Winkler et al. 2010). Moreover, nonmyelinating Schwann cells, found in proximity to HSCs, have been demonstrated to play a role in maintaining the quiescence of HSCs through the activation of transforming growth factor-β (TGF-β)-SMAD signaling pathway (Yamazaki et al. 2011).

The ECM within the hematopoietic niche has a crucial role in HSC regulation. Components such as fibronectin, collagen, and hyaluronic acid provide structural support and act as reservoirs for growth factors and signaling molecules. The interaction between HSCs and ECM components involves various

cell receptors, including integrins and other receptors such as CD44. CD44 is known to cooperate with CXCL12 in the homing of $CD34^+$ HSCs to the BM (Avigdor et al. 2004). Integrins can bind to ECM and activate downstream signaling through PI3K and focal adhesion kinase (FAK) (Buitenhuis 2011; Lu et al. 2012).

Soluble factors such as SCF are secreted by niche cells as presented above. CXCL12 binds to the CXCR4 receptor on HSCs, promoting their retention within the niche and quiescence (Ara et al. 2003; Sugiyama et al. 2006). TGF-β regulates HSC quiescence and exhibits immunomodulatory effects (Blank & Karlsson 2015). Notch ligands activate Notch signaling in HSCs, impacting their fate decisions and self-renewal (Lampreia et al. 2017). Interestingly, TPO, CXCL12 and TGF-β have been shown to modulate $p21^{Cip1}$ and $p57^{Kip2}$ expressions, suggesting a role for the BM niche in regulating expression of these CKIs in HSCs (Scandura et al. 2004; Qian et al. 2007; Nie et al. 2008).

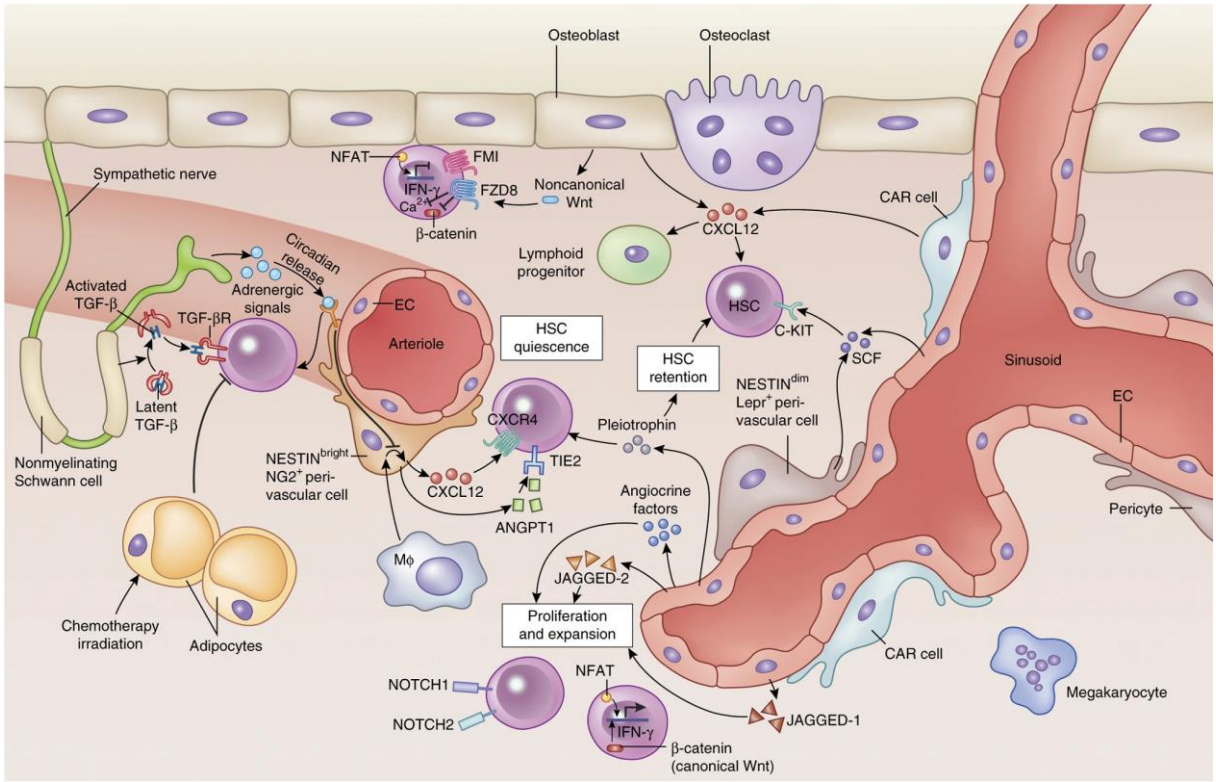

Figure 10: Regulation of HSC maintenance by the cells of the hematopoietic niche. *Different cell types are implicated in the maintenance of HSCs. These include perivascular stromal cells expressing CXCL12 (CXCL12-abundant reticular, CAR) cells, endothelial cells (ECs), macrophages, sympathetic neurons, and nonmyelinating Schwann cells. HSC maintenance is regulated by numerous factors, including CXCL12 and SCF, as well as additional factors like pleiotrophin, angiopoietin 1 (ANGPT1), and TGF-β. In addition, signaling pathways such as Notch and Wnt contribute to the regulation of the microenvironment (Mendelson & Frenette 2014).*

The physical properties of the niche, such as stiffness and oxygen tension may also influence HSC fate decisions and functional properties (Zhang et al. 2019). Moreover, emerging evidence suggests that the niche can dynamically respond to physiological and pathological conditions, adapting its properties to support HSC homeostasis or respond to stress and injury (Calvi & Link 2015).

Understanding the complex interplay between HSCs and their niche has profound implications for the development of novel therapeutic strategies targeting hematopoietic disorders and improving HSC transplantation outcomes.

2.2.4.4. Stress-induced regulation of hematopoiesis

Comprehending the development of lineage preferences due to the diversity of HSCs and their susceptibility to external signals is crucial for understanding how the hematopoietic system adapts to physiological stress. In this context, inflammation plays a prominent role in coordinating a demand-driven hematopoietic response. It has the capacity to either activate specific subsets of lineage-biased HSCs or to reprogram lineage bias in HSPCs through the secretion of cytokines. Both forms of regulation come into play in response to various physiological stressors, such as injuries.

For instance, TGF-β1 can promote the activation and differentiation of myeloid-biased HSCs, while myeloid-biased HSCs exhibit reduced responsiveness to the lymphopoietic IL-7 (Challen et al. 2010; Muller-Sieburg et al. 2004). Moreover, as mentioned earlier, certain HSCs can give rise directly to megakaryocytes, thus replenishing platelet levels in response to infection or tissue damage (Sanjuan-Pla et al. 2013; Haas et al. 2015). The MPP compartment also displays dynamic reactions to inflammatory signals, leading to alterations in blood cell production. Specifically, the secretion of IL-1 and M-CSF signals triggers the activation of the myeloid lineage transcription factor PU.1 in HSCs (Mossadegh-Keller et al. 2013; Pietras et al. 2016). This activation causes a shift from lymphoid-biased MPPs to myeloid-biased MPPs. This adaptability is also observed following transplantation, indicating the presence of a common regulatory mechanism in both scenarios (Olson et al. 2020). In the BM, rapidly differentiating GMP clusters support the production of mature myeloid cells during emergency hematopoiesis (Hérault et al. 2017).

Inflammation leads to the reprogramming the entire HSPC compartment, channeling the production of specific blood cell lineages helped by the activation of lineage-biased HSC subpopulations. The degree to which this HSC-level bias influences downstream progenitors is a subject of ongoing investigation. These findings raise intriguing questions regarding the versatility of HSPCs in responding to danger signals and their ability to guide hematopoietic outcomes through paracrine signaling.

2.2.4.5. Maintenance and expansion of HSCs *in vitro*

Researchers are actively working to enhance the success of HSC engraftment as a therapeutic approach for patients with hematopoietic disorders. A paramount objective in clinical therapy is to generate a substantial quantity of transplantable HSCs by amplifying the population of LT-HSCs while impeding their differentiation into committed progenitor cells (**Figure 11**). Over the years,

considerable progress has been made to develop various culture systems that enable the maintenance, manipulation, and expansion of HSCs *in vitro.*

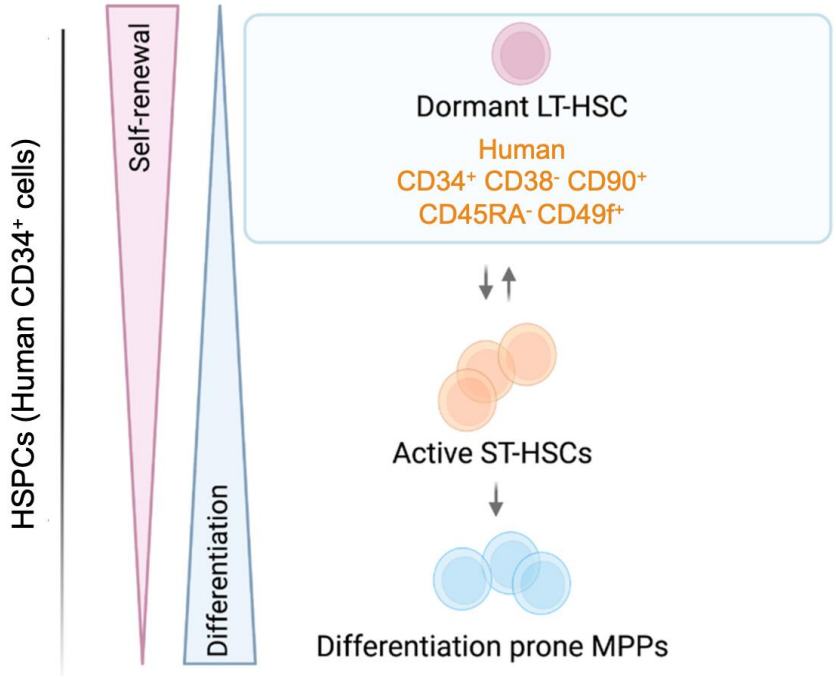

Figure 11: Model of HSCs and progenitor cells. *Dormant LT-HSC expressing Lin⁻ CD34⁺ CD38⁻ CD90⁺ CD45RA⁻ CD49f⁺. They possess the ability to self-renew, are quiescent and contribute to the replenishment of the ST-HSC pool. Active ST-HSCs act as an intermediate state between LT-HSCs and multipotent progenitor cells (MPPs), playing a vital role in replenishing progenitor cells and maintaining the balance of the hematopoietic system. (Adapted from Mayer et al. 2022).*

In vitro culture approaches aim to recreate the physiological conditions of the BM niche and provide growth factors and cytokines that support HSC quiescence or induce proliferation. Early attempts at HSC culture relied solely on media supplements such as cytokines and growth factors, without incorporating supporting BM cells. Mouse HSCs were cultured in media containing FCS, bovine serum albumin (BSA), and specific cytokines such as SCF, IL-11 and, FLT3/FLK-2 ligand (FLT3L) (Yonemura et al. 1997; Miller & Eaves 1997). Subsequent modifications of these culture conditions involved the addition of other supplements like ITS-X (insulin, transferrin, selenium, ethanolamine) or TPO in the culture medium resulting in the enhancement of the number of HSCs and the improvement of bone marrow reconstitution efficiency (Yagi et al. 1999). Eliminating FCS from the culture media composition, which can vary in quality between batches, and substituting BSA with polyvinyl alcohol (PVA), has additionally enhanced the extended culture of HSCs (Wilkinson et al. 2019).

The addition of small molecules such as StemRegenin-1 (SR1) and UM171 has been shown to be beneficial for HSCs expansion (Boitano et al. 2010; Fares et al. 2014). SR1 acts as an antagonist of the aryl hydrocarbon receptor, which is a negative regulator of hematopoiesis, while UM171 is believed to facilitate homeostatic inflammatory detoxification of ROS (Singh et al. 2009; Chagraoui et al. 2019).

When combined with cytokines such as TPO, SCF, FLT3L, and IL-6, SR1 and UM171 have been shown to induce an estimated 30-fold expansion of HSCs in *vitro* over a period of two weeks.

Advancements in our understanding of HSC self-renewal and its regulation by niche components paved the way for the development of novel *in vitro* expansion approaches. In the BM niche endothelial cells stimulate HSC self-renewal through Notch signaling (Lampreia et al. 2017). Researchers have shown engineered Notch ligands can be employed to culture HSCs, resulting in prolonged expansion and improved reconstitution ability (Varnum-Finney et al. 2003). More generally, the co-culture of HSCs on an extracellular matrix composed of BM mesenchymal stem or stromal cells (MSCs) has allowed for the improvement of HSCs maintenance (Butler et al. 2010; Nakahara et al. 2019). Research efforts are now focused on developing 3D culture methods to replicate the spatial structure of the BM microenvironment more accurately (Raic et al. 2019). These methods include the co-culture of HSCs inside an MSCs spheroid or the use of cross-linked polymers to form a 3D hydrogel scaffold (Cook et al. 2012; Bai et al. 2019). Overall, these 3D culture approaches offer advantages such as proper cell-cell contacts, maintenance of cell shape, controlled signaling molecule concentration, and enhanced communication between cells.

2.2.5. Challenges in HSC transplantation therapies

Alterations in HSCs or disturbances in BM homeostasis are known to be significant contributors to the development of various blood diseases, including leukemia, lymphoma, and myeloma (Li, Xue, et al. 2015; Maswabi et al. 2017; Toscani et al. 2015). Hematopoietic stem cell transplantation (HSCT) aims to restore normal hematopoiesis and continues to be a crucial therapeutic approach for treating acute leukemias in allogeneic settings and other hematopoietic malignancies in autologous settings, particularly high-risk multiple myeloma (Ntanasis-Stathopoulos et al. 2020; Cowan et al. 2022) and aggressive refractory/relapsed lymphomas (Zahid et al. 2017).

HSCT can be classified based on the source of the graft and the relationship between the donor and recipient (Bazinet & Popradi 2019). HSCs can be obtained from peripheral blood, BM, or UCB units. HSCT can be autologous, where the recipient's own stem cells are collected, or allogeneic, where the cells are obtained from another individual. In autologous HSCT, stem cells are collected from the recipient and cryopreserved. These cells are later re-infused after high-dose chemotherapy with or without radiotherapy. For allogeneic grafts, a healthy donor with human leukocyte antigen (HLA) compatibility is required. If a suitable donor is not available, banked UCB units or a partially matched family member (haploidentical donor) can be used (Wagner et al. 2002; Kanakry et al. 2016). However, the scarcity of HSCs from unrelated donors and the risk of graft-versus-host disease (GvHD) present ongoing challenges.

To overcome these challenges, several attempts have been made in the past to expand true LT-HSCs using *in vitro* established techniques in the presence of cytokines (see section **2.2.4.5. Maintenance and expansion of HSCs *in vitro***). However, these attempts have not yet yielded a methodology capable of producing transplantable LT-HSCs in clinically applicable settings. To address these limitations, double cord blood transplantation has been employed, particularly in adult patients, as an alternative approach to bypass these difficulties (Gutman et al. 2010).

The limitations in expanding true HSCs in vitro highlight the complexity of the HSC niche and the intricate regulatory mechanisms involved in HSC maintenance and self-renewal. Further research is needed to elucidate the precise signals and factors necessary for the successful expansion of functional HSCs. By gaining a deeper understanding of the biology of HSCs it may be possible to develop novel approaches for HSC expansion and overcome the challenges associated with transplantation therapies. Another approach for improving BM transplantation would be the generation of functional and engraftable HSCs from iPSC.

2.3. HSCs generation from iPSCs

The generation of HSCs from iPSCs holds great promise for regenerative medicine and personalized cell therapies. However, several challenges need to be addressed to achieve efficient and functional HSC generation from iPSCs.

2.3.1. Challenges in HSCs generation from iPSCs

Indeed, recapitulating the complex process of HSC development *in vitro* is a major hurdle as researchers need to understand the precise molecular cues and signaling pathways to effectively guide iPSCs towards the HSC fate. Studies have generated HSC-like cells from PSCs, but they recapitulate engraftment-deficient yolk sac hematopoiesis rather than the definitive hematopoiesis (Kaufman et al. 2001; Chadwick et al. 2003; Zambidis et al. 2005). Subsequently, protocols for generating terminally differentiated blood cells from PSCs have been developed, enabling the possibility of iPSC-derived erythrocyte transplantation (Ma et al. 2008; Kobari et al. 2012). Unfortunately, these protocols are not suitable for generating true engraftable LT-HSCs (Lim et al. 2021).

Until now, the only protocols for generating HSCs from iPSCs are those that involve *in vivo* teratoma formation in immunocompromised mice (Amabile et al. 2013; Suzuki et al. 2013). In these cases, iPSC-derived HSCs migrated from teratomas to the BM leading to the long-term reconstitution of the hematopoietic system with multilineage potential in serial transplantation. However, these protocols are problematic for clinical applications because the use of cells obtained via a culture within a mouse teratoma is not clinically acceptable.

Transcription factor screening has been a major focus of research to enhance *in vitro* hematopoiesis from iPSCs. Specific transcription factor combinations have been identified that can generate serially transplantable HSCs with multilineage differentiation potential (Riddell et al. 2014). These findings in mice have provided proof-of-principle data for modeling genetic blood diseases and therapeutic strategies. However, this method relies on ectopic expression of transcription factors and remains challenging to adapt in a clinical context due to practical limitations, such as the need for specialized laboratory conditions, time consumption, and cost. The same approach with overexpression of 5 transcription factors have also been reported but obviously these approaches are not currently clinically applicable (Doulatov et al. 2013). These experiments demonstrate however that iPSCs have the potential to generate long-term HSC.

Enhancing our understanding of the mechanisms underlying the hematopoietic differentiation of iPSCs and refining existing protocols is essential to pave the way for the generation of functional iPSC-derived HSCs. These cells would be used for various therapeutic applications, including hematopoietic disorders, immune reconstitution, and personalized medicine.

2.3.2. Current protocols for *in vitro* iPSC-derived hematopoiesis

Over the past decade, considerable progress has been made in the development of iPSC-derived blood therapeutics. Differentiation protocols for iPSCs follow a similar path that mimics embryonic development, involving key stages such as mesoderm induction, hematopoietic commitment, generation of hematopoietic progenitors and finally terminal differentiation into mature blood cells (**Figure 12**).

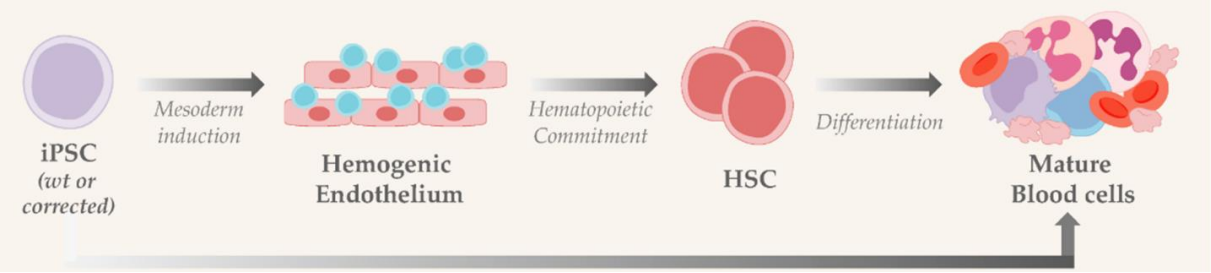

Figure 12: Simplified protocol of hematopoietic differentiation from iPSCs *(Rao et al. 2022).*

Co-culture with feeder cells or the use of small molecules has been shown to enhance hematopoietic output. However, the precise program of primitive versus definitive hematopoiesis in iPSCs is still under investigation, with efforts to improve engraftment potential and achieve more mature erythroid cells. Herein are presented several protocols of hematopoietic differentiation from iPSCs:

- **2D protocols** are easier and shorter but do not fully recapitulate the niche microenvironment and essential signaling pathways such as Notch resulting in fewer $CD34^+$ cells and lower colony-

forming capacity (Mora-Roldan et al. 2021). However, they are more reproducible, cheaper, and easier to use (Tursky et al. 2020). Commercial kits like STEMdiff™ Hematopoietic Kit provide standardization for 2D differentiation. The process induces mesoderm with factors like BMP-4, VEGF-A, and b-FGF. Hematopoietic differentiation is then achieved using factors like b-FGF, BMP-4, VEGF-A, SCF, Flt3-L, and TPO. Hematopoietic cells appear around day +12 of differentiation. However, the lack of a representative niche in 2D cultures leads to the rapid loss of self-renewal potential in favor of differentiation (Walasek et al. 2012).

- **3D strategies** aim to overcome the limitations of 2D culture by reconstituting the hematopoietic niche more closely (Rödling et al. 2017). Various approaches, including biomaterials and bioreactors, are used to mimic the complexity of the niche, considering paracrine functions, cellular heterogeneity, mechanical environment, and hypoxia (Leisten et al. 2012; Raic et al. 2014; Lee-Thedieck & Spatz 2014). iPSCs can spontaneously differentiate into embryoid bodies (EBs), which can be further differentiated into hematopoietic cells. EBs can be obtained through bioreactor cultures, hanging drop cultures, or microwell technology (Höpfl et al. 2004; Mohr et al. 2006; Lim et al. 2013). EBs can also be co-cultured with mouse stromal cells (such as MS-5, OP-9) that mimic the hematopoietic niche. These stromal cells can be modified to express specific transcription factors like HOXB4, DLL1, and DLL4 (Nakano et al. 1994; Mohtashami et al. 2010; Larbi et al. 2012). OP-9 cells, derived from mouse bone marrow stromal cells, possess hematopoietic supportive capacity similar to MS-5 cells (Gao et al. 2010). When co-cultured with ESC/iPSC, these stromal cells induce the differentiation of ESC/iPSC into various blood cell lineages (erythroid, myeloid, lymphoid).

Overall, 3D techniques aim to recreate the hematopoietic niche more accurately, while 2D techniques offer reproducibility and simplicity, albeit with some limitations.

In conclusion, the advancement of HSC engraftment for therapeutic applications remains an ongoing pursuit in the field of regenerative medicine. The primary goal is to expand the pool of long-term HSCs while impeding their differentiation into committed progenitors, ultimately facilitating the replenishment of the hematopoietic system. Notable progresses have been achieved through the development of various *in vitro* culture systems that permit the manipulation, expansion, and maintenance of HSCs. The promise of generating functional HSCs from iPSCs offers great potential for personalized cell therapies. Nonetheless, significant obstacles remain in achieving efficient and clinically applicable protocols for iPSC-derived HSC generation.

3. The RET proto-oncogene

The discovery of cytoplasmic and receptor tyrosine kinases as main drivers of cancer positioned them as promising targets for the treatment of malignant diseases (Sawyers 2002). In 1985, a specific tyrosine kinase receptor REarranged during Transfection (RET) was initially identified as a transforming gene (Takahashi et al. 1985). This finding occurred when DNA from human lymphoma cells was introduced into NIH3T3 cells leading to their oncogenic transformation. Takahashi and colleagues conducted Southern blot analysis and determined that the transforming gene resulted from the combination of two separate DNA sequences located over 25kb apart. This genetic recombination was named RET referring to the experiments leading to its discovery.

3.1. Role of RET in embryonic development and adult cells

3.1.1. Structure of RET Protein

The *RET* proto-oncogene is located on the human chromosome 10q11.2 and encodes a transmembrane protein member of the tyrosine kinase family. Its extracellular domain is constituted of four cadherin repeats, called cadherin-like domains (CLDs), and one $Ca2^{+}$ binding site situated between CLD2 and CLD3 (**Figure 13**) (Anders et al. 2001). Following CLD4, a region of 120 amino acids containing 16 cysteine residues (cysteine-rich domain, CRD) is connected to the transmembrane domain (TMD). The intracellular domain is a typical tyrosine kinase domain (TK). There are two RET isoforms after alternative splicing: one short with 9 residues after position 1063 (RET9) and one long with 51 residues (RET51).

The ligands that bind to RET belong to the Glial cell line Derived Neurotrophic Factor (GDNF) family known as GDNF family ligands (GFLs). The first identified member of this family was GDNF, which gave its name to the family (Durbec et al. 1996). In addition to GDNF, three others RET ligands have been identified and are closely related in sequence to GDNF. These include Artemin (ARTN) (Baloh et al. 1998), Neurturin (NRTN) (Kotzbauer et al. 1996) and Persephin (PSPN) (Milbrandt et al. 1998). GFLs are dimeric proteins with growth factor-like properties that form a family distantly related to the transforming growth factor-β (TGF-β) superfamily (Saarma 2000).

RET and its ligands cannot directly bind each other, instead GFLs first bind with a family of glycosyl-phosphatidylinositol (GPI) anchored co-receptor proteins called GDNF family receptor alpha (GFRα). There are four GFRα receptors (GFRα1–4), and each one preferentially interacts with a specific GFL. GDNF binds to GFRα1, NRTN to GFRα2, ARTN to GFRα3, and PSPN to GFRα4. Once the GFL and GFRα subunit have formed, it interacts with RET CLDs to form a complex. Therefore, RET activation occurs after the binding of a GFL dimer to a GFRα co-receptor.

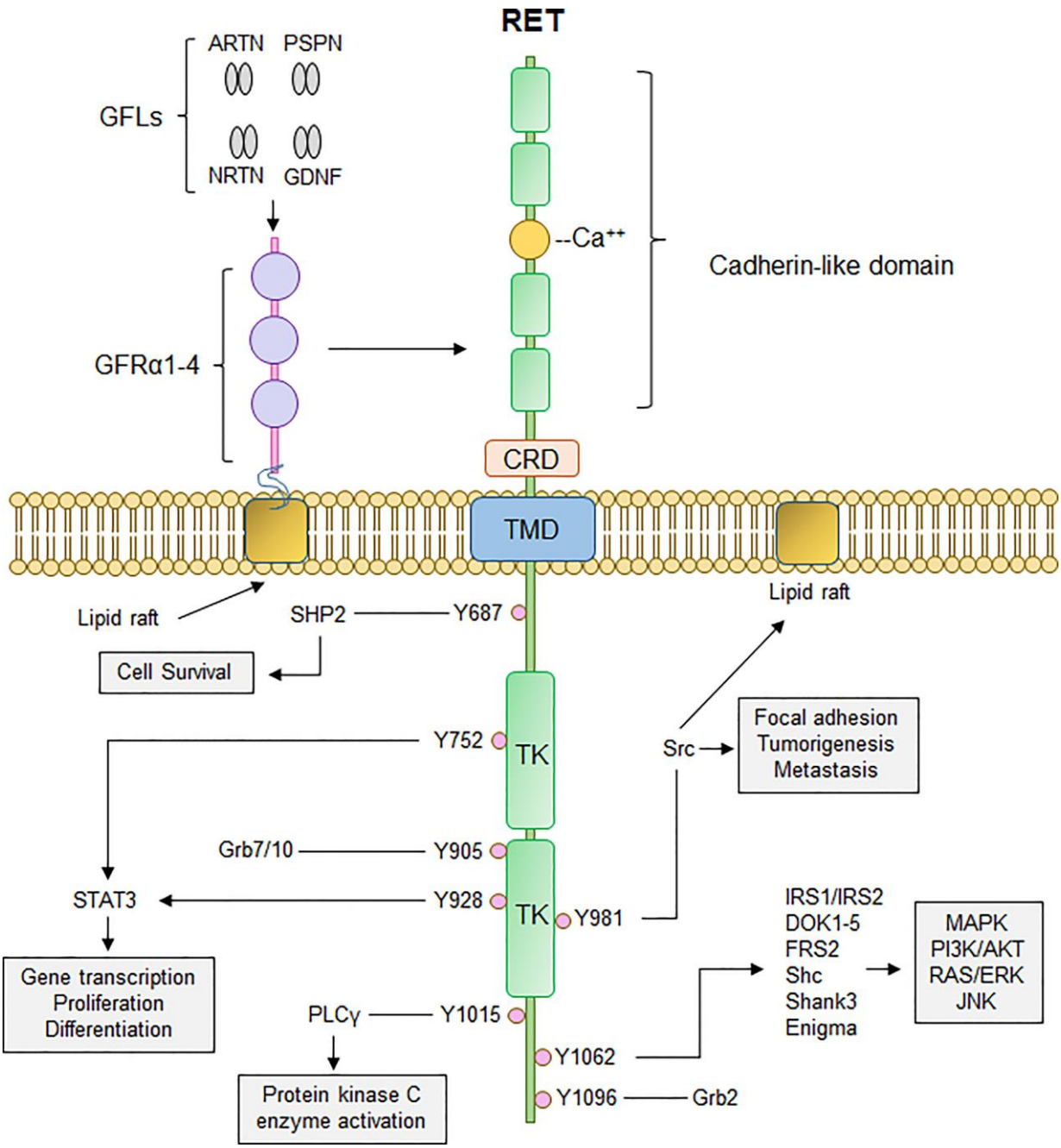

Figure 13: Canonical RET signaling. *GDNF-family ligands (GFLs) such as Artemin, Neurturin, Persephin (ARTN, NRTN, PSPN), and GDNF bind the co-receptor GFRα1-4. Simultaneously, calcium ions interact with the calcium-binding domain, leading to the recruitment of RET and the formation of a RET-GFRα complex. This complex brings two RET monomers close together, resulting in homodimerization and cross-phosphorylation of critical tyrosine residues within RET. These phosphorylated tyrosine residues serve as docking sites for adaptor proteins that play crucial roles in propagating RET signaling, including PI3K/AKT, MAPK, PLCγ, and RAS/RAF/ERK. Consequently, the activation of RET signaling facilitates cell proliferation, growth, and survival by triggering multiple downstream signaling cascades. The components involved in this process include the cysteine-rich domain (CRD), transmembrane domain (TMD), and tyrosine kinase domain (TK) (Regua et al. 2022).*

Concurrently, $Ca2^{+}$ ions bind on RET calcium binding domain to stabilize RET protein structure and its interactions with ligands. The GFL-GFRα subunit interacts with RET and induces the recruitment of 2 RET monomers leading to their homodimerization and the autophosphorylation of the TK (**Figure 13)** (Li, Shang, et al. 2019). They are 18 tyrosine residues in the intracellular kinase domain, including 14

that can become phosphorylated (Kawamoto et al. 2004). The cross-phosphorylation of RET tyrosine residues allows for the recruitment of adaptor proteins needed for transmitting external signals and initiating downstream signaling pathways. These proteins are well-known tyrosine kinases effectors such as phospholipase C-γ (PLCγ), PI3K/AKT, RAS/RAF/MAPK and JAK/STAT. The effects of the phosphorylation of several tyrosine residues are listed in the **Table 1** below:

Table 1: Effect of the phosphorylation of RET tyrosine kinase residues.

Kinases	*Effects*	*References*
Tyr^{687}	*Recruits and binds SHP2 phosphatase, leading to the activation of PI3K/AKT*	*(Perrinjaquet et al. 2010)*
Tyr^{752}	*Docking site STAT3*	*(Schuringa et al. 2001)*
Tyr^{900}	*Kinase activation loop*	*(Knowles et al. 2006)*
Tyr^{905}	*Stabilization of the active RET conformation. Binding of adaptor protein Grb7/10*	*(Iwashita, Asai, et al. 1996)*
Tyr^{928}	*Docking site for STAT3*	*(Schuringa et al. 2001)*
Tyr^{981}	*Binding and activation of SRC kinase*	*(Encinas et al. 2004)*
Tyr^{1015}	*Activation of PLCγ*	*(Borrello et al. 1996)*
Tyr^{1062}	*Activation of RAS/MAP kinase and PI3K/AKT*	*(Coulpier et al. 2002)*
Tyr^{1096}	*Present only in RET51 isoform. Activation of RAS/MAPK via Grb2 binding*	*(Liu et al. 1996)*

Altogether, activation of RET signaling promotes cell growth, differentiation, survival, and proliferation.

3.1.2. Normal functions of the RET receptor signaling

The RET protein is a key player in several physiological processes essential for normal development and tissue homeostasis.

During embryogenesis, RET is critical for the development and maintenance of the enteric nervous system (Schuchardt et al. 1994). It acts as a guiding force for neural crest cells, promoting their survival, migration, and differentiation into enteric neurons that control gastrointestinal functions (Lake & Heuckeroth 2013). Furthermore, RET plays a fundamental role in kidney development by regulating the process of branching morphogenesis in the ureteric bud, ensuring the formation of the functional collecting duct system (Sánchez et al. 1996; Pichel et al. 1996).

In addition to its role in organogenesis, RET is crucial for neurotrophic signaling. Activation of RET by GFLs triggers intracellular signaling cascades that promote neuronal survival, growth, and

differentiation (Moore et al. 1996). This is crucial in the development and maintenance of a variety of neuronal populations, such as motor neurons, sympathetic neurons, and sensory neurons (Cacalano et al. 1998). Moreover, a study revealed progressive and late degeneration of dopaminergic neurons, accompanied by inflammation and gliosis, in RET conditional knock-out mice over a two-year monitoring period (Kramer et al. 2007). This suggests RET plays a crucial role in the long-term maintenance of the nigrostriatal dopamine system.

RET signaling is implicated in the regulation of spermatogenesis. GDNF secreted by Sertoli cells plays a crucial role in the maintenance and the maturation of spermatogonial stem cells (SpSC) (Meng et al. 2000; Kubota et al. 2004). Studies have shown that mice expressing a dominant-negative RET exhibit defective spermatogenesis, indicating the involvement of RET in this process (Jain et al. 2004). Further research revealed that RET and GFRα1 are co-expressed in germ cells and SpSCs during early spermatogenesis and their signaling is necessary for complete spermatogenesis and SpSCs self-renewal. (Naughton et al. 2006). These findings highlight the importance of the GDNF-RET axis in spermatogenesis and the regulation of SSC fate.

RET is also involved in the regulation of hematopoiesis. This is addressed in detail in section **2.2.4.2.2. Role of the RET RTK during hematopoiesis** of this manuscript.

3.2. Roles of RET in disease

RET has emerged as a causative gene in several human diseases. *RET* mutations are responsible for the onset of diverse neuroendocrine cancers such as medullary thyroid carcinoma (MTC) and pheochromocytoma. Additionally, RET activation through gene rearrangements have been observed in papillary thyroid carcinoma (PTC), non-small cell lung cancer (NSCLC), salivary gland intraductal carcinoma, and other cancer types. In contrast, RET-inactivating point mutations or deletions contribute to the development of Hirschsprung's disease (HSCR).

3.2.1. RET and cancers

3.2.1.1. *RET* mutations in cancer

Mutations in the *RET* gene can lead to the development of various types of cancer, including MTC, multiple endocrine neoplasia type 2 (MEN2), and familial medullary thyroid carcinoma (FMTC). These mutations can be germline mutations, inherited from parents, or somatic mutations, acquired during a person's lifetime. The presence of these mutations leads to the abnormal activation of the RET protein, which promotes uncontrolled cell growth and division, resulting in the formation of tumors (Plaza-Menacho et al. 2014).

In 1961, a review of 537 pheochromocytoma cases revealed an unexpectedly high incidence of thyroid neoplasms co-occurrence, leading to the hypothesis of an association between the two

diseases (Sipple 1961). In 1965, Williams examined 17 cases of associations between thyroid cancer and pheochromocytomas and hypothesized that a genetic predisposition could be the cause of this association (Williams 1965). These seminal studies led to the identification of multiple endocrine neoplasia type 2 (MEN2) syndrome, which is further divided into two subtypes: MEN2A and MEN2B. Both types are characterized by MTC pheochromocytoma, but MEN2A also causes primary hyperparathyroidism (Wells et al. 2013).

MEN2 is an autosomal dominant inherited disease where nearly all patients carry a hereditary mutation in the *RET* proto-oncogene (Wells et al. 2013). These point mutations can lead to constitutive activation of the tyrosine kinase domain. In MEN2A, mutations affecting the extracellular cysteine-rich domain are responsible for the RET dimerization in the absence of its ligands, leading to autophosphorylation of the tyrosine kinase domain and constitutive activation of downstream signaling pathways. These mutations occur at either codon 634 (exon 11) or codons 609, 611, 618, and 620 (exon 10) and account for 98% of all mutations associated with MEN2A. The most common mutation affects codon 634 (mutation RET^{C634Y}) and represents over 80% of all MEN2A-associated mutations (Kouvaraki et al. 2005). The patient-derived iPSC used in the **Results** section of this manuscript is carrying this mutation ($iRET^{C634Y}$). For MEN2B a single mutation converting a methionine to a threonine at codon 918 (exon 16) has been identified in 95% of patients, with other mutations involving codon 883 (exon 15) or double mutations (Carlson et al. 1994; Eng et al. 1994). The mutation RET^{M918T} causes constitutive autophosphorylation of RET without receptor dimerization because it modifies a tyrosine kinase domain (Gujral et al. 2006).

3.2.1.2. *RET* rearrangements in cancer

Somatic *RET* rearrangements have been identified in various human cancers. Oncogenic gene rearrangements occur when two separate genes become joined together due to structural changes. In the case of RET fusions, the RET tyrosine kinase domain is often linked with a partner gene containing a dimerization domain leading to the constitutive activation of RET signaling. The majority of the chimeric proteins do not have a transmembrane domain, resulting in cytoplasmic proteins. Over 35 genes have been reported to form rearrangement genes with *RET*, leading to abnormal activated fusion protein (Subbiah et al. 2020).

RET rearrangements has been detected in 5-35% of adult PTCs, particularly with *CCDC6* (RET/PTC1) (Grieco et al. 1990). Additional gene partners involved in PTC consist of *PRKAR1A, NCOA4, GOLGA5, TRIM24, TRIM33, KTN1,* and *RFG9RET*. The greatest occurrence of rearrangement was observed in children exposed to the aftermath of the Chernobyl disaster, with a notable prevalence of *RET* rearrangements involving the *NCOA4* gene (RET/PTC3) (Hamatani et al. 2008; Ricarte-Filho et al. 2013).

In NSCLCs, *RET* rearrangements, such as KIF5B-RET fusion, are present in a subset of cases (1-2%) and associated with unique clinicopathological characteristics (Kohno et al. 2012). The implication of RET in NSCLC will be reviewed in detail in **section 4.3.3 Role of RET in NSCLC**.

In recent studies, a significant prevalence of *RET* rearrangements (>40%) has been identified in salivary intraductal carcinomas, specifically involving NCOA4-RET and TRIM27-RET fusions (Skálová et al. 2018; Skálová et al. 2019). These findings suggest that the detection of *RET* rearrangements is valuable in diagnosing a specific subtype of salivary carcinoma.

Next-generation sequencing approaches have identified less frequent *RET* rearrangements in colorectal, breast, ovarian and chronic myelomonocytic leukemia (Le Rolle et al. 2015; Paratala et al. 2018; Kato et al. 2017; Ballerini et al. 2012).

3.2.2. RET in Hirschsprung's disease

Hirschsprung's disease (HSCR) is a congenital disorder characterized by the absence of neuronal ganglion cells in the distal gastrointestinal tract leading to intestinal obstruction (Romeo et al. 1994; Edery et al. 1994). *RET* mutations are found in approximately 50% of patients with familial HSCR and 10-20% of sporadic cases (Lake & Heuckeroth 2013). Unlike gain-of-function mutations in cancer cases, HSCR-associated mutations are *RET*-inactivating ones and lead to impairment of RET signaling which is crucial for the migration and proliferation of enteric neural crest cells during embryogenesis (Brooks et al. 2005). These mutations target various aspects of RET, including its kinase activity or its docking sites for intracellular signaling molecules (Iwashita, Murakami, et al. 1996; Geneste et al. 1999). Other mutations are known to modify the extracellular domain of RET affecting its trafficking to the endoplasmic reticulum and therefore preventing its expression at the cellular surface (Cosma et al. 1998; Kjaer & Ibáñez 2003).

In conclusion, the discovery of cytoplasmic and receptor tyrosine kinases as major drivers of cancer has positioned them as promising targets for treating malignant diseases. RET involvement extends beyond normal physiological functions as it is implicated in a range of diseases, particularly cancer. *RET* mutations have been identified in neuroendocrine cancers such as MTC, pheochromocytoma, and various thyroid carcinomas. While oncogenic *RET* gene rearrangements are found in cancers like PTC, NSCLC and, salivary gland intraductal carcinoma. In-depth understanding of RET signaling mechanisms holds paramount importance in the development of precise treatments for the diseases associated with RET.

4. Non-Small Cell Lung Cancer

4.1. Normal human lung development

4.1.1. The human adult lung

The lungs form the fundamental components of the respiratory system with intricate branching airways and blood vessels, essential for gas exchange. Positioned adjacent to the heart, human lungs consist of three right and two left lobes, supported by the concave-shaped diaphragm and enclosed by a membrane called the pleura (**Figure 14**). Air travels through the airways until it reaches the alveoli, where the exchange of gases occurs between the alveolar epithelial cells and the network of capillaries that envelop them (Weibel 1963).

Lungs encompass various cell types, including epithelium, endothelium, airway and vascular smooth muscle, fibroblasts, neurons, and immune cells like alveolar macrophages. Cellular markers of the principal human lung cell populations are shown in the **Table 2**.

Table 2: Principal cell markers in human lung *(From Nikolić et al. 2018)**.***

Human cell population	*Markers*	*References*
Basal cell	*KRT5, TP63, PDPN*	*(Hackett et al. 2011; Rock et al. 2009; Teixeira et al. 2013)*
Ciliated cell	*Acetylated tubulin, β3-tubulin, FOXJ1*	*(Dye et al. 2016; Gao et al. 2015; Look et al. 2001)*
Secretory club cell	*SCGB1A1*	*(Khoor et al. 1996)*
Secretory goblet cell	*MUC5AC, MUC5B, SPDEF*	*(Dye et al. 2016; Yu et al. 2010)*
Type 1 alveolar epithelial cell	*AQP5, HOPX, HTI-56, PDPN, RAGE*	*(Fujino et al. 2012; Dobbs et al. 1999; Nikolić et al. 2017; Shirasawa et al. 2004)*
Type 2 alveolar epithelial cell	*ABCA3, HTII-280, LAMP3, LPCAT1, pro-SFTPC, SPA, SPB*	*(Barkauskas et al. 2013; Stahlman et al. 2007; Gonzalez et al. 2010; Cau et al. 2016; Khoor et al. 1994; Nikolić et al. 2017; Phelps & Floros 1988)*
Distal tip	*SOX9, SOX2, MYCN, GATA6, ETV5, HMGA1, HMGA2, HNF1B, ID2, CPM, CD47*	*(Gotoh et al. 2014; Hawkins et al. 2017; Miller et al. 2018; Nikolić et al. 2017)*
Stalk bronchiolar progenitors	*SOX2*	*(Danopoulos et al. 2018; Miller et al. 2018; Nikolić et al. 2017)*

Lung epithelial cells are categorized into airway and alveolar types:

- **The human tracheobronchial airways** exhibit a pseudostratified epithelium where cells are in contact with the basement membrane and surrounded by blood vessels, lymphatics, smooth muscle, fibroblasts, and nerves (**Figure 14**) (Hogan et al. 2014). Conducting airway epithelia are composed of basal cells, secretory cells (mainly of the mucous subtype) and ciliated cells, forming the “mucociliary escalator” for particles clearance. Basal cells are found throughout the human conducting airways and function as stem cells, capable of both self-renewal and differentiation into secretory and ciliated cells (Rock et al. 2009).

- **The alveolar epithelium** comprises type I (AT1) and type II (AT2) alveolar cells surrounded by capillaries and fibroblasts (Williams 2003; Weibel 2015). AT1 cells are flat and cover over 95% of the gas exchange surface, while AT2 cells are cuboidal, producing surfactant to reduce surface tension in the alveoli (**Figure 14**) (Crapo et al. 1982). AT2 cells are primary stem cells, capable of self-renewal and differentiation into AT1 cells (Barkauskas et al. 2013; Desai et al. 2014a). Adult human AT1 cells have limited proliferative capacity post-injury *in vivo* and they can de-differentiate to AT2-like cells *in vitro* (Danto et al. 1995; Hogan et al. 2014). Finally, alveolar epithelium also contains alveolar macrophages that play pivotal roles in surfactant equilibrium and innate immunity (Bhattacharya & Westphalen 2016).

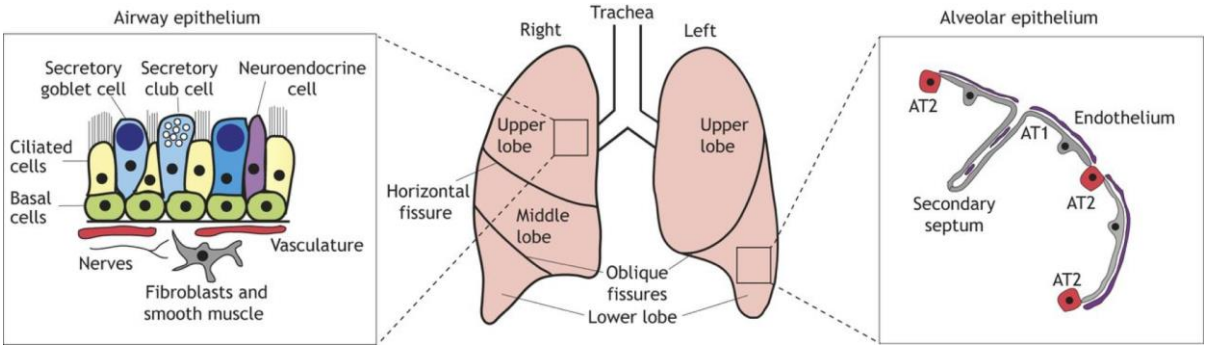

Figure 14: Structure and cell types in the adult human lung*. Close-ups showing the cell varieties present in the airway epithelium (left) and the alveolar epithelium (right) (From Nikolić et al. 2018).*

The submucosal glands, which are interconnected with the airway epithelium, are positioned beneath the luminal surface. These glands secrete mucus and other substances that play a role in safeguarding the lungs against particles and infectious agents (Liu et al. 2004). In humans, these glands are found throughout the cartilaginous airways (Meyrick et al. 1969).

Blood vessels play a vital role in the lung overall structure, with a particular importance in the alveolar gas exchange region. The organization of the vasculature, including smooth muscle, pericytes, and fibroblasts, varies based on their localization within the lung (Kool et al. 2014). Endothelial cells that line capillaries are not solely passive transport channels for blood; instead, they create specialized vascular environments that release sets of growth factors, termed angiocrine factors (Rafii et al. 2016). These signals actively contribute to directing organ regeneration, maintaining balance, and managing metabolism. After injury, these factors are elevated to coordinate the renewal and differentiation of resident stem and progenitor cells.

In summary, the lung stands as a multifaceted organ composed of an array of diverse cell types, and its intricate structure takes shape through a highly orchestrated process during embryonic development.

4.1.2. Stages of human lung development

The progression of human lung development can be categorized into specific morphological stages: embryonic, pseudoglandular, canalicular, saccular, and alveolar stages (**Figure 15A**) (Burri 1984; Rackley & Stripp 2012).

During the embryonic stage (4-7 post-conception weeks, pcw), the initial lung buds originate from the foregut endoderm around the fourth week. These buds then rapidly extend their branches, thus establishing the lobular configuration of the lung by the fifth week (**Figure 15B**).

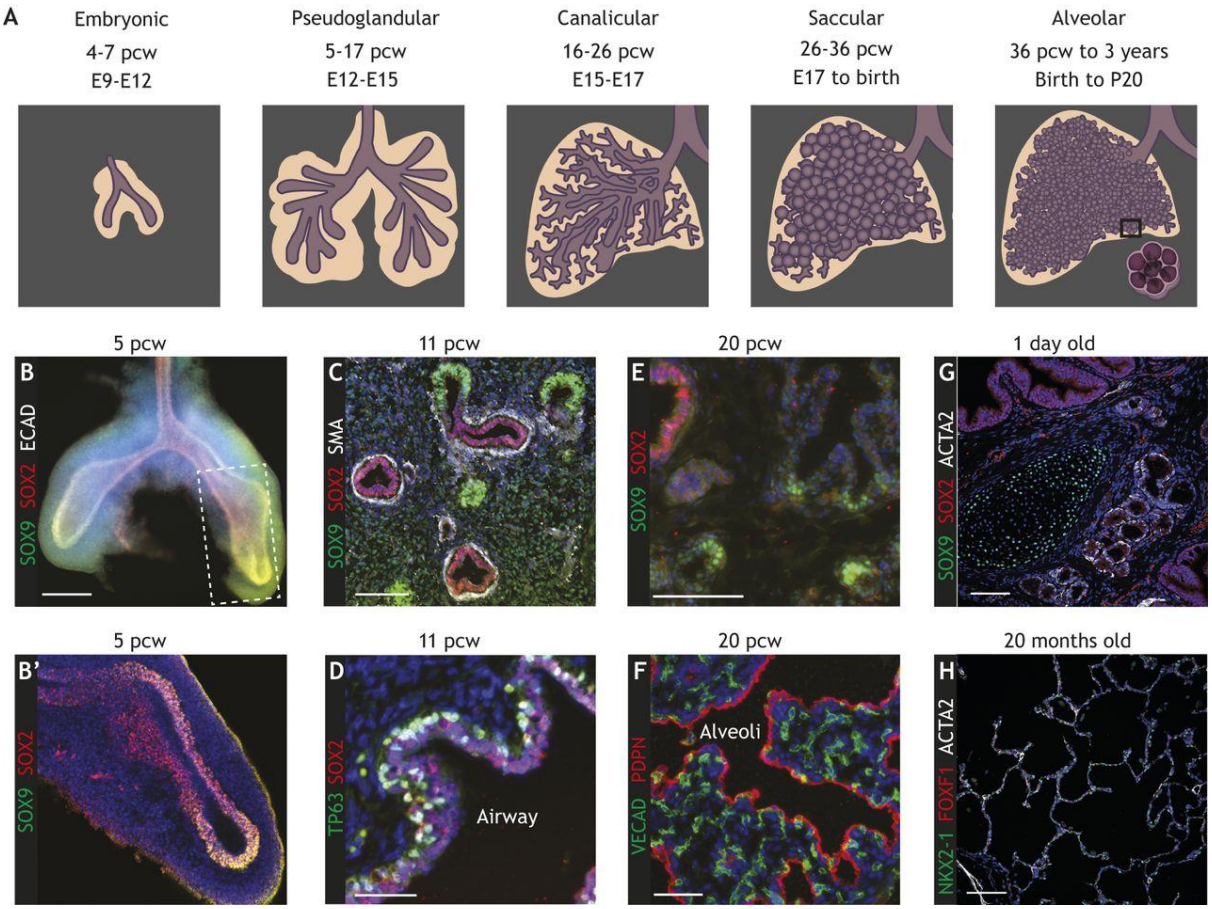

***Figure 15: Stages of human lung development**. **(A)** Schematics of the different stages of human lung development (post conception weeks; pcw). **(B-B')** Cryosection of a lung during embryonic stage (5 pcw). The primary branches and the co-expression of SOX2 and SOX9 at the tips can be observed. **(C-D)** Cryosections of lungs during pseudoglandular stage (11 pcw) showing the co-expression of SOX2 and SOX9 at the tips. Smooth muscle actin (SMA; C white) staining indicates airway differentiation while TP63 (D, green) marks the differentiating basal cells. **(E-F)** Cryosections of lungs in the canalicular stage showing **(E)** distal tips $SOX9^{+}$ but $SOX2^{-}$. **(F)** Emerging vasculature with VE-cadherin (VECAD; CDH5) in green and podoplanin (PDPN) in red. **(G-H)** Cryosections of lungs in the alveolar stage during postnatal development showing **(G)** the presence of SOX9 (in green, indicating cartilage), SOX2 (in red, marking airway cells), and ACTA2 (in white, representing smooth muscle). **(H)** the expression of NKX2-1 (in green, representing lung epithelium), FOXF1 (indicating mesenchyme), and ACTA2 (in white, denoting smooth muscle) is observed. Scale bars: 200 µm (B); 50 µm (C,D,F); 100 µm (E,G,H) (From Nikolić et al. 2018).*

Following this, during the pseudoglandular phase (5-17 pcw), the foundational structure of the airway tree is shaped through branching morphogenesis (Kitaoka et al. 1996). This stage is

accompanied by the differentiation of blood vessels in coordination with airway branching, as well as the development of cartilage, smooth muscle, mucous glands, and the epithelial lining (**Figure 15C-D)** (deMello & Reid 2000).

Between the 16th and 26th pcw, the canalicular phase takes place, characterized by multiple cycles of epithelial branching that contribute to the formation of the future alveolar regions (**Figure 15E-F**). The process of alveolar epithelial differentiation is initiated during this phase. As the existing airways continue to expand, the distal airspaces undergo a transformation into delicate terminal sacs, closely associated with neighboring capillaries (deMello & Reid 2000).

During the saccular phase (24-38 pcw), the differentiation of alveolar epithelium continues, particularly focusing on the maturation of the surfactant system within AT2 cells (Khoor et al. 1994). Concurrently, the terminal saccules emerge, growing and becoming enclosed by a bilayer of capillaries (Burri 1984).

Finally, during the alveolar stage (extending from 36 weeks to 3 years after birth), septae emerge from the walls of the saccules and subdivide the distal saccules into alveoli to enhance gas exchange efficiency. The maturation of microvasculature takes place, transitioning from a dual to a single capillary network configuration (Schittny 2017). The process of alveolar formation continues into young adulthood (Narayanan et al. 2012).

The process of lung embryogenesis is a sophisticated morphological process that is finely tuned and regulated by several molecular signals.

4.1.3. The molecular regulation of human lung development

Extensive research has been conducted on the molecular regulation of mouse lung development, yet there is a notable lack of information regarding the molecular aspects of human lung development (Cardoso & Lü 2006; Swarr & Morrisey 2015). Much of the investigation in this area has revolved around identifying mutant genes from patients with congenital lung diseases and examining their effects in genetically modified mice. For instance, the transcription factor NKX2-1 plays a critical role in the initial formation of the lung buds in the embryonic foregut endoderm in mice (Lazzaro et al. 1991; Ikeda et al. 1995). In human, mutations in this gene lead to lung developmental failures suggesting a similar function (Devriendt et al. 1998).

To evaluate if NKX2-1 expression accurately identifies human lung-competent foregut progenitors akin to the mouse lung development paradigm, investigations were conducted to determine if hPSC-derived NKX2-1^{+} and NKX2-1^{-} foregut progenitors equally possess the potential to produce lung lineages. To distinguish NKX2-1^{+} and NKX2-1^{-} foregut cells, researchers identified the

Carboxypeptidase M (CPM) as a marker for NKX2-1$^+$ pulmonary lineage progenitors (Gotoh et al. 2014). After sorting, CPM$^+$ cells exhibited substantial NKX2-1 enrichment (~90%) and demonstrated the capacity to generate bronchiolar and alveolar lineages under various differentiation conditions (Gotoh et al. 2014; Konishi et al. 2016; Yamamoto et al. 2017). The identification of surface markers for NKX2-1$^+$ population was further advanced by utilizing a GFP reporter integrated into the endogenous NKX2-1 locus (Hawkins et al., 2017) (Hawkins et al. 2017). Single-cell RNA-Seq (scRNA-Seq) analysis of NKX2-1$^+$ populations highlighted CD47 as the most correlated cell surface marker with NKX2-1 levels, alongside a similar correlation with CPM expression. Flow cytometry sorting for CD47$^+$ cells coupled with the negative selection marker CD26 achieved a high enrichment percentage (~90%) of NKX2-1$^+$ cells. Moreover, NKX2-1$^-$ cells exhibited a propensity for non-lung lineage differentiation, including oesophageal, liver, and intestinal lineage-like cells. The results from *in vitro* hPSCs differentiation experiments confirmed the identity of NKX2-1$^+$ foregut cells as human lung progenitors, as suggested by *in vivo* mouse experiments (Minoo et al. 1999).

Furthermore, RNA-Seq has played a significant role in elucidating comprehensive changes in gene expression across various developmental stages of entire human lungs (Kho et al. 2016). Comparative exploration has been conducted between the transcriptomes of human epithelial tip cells and previously reported mouse tip microarray data (Laresgoiti et al. 2016). Notably, nearly 96% of orthologous genes expressed in human tip cells are also detected in mice, indicating a high degree of conservation (Nikolić et al. 2017). In the context of mouse lung development, distal tip epithelial cells have been recognized as multipotent progenitors with Sox9$^+$/Id2$^+$ expression profiles, giving rise to bronchiolar and subsequently alveolar lineages (Rawlins et al. 2009; Alanis et al. 2014). Notably, during the pseudoglandular stage in mice, there is a distinct segregation between Sox9$^+$ tip cells and Sox2$^+$ stalk bronchiolar progenitors. However, a remarkable contrast emerges in human lungs where SOX2 is consistently co-expressed with SOX9 in tip cells throughout the pseudoglandular stage (Nikolić et al. 2017; Miller et al. 2018; Danopoulos et al. 2018). This distinctive expression pattern raises questions concerning the functional role of SOX2 in human epithelial tip progenitors and underscores the molecular disparities between human and mouse lung development. Furthermore, other disparities between human and mouse systems have been identified. Notably, human tip cells demonstrate high expression levels of BMP2 and BMP7 in contrast to Bmp4 in mice, implying substantial functional variations between the two species (Bellusci et al. 1996).

These two examples demonstrate the shared similarities in the molecular regulation of lung embryogenesis between mice and humans. However, cellular and molecular variations have been identified between mouse and human lungs underscoring the importance of investigating human-specific mechanisms to comprehend disease processes.

4.2. General overview of lung cancer

4.2.1. Epidemiology of lung cancer

Lung cancer is the second most common cancer worldwide with more than 2.2 million new cases in 2020 (Sung et al. 2021). It is the most common cancer in men and the second most common cancer in women. Lung cancer is also the leading cause of cancer death, with approximately 1.8 million deaths in 2020, accounting for nearly 20% of cancer deaths (Siegel et al. 2022). However, there are significant differences between lung cancer incidence and mortality rates around the world that reflect the evolution of the tobacco epidemic (Thun et al. 2012). Indeed, tobacco is the number one risk factor for lung cancer with more than 80% of lung cancer deaths related to smoking (Walser et al. 2008). It can be noted that in many industrialized countries where antitobacco policies are enforced, particularly in the United States and the United Kingdom, the incidence of lung cancer has decreased whereas it is increasing in developing countries where smoking has either peaked or continues to increase (Jha 2009).

In France, it is the third most frequent cancer with approximately 46 300 new cases diagnosed in 2018, including approximately 31 200 in men and 15 100 in women (Defossez G, et al. 2019, INCA 2019). It is also the leading cause of cancer death in France with 33 100 deaths in 2018 (approximately 22 800 men and 10 300 woman). The survival rate is low, about 20% at 5 years (24% for women and 18% for men) (Defossez G, et al. 2019). While in men, the incidence rate and the mortality rate are decreasing (-0.3% and -1.6% respectively), these indicators are increasing in women (incidence rate is increased by 5% and mortality by 3%). These disparities in terms of incidence and prognosis between gender are observed widespread but are not fully explained by sex differences in smoking patterns (Fidler-Benaoudia et al. 2020; Jemal et al. 2018).

As presented, most cases of lung cancer are related to long-term tobacco smoking. Smokers have more than a 20-fold increase in lung cancer risk compared to non-smokers (Alberg et al. 2013; Simonato et al. 2001). All the types of tobacco products are concerned: cigarettes, cigars, cigarillos, e-cigarette, etc. Cigarette smoke contains more than 55 substances that were found out to be carcinogenic by the International Agency for Research on Cancer (IARC). For example, the polycyclic aromatic hydrocarbons can lead upon activation to DNA methylation, DNA segment amplification or deletion, or whole chromosome gains or losses (Hecht 1999). Secondhand smoke-exposure is also increasing the risk of lung cancer. A study shows that 40% of children and 33-35% of non-smokers were exposed to secondhand smoke and 600 000 deaths worldwide were linked with secondhand smoking in 2004 (Oberg et al. 2011).

The other risk factors associated with lung cancer are prolonged exposure to certain substances and chemicals in the workplace such Radon, genetic mutations and predispositions or air pollution (Dela Cruz et al. 2011).

4.2.2. Lung cancer classification

Lung cancer classification involves categorizing tumors based on their histology, molecular features, and staging. Traditionally, lung cancer classification has relied on histological subtypes, with small cell lung cancer and non-small cell lung cancer representing the primary categories (**Figure 16**):

Small cell lung cancer (SCLC) represents about 10-15% of all lung cancer cases and is characterized by its rapid growth, high metastatic potential, and strong association with smoking (Gazdar et al. 2017). SCLC cells exhibit small size, scant cytoplasm, and high nuclear-to-cytoplasmic ratio. This aggressive subtype of lung cancer is prone to early dissemination and is frequently diagnosed at advanced stages.

Non-small cell lung cancer (NSCLC) comprises approximately 85% of all lung cancer cases and includes several histological subtypes such as adenocarcinoma, squamous cell carcinoma, and large cell carcinoma (Nicholson et al. 2022):

- **Adenocarcinoma** is the most common type of lung cancer, representing over 40% of all lung cancers (Lewis et al. 2014). Its incidence has been increasing steadily. It typically forms a mass in the outer part of the lungs but can also have different appearances. Lung adenocarcinoma is characterized by malignant epithelial cells with glandular differentiation or mucin production. Pneumocytic markers, such as thyroid transcription factor (TTF-1/NKX2-1) and NapsinA, are often expressed in these tumors and serve as diagnostic markers (Stenhouse et al. 2004; Tacha et al. 2012).
- **Squamous cell carcinoma (SSC**) accounts for approximately 25% of lung cancer (Lewis et al. 2014). It arises from the central bronchi and is strongly associated with smoking. It typically presents as a centrally located tumor and is characterized by the presence of squamous differentiation.
- **Large cell carcinoma (LCC)** is a heterogeneous group of NSCLC with poorly differentiated or undifferentiated morphology (Weissferdt 2014). It accounts for 3-9% of lung cancer cases. Large cell carcinoma lacks specific features of adenocarcinoma or squamous cell carcinoma.

The focus of this manuscript will be NSCLC, particularly adenocarcinoma, which represents the main subtype of lung cancer where patients with *RET* rearrangements are diagnosed.

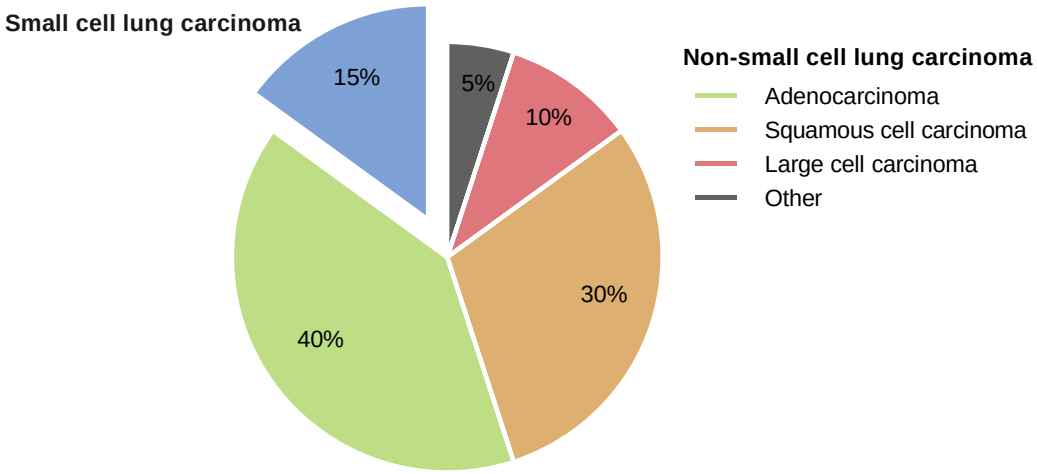

Figure 16: Classification of lung cancer subtypes based on histology. *(Data from Lewis et al. 2014)*

4.3. Non-small cell lung cancer (NSCLC)

4.3.1. Staging of NSCLC

Staging is an important aspect of lung cancer classification, which determines the extent of cancer spread. The most commonly used staging system is the TNM system, which considers the size of the primary tumor (T), the involvement of nearby lymph nodes (N), and the presence of distant metastasis (M) (Lim et al. 2018).

NSCLC is staged from I to IV, with subdivisions within each stage. During stage I, the tumor is limited to the lung without lymph node involvement. In stage II the tumor becomes larger with potential invasion of nearby structures and lymph nodes. At stage III the tumor spreads to lymph nodes in the chest and mediastinum. Stage IV is further divided into IVA, with the tumor spreading to distant organs within the chest, and IVB, indicating extensive metastasis outside the chest (Tsim et al. 2010).

In general NSCLC has a poor prognosis with an overall five-year survival rate of 15% across all stages (Zappa & Mousa 2016). This is primarily attributed to factors such as late diagnosis, frequent occurrence of metastasis, and high relapse rates, despite available treatments. However, there has been an improvement in lung cancer-specific survival rates over time, with an increase from 26% in men diagnosed with NSCLC in 2001 to 35% in those diagnosed in 2014 in the USA (Howlader et al. 2020). This progress is mainly due to the identification of the identification of “druggable” oncogenes and the development of targeted therapies (**see section 4.3.5 Targeted therapies for NSCLC**) (Shaw et al. 2016; Soria et al. 2018). Moreover, the recent success of checkpoint inhibitors positions them as the first line therapies in metastatic NSCLC (Huang et al. 2020).The majority of NSCLC cases are diagnosed at stage IV (46%), followed by stage III (24%) (Ruano-Raviña et al. 2020). Late diagnostics are common due to the nonspecific nature of most symptoms, which are often less frequent than

expected. Accurate staging of NSCLC is crucial for treatment decisions and prognosis assessment, as it helps determine the most suitable therapeutic approaches.

Moreover, advancements in molecular profiling technologies and the discovery of key genetic alterations in NSCLC have changed our understanding of lung cancer, allowing for a deeper insight into its pathogenesis and the development of targeted therapies.

4.3.2. Molecular classification of adenocarcinomas

The classification of lung adenocarcinomas into molecular subtypes is determined by the presence of well-defined molecular alterations that contribute to the initiation and advancement of cancer (Cancer Genome Atlas Research Network 2014). This categorization is established by identifying specific genetic modifications, such as point mutations, copy number alterations, rearrangements, insertions, and deletions, in key oncogenes that significantly influence cancer progression and can be specifically targeted for therapeutic strategies. The integration of molecular testing into routine clinical practice has enabled personalized treatment strategies, resulting in improved outcomes for lung cancer patients.

Most of these oncogenic drivers are RTKs and protein kinases that regulate intracellular signaling pathways. Key oncogene drivers and molecular alterations that contribute to the genomic subtypes of lung adenocarcinoma include *EGFR* alterations, *HER2*, *KRAS*, *BRAF* mutations, ALK and ROS1 fusions, *MET* exon 14 skipping mutations, and RET fusions (**Figure 17**) (Jordan et al. 2017).

EGFR mutations represent one of the most clinically relevant molecular alterations in adenocarcinoma (12-15%). In-frame deletions in exon 19 and the L858R point mutation in exon 21 are the most observed molecular alterations and account for approximately 90% of cases (Shigematsu & Gazdar 2006). These alterations activate EGFR signaling pathways that promote cell growth and survival. The identification of *EGFR* mutations has paved the way for the development of targeted therapies, such as EGFR tyrosine kinase inhibitors (TKIs), which have demonstrated significant clinical efficacy and improved outcomes in patients with *EGFR*-mutated lung cancer.

HER2 is a member of the ErbB family of tyrosine kinase receptors and shares similarities with EGFR. HER2 amplification is rarely observed in lung cancer, occurring in only about 1-2% of cases (Arcila et al. 2012). However, in approximately 3-4% of patients with metastatic lung adenocarcinoma, there are insertions or duplications affecting the kinase domain in exon 20 of *HER2*. These exon 20 insertions result in a structurally modified drug binding pocket and a rigid active conformation of the receptor, leading to resistance against commonly used TKIs (Robichaux et al. 2018).

KRAS, an oncogene encoding a small GTP binding protein, is frequently activated by missense mutations in various human cancers. In NSCLC *KRAS* mutations are detected in approximately 25% of cases, particularly in adenocarcinoma and among smokers. Several studies have shown that *EGFR* and *KRAS* mutations are mutually exclusive in NSCLC tumors (Kosaka et al. 2004; Marchetti et al. 2005). Furthermore, *KRAS* mutations have been associated with a lack of sensitivity to TKIs in lung adenocarcinoma (Pao, Wang, et al. 2005). The observation that *EGFR* and *HER2* gene mutations are more prevalent in non-smokers, whereas *KRAS* mutations are more common in smokers, indicates that the development of adenocarcinomas in those two groups involves distinct pathogenic pathways.

While KRAS binds to BRAF as part of the EGFR signaling cascade, *BRAF* mutations are rarely observed in lung cancer compared to *KRAS* mutations (3% of cases). The mutations of *EGFR*, *HER2*, *KRAS*, and *BRAF* were found to be mutually exclusive indicating that a single mutation in any of these genes may be sufficient for lung cancer pathogenesis (Shigematsu & Gazdar 2006). Interestingly, mutations in *RET*, *RAS*, and *BRAF* are also mutually exclusive in thyroid papillary cancer, suggesting similar patterns of exclusive mutations in different cancer types (Kimura et al. 2003).

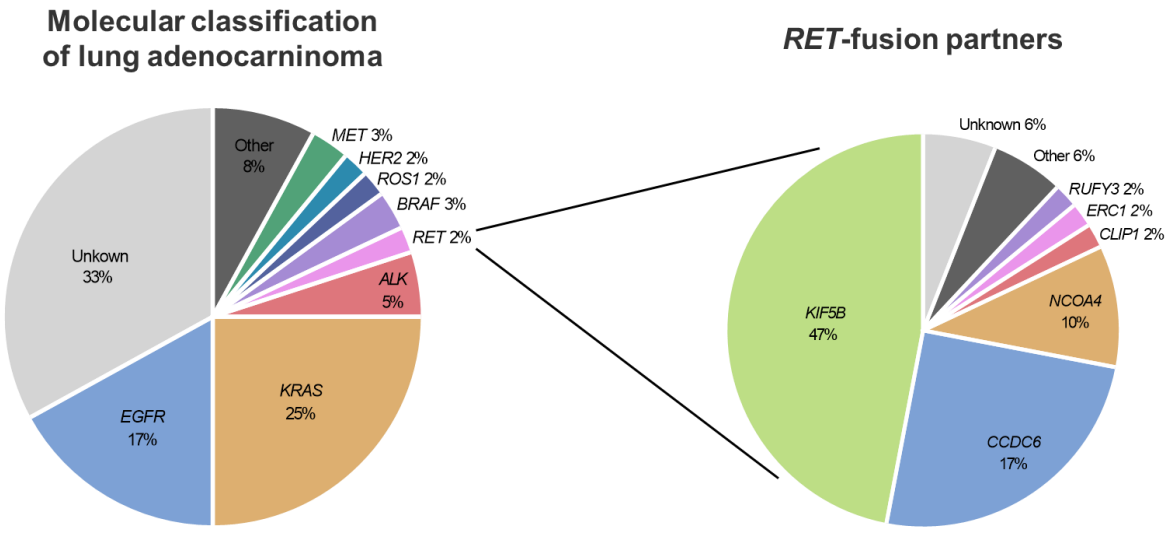

Figure 17: Molecular classification of lung adenocarcinoma and RET-fusion partners. *(Data from Pakkala & Ramalingam 2018 and Drilon et al. 2020).*

ALK and *ROS1* gene rearrangements represent another subset of driver alteration in NSCLC. They represent respectively 5% and 1-2% of all NSCLC cases, and are mostly adenocarcinoma (Du et al. 2018; Bergethon et al. 2012). These rearrangements lead to the formation of fusion proteins with constitutive kinase activity, promoting cell proliferation and survival thus driving tumor growth.

The Mesenchymal-Epithelial Transition (MET) proto-oncogene is an RTK which plays a crucial role in the MET process. MET oncogenesis is associated to the alterations in the splicing regulatory sites of exon 14 and/or MET amplification. These alterations are leading to exon 14 skipping, resulting in the

disruption of MET degradation process (Petrelli et al. 2002). *MET* exon 14 mutations are found in approximately 3% of NSCLC and can be targeted with MET TKIs (Awad et al. 2016). *MET* amplification, though less frequent, is often acquired during treatment with EGFR TKIs in *EGFR*-mutant patients as a resistance mechanism (Engelman et al. 2007a).

4.3.3. Role of RET in NSCLC

As mentioned in the **3.2.1 RET and cancers** section, RET has been implicated in various types of cancer. Recent studies have revealed the presence of *RET* rearrangements in 1-2% of cases of lung adenocarcinoma (Tsuta et al. 2014). Patients with RET-fusion positive NSCLC are mostly young-never smokers (Hess et al. 2021). The rearrangement between *RET* and another gene of unrelated origin arises from an abnormal DNA repair mechanism and leads to the activation of downstream signaling pathways involved in cell proliferation and survival (Mizukami et al. 2014) (**Figure 18**). There are at least 48 unique RET fusion partners identified in NSCLC, with the most common ones being KIF5B-RET and CCDC6-RET and others including NCOA4, CLIP1, ERC1, RUFY3 (**Figure 17**) (Ou & Zhu 2020). KIF5B-RET fusions are responsible for the activation of STAT3 and RAS-MAPK signaling pathway thus promoting tumor growth (**Figure 18**) (Qian et al. 2014; Schubert et al. 2021). *In vitro* studies using BaF3 cells transduced with a KIF5B-RET vector have demonstrated that KIF5B-RET enhances cell growth (Huang et al. 2016). Moreover, its role in promoting lung tumorigenesis has also been confirmed *in vivo* using *KIF5B-RET* transgenic mouse (Saito et al. 2014a).

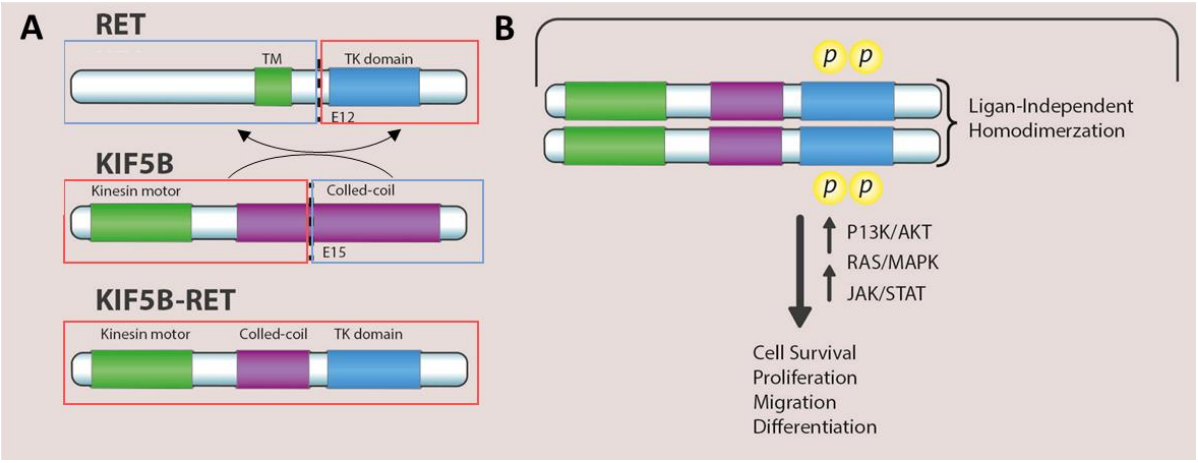

Figure 18: Example of a RET rearrangement causing constitutive activation of RET pathways. *(A) Rearrangement between RET and KIF5B caused by pericentric inversion of chromosome 10 leads to KIF5B-RET fusion protein and (B) activation of downstream pathways associated with cell survival, proliferation, migration and differentiation (Adapted from Ferrara et al. 2018).*

RET fusion-positive lung carcinomas exhibited more poorly differentiated tumors compared to those with *ALK* or *EGFR* alterations, indicating that RET fusions define a distinct molecular and clinicopathological subtype of NSCLC (Wang et al. 2012). Moreover, while *RET*-rearranged tumors are more sensitive to RET TKIs, previous evidence has indicated that RET signaling plays a significant role

in drug resistance, including resistance to EGFR TKIs and emerging $KRAS^{G12C}$ inhibitors in NSCLC (Piotrowska et al. 2018; Awad et al. 2021). Additionally, *RET*-rearranged patients typically exhibit low levels of PD-L1 expression and a low tumor mutational burden, but they tend to have unfavorable outcomes when treated with immunotherapies (Offin et al. 2019).

Gathering evidence suggests the presence of considerable clinical diversity within oncogenic driver-defined NSCLC subgroups, which the current single oncogenic driver model fails to fully address. For example, a study found co-occurrence of RET fusions with other genetic alterations, such as PI3K-associated genes or MAPK effector genes, in up to 82% of NSCLC patients (Kato et al. 2017). Moreover, *RET*-rearranged adenocarcinomas display high rate of *CDKN2A* loss (29% of tumors) and *CDKN2B* loss (23% of tumors), along with a high occurrence of *TP53* mutations (43%) (Parimi et al. 2023). Co-occurring genomic alterations in oncogenic drivers and tumor suppressor genes are emerging as crucial aspects of the molecular diversity of NSCLC as the therapeutic response of patients will be influenced by the presence of concurrent mutations alongside RET alterations.(Skoulidis & Heymach 2019).

The response to therapy will also depend on the recently identified stem cell plasticity state in lung cancers (Marjanovic et al. 2020). In this study, the evolution of tumor cells in a mouse model of adenocarcinoma was investigated using scRNA-Seq. Tumorigenesis was found to be associated with an increase in transcriptional heterogeneity independent of genetic variation, indicating the presence of structured mechanisms that control the emergence and persistence of heterogeneity. In contrast to embryonic development, where new states replace previous ones, this study shows that during tumor progression new states are acquired while existing ones are retained, resulting in progressively diverse cell populations within advanced tumors. A particular cell state emerged as a hub for transitions among cell states and is described as high-plasticity cell state (HPCS). The HPCS play a crucial role in generating diversity and aggressive cell states in advanced adenocarcinomas. These findings reveal that adenocarcinoma heterogeneity emerges rapidly from a highly plastic cells during tumorigenesis, shedding light on the importance of targeting such plastic cell states for cancer therapy.

Despite the complexity of lung cancer oncogenesis, RET signaling is a promising therapeutic target for the development of specific RET inhibitors in the treatment of cancer.

4.3.4. Current treatments for NSCLC

Historically, surgery has been the primary treatment modality for early-stage NSCLC. Patients with stage I, II, and IIIA NSCLC who are suitable for surgery may undergo tumor resection (Howington et al. 2013). Adjuvant therapy, such as radiation, chemotherapy, or targeted therapy, may be recommended after surgery to reduce the risk of disease recurrence and improve long-term outcomes. For example,

at stage IIA, IIB, and IIIA NSCLC, chemotherapy is often administered following surgery to eliminate any remaining cancer cells and improve long-term survival.

Radiotherapy is a treatment that utilizes high-energy beams to target and damage the DNA of cancer cells, leading to their destruction. It is particularly beneficial for patients with NSCLC that are confined to the chest and who are not suitable candidates for surgical resection. Radiotherapy can help control or eliminate tumors localized in specific areas of the body.

In advanced or metastatic NSCLC (stage IV), the treatment approach aims to extend survival and improve the quality of life. In this stage, a combination of cytotoxic chemotherapies has been the standard first-line therapy, offering modest improvements in overall survival for these patients (Ramalingam & Belani 2008). The median overall survival for these patients is typically around 8-10 months.

Despite advances in systemic therapy, the prognosis for stage IV NSCLC remains relatively poor, highlighting the need for more effective and targeted treatment options.

4.3.5. Targeted therapies for NSCLC

In recent years, the advent of precision medicine and the identification of targetable genetic alterations have revolutionized NSCLC therapy. As described above, most NSCLC oncogenic drivers are RTKs, or TK associated proteins. Consequently, TKIs have been developed and successfully employed to target these specific molecular alterations such as *EGFR* mutations, ALK, ROS1 and RET fusions, and others. These targeted therapies are responsible for improved response rates and prolonged progression-free survival. TKIs can be divided into two groups: multi-kinase inhibitors (MKIs), which are designed to inhibit multiple RTKs, and selective TKIs, which specifically target a single TK domain.

For the sake of simplicity and coherence, only targeted therapies against *RET*-rearranged NSCLC will be presented in this manuscript.

4.3.5.1. Multi-kinase inhibitors against *RET*-rearranged NSCLC

Several MKIs have shown activity against RET in the context of MTC, including Cabozantinib, Lenvatinib, Vandetanib, and Alectinib (Wells 2018). Among them, Cabozantinib and Vandetanib have been approved for advanced MTC by both the US Food and Drug Administration (FDA) and the European Medicines Agency (EMA). These MKIs have also been tested in the context of *RET*-rearranged NSCLC.

- **Cabozantinib** (XL-184) is a small molecule that primarily targets RET, VEGFR-2, and MET (Bowles et al. 2011). Initially used for treating thyroid cancers, its effectiveness has not been demonstrated except in the case of RET^{M918T} mutation (Kurzrock et al. 2011; Schlumberger et

al. 2017). However, it has been tested in various other types of tumors and showed anti-proliferative and pro-apoptotic effects in breast, lung, and glioma tumor model (Yakes et al. 2011). Moreover, several studies show that patients with *RET*-rearranged NSCLC treated with Cabozantinib present an increase in overall response rate (ORR), in progression-free survival (PFS) as well as in overall survival (OS) (Drilon et al. 2016; Schöffski et al. 2017; Nokihara et al. 2019).

- **Vandetanib** (ZD6474) is a drug that inhibits VEGFR2, EGFR, and RET (Morabito et al. 2009). Only two studies have investigated the effects of Vandetanib specifically in patients with *RET*-rearranged NSCLC. The phase II LURET trial examined Vandetanib in 19 advanced *RET*-rearranged NSCLC patients. The experimental drug resulted in a 47.4% ORR, a PFS of 6.5 months, and OS of 13.5 months (Yoh et al. 2021). Another phase II trial assessed Vandetanib and led to an ORR of 18%, an PFS of 4.5 months, and an OS of 11.5 months (Lee et al. 2017).
- **Lenvatinib** (E7080) is a MKI that inhibits VEGFR1-3, FGFR1-4, RET, and various other targets. A phase II trial showed an ORR of 16% and a median PFS of 7.3 months in patients with *RET*-rearranged adenocarcinoma treated with Lenvatinib (Hida et al. 2019).

It should be noted that there are preliminary studies reporting positive effects of other MKIs such as Alectinib or Apatinib on patients with RET-rearranged NSCLC (Lin, Kennedy, et al. 2016; Lin, Wang, et al. 2016).

MKIs have shown clinical utility in RET-driven cancers but their ORRs and PFS in *RET*-rearranged NSCLC are lower than those seen in other oncogene-driven NSCLCs treated with targeted TKIs. Complete response was also rarely reported in all clinical trials mentioned previously. The limited efficacy of MKIs on RET-driven cancers can be partially attributed to their off-target activity. Indeed, MKIs can target a wide spectrum of kinases beside RET, and the off-target effect can result in inferior inhibition of RET by non-specific interactions or pathway crosstalk. Additionally, an inhibitor may have different efficacies against various *RET* mutations and/or rearrangements with different fusion partners (Carlomagno et al. 2004). For instance, a study utilizing a Drosophila model of RET fusion cancer demonstrated that CCDC6-RET and NCOA4-RET fusions exhibit different sensitivities to TKIs (Levinson & Cagan 2016). Moreover, acquired resistance to MKIs can also occur through mutations in other genes or activation of bypass signaling pathways (Somwar et al. 2016; Nelson-Taylor et al. 2017). Hence, there is a need to develop selective RET inhibitors.

4.3.5.2. Selective RET tyrosine kinase inhibitors

Results of clinical trials led to the approval of novel potent and selective RET inhibitors, Pralsetinib (BLU-667) and Selpercatinib (LOXO-292), able to overcome the limits of previously used MKIs (Subbiah, Gainor, et al. 2018; Subbiah, Velcheti, et al. 2018). Both drugs have shown superior activity and

tolerability in early-phase trials and have received US FDA breakthrough designation. They showed high overall response rates in *RET*-mutated MTC and RET fusion-positive NSCLC.

- **Selpercatinib** is a drug that inhibits RET and has shown CNS penetration (Subbiah, Velcheti, et al. 2018). It has been effective in treating patients with RET-fusion positive NSCLC, even those with brain metastases (Guo et al. 2019; Tsui et al. 2022). The FDA granted its regular approval in September 2022. The most common adverse events were hypertension, increased liver enzyme levels, hyponatremia, and lymphopenia. The phase I-II LIBRETTOA trial, comprising 105 patients with RET-fusion positive NSCLC, showed an ORR of 64% and a PFS of 17.5 months (Drilon et al. 2020). Phase III trial comparing Selpercatinib to other treatments in treatment-naive patients is ongoing (Solomon et al. 2021).
- **Pralsetinib** is a drug designed to selectively target oncogenic RET alterations such as KIF5B-RET and CCDC6-RET fusions and RET^{C634Y} or RET^{M918T} mutations (Subbiah, Gainor, et al. 2018). It has lower affinity for VEGFR2 compared to Vandetanib and Cabozantinib. In the phase II part of the ARROW trial, 233 patients with RET-fusion positive NSCLC were enrolled and treated with Pralsetinib. This treatment showed an ORR of 61% in chemotherapy-treated patients and 70% in treatment-naïve and complete responses were observed in 6% and 11% of these two groups, respectively. (Gainor et al. 2021). It also induced intracranial response in patients with intracranial metastases.

Other selective RET inhibitors such as BOS172738 or TPX-0046 are in early stages of development (Drilon et al. 2019; Schoffski et al. 2019).

The adverse events associated with these TKIs are generally mild and drug discontinuation rates are low. However, more research is needed to fully understand the safety profiles of these RET inhibitors. Moreover, resistance mechanisms to these drugs are an active area of research.

4.3.5.3. Mechanisms of resistance

Despite the initial success of targeted therapies, the development of resistance remains a significant challenge in NSCLC treatment. Resistance mechanisms can arise due to acquired secondary *RET* mutations or to the activation of alternative signaling pathways.

Acquired secondary *RET* mutations, including gatekeeper mutations $RET^{V804L/M}$, have been associated with resistance to MKIs such as Vandetanib (Carlomagno et al. 2004; Dagogo-Jack et al. 2018). Another example is the mutation RET^{S904F} that also confers resistance to Vandetanib (Nakaoku et al. 2018). Moreover, in a multi-institutional study of 23 patients with advanced RET fusion-positive NSCLC treated with selective RET TKIs Pralsetinib and Selpercatinib, acquired *RET* mutation were identified as recurrent mechanisms of resistance (Lin et al. 2020). For example, RET^{G810R} mutation has

been identified as a mechanism of resistance to Selpercatinib in NSCLC and MTC (Solomon et al. 2020). However, *RET* resistance mutations were detected at a low frequency and most of the resistance appears to be driven by RET-independent mechanisms.

Studies have identified co-occurrence of *RET* rearrangements with somatic alterations in MAPK and PI3K pathways, potentially contributing to the development of drug resistance (Nelson-Taylor et al. 2017). These genetic alterations worked together to restore RAS/MAPK activation and counteracted the effect of RET inhibition. Furthermore, *MET* gene amplification is another mechanism of RET-independent resistance (Lin et al. 2020). It is also a well-known resistance mechanism to EGFR inhibitors in *EGFR*-mutant NSCLC (Engelman et al. 2007b). The combination of EGFR and MET inhibitors has demonstrated efficacy in overcoming MET-driven resistance, indicating its potential for addressing RET-independent resistance in patients with *RET*-rearranged NSCLC (Sequist et al. 2020). Finally, *KRAS* amplification has been identified as a causative factor for resistance to targeted therapies in various scenarios such as resistance to ALK or MET TKIs in NSCLC (Hrustanovic et al. 2015; Bahcall et al. 2018). It also has been detected in Selpercatinib resistant patient which makes it a potential driver in *RET*-rearranged NSCLC TKIs resistance (Lin et al. 2020).

The introduction of potent selective RET inhibitors, such as Pralsetinib and Selpercatinib, represented a breakthrough in managing patients with RET fusion-positive NSCLC. However, it is imperative to continue developing next-generation inhibitors, exploring combination strategies, and deepening our understanding of resistance mechanisms. These efforts are crucial to overcome treatment failures and further improve the efficacy of these therapies. Achieving that requires the utilization and the development of accurate models of lung cancer.

4.4. Experimental models of lung cancer

Human preclinical models that accurately capture the heterogeneity of cancer are crucial for understanding cancer biology and developing effective treatments. Several major approaches are currently available including cancer cell lines, genetically engineered mouse (GEM) models, patient-derived xenograft (PDX) models and organoid models. The following discussion explores these strategies along with their respective advantages and limitations.

4.4.1. Cancer cell lines

Cancer cell lines have been extensively utilized in lung cancer research to gain insights into the biology of the disease and develop potential treatments. These cell lines are derived from tumor tissue obtained from lung cancer patients and cultured *in vitro.* More than 300 cell lines have been established from NSCLC and SCLC (Gazdar et al. 2010). They provide a renewable resource of pure

cancer cells that are relevant to the parental tumor (Wistuba et al. 1999). They can be easily propagated and manipulated for experimental purposes.

Cancer cell lines offer several advantages in studying lung cancer, including the ability to investigate the molecular mechanisms underlying tumor development, progression, and response to therapies. They allow researchers to perform high-throughput drug screening and assess the efficacy of potential anti-cancer agents (Luo et al. 2009). Furthermore, cancer cell lines serve as valuable models for studying drug resistance mechanisms and identifying predictive biomarkers (Pao, Miller, et al. 2005; Gandhi et al. 2009). For example, several *RET*-rearranged derived cell lines have been derived from patients and have shown a differential response to RET inhibitors (Nelson-Taylor et al. 2017).

However, it is important to note that the experiments using cancer cell lines have limitations, such as genetic and phenotypic drift from the original tumor after extensive passages and the lack of a tumor microenvironment (Grigorova et al. 2005). Although useful in some circumstances, cancer cell line models may not fully recapitulate the complexity and heterogeneity of tumors *in vivo*. Therefore, it is crucial to complement studies using cancer cell lines with other models, such as GEM models, PDXs, or organoids to better recapitulate the complexity of lung cancer.

4.4.2. Genetically engineered mouse models

Genetically engineered mouse (GEM) models provide a powerful tool for studying lung cancer by introducing specific genetic alterations in mice relevant to human lung tumorigenesis. These alterations can include the activation of oncogenes or the inactivation of tumor suppressor genes, mirroring the molecular events observed in human lung cancer. GEM models can be engineered to develop spontaneous lung tumors or specific lung cancer subtypes, allowing the study of tumor initiation, progression, and metastasis. They enable the investigation of tumor biology, the evaluation of therapeutic interventions, and the exploration of mechanisms underlying drug resistance. GEM models closely mimic the genetic and histopathological characteristics of human lung cancer, making them highly valuable for translational research.

The initial *KRAS* mutant lung cancer model demonstrated that activating KRAS alone is sufficient to induce adenocarcinoma in mice (Jackson et al. 2001). Various GEM models have since been created, utilizing conditional systems and inducible models. The majority of these studies employ a conditional allele that activates the $KRAS^{G12D}$ mutation via Cre-mediated recombination (DuPage et al. 2009). Other KRAS alleles, including $KRAS^{G12C}$, have been modeled using similar approaches and are valuable for investigating new KRAS inhibitors (Li et al. 2018). Similarly, GEM models were developed for *EGFR*-mutant lung cancer following the discovery of *EGFR* mutations as a driver for NSCLC and therefore a potential target for TKIs (Lynch et al. 2004; Paez et al. 2004). These models express specific *EGFR*

mutations, such as *EGFR*^{L858R}, in lung type II pneumocytes upon doxycycline administration (Politi et al. 2006; Ji et al. 2006). These models recapitulate EGFR driven adenocarcinoma development and have provided insights into tumor initiation and the dependence of tumor cells on mutant oncogene expression for survival. Furthermore, GEM models have also been developed for other lung adenocarcinoma drivers, including ROS1 or ALK as well as KIF5B-RET (Arai et al. 2013; Pyo et al. 2017; Saito et al. 2014a), as well as for different lung cancer types such as SCLC or SCC (Schaffer et al. 2010; Xiao et al. 2013).

4.4.3. Patient-derived xenograft models

While traditional 2D cell cultures can be used to grow primary tumor tissues *in vitro,* they lack the phenotypic and genetic diversity present in the original tumors. To address this limitation, surgically isolated primary clinical tumor samples can be grafted into mice, known as patient-derived xenografts (PDX). PDX models maintain the tumor architecture and the proportion of cancer cells and stromal cells, providing a better representation of the original tumor compared to cell lines (Byrne et al. 2017). PDX models have been developed for a variety of cancers, including lung cancer (Cutz et al. 2006). The success rate of PDX establishment has improved with the use of immunocompromised mice such as NOD/SCID/IL2Rγ_{null} (NSG) (Shultz et al. 2005).

However, the limited availability of tumor material may result in incomplete representation of tumor heterogeneity (Kemper et al. 2015). Additionally, clonal selection and evolution may occur during tumor tissue engraftment, leading to variations between the primary tumor and PDXs. For example, a study revealed that only 43% of the mutations identified in primary non-NSCLC tumors were found in the corresponding PDX (Morgan et al. 2017). Additionally, four new mutations emerged in early passages of PDXs that were not present in the original tumor.

Multiple biopsies from different regions of a tumor and early passages of PDXs are recommended to capture the complete tumor architecture and ensure translational relevance. Furthermore, not all patient-derived tumors can be successfully engrafted as the engraftment rates of PDXs vary among different cancers, with sub-clones of advanced tumors demonstrating better growth as PDXs (Rosfjord et al. 2014). Moreover, clonal selection is observed over passages of PDXs, with higher passage numbers correlating with higher tumor grade (Pearson et al. 2016).

In recent years, it has become evident that orthotopic transplantation (ie, in the original organ) offers a more physiologically relevant model for PDXs compared to heterotopic engraftment. Orthotopic transplantation allows for the investigation of tumor-host interactions in the specific anatomical site of primary and secondary tumor growth, as well as metastasis development (DAI et al. 2015; Hoffman 2015). Studies comparing orthotopic and subcutaneous xenografts of pancreatic ductal

adenocarcinoma have revealed metabolic differences attributed to variations in the tumor microenvironment resulting from different engraftment sites (Zhan et al. 2017). These findings emphasize the complexity of cancer and the significance of the transplantation site and environment. However, despite the superior resemblance to primary tumors offered by orthotopic PDXs, this method is technically challenging and time-consuming, leading most studies to still rely on subcutaneous engraftment of tumor tissue.

4.4.4. Organoid models

4.4.4.1. Lung cancer organoids

Organoids are defined as a 3D structure that develops from stem cells and exhibiting self-organization giving rise the architectural complexity and multi cell lineages closely resembling the organs. In 2009, Sato et al. achieved a significant breakthrough by establishing 3D epithelial organoids from mouse intestinal stem cells (Sato et al. 2009). By adapting this protocol to other tissues, it was possible to develop lung organoids from lung stem cells. Indeed, a study demonstrated the formation of tracheospheres by basal cells and the successful culture of different types of lung epithelial cells, such as distal epithelial cells and alveolar epithelial progenitor cells in organoid models (Rock et al. 2009). In 2010, McQualter and colleagues demonstrated that specific population of lung epithelial cells form distinct spherical structures when co-cultured with freshly isolated lung mesenchymal cells (McQualter et al. 2010). Additionally, Chapman and colleagues successfully established organoid cultures derived from integrin $\alpha6\beta4^{+}$ alveolar epithelial progenitor cells (Chapman et al. 2011). These experiments have shown the existence of a cell hierarchy within the adult lung and the existence of a lung stem/progenitor cell capable of generating a lung organoid *in vitro.* Therefore, lung organoids have proven to be a valuable tool for studying lung epithelial stem/progenitor cells i*n vitro*.

Organoids have also been used for studying lung cancer processes as they offer a more sophisticated representation of the tumor microenvironment. Patient-derived tumor spheroids have been successfully established, exhibiting characteristics consistent with matched patient tumor samples, including interactions between cancer cells, stromal cells, and immune cells (Di Liello et al. 2019). These spheroids also display tubular structures and branching morphogenesis. They express markers confirming their adenocarcinoma origin, such as TTF-1/NKX2-1 (Zhang et al. 2018). Another study shows that lung cancer organoids derived from adenocarcinoma tissues exhibit acinar or large glandular patterns and express specific markers like TTF-1/NKX2-1, napsin-A, and cytokeratin 7 (Kim et al. 2019). These findings highlight the similarity between tumor and cancer organoids, therefore demonstrating their potential for studying lung cancer and developing targeted treatments.

By replicating the specificity of a cancer, organoids can capture the genetic heterogeneity and progression-related modifications observed in the original tumors. Therefore, they can recapitulate drug responses and provide a more physiologically relevant model for testing anti-cancer drugs (Xu et al. 2018). For example, multicellular tumor spheroids have been used to analyze drug sensitivity and investigate the molecular mechanisms involved in drug resistance (Barrera-Rodríguez & Fuentes 2015). Moreover, lung cancer organoids derived from individual patients have been employed in high-throughput drug screening assays (Sachs et al. 2019).

Organoids have emerged as a valuable model for studying patient-specific responses to anti-cancer drugs, particularly in lung cancer. For example, organoids derived from a patient with *HER2*-mutant lung cancer helped identify Pyrotinib as the most effective drug among various anti-HER2 therapies *in vitro* but also *in vivo* (Wang et al. 2019). Subsequent clinical studies confirmed the efficacy of Pyrotinib in *HER2*-mutant NSCLC patients.

However, a limitation to this approach is the requirement for tissue samples, which may not always be available or representative of the hierarchical subtypes of a tumor. This issue could be solved by iPSC-derived organoids.

4.4.4.2. iPSC-derived organoids

More recently, iPSC-derived organoids have gained attention because they combine the self-organization potential of iPSCs with the ability to differentiate into organ-specific cell types (Garreta et al. 2021). Researchers have successfully generated organoids resembling various organs using iPSC-derived technology. For example, iPSC-derived intestinal organoids have been developed by mimicking human embryonic gut development, allowing the generation of functional structures with absorption and exocrine functions (Spence et al. 2011). Similarly, iPSC-derived brain organoids, including specialized cells such as oligodendrocytes and astrocytes, have been generated in 3D culture systems (Lancaster et al. 2013; Giandomenico et al. 2021). These brain organoids have been used to model microcephaly and study neural development (Lancaster et al. 2013; Renner et al. 2017). Furthermore, iPSC-derived liver, kidney and cardiac organoids have also been generated in the past years (Takebe et al. 2013; Takasato et al. 2015; Cyganek et al. 2018).

As described in section **1.4 Utilization of iPSCs for disease modeling and therapy**, iPSCs have revolutionized the field of disease modeling and regenerative medicine. These cells have the remarkable ability to serve as an inexhaustible source of patient-specific cells, enabling researchers to study disease mechanisms, facilitate drug discovery, and develop personalized cell-based therapies with unprecedented potential (Turhan et al. 2021). Indeed, the generation of iPSC-derived lung organoid from diverse individuals with different genetic susceptibilities allows for the creation of

patient-specific lung organoids. These organoids have the potential to shed light on the variations in disease susceptibility and aid in optimizing therapeutic interventions by enabling the adjustment of drug doses to mitigate such disparities. In conclusion healthy iPSC-derived organoids could be a source of transplantable tissues on a large scale in the future while patient-derived organoids could be major tools for diseases modeling.

4.4.4.3. iPSC-derived lung organoid models

With their 3D organization, iPSC-derived organoids can reconstruct the interactions between different tissues involved in oncogenesis and precisely imitate organ dysfunction. The generation of iPSC-derived lung organoids mirrors the steps observed during lung embryonic development. As discussed previously (see section **4.1.2 Stages of human lung development**), during embryogenesis, lung buds emerge from the foregut and then undergo branching morphogenesis forming a tree-like structure. As development progresses, the cells will differentiate into the components of the lung, including the airways, alveoli, and blood vessels. Signaling pathways, such as the FGF, BMP and Wnt pathways, play crucial roles in directing the differentiation and patterning of these cell types (Rankin & Zorn 2014).

Hence, generation of iPSC-derived lung organoid should follow the same steps. For example, Dye et al. have developed a novel three-dimensional model of the human lung using stem cells. By inducing FGF-2 they guided hESC to form human foregut expressing NKX2-1, a marker of lung progenitor (Dye et al. 2015). This tissue then developed into three-dimensional spherical structures when cultivated in $Hedgehog^{High}$ condition supplemented with FGF10. The resulting lung organoids survived and matured, expressing progenitor markers SFTPC/SOX9 and HOPX/SOX9 consistent with alveolar progenitors identities (Treutlein et al. 2014; Desai et al. 2014b). This research offers a promising method for creating human lung organoids in culture, providing opportunities to explore lung development and diseases. Consequently, we used a similar protocol for the research presented in this manuscript (**Figure 19**) (Leibel et al. 2020). The process involves enzymatic disruption of iPSCs and their differentiation into lung progenitor cells expressing NKX2-1 following sequential steps. First the induction of the definitive endoderm (DE) expressing CXCR4 and SOX17 (D'Amour et al. 2005). Then the generation of anterior foregut endoderm (AFE), characterized with the expression of FOXA2 and SOX2, by the inhibition of BMP and TGF-β signaling pathway (Green et al. 2011). Finally, the cells are specified into lung progenitor cells (LPC) expressing NKX2-1 (Minoo et al. 2007). These cells are then suspended in a matrix and cultured as 3D organoids, mimicking lung branching and maturation.

Maintaining the 3D configuration allows the development of surfactant-producing alveolar cells and ciliated cells when exposed to an air-liquid interface.

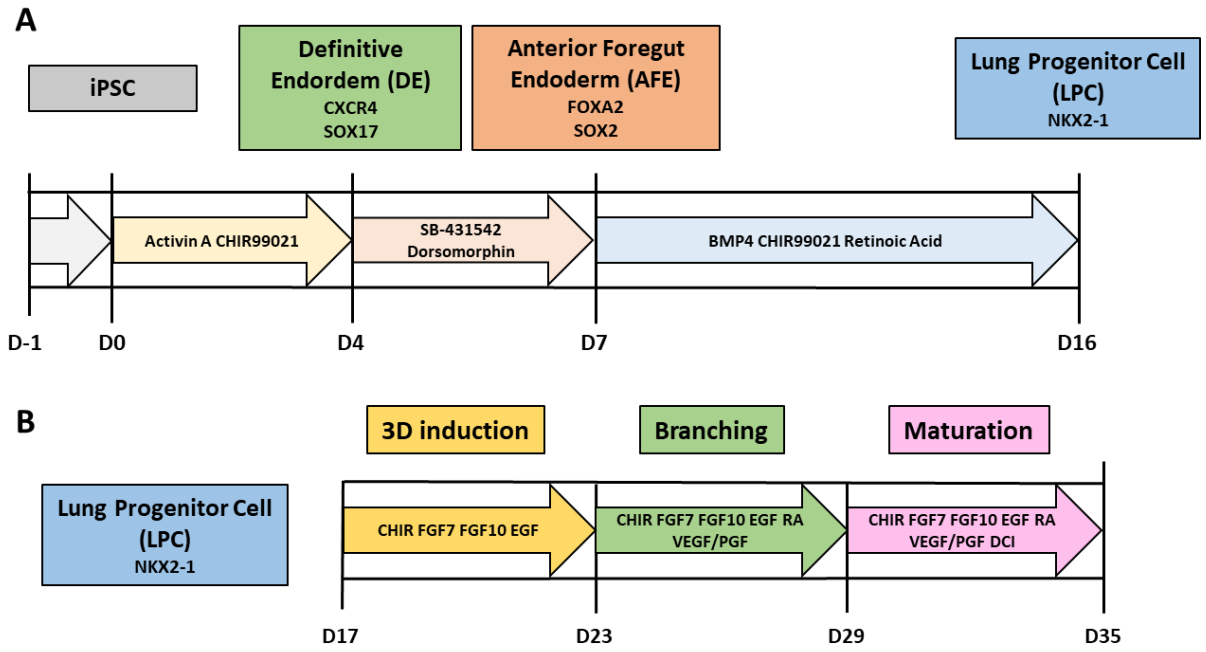

***Figure 19: Chronological progression of iPSCs differentiation to lung organoids**. **(A)** Monolayer culture stages from iPSC to definitive endoderm (DE) characterize by CXCR4 and SOX17 expression, anterior foregut endoderm (AFE) expressing FOXA2 and SOX2, and ultimately lung progenitor cells (LPCs) NKX2-1 positive. **(B)** Step-by-step process for differentiating LPCs into 3D lung (adapted from Leibel et al. 2020).*

A model of lung cancer from iPSC-derived organoids has been developed with the induction of *KRAS*^{G12D} during iPSC lung differentiation (Dost et al. 2020). This work reveals that iPSC-derived *KRAS*^{G12D} lung organoids exhibit a distinct transcriptional profile compared to normal lung organoids. Specifically, they display a gene expression signature characteristic of early-stage adenocarcinoma. Overall, this study establishes the viability of iPSC-derived lung cancer model and paves the way for the creation of additional lung cancer organoids incorporating other oncogenic drivers such as RET.

Patient-derived iPSC lung organoids have the potential to provide even greater accuracy in modeling lung cancer due to their expression of endogenous levels of oncogenic drivers. By differentiating in parallel organoids from patient-derived iPSCs and their CRISPR-corrected isogenic control iPSCs it is possible to identify the distinct characteristics linked to the mutation (**Figure 20**). These organoid models hold great promise for identifying novel targets and facilitating drug screening processes. However, there are currently no models of patient-derived-iPSC lung organoid. The development of such models could replicate cancers and help capture the genetic heterogeneity and progression-related modifications observed in the original tumors.

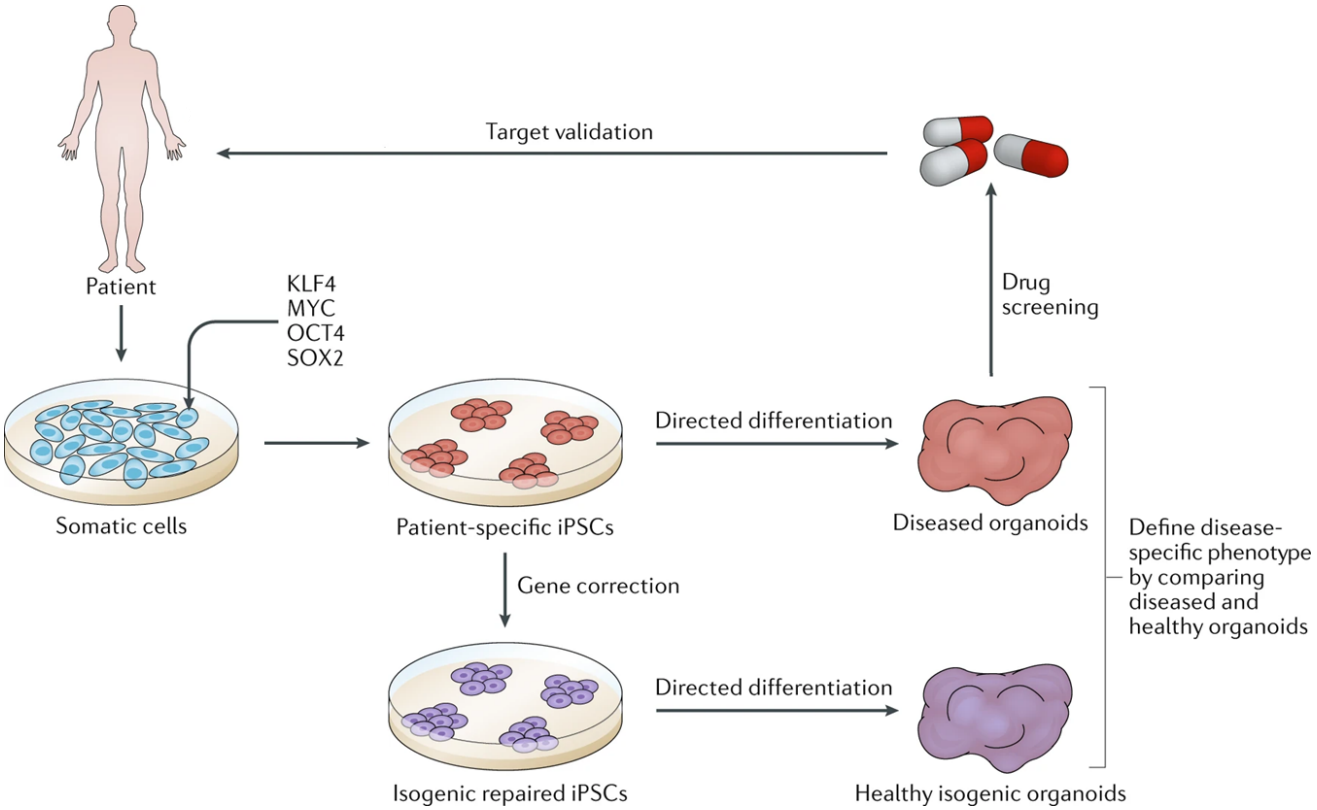

Figure 20: iPSC-derived organoids for disease modelling and drug discovery. *Simultaneously differentiation of organoids from patient-derived iPSCs and its CRISPR corrected isogenic control iPSC allows for identifying the specific characteristics associated with the mutation. These organoid models have the potential to be used for the identification of new targets and for conducting drug screening (Rowe & Daley 2019).*

In conclusion, the development of organoids has revolutionized the field of disease modeling, including lung cancer research. Lung cancer organoids have been successfully generated, offering a more sophisticated representation of the tumor microenvironment. Moving forward, patient-derived iPSC lung organoids hold great promise for modeling lung cancer with higher accuracy, capturing genetic heterogeneity, and reflecting the progression-related modifications observed in original tumors.

PHD OBJECTIVES

The first objective of my PHD was to investigate the role of the tyrosine kinase receptor RET in iPSC derived hematopoiesis. The first article aims to understand the impact of RET activation on the differentiation of iPSCs into hematopoietic stem cells (HSCs). Previous research has shown positive effects of RET activation in mice and cord blood HSCs, but its role in iPSC-derived hematopoiesis is not yet known. By differentiating iPSCs with the *RET*^{C634Y} somatic mutation and comparing them with control iPSCs, the study aims to unravel the specific characteristics linked to RET activation during hematopoietic differentiation.

The second objective of my PHD consisted in establishing a model of RET-driven NSCLC using iPSCs. The second article described the generation of lung cell progenitors (LPCs) from patient-derived iPSCs carrying the *RET*^{C634Y} somatic mutation and the validation of the effect of this mutation. Through phenotypic and molecular analysis, this article seeks to demonstrate that these RETC^{634Y} iPSC-derived LPCs exhibit characteristics resembling those of RET-driven NSCLC. This study also intends to evaluate the response of these cells to a specific RET inhibitor, Pralsetinib, providing insights into potential therapeutic interventions. Ultimately, this article aims to establish a novel patient-derived iPSC model for RET-driven NSCLC, which can be utilized for studying disease mechanisms, exploring disease progression, and identifying potential new therapeutic targets.

Overall, the goal of this thesis was to use iPSCs as a versatile tool to investigate the role of a major driver gene on different biological processes and model different tissue with the same iPSCs. I focused my work on understanding the role of RET in hematopoiesis and its implications in RET-driven NSCLC for the development of novel therapies.

RESULTS

RESULTS

1. Article 1: Impact of the Overexpression of the Tyrosine Kinase Receptor RET in the Hematopoietic Potential of Induced Pluripotent Stem Cells (iPSCs)

This article is the first part of my PhD manuscript, where I explored the role of RET in iPSC-derived hematopoiesis. Indeed, previous studies have suggested that RET plays a significant role in the hematopoietic potential in mice and could also be used to expand UCB derived HSC (Fonseca-Pereira et al. 2014; Grey et al. 2020). The potential role of RET in the iPSC-derived hematopoiesis has not been tested so far. This question is of major interest since obtaining ES or iPSC-derived HSCs is not currently achievable, thus the possibility of inducing HSCs from iPSCs would have major medical implications.

To assess how RET affects the hematopoietic potential of iPSC, we used several strategies. These methods involved activating the RET pathway by either its ligand GDNF or either by the overexpression of *RET* wild type (WT) and RET^{C634Y} mutation in iPSCs. We also used an iPSC derived from a patient harboring the RET^{C634Y} mutation and its CRISPR-corrected isogenic control. Hematopoietic potential was tested using 2D cultures allowing generation of large numbers of hematopoietic cells evaluated regarding their phenotype and their clonogenic potential. We then performed transcriptomic analyses on these cells, and we verified with qPCR the expression of genes found to be modulated by RET.

Two normal iPSC lines cultured with or without GDNF generated similar numbers of $CD34^+$ and $CD34^+/CD38^-$ cells. On the other hand, the same experiments performed using iPSC with RET overexpression led to a significant reduction in the number of HSCs ($CD34^+/CD38^-/CD49f^+$) as compared to control iPSC. RET overexpression was also found to alter the clonogenic potential of HSCs. Similarly, the hematopoietic potential of a patient-derived iPSC line with a constitutive RET^{C634Y} mutation was reduced as compared to its CRISPR-corrected isogenic control. Transcriptomic analyses revealed a specific activated expression profile for RETC634Y compared to its control with evidence of overexpression of genes which are part of the MAPK network with negative hematopoietic regulator activities.

Thus, as opposed to the findings reported in mice knock-out model and in UCB expansion, RET activation/overexpression in iPSCs does not give rise to an increased hematopoietic potential but is rather associated with an inhibitory activity, potentially related to MAPK activation.

Cytotherapy 000 (2023) 1–10

Contents lists available at ScienceDirect

CYTOTHERAPY

journal homepage: www.isct-cytotherapy.org

International Society ISCT Cell & Gene Therapy®

Full-length article

Impact of the overexpression of the tyrosine kinase receptor RET in the hematopoietic potential of induced pluripotent stem cells (iPSCs)

Paul Marcoux[1,2], Jusuf Imeri[1,2], Christophe Desterke[1,2], Theodoros Latsis[1], Diana Chaker[1,4], Patricia Hugues[1,2], Annelise Bennaceur Griscelli[1,2,3,4,5], Ali G. Turhan[1,2,3,4,5,*]

[1] *INSERM UMR-S-1310, Université Paris Saclay, Villejuif, France*
[2] *Université Paris-Saclay, Faculté de Médecine, Le Kremlin Bicetre France*
[3] *Department of Hematology, APHP Paris Saclay, Hôpital Bicetre, Le Kremlin Bicetre France*
[4] *CITHERA, Centre for iPSC Therapies, INSERM UMS-45, Genopole Campus, Evry, France*
[5] *Department of Hematology, APHP Paris Saclay, Hôpital Paul Brousse, Villejuif, France*

ARTICLE INFO

Article History:
Received 7 August 2023
Accepted 5 October 2023
Available online xxx

Key Words:
CD34
hematopoietic differentiation
HSCs
iPSCs
RET

ABSTRACT

Introduction: Previous studies have suggested that the tyrosine kinase receptor RET plays a significant role in the hematopoietic potential in mice and could also be used to expand cord-blood derived hematopoietic stem cells (HSCs). The role of RET in human iPSC-derived hematopoiesis has not been tested so far.
Methods: To test the implication of RET on the hematopoietic potential of iPSCs, we activated its pathway with the lentiviral overexpression of RET^{WT} or RET^{C634Y} mutation in normal iPSCs. An iPSC derived from a patient harboring the RET^{C634Y} mutation ($iRET^{C634Y}$) and its CRISPR-corrected isogenic control iPSC ($iRET^{CTRL}$) were also used. The hematopoietic potential was tested using 2D cultures and evaluated regarding the phenotype and the clonogenic potential of generated cells.
Results: Hematopoietic differentiation from iPSCs with RET overexpression (WT or C634Y) led to a significant reduction in the number and in the clonogenic potential of primitive hematopoietic cells ($CD34^+/CD38^-/CD49f^+$) as compared to control iPSCs. Similarly, the hematopoietic potential of $iRET^{C634Y}$ was reduced as compared to $iRET^{CTRL}$. Transcriptomic analyses revealed a specific activated expression profile for $iRET^{C634Y}$ compared to its control with evidence of overexpression of genes which are part of the MAPK network with negative hematopoietic regulator activities.
Conclusion: RET activation in iPSCs is associated with an inhibitory activity in iPSC-derived hematopoiesis, potentially related to MAPK activation.
© 2023 International Society for Cell & Gene Therapy. Published by Elsevier Inc. All rights reserved.

Introduction

Hematopoietic stem cells (HSCs) are multipotent cells that give rise to all blood cells [1]. They are located in the bone marrow (BM) niche where they maintain blood and immune cell homeostasis through a balance of self-renewal and differentiation [2]. Alterations of HSCs or bone marrow homeostasis are a major cause of blood diseases such as leukemia, lymphoma or myeloma [3–5]. Hematopoietic stem cell transplantation (HSCT) remains the mainstay of the therapies for acute leukemias in allogeneic settings, and that of other hematopoietic malignancies in autologous settings in high-risk multiple myeloma [6,7] and aggressive refractory/relapses lymphomas [8].

Several attempts have been made in the past to expand true HSCs using *in vitro* established techniques in the presence of cytokines and starting with bone marrow (BM), umbilical cord blood (UCB) or mobilized peripheral blood cells [9–13]. These attempts have not generated so far a methodology to manufacture transplantable true HSCs in clinically applicable settings. The use of double cord blood transplantation, especially in adults, has been used to circumvent these difficulties [14].

The generation of functional and engraftable HSCs from induced pluripotent stem cells (iPSC) is a major goal that would lead to clinical applications. However, current protocols do not enable the generation of mature and engraftable HSCs [15]. With the current protocols, iPSC-derived HSCs can produce matured blood cells in a process resembling primitive hematopoiesis [16,17] but they lack engraftment and repopulation capacities. A better knowledge of the mechanisms of iPSCs hematopoietic differentiation and the improvement of the current protocols to generate more BM/UCB HSCs-like cells from iPSCs are needed for developing HSCs generation from iPSCs.

Previous studies have shown the implications of receptor tyrosine kinases (RTKs) in hematopoietic stemness potential and maintenance

* Correspondence: Ali G. Turhan, INSERM UMR-S-1310, Université Paris Saclay, Villejuif, France.
E-mail address: ali.turhan@inserm.fr (A.G. Turhan).

https://doi.org/10.1016/j.jcyt.2023.10.003
1465-3249/© 2023 International Society for Cell & Gene Therapy. Published by Elsevier Inc. All rights reserved.

[18,19]. RET (rearranged during transfection) protooncogene is an RTK that transmits a proliferative signal in the presence of its co-receptor GDNF (glial cell line-derived neurotrophic factor) family receptor alpha-1 (GFRα1) and in response to GDNF-ligands families (GLF). RET is known to be expressed in intermediate mature myeloid cells and in acute myeloid leukemia [20,21]. Previous studies have suggested that RET plays a key role in the emergence of hematopoietic potential in mice [22]. Others showed the improvement of cord blood (CB) HSCs survival and expansion when the RET pathway is activated by the addition of its ligand/coreceptor GDNF/GFRα1 [23]. Moreover, HSCs frequency is 4-fold higher in the RET-positive compartment compared to RET-negative cells [23]. However, the effect of RET expression during iPSC-derived hematopoietic differentiation has not been evaluated so far.

The mutation *RET*^{C634Y} (exon 11) is responsible for the RET dimerization in the absence of its ligands, leading to autophosphorylation of the tyrosine kinase domain and constitutive activation of downstream signaling pathways [24]. We have used this property to test the effect of RET during iPSC-derived hematopoietic differentiation. We have generated different RET-overexpressing iPSC models with either wild-type RET (RET^{WT}) or mutated RET (RET^{C634Y}) receptors. Additionally, we have used a patient-derived iPSC line carrying the RET^{C634Y} somatic mutation (iRET^{C634Y}) and its CRISPR-corrected isogenic control (iRET^{CTRL}). With the use of these tools, we have tested the hematopoietic potential of iPSCs using *in vitro* assays. Interestingly, as opposed to the results obtained in mice KO model and in cord blood cells, we show that RET activation during iPSCs hematopoietic differentiation reduces the hematopoietic potential. We have performed transcriptome analyses revealing the activation of some regulatory factors, such as DLK1, that could be involved in hematopoietic inhibition. This work provides a better understanding of the effects of RET activation during iPSC-derived hematopoietic differentiation.

Materials and Methods

Generation of iPSCs

PB33-WT and PB68-WT iPSCs were both generated from peripheral blood mononuclear cells from healthy donors with the informed consents according to the Declaration of Helsinki. Peripheral blood mononuclear cells were reprogrammed by non-integrative Sendai viral transduction. Pluripotency was characterized by FACS and teratoma assays. Generation of RET mutated iPSC iRET^{C634Y} and its isogenic CRIPSR corrected control iRET^{CTRL} have been previously described [25,26].

iPSC cultures

iPSCs were cultured in feeder-free condition on Geltrex coated dishes (A1413201; ThermoFisher Scientific, France) and fed daily with Essential 8 flex Medium (A2858501; ThermoFisher Scientific, France). iPSCs were passaged twice a week with EDTA dissociation (0.5 mM).

Hematopoietic differentiation from iPSCs

Hematopoietic differentiation of iPSCs has been performed using a STEMDiff hematopoietic kit (05310; STEMCELL Technologies, France) according to the manufacturer's recommendations. Briefly, iPSCs have been dissociated in aggregates of 50–100 μm by using EDTA (0.5 mM). Fifty aggregates have been seeded per well in a 12-well cell culture plate (Corning, France) coated with Geltrex (A1413202; Gibco, France). The medium was changed according to the manufacturer's instruction and floating cells were harvested on day +13 of hematopoietic differentiation. For the GDNF/GFRα1 experiment, 100 ng/mL of GDNF & GFRα1 mixed 1:1; (212-GD-010, 714-GR-100; R&D Systems, France) were added to the media. Cells were thereafter washed and resuspended in PBS. Stained cells were analyzed with a BD LSRFortessaTM (BD Biosciences, USA) flow cytometer and FlowJo analysis software.

Table 1
Antibody fluorophores and references.

Antibody	*Fluorophore*	*Reference*
CD34	*APC*	*BD 555824*
CD38	*PE-Cy7*	*BD 560677*
CD45	*FITC*	*BD 555482*
CD49f	*PE*	*BD 555736*
CD201	*BV421*	*BD 743552*

Flow cytometry

The viability of the cells collected from day +13 of hematopoietic differentiation was evaluated with Trypan blue. Cells were stained with the following antibodies (Table 1) in PBS at 4°C for 20 minutes.

Clonogenic assays

Non-adherent cells collected at day +13 of hematopoietic differentiation were counted and plated in methylcellulose-based medium (MethoCultTM H4434; STEMCELL Technologies, France), containing SCF, IL-3, IL-6, EPO, GM-CSF, G-CSF, at the concentration of 5000 cells/dish and incubated for 14 days in a 37°C incubator with 5% CO_2. After 14 days of culture in methylcellulose, colonies were enumerated using established criteria as erythroid colonies (BFU-Es) as well as granulocytic and macrophagic colonies (CFU-GMs).

RNA extraction, reverse transcription and quantitative qRT-PCR

Total intracellular RNA was extracted using RNeasy Mini Kit (74104; Qiagen, Germany) and 1 μg was reverse transcribed using a reverse transcription (RT)-PCR kit (Superscript III 18080-44; ThermoFisher Scientific, France). An aliquot of cDNA was used as a template for qRT-PCR analysis using a fluorescence thermocycler (ThermoFisher Scientific QuantStudio 3^{TM}) with FastStart Universal SYBR Green (04913914001, Roche, Lithuania) DNA dye. The primer sequences used for qRT-PCR are shown in Supplementary Material Table 1. Relative expression was normalized to the geometric mean of housekeeping gene expression and was calculated using the 2-$\Delta\Delta$Ct method.

Western blots

Cells were lysed in ice with RIPA buffer. Separation of proteins was done by electrophoretic migration on a NuPAGE^{TM} 4–12% Bis-Tris gel (NP0323BOX; ThermoFisher, France) under denaturing conditions. The proteins were transferred onto a PVDF membrane pre-activated with methanol. After saturation with TBS-Tween 5% BSA for 1h and hybridization of the membranes with primary antibody overnight (1:500, Ret #132507, R&D System, USA; 1:1000, Phospho-p44/42 MAPK (Erk1/2) (Thr202/Tyr204) (E10) #9106, CellSignaling, USA; 1:200, p-Ret (Tyr 1062)-R: sc-20252-R, SantaCruz, USA; p63 [EPR5701] #ab124762, Abcam, USA; 1:60000, B-Actin-Peroxidase #A3854, Sigma, France) and secondary antibodies coupled to HRP. Membranes were revealed by chemiluminescence with SuperSignal West Dura or Femto reagents and data were acquired using G:BOX iChemi Chemiluminescence Image Capture system.

Production of lentiviruses and viral transduction

To produce RET-expressing lentiviruses, we used Lenti-X 293T as a packaging cell line and psPAX2.2, and pMD2.G as packaging vector and envelope vector, respectively. Briefly, the Lentix-293T cell line was cultured on a T150 mm in Dulbecco's Modified Eagle's Medium (DMEM) supplemented with 10% fetal bovine serum (FBS) (11560636; Gibco, France) and 100 U/mL of penicillin-streptomycin (PenStrep) solution (11548876; Gibco, France) and co-transfected with Lipofectamine 3000 reagent (L3000015; ThermoFisher, France) with 20 μg of packaging vector ps-PAX2.2 (Addgene, USA), 10 μg envelope vector of pMD2.G (Addgene, USA) and 30 μg transfer vector. The supernatant was collected at 24h and 48h. RET^{WT} overexpression plasmid was a gift from Gordon Mills & Kenneth Scott (Addgene plasmid # 116787; RRID:Addgene 116787). The plasmid RET^{C634Y} was purchased from VectorBuilder (Guangzhou, China).

Transduction of iPSC with RET lentiviruses was performed by using freshly passaged iPSC. Puromycin selection was performed by using 1 μg/mL of Puromycin (12122530; Fisher Scientific, France).

Transcriptomic experiments

Total RNA from hematopoietic cells derived from $iRET^{C634Y}$ and from its CRISPR correction $iRET^{CTRL}$ were treated in duplicates to performed Clarium S Assay human microarray (902927; ThermoFisher Scientific, USA). Robust microarray analysis (RMA) [27] normalization was applied to the resulting transcriptome matrix with Transcriptome Analysis Console (TAC) version 4.0.1.36 (ThermoFisher Scientific, USA).

Bioinformatics analysis

Bioinformatics analyses were performed in R software environment version 4.1.0. Supervised differential expression analysis between RET-mutated cells and their CRISPR-corrected counterparts was performed LIMMA R bioconductor package version 3.48.3 [28]. Expression heatmap upregulated genes by *RET* mutation was drawn with pheatmap R-package version 1.0.12. Heatmap classification was performed with Euclidean distances and Ward.D2 method. Functional enrichment was performed with Toppgene website on Gene Ontology Biological Function and DisGeNET diseases databases [29]. Functional molecular networks were drawn with Cytoscape standalone software version 3.6.0 [30].

Results

Endogenous RET activation with GDNF/GFRα1 during iPSC-derived hematopoietic differentiation does not affect the hematopoietic potential

We started by studying the effect of the activation of endogenous RET by adding the RET primary ligand/coreceptor combination GDNF/GFRα1 during hematopoietic differentiation of iPSCs. We induced hematopoietic differentiation of 2 normal wild-type (WT) iPS cell lines (PB33-WT and PB68-WT) using the STEMdiff hematopoietic kit. This protocol allows the generation of non-adherent, round, hematopoietic cells from iPSCs after day +10–13 of culture (Figure 1A). The May-Grünwald and Giemsa (MGG) coloration showed a normal hematopoietic phenotype for the cells generated (Figure 1B) and the colony-forming cell (CFC) assay displayed normal morphological colonies (Figure 1C).

On day +3 of differentiation, we added 100 ng/mL of GDNF/GFRα1 at each medium change for the test groups. We collected the non-adherent cells at the end of the culture procedure on day +13 and characterized them. Western blot analysis showed an increase in the expression of phosphoRET (pRET) in the conditions where GDNF/GFRα1 was added, strongly suggesting the activation of the RET pathway (Supplementary Figure 1A). On day +13 of differentiation, we also analyzed hematopoietic cells by flow cytometry using surface markers representative of HSC (CD34, CD45, CD38 and CD49f).

The cocktail of antibodies was chosen on the basis of the fact that the $CD34^+$ population is heterogenous [31]. Most of the $CD34^+$ cells co-express CD38 but only the $CD38^-$ fraction can generate multi-lineage colonies in immune-deficient mice [32,33]. In addition to well-established HSC markers [31–33], CD49f has been shown to be a specific marker of HSC and a demarcation between HSCs and multipotent progenitors. Moreover, $CD49f^+$ cells were highly efficient in generating long-term multilineage grafts [34].

As it can be seen in Figure 1, for both iPS cell lines, the addition of GDNF/GFRα1 did not significantly modify the percentage of the total $CD34^+$ cell population (Figure 1D) nor the percentage of the $CD34^+/CD38^-$ cell fraction, which are highly enriched in the primitive hematopoietic stem and progenitor cells (Figure 1E). Similarly, no significant change in the HSC-enriched fraction ($CD34^+$ $CD38^-$ $CD49f^+$) was observed after the addition of GDNF/GFRα1 (Figure 1F). Finally, RET activation with GDNF did not show a significant effect on the total percentage of hematopoietic cells ($CD45^+$) (Figure 1G). The hematopoietic cells were tested for their clonogenic potential using CFC assays. Non-adherent cells from day +13 of hematopoietic differentiation, were plated in methylcellulose, and colonies were enumerated 14 days after. As it is shown in Figure 1H, for both PB33-WT and PB68-WT no significant differences were observed in the number of colonies (Figure 1H). Interestingly, the phenotypic characteristics of the progenitors have been found to be different between the 2 iPS cell lines. Indeed, with or without GDNF, PB33-WT hematopoietic progenitors gave rise to BFU-Es whereas PB68-WT colonies gave almost only CFU-GMs (n=5 experiments) (Figure 1I).

Lentiviral-vector mediated overexpression of RET decreases the clonogenic potential of iPSCs during hematopoietic differentiation

Since we observed no significant effect of endogenous RET activation with GDNF on hematopoietic cells derived from iPSCs, we hypothesized that RET activation with GDNF may not be sufficient. Therefore, we overexpressed the RET^{WT} gene with a lentiviral system inside both iPSCs (PB33-RET^{WT} and PB68-RET^{WT}). Expression of the RET^{WT} protein was verified by qRT-PCR quantification (Supplementary Figure 1B) and Western blot analysis (Supplementary Figure 1C) for both iPSCs. Then the same hematopoietic differentiation technology was performed using the same protocol as described above. On day +13 of hematopoietic differentiation, cells were collected and analyzed by flow cytometry. The overexpression of RET^{WT} in PB33 led to a significant decrease in the percentage of the $CD34^+$ population as compared to the control (PB33-WT) whereas for the PB68 no differences were observed between PB68-WT and PB68-RET^{WT} overexpression (Figure 2A).

In PB33-RET^{WT}, the effect of RET overexpression was even stronger on the fraction of cells expressing a more primitive hematopoietic potential. Indeed, the production of $CD34^+/CD38^-$ and $CD49f^+$ positive cells was reduced by a third as compared to hematopoietic progenitors derived from PB33-WT iPSC (Figure 2B–C). Then we tested whether we could potentialize the effect of the RET pathway activation by the addition of GDNF/GFRα1 and whether it would increase the inhibitory effect of RET on hematopoietic potential. Indeed, the percentage of $CD34^+/CD38^-/CD49f^+$ was even lower and the number of $CD45^+$ cells was reduced by 60% after the combination of RET overexpression and GDNF/GFRα1 activation (Figure 2C–D).

On the other hand, no statistically significant effects were observed for the PB68-RET^{WT} after the overexpression of RET in

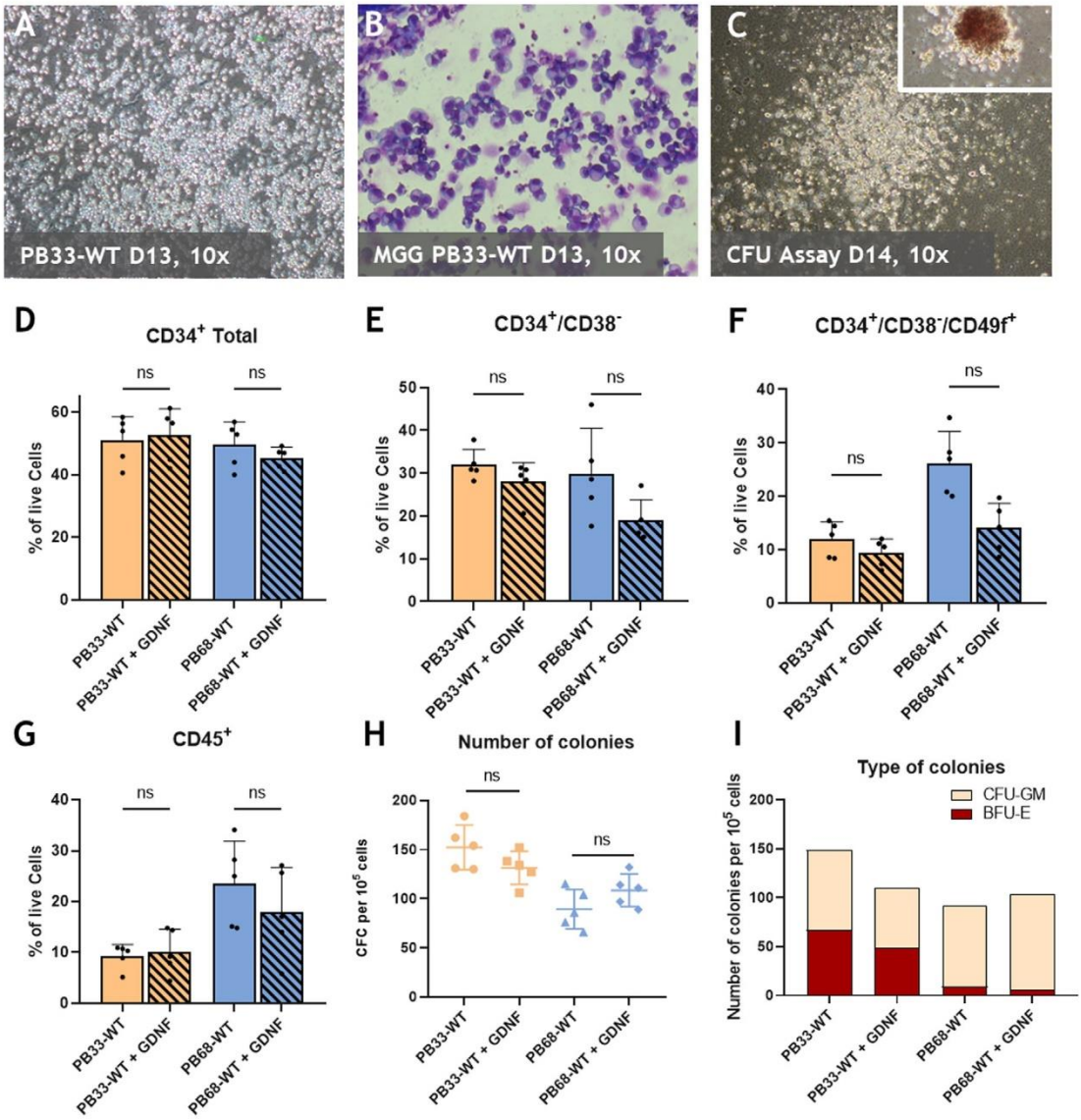

Figure 1. RET activation with GDNF/GFRα1 has no effect on hematopoietic potential at D13 of iPSCs hematopoietic differentiation. (A) Morphology of non-adherent, round, hematopoietic cells derived from PB33-WT iPSC at D13 of differentiation. (B) Microscope pictures (magnification 10x) of May-Grunwald and Giemsa (MGG) staining at day +13 of floating hematopoietic cells differentiated from PB33-WT. (C) Microscope picture of CFU assay at D+14 of the culture displaying a CFU-GM (*white*) and BFU-E (*red*) colony. (D–G) Phenotypic analysis of hematopoietic cells initially gated on live cells. Proportion of CD34 total (D), primitive hematopoietic stem and progenitor cells ($CD34^+/CD38^-$) (E), HSC phenotype bearing cells ($CD34^+/CD38^-/CD49f^+$) (F), or total hematopoietic cells ($CD45^+$) (G) at day +13 of hematopoietic differentiation with or without GDNF for 2 different iPSC cell lines (PB33-WT and PB68-WT). (H) CFC assays derived from PB33-WT and PB68-WT with or without GDNF showing the number of colonies per 5000 cells (Means and SD are represented) and the type of colonies (I). All experiments have been performed 5 times. *P*-values were calculated using a 2-tailed Student's t-test. ns, not significant.

none of the cell populations despite a decreasing tendency (Figure 2A–D). However, the addition of GDNF/GFRα1, led to a significant decrease of $CD34^+/CD38^-$ and $CD49f^+$ positive cells as compared to PB68-WT (Figure 2B–C). The percentage of hematopoietic cells ($CD45^+$) also decreased by half after the activation of the RET pathway (Figure 2D).

The clonogenic potential of the hematopoietic-derived cells was evaluated by CFC assays. RET overexpression in the PB33-RET^{WT} condition results in more than 30% decrease in the total number of colonies, which is coherent with the results obtained by cytometry, whereas no significant differences were observed between PB68-RET^{WT} and PB68-WT (Figure 2E). CFU-GM is the main class of colony affected by the decrease in PB33-RET^{WT} while almost no BFU-Es can be found in PB68-RET^{WT} condition (Figure 2F).

Overexpression of the RET^{C634Y} *mutation amplifies the inhibitory phenotype of the iPSC-derived hematopoietic differentiation*

Since the addition of GDNF/GFRα1 induces a potentializing effect of RET^{WT} overexpression, we tested the effect of a constitutively active *RET* mutation on the hematopoietic differentiation of iPSCs. The RET^{C634Y} mutation is known to be involved in medullary thyroid cancer patients with MEN2A syndrome [35]. This mutation located in the extracellular domain of the protein, leads to the dimerization of RET and its activation independently from its ligand/coreceptor GDNF/GFRα1. We overexpressed the RET^{C634Y} mutation with a lentiviral construction in both PB33 and PB68 (PB33-RET^{C634Y} and PB68-RET^{C634Y}). After the evaluation of the RET overexpression in iPSCs (Supplementary Figure 1B), we performed hematopoietic differentiation using the same protocol as above.

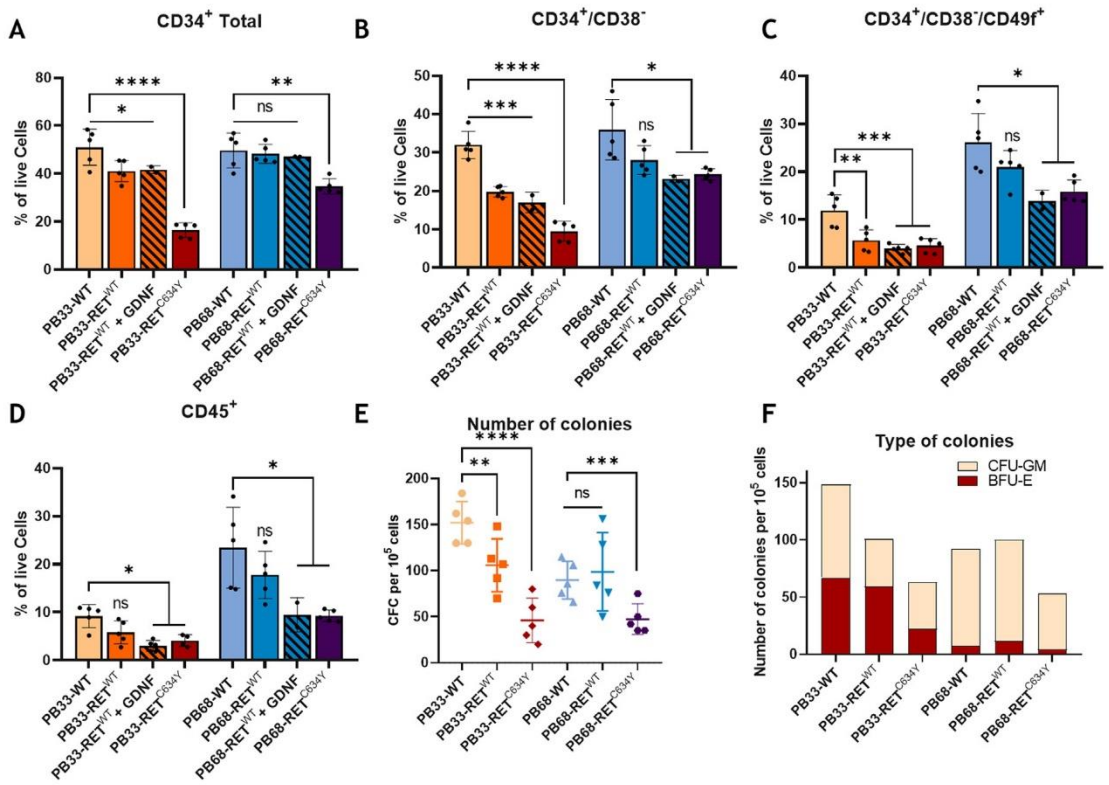

Figure 2. Overexpression of RET^{WT} and RET^{C634Y} during iPSCs-derived hematopoiesis decreases the percentage of hematopoietic progenitors and their capability. (A–D) FACS phenotypic panel gated on live cells. Proportion of CD34 total (A), primitive hematopoietic stem and progenitor cells ($CD34^+/CD38^-$) (B), HSC phenotype bearing cells ($CD34^+/CD38^-/CD49f^+$) (C), or hematopoietic cells ($CD45^+$) (D) at day +13 of hematopoietic differentiation for WT iPSC cell lines (PB33-WT and PB68-WT), with RET^{WT} overexpression with or without GDNF or with RET^{C634Y} overexpression. (E) CFC assays for PB33-WT/PB33-RET^{WT}/PB33-RET^{C634Y} and for PB68-WT/PB68-RET^{WT}/PB68-RET^{C634Y} showing the number of colonies per 5000 cells and the type of colonies (F) (Means and SD are represented). All experiments have been performed 5 times. *P*-values were calculated using a 2-tailed Student's t-test. ns, not significant; *, $P < 0.05$; **, $P < 0.01$; ***, $P < 0.001$; ****, $P < 0.0001$.

After 13 days of hematopoietic differentiation, we observed a drastic reduction in the number of $CD34^+$ and $CD38^-$ cells in the PB33-RET^{C634Y} condition as compared to PB33-WT (Figure 2A–B). The percentages of $CD34^+/CD38^-/CD49f^+$ and $CD45^+$ were decreased in a similar range to the one observed after the addition of GDNF/GFRα1 on PB33-RET^{WT} (Figure 2C–D). Comparable results were observed with the second iPS cell line PB68-RET^{C634Y} (Figure 2A–D). The number of colonies was also evaluated by CFC assay. A striking decrease in the number of CFC was observed in both RET^{C634Y} iPSCs as compared to their respective control (Figure 2E). These results are consistent with an inhibition of the hematopoietic potential by RET^{C634Y} overexpression. We next wished to test these findings using a RET^{C634Y} patient-derived iPSC, which expresses RET^{C634Y} at levels observed in patients and could be considered as a more accurate model. To this end, we have used an iPSC line generated from a patient with hereditary medullary thyroid cancer (MTC).

The inhibitory effect of the constitutive RET^{C634Y} mutation on hematopoietic potential correlates with MAPK2/3 activity

In previous works, we reprogrammed iPSCs from a patient with a *RET* mutation at the codon 634 (RET^{C634Y}) who developed pheochromocytoma and MTC [25]. RET^{C634Y}-mutated cells were reprogrammed by non-integrative viral transduction. As described previously, these iPSCs ($iRET^{C634Y}$) had a normal karyotype, harbored the RET^{C634Y} mutation and expressed pluripotency hallmarks as well as RET protein [25]. We have also generated a CRISPR Cas9-corrected version of this iPS cell line, allowing to evaluate the hematopoietic potential of RET-mutated iPSC as compared to its isogenic RET-corrected iPS cell line ($iRET^{CTRL}$) [26]. $iRET^{CTRL}$ and $iRET^{C634Y}$ were induced to hematopoietic differentiation as described above. No differences were observed in the percentage of $CD34^+$ total population between $iRET^{CTRL}$ and $iRET^{C634Y}$ (Figure 3A). Interestingly, the progenitors and stem cell-enriched fraction ($CD34^+/CD38^-$) was significantly lower in the $iRET^{C634Y}$ as compared to the $iRET^{CTRL}$ (Figure 3B). We observed an even more important decrease when we restricted the analysis to the cells with HSC phenotype (Figure 3C). Finally, no significant changes were observed for the total hematopoietic cell fraction ($CD45^+$) (Figure 3D). CFC assays showed a significantly lower number of colonies in the $iRET^{C634Y}$ condition, thus indicating a lower hematopoietic potential (Figure 3E). These results are consistent with what we observed with the RET^{WT} and RET^{C634Y} overexpression in normal iPSCs.

Western blots were performed with protein extracts collected at the iPSC stage or after 13 days of hematopoietic differentiation. As it can be seen in Figure 3F, pMAPK1/2, RET and pRET expression has been found to be increased during $iRET^{C634Y}$ differentiation whereas they were reduced in hematopoietic cells derived from $iRET^{CTRL}$ (Figure 3F). We have estimated that pRET and RET proteins were enriched by 120% and 230% respectively during $iRET^{C634Y}$ hematopoietic differentiation (Figure 3G) Phospho-p44 MAPK expression is increased by more than 5 times while pMAPK p42 quantity is up by 110%. On the other hand, the quantity of all these proteins was decreased during the differentiation of $iRET^{CTRL}$ (Figure 3G). MAPKs are known to be phosphorylated by RET [36] therefore, we hypothesized that they could play a role in the inhibition of the RET-mediated hematopoietic potential.

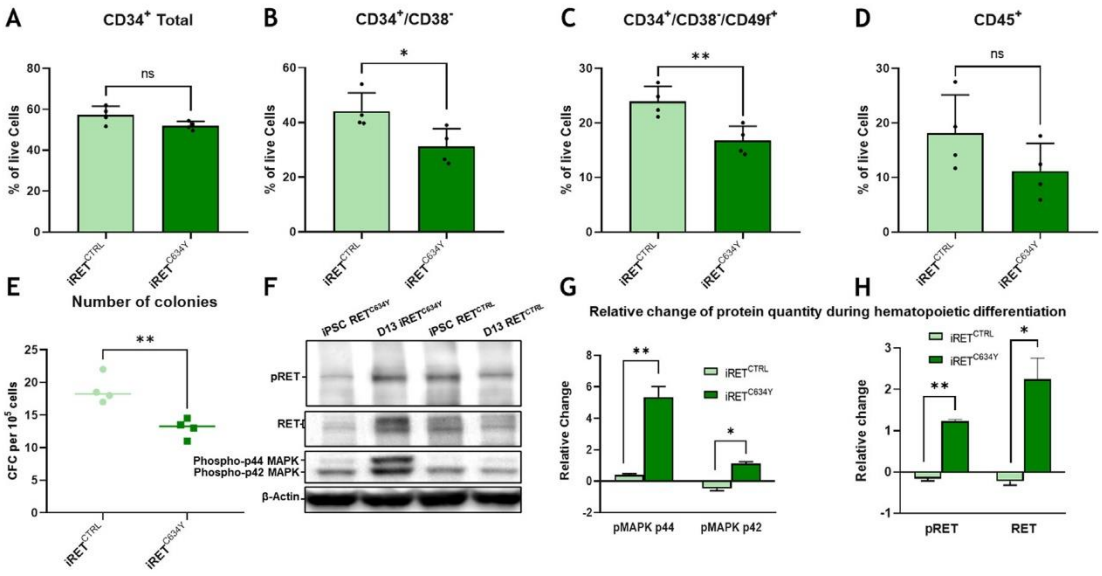

Figure 3. RET^{C634Y} mutation from a patient has an inhibitory effect on the hematopoietic potential that correlated with MAPK1/2 activity. (A–D) FACS phenotypic panel gated on live cells. Proportion of CD34 total (A), primitive hematopoietic stem and progenitor cells (CD34$^+$/CD38$^-$) (B), HSC phenotype bearing cells (CD34$^+$/CD38$^-$/CD49f$^+$) (C), or hematopoietic cells (CD45$^+$) (D) at day +13 of hematopoietic differentiation for RET^{C634Y} mutated iPSC (iRET^{C634Y}) and its isogenic CRISPR control (iRET^{CTRL}). (E) CFC assays showing the number of colonies per 5000 cells. (F) Western blot showing iRET^{C634Y} and iRET^{CTRL} at the iPSC stage or after 13 days of hematopoietic differentiation. (G–H) Relative change of the phospho-p44/42 MAPK (G) and pRET/RET (H) quantity during hematopoietic differentiation. All experiments have been performed 4 times. *P*-values were calculated using a 2-tailed Student's t-test. ns, not significant; *, $P < 0.05$; **.

RET^{C634Y} *mutation activates a specific transcriptional program in hematopoietic cells generated from iPSCs*

To evaluate the effect of the hereditary *RET^{C634Y}* mutation on transcriptional regulation during iPSC-derived hematopoietic differentiation, RET-mutated cells iRET^{C634Y} and its isogenic corrected control iRET^{CTRL} cells were collected at day +13 of hematopoietic differentiation to perform whole transcriptomic experiments in duplicates. Unsupervised principal component analysis performed at the whole transcriptome level allowed a good stratification of sample groups (Figure 4A) suggesting a major impact of *RET* mutation on the transcriptional regulation. Differential expression analysis performed with LIMMA algorithm between iRET^{C634Y} cells and iRET^{CTRL} allowed the identification of a specific transcriptional program between these 2 experimental constituted of 109 upregulated genes (log2 FC > 2, adjusted *P*-values ≤ 0.05) (Figure 4B, Supplementary Table 1). Expression Heatmap performed with these 109 genes upregulated by *RET^{C634Y}* mutation during hematopoietic differentiation of iPSCs allowed to well discriminate 2 experimental groups: samples from iRET^{C634Y} versus their CRISPR controls (Figure 4C). These results suggest that *RET^{C634Y}* mutation could impact hematopoietic differentiation of human iPSCs even at endogenous levels of expression.

RET^{C634Y} *mutation activates a hematopoietic molecular network that overlaps with MAPK cascade*

With the 109 genes found upregulated by *RET^{C634Y}* mutation during iRET^{C634Y} hematopoietic differentiation, a functional enrichment was performed with the Gene Ontology Biological Process database (GO-BP) (Figure 5A). This analysis highlighted best-ranking enrichment with several gene sets implicated in the MAPK cascade, followed by enrichment with gene set implicated in the immune system and hemopoiesis (Figure 5A). Overlap between these enrichments shows that 4 genes belonging to the 3 enriched functions including SRFP1, FCGR2B, HLA-DRB1, JUN (Figure 5B). Similarly, 6 genes were both implicated in the immune system and hemopoietic regulations including NR4A3, DLK1, TMEM17B, JAG1, TCTA and TMEM176A (Figure 5B). DLK1 is known to be a negative regulator of emerging hematopoietic stem and progenitor cells [37] and NR4A3 is known to restrict HSC proliferation via reciprocal regulation of C/EBPα and inflammatory signaling [38]. All together, these results suggest that MAPK cascade could potentially be activated downstream to *RET^{C634Y}* mutation and promote the regulation of HSCs potential during iPSC-derived hematopoietic differentiation. The action of *RET^{C634Y}* mutation could occur at a primitive stage of hematopoiesis because both hemopoiesis and lymphopoiesis are affected by these regulations (Figure 5C). This idea was confirmed by the fact that after functional enrichment on disease, with the DisGeNET database, a larger functional enrichment network could be built with molecules implicated both in lymphoid (Chronic lymphoid leukemia, multiple myeloma) and myeloid (acute promyelocytic leukemia, myelodysplastic syndrome) disorders (Supplemental Figure 2A–B).

Finally, the expressions of a set of genes found upregulated by *RET^{C634Y}* in the transcriptomics data were quantified by qRT-PCR in WT, RET^{WT} or RET^{C634Y} iPS cell lines at iPSCs stage (Supplemental Figure 2C) or after 13 days of hematopoietic differentiation (Figure 5D). The results show a significant overexpression of *GFRα1* and *DLK1* correlating with the increased activity of RET at both iPSC and day +13 hematopoietic stages. This highlights a correlation between RET and *DLK1* expression. Depending on the iPS cell line, *JUN, NR4A3* and *C/EBPα* were also found to be upregulated by RET activation and therefore validating the transcriptomic data.

Discussion

We have tested in this work, the impact of the overexpression of either wild-type or mutated RET gene in the generation of a hematopoietic potential of derived from iPSCs. Although almost all differentiated hematopoietic cells can be derived from iPSCs and ESCs with several in vitro culture strategies, there are currently no data showing the possibility of producing bona fide HSC from iPSCs. Generation of HSC with long-term potential from iPSCs is a major goal of research which could circumvent the unmet need for new sources for HSCT. However, iPSC-derived hematopoiesis resembles the first wave of

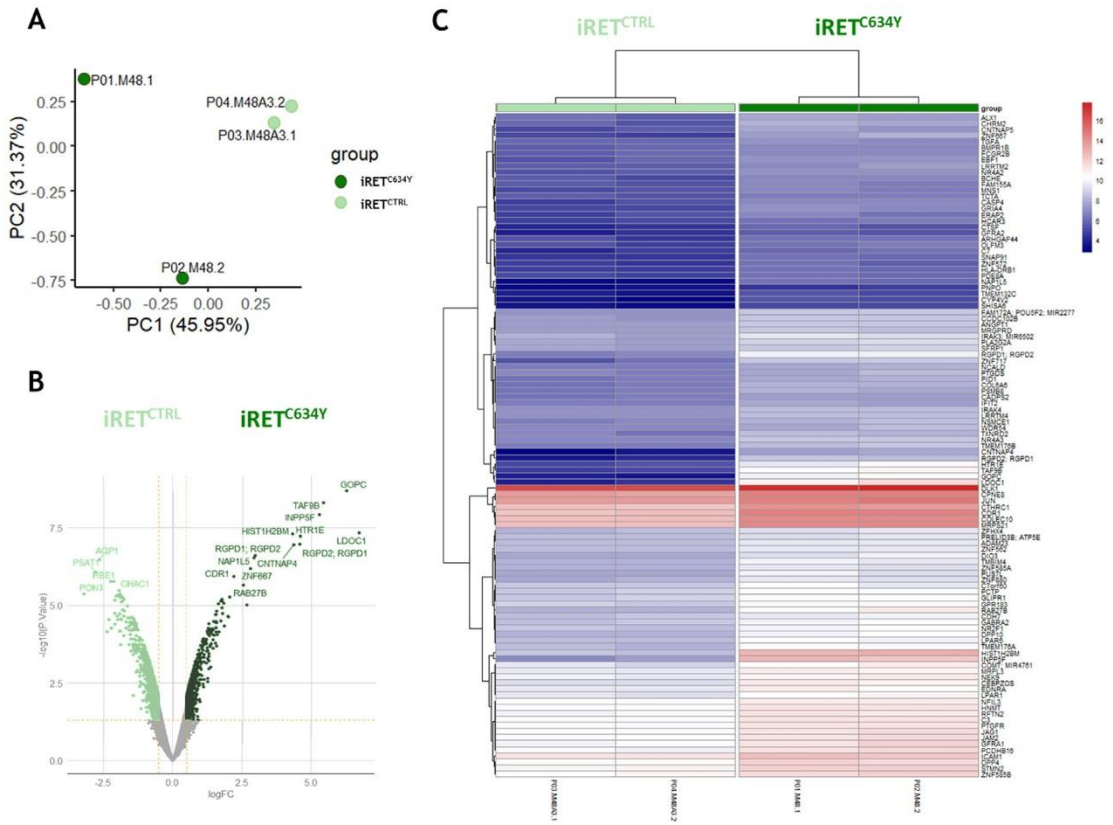

Figure 4. iRET^{C634Y} mutated hematopoietic cells derived from iPSCs harbored a specific activated expression profile as compared to iRET^{CTRL}. (A) Whole transcriptomic principal component analysis stratified on a group of samples. (B) Volcano plot of differential expressed between iRET^{C634Y} mutated cells and its isogenic CRISPR correction iRET^{CTRL}. (C) Expression heatmap of 109 genes upregulated in iRET^{C634Y} cells as compared to its CRISPR corrected control iRET^{CTRL}.

hematopoiesis because it produces mature blood cells only and not long-term engraftable HSCs [16,17]. Previous experimental work showed the possibility of HSC generation inside teratomas generated in immunodeficient mice, able to migrate and repopulate mice BM demonstrating that this potential truly exists [39,40]. Other studies by genetic modification of iPSCs via the ectopic expression of transcriptional factors such as HOXA9, ERG, RORA, SOX4 and MYB showed the possibility of inducing HSC potential [41,42]. Obviously, none of these strategies could be applicable to future generations of iPSC-derived HSC for clinical purposes. Therefore, protocols for hematopoietic differentiation must be optimized, or mechanisms of differentiation must be better understood to develop iPSCs-derived HSCs for clinical applications.

It was therefore of interest to evaluate the hematopoietic potential of iPSCs under the influence of the tyrosine kinase receptor RET for 2 different reasons. The first is the fact that RET has been identified as a crucial player in the development of hematopoietic potential in mice invalidated for the RET gene [22]. This study shows that RET neurotrophic factor partners are produced in the HSCs environment and stimulate the survival, expansion and function of HSCs. Moreover, mice lacking the RET receptor (Ret$^{-/-}$) exhibited a reduction in HSC numbers and compromised transplantation potential. RET-deficient HSCs were more susceptible to apoptosis because of to the loss of Bcl2 and Bcl2l1 surviving cues and demonstrated reduced long-term transplantation fitness [22]. The second work has studied the effect of the activation of the RET pathway by the addition of its ligand/coreceptor GDNF/GFRα1a and showed an improvement in CB HSCs survival and expansion [23]. However, the impact of RET during iPSCs hematopoietic differentiation remains to be characterized. Here, we observed no effect of RET activation by GDNF/GFRα1 addition during hematopoietic differentiation of WT iPSCs (Figure 1). Then we generated iPSC overexpressing the gene *RET^{WT}* and the mutant *RET^{C634Y}*. Our results show that RET activation decreases the number of hematopoietic cells with HSC phenotype as well as that of hematopoietic progenitors (Figure 2). The hematopoietic potential of iPSCs is also altered by the activation of exogenous RET because their capacity to form hematopoietic colonies is also reduced. This inhibitory effect is enhanced with the level of RET activation as shown by the addition of GDNF in the RET^{WT} conditions (Figure 2). We have observed that constitutive activation of the *RET^{C634Y}* mutant is associated with the most severe inhibitory effect in both iPSCs. These results strongly suggest a relationship between RET constitutive phosphorylation and hematopoietic differentiation.

We have evaluated the effect of RET activation in 2 different iPS cell lines (PB33-WT and PB68-WT) by overexpression of RET. Interestingly, hematopoietic differentiation gave rise to different outcomes in these 2 cell lines. As shown in Figure 1, the percentage of CD45^{+} hematopoietic cells and that of hematopoietic cells with the more primitive phenotype (CD34^{+}/CD68^{-}/CD49f^{+}) were found to be different between the hematopoietic progeny from 2 WT iPSCs (Figure 1). The number and the type of colonies were found to be different as well. Indeed, there were almost no BFU-Es observed for PB68-WT whereas in PB33-WT almost 50% of the colonies formed erythroid colonies. The effect of RET^{WT} overexpression is also different between the 2 cell lines where a much stronger activation of RET is needed to observe an effect in PB68 (Figure 2). These differences could be explained by the genotypic background of the donors and the well-known heterogeneity between different iPSCs. Indeed, a study shows that high variation in different iPSC phenotypes arises from differences between individuals [43].

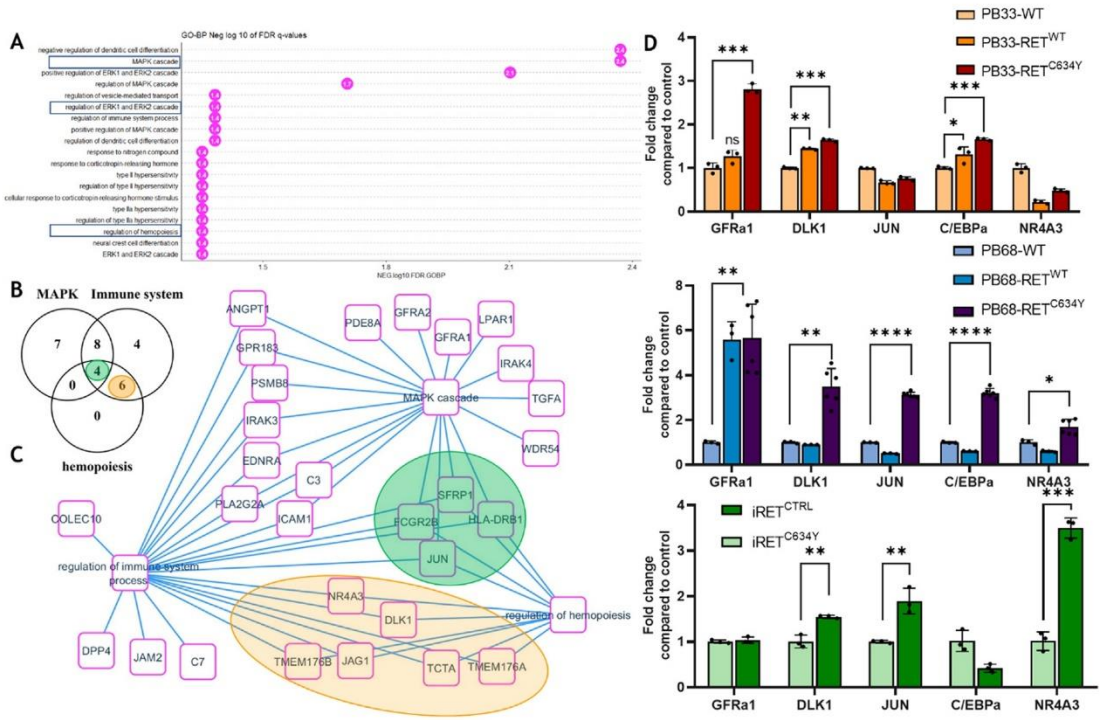

Figure 5. MAPK cascade overlaps the immune system and hemopoiesis network induced by RET^{C634Y} mutation in hematopoietic cells derived from iPSCs. (A) Bar plot of functional enrichment performed on GO-BP database with the 109 coding genes found upregulated in iRET^{C634Y} hematopoietic cells. (B) Venn diagram for overlapping of MAPK, immune system, hemopoiesis gene sets upregulated by RET^{C634Y} mutation. (C) MAPK and hematopoiesis regulation molecular network activated by RET^{C634Y}. (D) Expression of RET-regulated candidate genes quantified by qRT-PCR in iPSCs-derived hematopoietic cells after 13 days of differentiation. Experiments have been performed 3 times. *P*-values were calculated using a 2-tailed Student's t-test. ns, not significant; *, $P < 0.05$; **, $P < 0.01$; ***, $P < 0.001$; ****, $P < 0.0001$.

We next tested the effect of an endogenous *RET*^{C634Y} mutation from a patient-derived iPSC and we compared the results with its CRISPR-corrected isogenic control. This model is derived from a patient and therefore is more suitable to study the endogenous effect of *RET*^{C634Y} (Figure 3). Interestingly, we found the same inhibitory effect than with the overexpression of the mutation in WT background iPSCs. It indicates that our RET^{C634Y} lentiviral overexpression model is relevant to mimic the *in vivo* effect of the *RET* mutation and therefore it could serve as a drug screening model.

To get a better understanding of the RET activation effect on iPSC-derived hematopoiesis, we performed transcriptomic analysis on iRET^{C634Y} and its isogenic counterpart iRET^{CTRL} in hematopoietic cells collected at day +13 of differentiation. The data reveals a specific activated expression profile of iRET^{C634Y} compared to iRET^{CTRL} (Figure 4). Genes upregulated in iRET^{C634Y} are functionally enriched for MAPK, immune system and hematopoiesis regulation gene sets. Inside this network, we identified some relevant hematopoietic regulatory genes upregulated by *RET* mutation (Figure 5). DLK1 and NR4A3 are both known to be involved in the restriction of HSC proliferation and emerging hematopoiesis [37,38]. *C/EBPα* is downstream of NR4A3 and its conditional knock-out in adult HSC leads to the expansion of functional HSCs [44]. Moreover, upon its activation by the MAPK, JNK1 can act as a positive regulator of *C/EBPα* [45]. The implication of the MAPK pathway was also hinted by western blot analysis showing an increase of pMAPK1/2 protein quantity during iRET^{C634Y} hematopoietic differentiation. qRT-PCR performed at both iPSC stage and at day +13 of differentiation show a correlation between RET activation and the overexpression of *DLK1, NR4A3, GFRα1, JUN, C/EBPα*. Therefore, the inhibitory effect of RET activation on hematopoietic potential during hematopoietic differentiation could be mediated by MAPK/JNK and the transcriptional regulation of HSC inhibitory genes. Conditional knock-out of these candidate genes with siRNA during iPSC-derived hematopoiesis could provide useful information on their role and on the mechanism of RET hematopoietic potential inhibition.

Activation of the RET pathway by GDNF promotes the growth and survival of UCB-derived HSCs [23]. This activation induces an anti-apoptotic and anti-inflammatory response while reducing the accumulation of reactive oxygen species (ROS) in UCB HSCs. *In vivo*, the RET signal is likely provided by GDNF/GFRα1 from the bone marrow environment, playing a crucial role in maintaining HSC potential. However, our study reveals an inhibitory effect of RET activation during iPSC-derived hematopoiesis. Specifically, we observed a decrease in the number of HSC phenotype bearing-positive cells and their clonogenic potential in various models of RET activation. It is interesting that the same regulatory pathway can exhibit opposing effects depending on the developmental stages. In the context of hematopoietic differentiation, premature activation of a proliferative signal may impede the emergence of HSCs.

Overall, our results show that RET activation in the context of iPSC leads to an inhibitory effect on the hematopoietic potential of the pluripotent cells, as opposed to the hematopoietic promotion that has been observed in CB-derived hematopoiesis. We have identified in the context of iPSCs regulatory pathways (such as DLK1) whose activation could be at the origin of this effect. Genetic manipulation of these pathways could lead to a better understanding of this phenotype. It would be of interest in future studies, to use an inducible RET lentivirus which could be activated at different stages of hematopoietic differentiation after the mesoderm stage. Nevertheless, this study shows for the first time that the expression of wild-type or constitutively active RET at the iPSC stage leads to an inhibitory effect and is not recommended for future clinical use.

Institutional Review Board Statement

This study was conducted in accordance with the Declaration of Helsinki and approved by IRB from INSERM.

Funding

No funding was received.

Declaration of Competing Interest

The authors declare no conflict of interest.

Author Contributions

Conceptualization, PM, JI, CD, AT; methodology, PM, JI, CD, AT; software, CD; validation, PM, AB-G, AT; formal analysis, PM, CD; investigation, PM, JI; resources, TL, DC, PH; data curation, PM, JI, AT; writing—original draft preparation, PM JI, AT; writing—review and editing, PM, JI, CD, AT; visualization, PM, AT; supervision, PM, AT; project administration, PM; funding acquisition, AB-G, AT All authors have read and agreed to the published version of the manuscript.

Acknowledgments

We would like to acknowledge Vaincre le Cancer for funding the fellowships of PM and JI. Thanks to GENOM'IC Research facility from Institut Cochin (Paris) for the sequencing (bulk RNA).

Supplementary materials

Supplementary material associated with this article can be found in the online version at doi:10.1016/j.jcyt.2023.10.003.

References

[1] Bryder D, Rossi DJ, Weissman IL. Hematopoietic stem cells: the paradigmatic tissue-specific stem cell. Am J Pathol 2006;169:338–46. https://doi.org/10.2353/ajpath.2006.060312.
[2] Weissman IL. Stem cells: units of development, units of regeneration, and units in evolution. Cell 2000;100:157–68. https://doi.org/10.1016/S0092-8674(00)81692-X.
[3] Li X-L, Xue Y, Yang Y-J, Zhang C-X, Wang Y, Duan Y-Y, et al. Hematopoietic stem cells: cancer involvement and myeloid leukemia. Eur Rev Med Pharmacol Sci 2015;19:1829–36.
[4] Maswabi BCL, Molinsky J, Savvulidi F, Zikmund T, Prukova D, Tuskova D, et al. Hematopoiesis in patients with mature B-cell malignancies is deregulated even in patients with undetectable bone marrow involvement. Haematologica 2017;102:e152–5. https://doi.org/10.3324/haematol.2016.151571.
[5] Toscani D, Bolzoni M, Accardi F, Aversa F, Giuliani N. The osteoblastic niche in the context of multiple myeloma. Ann N Y Acad Sci 2015;1335:45–62. https://doi.org/10.1111/nyas.12578.
[6] Ntanasis-Stathopoulos I, Gavriatopoulou M, Kastritis E, Terpos E, Dimopoulos MA. Multiple myeloma: role of autologous transplantation. Cancer Treat Rev 2020;82:101929. https://doi.org/10.1016/j.ctrv.2019.101929.
[7] Cowan AJ, Green DJ, Kwok M, Lee S, Coffey DG, Holmberg LA, et al. Diagnosis and management of multiple myeloma: a review. JAMA 2022;327:464–77. https://doi.org/10.1001/jama.2022.0003.
[8] Zahid U, Akbar F, Amaraneni A, Husnain M, Chan O, Riaz IB, et al. A review of autologous stem cell transplantation in lymphoma. Curr Hematol Malig Rep 2017;12:217–26. https://doi.org/10.1007/s11899-017-0382-1.
[9] Boitano AE, Wang J, Romeo R, Bouchez LC, Parker AE, Sutton SE, et al. Aryl hydrocarbon receptor antagonists promote the expansion of human hematopoietic stem cells. Science 2010;329:1345–8. https://doi.org/10.1126/science.1191536.
[10] Fares I, Chagraoui J, Gareau Y, Gingras S, Ruel R, Mayotte N, et al. Cord blood expansion. Pyrimidoindole derivatives are agonists of human hematopoietic stem cell self-renewal. Science 2014;345:1509–12. https://doi.org/10.1126/science.1256337.
[11] Wagner JE, Brunstein CG, Boitano AE, DeFor TE, McKenna D, Sumstad D, et al. Phase I/II trial of stemregenin-1 expanded umbilical cord blood hematopoietic stem cells supports testing as a stand-alone graft. Cell Stem Cell 2016;18:144–55. https://doi.org/10.1016/j.stem.2015.10.004.
[12] Papa L, Djedaini M, Hoffman R. Ex vivo HSC expansion challenges the paradigm of unidirectional human hematopoiesis. Ann N Y Acad Sci 2020;1466:39–50. https://doi.org/10.1111/nyas.14133.
[13] Mayer IM, Hoelbl-Kovacic A, Sexl V, Doma E. Isolation, maintenance and expansion of adult hematopoietic stem/progenitor cells and leukemic stem cells. Cancers (Basel) 2022;14:1723. https://doi.org/10.3390/cancers14071723.
[14] Gutman JA, Riddell SR, McGoldrick S, Delaney C. Double unit cord blood transplantation. Chimerism 2010;1:21–2. https://doi.org/10.4161/chim.1.1.12141.
[15] Demirci S, Leonard A, Tisdale JF. Hematopoietic stem cells from pluripotent stem cells: clinical potential, challenges, and future perspectives. Stem Cells Transl Med 2020;9:1549–57. https://doi.org/10.1002/sctm.20-0247.
[16] Lapillonne H, Kobari L, Mazurier C, Tropel P, Giarratana M-C, Zanella-Cleon I, et al. Red blood cell generation from human induced pluripotent stem cells: perspectives for transfusion medicine. Haematologica 2010;95:1651–9. https://doi.org/10.3324/haematol.2010.023556.
[17] Slukvin II. Generation of mature blood cells from pluripotent stem cells. Haematologica 2010;95:1621–3. https://doi.org/10.3324/haematol.2010.029231.
[18] Reilly JT. Receptor tyrosine kinases in normal and malignant haematopoiesis. Blood Rev 2003;17:241–8. https://doi.org/10.1016/S0268-960X(03)00024-9.
[19] Fares I, Calvanese V, Mikkola HKA. Decoding human hematopoietic stem cell self-renewal. Curr Stem Cell Rep 2022;8:93–106. https://doi.org/10.1007/s40778-022-00209-w.
[20] Gattei V, Celetti A, Cerrato A, Degan M, De Iuliis A, Rossi FM, et al. Expression of the RET receptor tyrosine kinase and GDNFR-alpha in normal and leukemic human hematopoietic cells and stromal cells of the bone marrow microenvironment. Blood 1997;89:2925–37.
[21] Nakayama S, Iida K, Tsuzuki T, Iwashita T, Murakami H, Asai N, et al. Implication of expression of GDNF/Ret signalling components in differentiation of bone marrow haemopoietic cells. Brit J Haematol 1999;105:50–7. https://doi.org/10.1111/j.1365-2141.1999.01311.x.
[22] Fonseca-Pereira D, Arroz-Madeira S, Rodrigues-Campos M, Barbosa IAM, Domingues RG, Bento T, et al. The neurotrophic factor receptor RET drives haematopoietic stem cell survival and function. Nature 2014;514:98–101. https://doi.org/10.1038/nature13498.
[23] Grey W, Chauhan R, Piganeau M, Huerga Encabo H, Garcia-Albornoz M, McDonald NQ, et al. Activation of the receptor tyrosine kinase ret improves long-term hematopoietic stem cell outgrowth and potency. Blood 2020;136:2535–47. https://doi.org/10.1182/blood.2020006302.
[24] Kouvaraki MA, Shapiro SE, Perrier ND, Cote GJ, Gagel RF, Hoff AO, et al. RET proto-oncogene: a review and update of genotype-phenotype correlations in hereditary medullary thyroid cancer and associated endocrine tumors. Thyroid 2005;15:531–44. https://doi.org/10.1089/thy.2005.15.531.
[25] Hadoux J, Féraud O, Griscelli F, Opolon P, Divers D, Gobbo E, et al. Generation of an induced pluripotent stem cell line from a patient with hereditary multiple endocrine neoplasia 2A (MEN2A) syndrome with RET mutation. Stem Cell Res 2016;17:154–7. https://doi.org/10.1016/j.scr.2016.06.008.
[26] Hadoux J, Desterke C, Féraud O, Guibert M, De Rose RF, Opolon P, et al. Transcriptional landscape of a RETC634Y-mutated IPSC and its CRISPR-corrected isogenic control reveals the putative role of EGR1 transcriptional program in the development of multiple endocrine neoplasia type 2A-associated cancers. Stem Cell Res 2018;26:8–16. https://doi.org/10.1016/j.scr.2017.11.015.
[27] Irizarry RA, Bolstad BM, Collin F, Cope LM, Hobbs B, Speed TP. Summaries of affymetrix GeneChip probe level data. Nucleic Acids Res 2003;31:e15.
[28] Ritchie ME, Phipson B, Wu D, Hu Y, Law CW, Shi W, et al. Limma powers differential expression analyses for RNA-sequencing and microarray studies. Nucleic Acids Res 2015;43:e47. https://doi.org/10.1093/nar/gkv007.
[29] Chen J, Bardes EE, Aronow BJ, Jegga AG. ToppGene suite for gene list enrichment analysis and candidate gene prioritization. Nucleic Acids Res 2009;37:W305–11. https://doi.org/10.1093/nar/gkp427.
[30] Cline MS, Smoot M, Cerami E, Kuchinsky A, Landys N, Workman C, et al. Integration of biological networks and gene expression data using cytoscape. Nat Protoc 2007;2:2366–82. https://doi.org/10.1038/nprot.2007.324.
[31] DiGiusto D, Chen S, Combs J, Webb S, Namikawa R, Tsukamoto A, et al. Human fetal bone marrow early progenitors for T, B, and myeloid cells are found exclusively in the population expressing high levels of CD34. Blood 1994;84:421–32.
[32] Huang S, Terstappen LW. Lymphoid and myeloid differentiation of single human CD34+, HLA-DR+, CD38- hematopoietic stem cells. Blood 1994;83:1515–26.
[33] Bhatia M, Bonnet D, Kapp U, Wang JC, Murdoch B, Dick JE. Quantitative analysis reveals expansion of human hematopoietic repopulating cells after short-term ex vivo culture. J Exp Med 1997;186:619–24. https://doi.org/10.1084/jem.186.4.619.
[34] Notta F, Doulatov S, Laurenti E, Poeppl A, Jurisica I, Dick JE. Isolation of single human hematopoietic stem cells capable of long-term multilineage engraftment. Science 2011;333:218–21. https://doi.org/10.1126/science.1201219.
[35] Sánchez B, Robledo M, Biarnes J, Sáez ME, Volpini V, Benítez J, et al. High prevalence of the C634Y mutation in the RET proto-oncogene in MEN 2A families in Spain. J Med Genet 1999;36:68–70.
[36] Regua AT, Najjar M, Lo H-W. RET signaling pathway and RET inhibitors in human cancer. Front Oncol 2022;12:932353. https://doi.org/10.3389/fonc.2022.932353.
[37] Mirshekar-Syahkal B, Haak E, Kimber GM, Leusden K van, Harvey K, O'Rourke J, et al. Dlk1 is a negative regulator of emerging hematopoietic stem and progenitor cells. Haematologica 2013;98:163–71. https://doi.org/10.3324/haematol.2012.070789.
[38] Freire PR, Conneely OM. NR4A1 and NR4A3 restrict HSC proliferation via reciprocal regulation of C/EBPα and inflammatory signaling. Blood 2018;131:1081–93. https://doi.org/10.1182/blood-2017-07-795757.

[39] Suzuki N, Yamazaki S, Yamaguchi T, Okabe M, Masaki H, Takaki S, et al. Generation of engraftable hematopoietic stem cells from induced pluripotent stem cells by way of teratoma formation. Mol Ther 2013;21:1424–31. https://doi.org/10.1038/mt.2013.71.

[40] Amabile G, Welner RS, Nombela-Arrieta C, D'Alise AM, Di Ruscio A, Ebralidze AK, et al. In vivo generation of transplantable human hematopoietic cells from induced pluripotent stem cells. Blood 2013;121:1255–64. https://doi.org/10.1182/blood-2012-06-434407.

[41] Doulatov S, Vo LT, Chou SS, Kim PG, Arora N, Li H, et al. Induction of multipotential hematopoietic progenitors from human pluripotent stem cells via respecification of lineage-restricted precursors. Cell Stem Cell 2013;13:459–70. https://doi.org/10.1016/j.stem.2013.09.002.

[42] Sugimura R, Jha DK, Han A, Soria-Valles C, da Rocha EL, Lu Y-F, et al. Haematopoietic stem and progenitor cells from human pluripotent stem cells. Nature 2017;545:432–8. https://doi.org/10.1038/nature22370.

[43] Kilpinen H, Goncalves A, Leha A, Afzal V, Alasoo K, Ashford S, et al. Common genetic variation drives molecular heterogeneity in human IPSCs. Nature 2017;546:370–5. https://doi.org/10.1038/nature22403.

[44] Ye M, Zhang H, Amabile G, Yang H, Staber PB, Zhang P, et al. C/EBPa controls acquisition and maintenance of adult haematopoietic stem cell quiescence. Nat Cell Biol 2013;15:385–94. https://doi.org/10.1038/ncb2698.

[45] Geest CR, Coffer PJ. MAPK signaling pathways in the regulation of hematopoiesis. J Leukocyte Biol 2009;86:237–50. https://doi.org/10.1189/jlb.0209097.

SUPPLEMENTARY MATERIALS

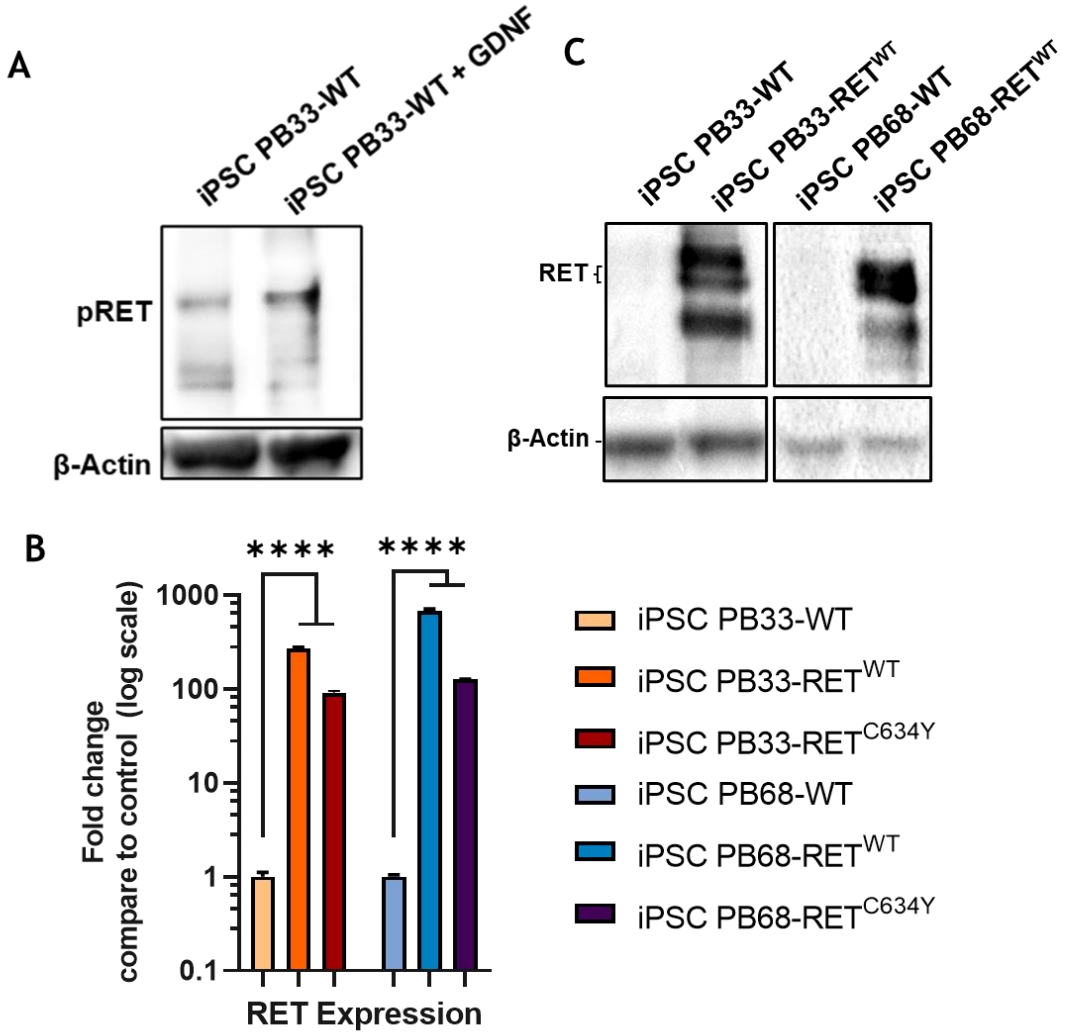

Supplementary Figure 1: (A) *Activation of the RET pathway by the addition of GDNF/GFRα1.* ***(B)*** *qRT-PCR quantification of* RET^{WT} *and* RET^{C634Y} *in PB33 and PB68 at iPSC stage.* ***(C)*** *Western blot analysis of* RET^{WT} *overexpression in PB33 and PB68*

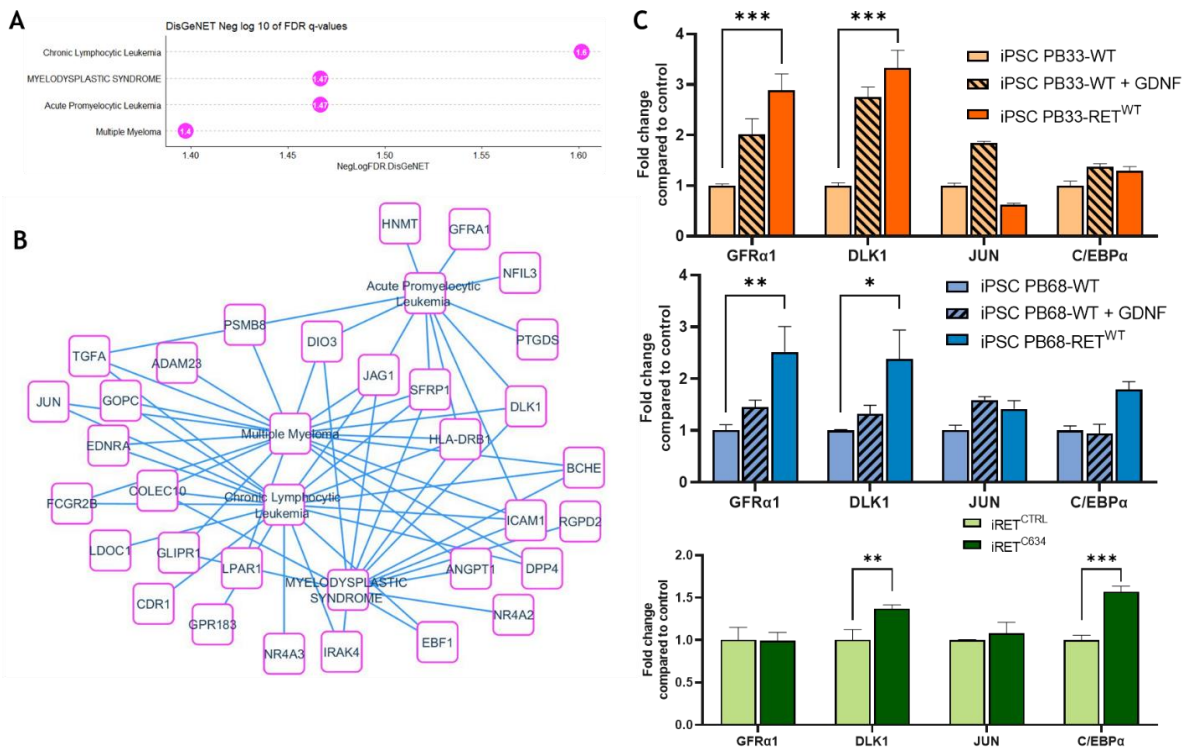

Supplementary Figure 2: (A) *Bar plot of functional enrichment performed on DisGeNET database and filtered on hematopoietic disorders.* ***(B)*** *Hematopoietic disorders molecular network induced by RET^{C634Y} mutation in hematopoietic cells derived from iPSCs.* ***(C)*** *Expression of RET regulated candidate genes quantified by qRT-PCR at iPSC stage. Experiments have been performed three times. P-values were calculated using a two-tailed Student's t-test. ns, not significant; *, P<0.05; **, P< 0.01; ***, P<0.001; ****, P<0.0001.*

Supplementary Material Table 1:

Primers	*Sequence*
ACTIN_FW	*CACCATTGGCAATGAGCGGTTC*
ACTIN_RV	*AGGTCTTTGCGGATGTCCACGT*
CEPBA_FW	*GGACCCTCAGCCTTGTTTGT*
CEPBA_RV	*TGTCATAACTCCGGTCCCTCT*
DLK1_FW	*TGCCTGCCGTGTTTACCTTG*
DLK1_RV	*TGTGTGTGGGTGACTGATGTG*
GFRA1_FW	*TATCAAAGCAAGCCAAGCAAG*
GFRA1_RV	*TAAGCACGCCAAGAAGAAGTG*
JUN_FW	*CAAGAACTCGGACCTCCTCAC*
JUN_RV	*TCCTGCTCATCTGTCACGTTC*
NR4A3_FW	*GAAGTGTCTCAGTGTTGGAATGG*
NR4A3_RV	*ATGGGCTCTTTGGTTTGGAAG*
RET_FW	*CATCAGCAAAGACCTGGAGAAG*
RET_RV	*AATCAGGGAGTCAGATGGAGTG*

Supplementary Table 1: List of the 109 genes upregulated by RET^{C634Y} mutation during iSPCs hematopoietic differentiation

Gene	*logFC*	*AveExpr*	*adj.P.Val*
GOPC	*6.39189*	*6.824905*	*3.839737724586e-05*
TAF9B	*5.552925*	*7.6517775*	*4.55189292473964e-05*
INPP5F	*5.39053*	*9.815355*	*7.29940973661325e-05*

LDOC1	*6.83768*	*7.6542*	*0.000186177747550023*
HIST1H2BM	*4.434215*	*10.7141625*	*0.000186177747550023*
HTR1E	*4.712515*	*7.4190375*	*0.000189093530472259*
RGPD2	*4.683155*	*6.0728075*	*0.000257125685418469*
CNTNAP4	*4.48187*	*5.30308*	*0.000257125685418469*
RGPD1	*3.08282*	*8.168405*	*0.000510825598115004*
NAP1L5	*3.038625*	*4.6231325*	*0.000552636174486203*
ZNF667	*2.913245*	*6.2546325*	*0.00102742664698341*
CDR1	*2.307375*	*13.5474575*	*0.00157295220217926*
RAB27B	*2.64627*	*9.349*	*0.00250610851294452*
DPP10	*2.15072*	*9.030765*	*0.00397837984024221*
NR4A3	*1.8779*	*7.685635*	*0.00418981529421182*
MRPS21	*1.87338*	*13.381125*	*0.00418981529421182*
GRIA4	*1.838055*	*5.9839325*	*0.00418981529421182*
TMEM176A	*1.949345*	*9.1347625*	*0.00477445401661958*
COLEC10	*1.75172*	*13.50653*	*0.00477445401661958*
ZNF717	*2.78298*	*7.20399*	*0.0050029213396522*
TMEM176B	*1.877415*	*7.5184825*	*0.00593613114366584*
SHISA6	*1.693635*	*4.1400525*	*0.00712521719554855*
DIO3	*1.90021*	*8.591525*	*0.00772463281293109*
TMBIM4	*1.66727*	*8.78482*	*0.00831238823421279*
NR4A2	*1.645535*	*6.2878225*	*0.00831238823421279*
CHRM2	*2.087845*	*6.7283675*	*0.00849654760886506*
CNTNAP5	*2.11457*	*6.394995*	*0.00849654760886506*
LPAR6	*1.843795*	*9.1825075*	*0.00942550433851747*
COL6A6	*1.58289*	*7.14962*	*0.00942550433851747*
PCDHB16	*1.6577*	*10.75213*	*0.00942550433851747*
DPP4	*1.578795*	*11.0388825*	*0.00942550433851747*
CEBPZOS	*1.659535*	*10.0678475*	*0.00946441527224467*
NR2F1	*1.696465*	*9.2369925*	*0.0095289485730007*
IRAK4	*1.413775*	*7.7066975*	*0.00964652889110839*
CYP4V2	*1.975685*	*4.2147475*	*0.0104863922619242*
ALX1	*1.6706*	*6.780535*	*0.011142321024797*
GLIPR1	*1.3864*	*9.443665*	*0.011142321024797*
BCHE	*1.56037*	*6.11527*	*0.011142321024797*
ZNF880	*1.517995*	*8.5236275*	*0.011142321024797*
CTHRC1	*1.42238*	*13.05974*	*0.0111885798351944*
FAM172A	*1.43141*	*7.8818*	*0.0111885798351944*
HCAR3	*1.550005*	*5.6404875*	*0.0111885798351944*
SNAP91	*1.453005*	*5.2175525*	*0.0120201363164359*
NSMCE1	*1.51567*	*7.509725*	*0.0120201363164359*
GPR183	*1.33453*	*9.476375*	*0.0120201363164359*
GABRA2	*1.65994*	*9.309935*	*0.0120571870641575*
TXNRD2	*1.76429*	*7.381675*	*0.0120571870641575*
PLA2G2A	*1.471405*	*8.2217275*	*0.0132059296878331*
SFRP1	*1.365095*	*8.1756275*	*0.013722700612905*

PID1	*1.41367*	*7.07916*	*0.0139581054732494*
TMEM132C	*1.546885*	*4.3803225*	*0.0139581054732494*
CASP4	*1.71681*	*5.938465*	*0.0139581054732494*
LRRTM2	*1.594415*	*6.3730175*	*0.0143179764931618*
PSMB8	*1.429735*	*7.1980625*	*0.0149774940033406*
C3	*1.21254*	*10.77043*	*0.0178176824349004*
CDH7	*1.312035*	*9.0969775*	*0.0180445208352434*
LRRTM4	*1.197085*	*7.6331675*	*0.0180879278843384*
PUS7L	*1.56445*	*8.626045*	*0.0180879278843384*
MRPL3	*1.310275*	*10.2708625*	*0.0180879278843384*
STMN2	*1.18248*	*11.36844*	*0.0192466567143874*
RFTN2	*1.30058*	*10.613425*	*0.0198375526063248*
ADAM23	*1.185965*	*8.8568675*	*0.0198375526063248*
PTGFR	*1.169195*	*10.7926325*	*0.0200756776981018*
PNPO	*1.197005*	*3.9925475*	*0.0216267920727596*
IRAK3	*1.6331*	*8.40788*	*0.0220852025295686*
PTGDS	*1.48716*	*7.339845*	*0.0220960844482512*
ZNF585B	*1.233265*	*11.1525975*	*0.0220960844482512*
JAG1	*1.324425*	*10.8424225*	*0.0220960844482512*
DLK1	*1.296805*	*16.9212025*	*0.0220960844482512*
JAM2	*1.208825*	*10.8772725*	*0.0224957181851337*
PCTP	*1.44364*	*9.52025*	*0.0227362826870834*
ANGPT1	*1.10835*	*8.07056*	*0.0228608965261987*
NEK9	*1.18655*	*10.267355*	*0.0228608965261987*
C7	*1.677465*	*5.2920675*	*0.0230378169659056*
CADPS2	*1.16517*	*6.90015*	*0.0232838609938617*
GFRA1	*1.448515*	*10.7839125*	*0.0238103172498784*
ZNF562	*1.17215*	*8.88995*	*0.0238193526012892*
NCALD	*1.34288*	*7.20356*	*0.0251331985626647*
COMT	*1.55994*	*9.98751*	*0.0253027873732179*
HNMT	*1.14319*	*10.71118*	*0.0254541264647253*
ZNF585A	*1.196235*	*8.6598775*	*0.0270754306280722*
NFIL3	*1.05123*	*10.567205*	*0.0270754306280722*
GFRA2	*1.36447*	*4.85712*	*0.0280723126469758*
MNS1	*1.32578*	*5.954835*	*0.0280773357444547*
ICAM1	*1.15306*	*11.79135*	*0.0296068165619322*
FCGR2B	*1.05993*	*6.340205*	*0.0296964339958956*
OLFM3	*1.4148*	*5.66399*	*0.0298444148420818*
TCTA	*1.02468*	*6.02184*	*0.0303148062108365*
JUN	*1.029955*	*14.1677475*	*0.0303148062108365*
FAM155A	*1.24339*	*6.139145*	*0.0310797970913604*
CCDC102B	*1.094785*	*7.9479125*	*0.0316292104513524*
TGFA	*1.084345*	*6.4699725*	*0.0316469976720747*
BMPR1B	*1.02368*	*6.26078*	*0.0326468613946061*
LPAR1	*1.05089*	*9.97868*	*0.0326468613946061*
ZNF572	*1.40546*	*5.27796*	*0.0332833952978816*

HLA-DRB1	*1.170975*	*5.3973475*	*0.0346673244909029*
PDE8A	*1.23345*	*5.518815*	*0.0352443612012122*
ZFHX4	*1.08177*	*8.8411*	*0.0365320473525916*
ARHGAP44	*1.370575*	*5.5606125*	*0.0365873464007626*
EBF1	*1.35567*	*6.350415*	*0.0383672864673443*
MRGPRD	*1.07915*	*7.951225*	*0.0390354468500145*
ERAP2	*1.400745*	*5.6965525*	*0.0410285718938848*
EDNRA	*1.140445*	*10.0933975*	*0.0429600142994066*
IFIT2	*1.074825*	*7.0686375*	*0.0431521978474641*
PRELID3B	*1.03029*	*8.82904*	*0.0431795144817928*
C7orf60	*1.22736*	*9.27379*	*0.0434340766371203*
CTSF	*1.32325*	*5.00302*	*0.0450019054447269*
WDR54	*1.11879*	*7.455195*	*0.0458443677121318*
CPNE8	*1.00153*	*14.093495*	*0.0462967389197386*

2. Article 2: Modeling *RET*-rearranged Non-Small Cell Lung Cancer (NSCLC): Generation of Lung Cell Progenitors (LPCs) from Patient-Derived Induced Pluripotent Stem Cells (iPSCs)

The objective of this second article was the development of a model of RET-driven NSCLC from patient-derived iPSCs. Indeed, *RET* rearrangements occur in approximately 1-2% of NSCLC cases and lead to the constitutive activation of the RET kinase domain, driving downstream signaling pathways critical to cancer cell behaviors like proliferation, invasion, and survival.

Although various models for RET-driven lung cancer exist, none have been based on patient-derived iPSC. These iPSCs hold promise for disease modeling and drug testing. Yet, generating iPSCs with specific oncogenic drivers like *RET* rearrangements faces challenges due to reprogramming efficiency and tumor genotypic variability.

To overcome these challenges, we tried to generate lung progenitor cells (LPCs) from patient-derived iPSCs harboring the RET^{C634Y} somatic mutation which is a major oncogenic event in medullary thyroid carcinoma. A RET^{C634Y} knock-in iPSC model was also engineered to validate the effect of the overexpression of this allele during differentiation of normal iPSCs towards lung progenitor cells.

In this work, we have successfully generated LPCs from RET^{C634Y} iPSCs and found that the differentiated cells mirrored *RET*-rearranged NSCLC characteristics. Indeed, upon differentiation towards lung progenitor lineage, LPCs exhibited overexpression of cancer associated markers reported in RET driven NSCLC. Transcriptomic analysis reveal that RET^{C634Y} signature is associated with multilineage lung dedifferentiation. Moreover, the comparison of these transcriptomic data with primary NSCLC cohorts revealed a group of genes associated with poor prognosis in NSCLC. Similar analysis performed with RET^{C634Y} knock-in model validates our finding. Moreover, RET^{C634Y} iPSC-derived LPCs demonstrated a positive response to the RET inhibitor Pralsetinib, as indicated by the downregulation of the cancer markers after the treatment.

This study successfully establishes a model of RET-driven NSCLC using patient-derived iPSCs and highlights the potential of iPSCs for drug testing and cancer marker discovery.

This article has been published in Cells 2023.

cells

MDPI

Article

Modeling RET-Rearranged Non-Small Cell Lung Cancer (NSCLC): Generation of Lung Progenitor Cells (LPCs) from Patient-Derived Induced Pluripotent Stem Cells (iPSCs)

Paul Marcoux [1,2,†], Jin Wook Hwang [1,2,†], Christophe Desterke [1,2], Jusuf Imeri [1,2], Annelise Bennaceur-Griscelli [1,2,3,4,5] and Ali G. Turhan [1,2,3,4,5,*]

1 INSERM UMR-S-1310, Université Paris Saclay, 94800 Villejuif, France; paul.marcoux@inserm.fr (P.M.); jinwook.hwang@inserm.fr (J.W.H.); christophe.desterke@gmail.com (C.D.); jusuf.imeri@inserm.fr (J.I.); abenna@hotmail.fr (A.B.-G.)
2 Faculty of Medicine, Paris-Saclay University, 94270 Le Kremlin Bicetre, France
3 APHP Paris Saclay, Department of Hematology, Hôpital Bicêtre, 94270 Le Kremlin Bicetre, France
4 Center for IPSC Therapies, CITHERA, INSERM UMS-45, Genopole Campus, 91100 Evry, France
5 APHP Paris Saclay, Department of Hematology, Hôpital Paul Brousse, 94800 Villejuif, France
* Correspondence: turviv33@gmail.com
† These authors contributed equally to this work.

Abstract: REarranged during Transfection (RET) oncogenic rearrangements can occur in 1–2% of lung adenocarcinomas. While RET-driven NSCLC models have been developed using various approaches, no model based on patient-derived induced pluripotent stem cells (iPSCs) has yet been described. Patient-derived iPSCs hold great promise for disease modeling and drug screening. However, generating iPSCs with specific oncogenic drivers, like *RET* rearrangements, presents challenges due to reprogramming efficiency and genotypic variability within tumors. To address this issue, we aimed to generate lung progenitor cells (LPCs) from patient-derived iPSCs carrying the mutation RET^{C634Y}, commonly associated with medullary thyroid carcinoma. Additionally, we established a RET^{C634Y} knock-in iPSC model to validate the effect of this oncogenic mutation during LPC differentiation. We successfully generated LPCs from RET^{C634Y} iPSCs using a 16-day protocol and detected an overexpression of cancer-associated markers as compared to control iPSCs. Transcriptomic analysis revealed a distinct signature of NSCLC tumor repression, suggesting a lung multilineage lung dedifferentiation, along with an upregulated signature associated with RET^{C634Y} mutation, potentially linked to poor NSCLC prognosis. These findings were validated using the RET^{C634Y} knock-in iPSC model, highlighting key cancerous targets such as *PROM2* and *C1QTNF6*, known to be associated with poor prognostic outcomes. Furthermore, the LPCs derived from RET^{C634Y} iPSCs exhibited a positive response to the RET inhibitor pralsetinib, evidenced by the downregulation of the cancer markers. This study provides a novel patient-derived off-the-shelf iPSC model of RET-driven NSCLC, paving the way for exploring the molecular mechanisms involved in RET-driven NSCLC to study disease progression and to uncover potential therapeutic targets.

Keywords: NSCLC; patient derived; iPSCs; RET; LPC differentiation; cancer; model; pralsetinib

check for updates

Citation: Marcoux, P.; Hwang, J.W.; Desterke, C.; Imeri, J.; Bennaceur-Griscelli, A.; Turhan, A.G. Modeling RET-Rearranged Non-Small Cell Lung Cancer (NSCLC): Generation of Lung Progenitor Cells (LPCs) from Patient-Derived Induced Pluripotent Stem Cells (iPSCs). *Cells* **2023**, *12*, 2847. https://doi.org/10.3390/cells12242847

Academic Editor: Gianpaolo Papaccio

Received: 7 November 2023
Revised: 3 December 2023
Accepted: 8 December 2023
Published: 15 December 2023

Copyright: © 2023 by the authors. Licensee MDPI, Basel, Switzerland. This article is an open access article distributed under the terms and conditions of the Creative Commons Attribution (CC BY) license (https://creativecommons.org/licenses/by/4.0/).

1. Introduction

Lung cancer is the second most prevalent cancer worldwide with over 2.2 million new cases reported in 2020 [1]. Non-small cell lung cancer (NSCLC) accounts for approximately 85% of these cases, with adenocarcinoma being the most common subtype among all lung cancers, comprising 40% of cases [2,3]. The classification of lung adenocarcinomas into molecular subtypes is determined by specific molecular alterations that contribute to cancer initiation and progression [4]. Many of these oncogenic drivers are receptor tyrosine kinases (RTKs) that regulate intracellular signaling pathways [5].

One of these RTK, REarranged during Transfection (RET), has been extensively studied in NSCLC. RET transmits a proliferative signal in the presence of its co-receptor GDNF (glial cell line derived neurotrophic factor) family receptor alpha-1 (GFRα1) and in response to GDNF-ligands families (GLF). Recent studies have revealed the presence of *RET* rearrangements in 1–2% of cases of lung adenocarcinoma [6]. Patients with RET-fusion positive NSCLC are mostly young-never smokers [7]. RET fusions lead to the activation of downstream signaling pathways such as STAT3 and RAS-MAPK involved in cell proliferation and survival, thus promoting tumor growth [8–10]. RET fusion-positive lung carcinomas exhibit poorer differentiated tumors compared to those with ALK or EGFR alterations [11]. Moreover, previous evidence has indicated that RET signaling plays a significant role in drug resistance, including resistance to EGFR TKIs and emerging $KRAS^{G12C}$ inhibitors in NSCLC [12,13]. Finally, *RET*-rearranged patients typically exhibit low levels of PD-L1 expression and a low tumor mutational burden, and they tend to have unfavorable outcomes when treated with immunotherapies [14]. These data show that *RET* rearrangements define a distinct molecular and clinicopathological subtype of NSCLC. Therefore, the development of a *RET*-rearranged lung cancer model would be highly valuable to investigate the unique characteristics of this disease and identify novel therapeutic targets.

Several models of *RET*-rearranged lung cancer have been developed during previous years. These models are based on cancer cell lines [15], genetically engineered mouse models expressing KIF5B-RET fusion protein [16], or PDX-derived lung adenocarcinoma cells harboring KIF5B-RET fusion [17].

iPSCs have been used previously to model several types of malignancies including leukemia [18–20], hereditary cancers such as Li-Fraumeni syndrome [21] kidney cancer [22], and hereditary retinoblastoma [23]. The role of oncogenic KRAS has been studied in alveolar cells derived from human iPSCs expressing Dox-inducible $KRAS^{G12D}$, revealing a down-regulation of maturation markers in alveolar cells expressing $KRAS^{G12D}$ with upregulation of progenitor and developmental markers [24]. However, this highly interesting model used normal donor-derived iPSCs to study the effect of the expression of oncogenic $KRAS^{G12D}$ in alveolar epithelial cells. Currently, no lung cancer model based on patient-derived induced pluripotent stem cells (iPSCs) has yet been developed. Such a model could constitute a valuable asset to study RET-driven NSCLC. Indeed, patient-derived iPSC models capture the unique genetic characteristics of individual patients and provide a more accurate representation of the disease biology compared to traditional cell lines [25]. By facilitating disease modeling and the creation of patient-specific organoids, patient-derived iPSCs enable the investigation of cancer development, high-throughput drug screening, and target discovery, paving the way for remarkable progress in these critical domains [22].

However, generation of patient-derived iPSCs from NSCLC patients carrying specific oncogenic drivers, such as *RET* rearrangements, presents significant challenges. Indeed, most reprogramming protocols are optimized for cells that are easily available and more efficient to reprogram, with high proliferation rate and chromatin accessibility, such as peripheral blood mononuclear cells (PBMC), mesenchymal stem cells, fibroblast, etc. [26]. Additionally, the low efficiency of reprogramming, coupled with the high genotypic variability within tumors, further complicates the generation of iPSCs with specific mutations of interest [27]. Finally, like other cancer cells, the reprogramming of NSCLC cells into iPSCs is impeded by various barriers, including genetic alterations and epigenetic memory [18]. Although, the generation of iPSCs carrying hereditary mutations is a more attainable objective due to their presence in all cells of an individual, it enables the utilization of existing reprogramming protocols [21]. Several studies have already used patient-derived iPSCs carrying mutations, such as *p53* or *RB1* mutations, to elucidate mechanisms related to cancer [23,28]. However, to the best of our knowledge, there are presently no NSCLC patient-derived iPS cell lines and therefore no model of a patient-derived-iPSC lung cancer model.

To tackle this challenge, we tested whether we could generate lung progenitor cells (LPCs) accurately recapitulating the characteristics of *RET*-rearranged NSCLC from a patient-derived iPSC carrying the RET^{C634Y} point mutation. RET^{C634Y} mutation is com-

monly associated with medullary thyroid carcinoma (MTC) and results in RET dimerization in the absence of its ligands, leading to the autophosphorylation of its tyrosine kinase domains. The constitutive activation of the RET pathway is equivalent to the consequences of *RET* rearrangements observed in NSCLC [29–31]. We also generated a RET^{C634Y} knock-in iPSC to validate the effect of the mutation on iPSC-derived lung progenitors. Therefore, this work aimed to establish the suitability of iPSCs carrying RET point mutations as the first model of patient-derived iPSCs RET-driven NSCLC.

Using a 16-day protocol [32], we successfully generated lung progenitors from patient-derived iPSCs harboring the RET^{C634Y} mutation ($iRET^{C634Y}$) and its CRISPR-corrected isogenic control iPSC ($iRET^{CTRL}$). Notably, progenitors derived from $iRET^{C634Y}$ exhibited an overexpression of cancer-associated markers as compared to WT progenitor derived from $iRET^{CTRL}$. Transcriptomic analysis uncovered a distinctive repressed signature of NSCLC that was dependent on the RET^{C634Y} mutation, indicating lung multilineage dedifferentiation. Additionally, the upregulated signature associated with RET^{C634Y} mutation could potentially be linked to poor prognosis for NSCLC. These findings were further validated by employing a knock-in of the RET^{C634Y} mutation in WT iPSCs (PB68-RET^{C634Y} and PB68-WT). In both approaches, key targets associated with poor prognostic outcomes, namely *PROM2* and *C1QTNF6*, were found to be upregulated by the RET^{C634Y} mutation. Finally, LPCs derived from iPSCs carrying the RET^{C634Y} mutation demonstrated a positive response to the RET inhibitor pralsetinib, as evidenced by the downregulation of these cancer markers.

2. Materials and Methods

2.1. Generation of iPSCs

The iPSC line PB68-WT was generated from peripheral blood mononuclear cells (PBMCs) obtained from the cord blood of healthy donors according to the Declaration of Helsinki. Cells were reprogrammed by non-integrative Sendai viral transduction. Pluripotency was characterized by FACS and teratoma assays. PB68-RET^{C634Y} was generated from the iPSC PB68-WT using lentiviral transduction described in a previous study [33]. Briefly, we used Lenti-X 293T as a packaging cell line and psPAX2.2, and pMD2.G as packaging vector and envelope vector, respectively. The plasmid RET^{C634Y} was purchased from VectorBuilder (Guangzhou, China). Generation of RET mutated iPSC $iRET^{C634Y}$ and its isogenic CRIPSR corrected control $iRET^{CTRL}$ were previously described [34,35].

iPSCs were cultured in feeder-free condition in Geltrex coated dishes (A1413201; ThermoFisher Scientific, Illkirch, France) and fed daily with Essential 8 flex Medium (A2858501; ThermoFisher Scientific, Illkirch, France). iPSCs were passaged twice a week with EDTA dissociation (0.5 mM).

2.2. Generation of Lung Progenitor Cells

This procedure was adapted from the work of Leibel and colleagues [32]. The protocol involves the stepwise differentiation of iPSCs to lung progenitor cells (LPCs). iPSCs were seeded at 55–70% confluency in 6-well plates coated with Geltrex the day before definitive endoderm induction (DE). DE induction medium is composed of RPMI1640 (11875093; Gibco, Illkirch, France) supplemented with Glutamax (35050061; Gibco, Illkirch, France), B27 (12587010; ThermoFisher, Illkirch, France), Pen/Strep (15140-122; Gibco, France), HEPES 1% (15630-080; Gibco, Illkirch, France), 100 ng/mL Human activin A (338-AC; R&D Systems, Lille, France) and 5 µM CHIR99021 (72054; Stemcell Technology, Grenoble, France). DE induction medium was replaced daily for 3 days. On day +4, the medium was changed and replaced daily until day +6 with anterior foregut endoderm (AFE) induction medium which is serum free basal media supplemented with 10 µM SB431542 (1614; Tocris Bioscience, Bristol, UK) and 2 µM dorsomorphin (72102; Stemcell, Grenoble, France). Serum free basal medium is composed of 75% IMDM+Glutamax (31980030; Gibco, Illkirch, France) and 25% Ham's F12 (11765054; Gibco, France) complemented with B27, N2 (17502048; ThermoFisher, Illkirch, France), Pen/Strep, 50 mg/mL L-Ascorbic acid 2-phosphate (A8960;

Sigma-Aldrich, Saint-Quentin-Fallavier, France), 500 µg/mL monothioglycerol (M6145; Sigma-Aldrich, Saint-Quentin-Fallavier, France), 7,5% BSA (15260-037; Gibco, Illkirch, France). On day +7, the AFE medium was aspirated, and replaced by LPC induction medium and changed every two days. LPC induction medium is composed of serum free basal medium complemented with 10 ng/mL human BMP4 (78211; Stemcell, Grenoble, France), 0.1 µM all-trans retinoic acid (72262; Stemcell, Grenoble, France), and 3 µM CHIR99021.

2.3. RNA Extraction, Reverse Transcription, and qRT-PCR

Total intracellular RNA was extracted using RNeasy Mini Kit (74104; Qiagen, Hilden, Germany) and 1 µg was reverse transcribed using a reverse transcription (RT)-PCR kit (Superscript III 18080-44; ThermoFisher Scientific, Illkirch, France). An aliquot of cDNA was used as a template for qRT-PCR analysis using a fluorescence thermocycler (ThermoFisher Scientific QuantStudio 3TM) with FastStart Universal SYBR Green (04913914001, Roche, Vilnius, Lithuania) DNA dye. The primer sequences used for qRT-PCR are listed in the Supplementary Table S1. Relative expression was normalized to the geometric mean of housekeeping gene expression and was calculated using the $2^{-\Delta\Delta Ct}$ method.

2.4. Immunofluorescence Staining

LPCs were washed with phosphate-buffered saline (PBS) fixed with 4% formaldehyde in PBS for 60 min, permeabilized with 0.2% Triton X-100 (Sigma-Aldrich, Saint-Quentin-Fallavier, France) in PBS and blocked with 10% serum. Primary antibodies were diluted in PBS 10% serum at the following concentrations: TP63 (1:100, ab124762; Abcam, Cambridge, UK) and Phospho-RET (Tyr1096) (1:100, PA5-105796; Thermo Fisher Scientific, Illkirch, France). Samples were incubated with secondary antibodies in antibody dilution buffer, then washed in PBS. Nuclei were labeled with DAPI (D9542; Sigma-Aldrich, Saint-Quentin-Fallavier, France) mounting medium. Visualization and capture were performed with a Leica confocal microscope and LAS AF software (v3.2).

2.5. RNA-Sequencing Experiments

iPSCs and iPSC-derived LPC samples were processed for transcriptome triplicate experiments. Before the preparation of the sequencing library, the quality of the RNAs was checked with bioanalyzer with an average RIN per sample of 9.6. Starting from 10 to 100 ng of total RNA, molecular library of sequencing (Illumina) preparation was conducted for paired end sequencing focused on 3′ coding ends of transcripts. A minimum of ten million of reads were sequenced by sample on GENOMIC platform from Cochin Institute (Paris, France).

2.6. RNA-Sequencing Analyses

Paired-end FASTQ files were aligned on human genome version Ensembl release 101, Homo sapiens GRCh38 with STAR algorithm version (v2.7.6a) in two pass mode [36]. Transcript count was counted with RSEM algorithm version (v1.3.1) [37]. Transcript normalization and differential expressed gene analysis was performed with DeSeq2 R package version 1.34.0 in R environment version 4.1.3 [38].

2.7. Transcriptome Datasets

Transcriptome data of NSCLC samples and normal lung adjacent tissue from frozen sampling of Gene Expression Omnibus (GEO) dataset GSE44077 [39] were collected at this address https://www.ncbi.nlm.nih.gov/geo/query/acc.cgi?acc=GSE44077 (accessed on 12 May 2022). This transcriptomic analysis was performed with Affymetrix Human Gene 1.0 ST Array technology and annotated with the corresponding platform GPL6244 https://www.ncbi.nlm.nih.gov/geo/query/acc.cgi?acc=GPL6244 (accessed on 12 May 2022).

2.8. TCGA RNA-Sequencing of Lung Adenocarcinoma Tumors

Lung adenocarcinoma tumor transcriptome dataset from The Cancer Genome Atlas (TCGA) consortium [40] was accessed through CBioPortal web tool [41]. This cohort of transcriptome is composed of 510 lung tumors from patients with a median age of 66 years old (range from 33 to 88 years).

2.9. Bioinformatics Analysis

Bioinformatics analyses were performed with R version 4.1.3. Unsupervised principal component analysis (PCA) was carried out with prcomp R base function and drawn with autoplot function from ggforitfy R-package version 0.4.14. Microarray transcriptome differentially expressed gene analysis was conducted with limma R-package version 3.50.3. Expression heatmaps were drawn with pheatmap R-package version 1.0.12 and clustering was conducted with the parameters clustering distance = "euclidean" and clustering method = "complete". Functional enrichment was performed by over representative analysis through two distinct webtool applications: Enrichr [42] and Toppgene suite [43]. These functional enrichment analyses were carried out with distinct databases: Gene Ontology [44], DisGeNET [45] and Co-expression Lung Atlas through GeneSigDB [46] and MsigDb [47]. Functional enrichment networks were built with Cytoscape standalone application version 3.6.0 [48]. Barplots were drawn with ggplot2 R-package 3.3.6 [49]. Iterative loop of univariate survival Cox model on expression of selected markers was performed with loopcolcox_1.0.0 R-package https://github.com/cdesterke/loopcolcox (accessed on 8 February 2023). Log rank survival analysis at univariate and multivariate levels was performed with survival R-package version 3.5-0. The expression risk score was computed with the sum of the mathematical products between the Cox beta coefficient and the expression of the selected molecular markers. The threshold on risk score and Kaplan–Meier graph were performed with survminer R-package version 0.4.9. Calibration of the Cox multivariable model was performed by bootstrapping with rms R-package version 6.4-1 and survival nomogram was drawn with regplot R-package version 1.1.

3. Results

3.1. $iRET^{CTRL}$ and $iRET^{C634Y}$ iPSCs Can Be Successfully Differentiated into Lung Progenitor Cells

To assess the potential of patient-derived iPSCs harboring inherited mutations as an accurate model of RET-driven NSCLC, we employed an iPS cell line derived from a patient carrying RET^{C634Y} mutation ($iRET^{C634Y}$) who developed medullary thyroid carcinoma (MTC) [34] Additionally, we included an isogenic CRISPR/Cas9-corrected iPSC line ($iRET^{CTRL}$) as a control [35]. This model has already proven to be valuable in investigating the RET-activation related mechanisms [33].

These two iPS cell lines were differentiated into NKX2-1^{+} lung progenitor cells (LPCs) with a 16-day protocol [32]. The process involves enzymatic dissociation of iPSCs and their differentiation into LPC following sequential steps (Figure 1A). The first step is the induction of the definitive endoderm (DE) expressing *CXCR4* and *SOX17* [50], and then the generation of anterior foregut endoderm (AFE), characterized with the expression of *FOXA2* and *SOX2* [51]. Finally, the cells are specified into LPCs (Figure 1A) [52].

Phase-contrast imaging during the differentiation of both $iRET^{CTRL}$ and $iRET^{C634Y}$ iPSC differentiation revealed expected morphology at each stage for respective cell types as compared to previously published data, thus showing a typical morphology consistent with an ongoing differentiation (Figure 1B) [32]. To further confirm the phenotype of the cells obtained at day +16, an immunostaining for TP63 was performed. Both NKX2-1 and TP63 were shown to be expressed upon differentiation of pluripotent stem cells towards LPCs [53]. TP63 is a marker for basal cells in the human airway epithelium, which are multipotent stem cells involved in epithelial repair and regeneration [54]. Immunofluorescence staining demonstrated that cells derived from both iPSCs expressed TP63, indicating a successful differentiation into LPCs (Figure 1C).

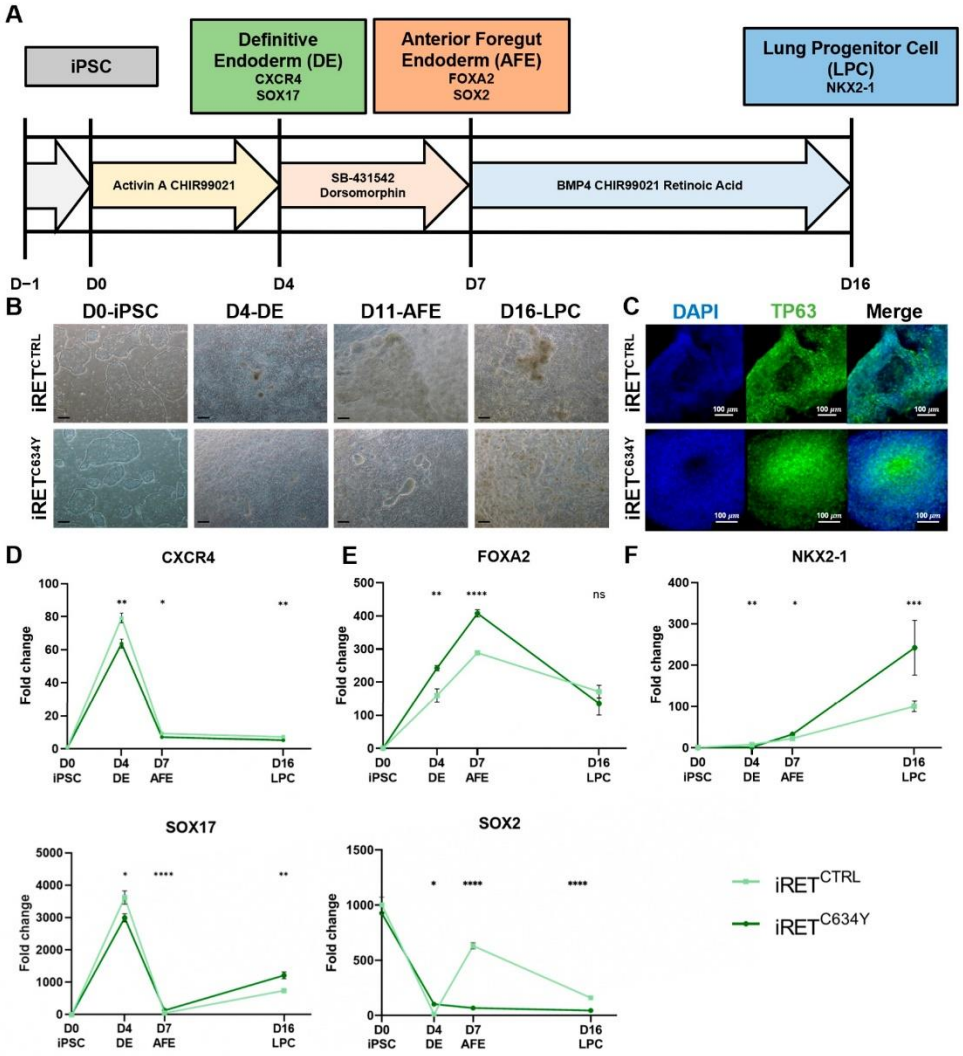

Figure 1. Generation of lung progenitor cells (LPCs) from iRET^{C634Y} is associated with the overexpression of FOXA2 and NKX2-1. (**A**) Schematic representation of the differentiation protocol from iPSC to NKX2-1^{+} lung progenitor cells (LPCs). (**B**) Morphology of *RET*^{C634Y} mutated iPSC (iRET^{C634Y}) and its isogenic CRISPR control (iRET^{CTRL}) during LPC differentiation at definitive endoderm (DE), anterior foregut endoderm (AFE), and LPC stages. Magnification 10×; scale bar 100 µm. (**C**) Immunostaining of LPCs derived from iRET^{C634Y} and iRET^{CTRL} iPSCs showing the expression of TP63 (green), DAPI (blue) or merged. (**D**–**F**) Expression of the differentiation markers specific to each stage; (**D**) DE, (**E**) AFE, and (**F**) LPC; quantified by qRT-PCR. Fold change ($2^{-\Delta\Delta Ct}$) was normalized to iPSC stage. Differentiation experiments were performed three times for each condition. *p*-values were calculated at each stage using a two-tailed Student's *t*-test. ns, not significant; * $p < 0.05$; ** $p < 0.01$; *** $p < 0.001$; **** $p < 0.0001$.

3.2. Generation of LPCs from iRET^{C634Y} Is Associated with the Overexpression of Cancer-Related Markers and a Delay of Differentiation

To gain deeper insights into the processes occurring during LPC differentiation, qRT-PCR analyses were performed to assess the expression levels of stage-specific markers at various time points. Specifically, the characteristic markers for each stage, namely *CXCR4* and *SOX17* for DE, *FOXA2* and *SOX2* for AFE, and *NKX2-1* for LPC, were examined at day +4 (DE), day +7 (AFE), and day +16 (LPC). (Figure 1D). During the differentiation process of both iRET^{CTRL} and iRET^{C634Y} cell lines, expression levels of *CXCR4* and *SOX17* peaked

at day +4, with a fold change of 60 and 3000, respectively, were compared to the expression levels in iPSCs (Figure 1D). Subsequently, their expression declined during the AFE stage and remained consistently low until the completion of differentiation. Interestingly, on day +4, the upregulation of *CXCR4* and *SOX17* was significantly higher in iRET^{CTRL} as compared to iRET^{C634Y}.

The expression of *FOXA2* was increased during the first day of the differentiation and reached its maximum level at the AFE stage before decreasing at the LPC stage (Figure 1E). At the DE and AFE stages, *FOXA2* was significantly overexpressed in iRET^{C634Y} as compared to iRET^{CTRL}. Interestingly, FOXA2 transcription factor is known to be upregulated in KIF5B-RET fusion adenocarcinomas through RET downstream signaling pathways such as ERK and AKT [55]. Hence, it is plausible that *RET^{C634Y}* could upregulate *FOXA2* expression similarly during the differentiation of iPSC-derived LPCs.

SOX2 is a pluripotency marker and is highly expressed in undifferentiated iPSCs (D0) (Figure 1E). As the iPSCs undergo differentiation, the expression of *SOX2* diminished in the initial days. Intriguingly, during the AFE stage, *SOX2* is re-expressed solely in iRET^{CTRL} cells and not in iRET^{C634Y} cells, before declining once more during the LPC stage. During the AFE stage, *SOX2* was shown to regulate the emergence of lung basal cells [56], consequently, its absence could potentially result in a differentiation defect associated with the *RET^{C634Y}* mutation.

The expression of *NKX2-1* exhibited a consistent increase throughout the entire differentiation process, reaching its peak at the LPC stage (Figure 1F). Interestingly, LPCs derived from iRET^{C634Y} demonstrated a three-fold higher expression of *NKX2-1* compared to iRET^{CTRL}-derived LPCs. NKX2-1 serves as a marker for LPC differentiation; however, it is also associated with cancer [57], particularly in lung adenocarcinoma where it is highly expressed [58,59]. Therefore, the overexpression of NKX2-1 in iRET^{C634Y}-derived LPCs could potentially be linked to the formation of cancerous tissues.

Hence, the *RET^{C634Y}* mutation appears to be linked to the upregulation of cancer-related markers and may be associated with a delay in the differentiation process, which is a characteristic feature of RET-driven NSCLC [11].

3.3. RET^{C634Y}-Dependent Gene Signature during iPSC-Derived LPC Differentiation Predicts a Major Transcriptional Repression in NSCLC

To evaluate the effect of *RET^{C634Y}* mutation on transcriptional regulation during iPSC-derived LPC differentiation, whole transcriptome sequencing was performed in triplicate for iRET^{C634Y} and iRET^{CTRL} at both iPSC and LPC stages. During LPC differentiation, a total of 1977 and 2139 genes were found to be overexpressed in iRET^{CTRL} and iRET^{C634Y}, respectively. The comparison between these two gene lists was performed and only 640 genes specifically overexpressed during iRET^{C634Y} LPC differentiation were retained constituting a specific *RET^{C634Y}*-dependent gene signature (Figure 2A). To estimate the validity of this patient-derived iPSC NSCLC model and the influence of the *RET^{C634Y}* mutation, *RET^{C634Y}*-dependent gene signature was used to perform unsupervised analysis of NSCLC transcriptome data as compared to adjacent normal lung tissues. Principal component analysis performed (PCA) on GSE44077 transcriptome dataset revealed a good stratification of NSCLC tumor samples as compared to normal lung sample on the first principal axis based on *RET^{C634Y}*-dependent gene signature (Figure 2B). Among the 640 *RET^{C634Y}*-dependent genes, 97 genes were found to be significantly suppressed in tumors (Supplementary Table S2), while 33 genes were significantly upregulated (Supplementary Table S3). Supervised gene expression analysis restricted to *RET^{C634Y}*-dependent gene signature highlighted a major differentiation inhibitory signature in NSCLC tumor samples as compared to normal lung tissue samples (Figure 2C). These results suggest that *RET^{C634Y}*-dependent gene signature can predict a set of repressed genes in NSCLC.

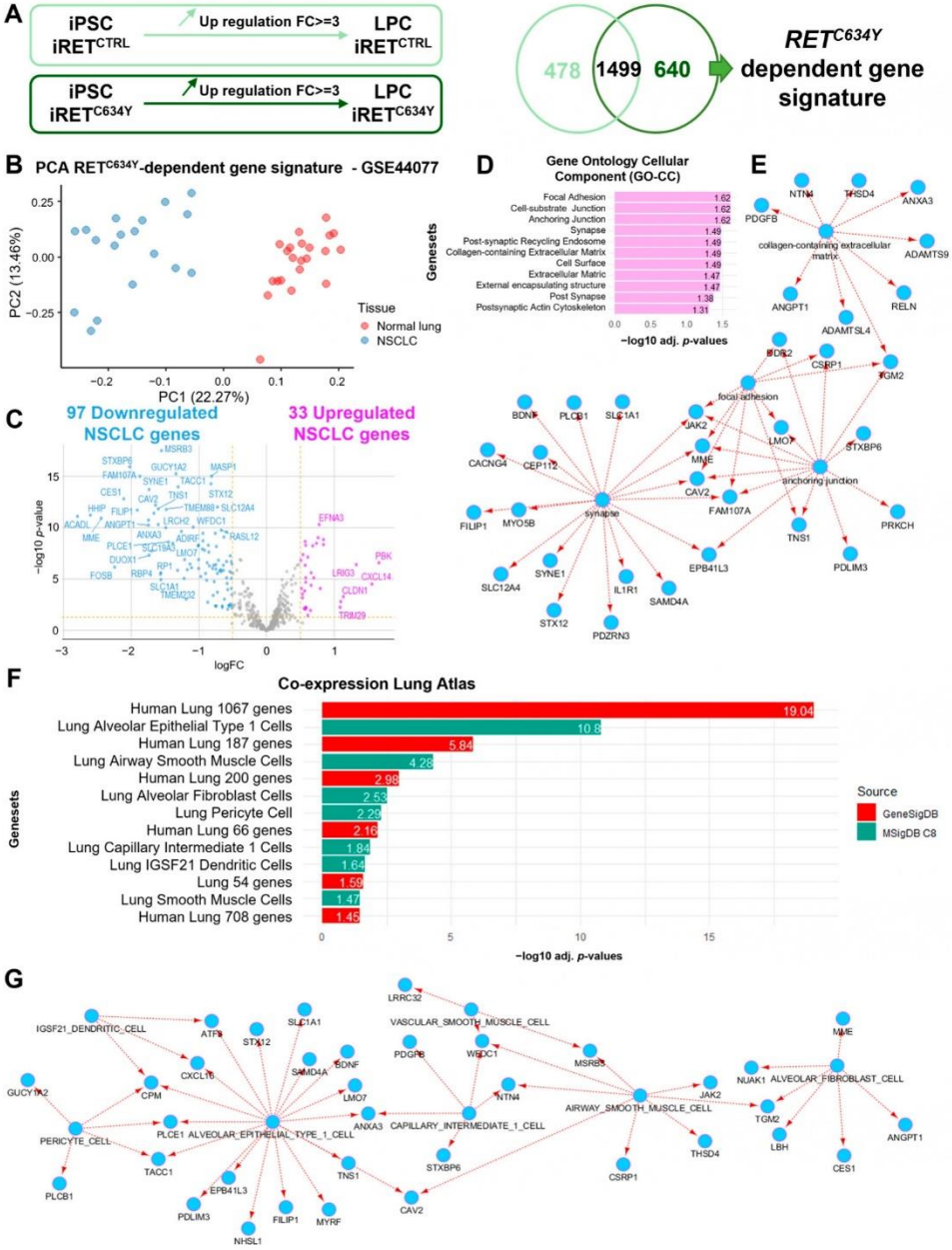

Figure 2. *RET*^{C634Y}-dependent gene signature during iPSC-derived LPC differentiation predicts a major transcriptional repression in NSCLC associated with a lung multilineage dedifferentiation. (**A**) Method for analyzing the *RET*^{C634Y}-dependent signature during iPSC-derived LPC differentiation. (**B**) Unsupervised principal component analysis based on *RET*^{C634Y}-dependent gene signature can stratify tumoral and normal lung adjacent samples from GSE44077 transcriptome dataset. (**C**) Volcano plot of differential expressed gene analysis between tumor and lung adjacent tissue of GSE44077 restricted to *RET*^{C634Y}-dependent gene signature (filter fixed over 0.5 log2 of fold change). (**D**) Barplot of functional enrichment performed with *RET*^{C634Y}-dependent repressed signature on Gene Ontology Cellular Component (GO-CC) database. (**E**) Functional enrichment network highlighting the implication of connected components like focal adhesion, anchoring junction, and synapse in *RET*^{C634Y}-dependent repressed signature in NSCLC tumors. (**F**) Barplot of functional enrichment performed on Co-expression Lung Atlas database with *RET*^{C634Y}-dependent repressed NSCLC signature. (**G**) Functional enrichment network identifying a lung multilineage implication of *RET*^{C634Y}-dependent repressed signature in NSCLC.

3.4. RET^{C634Y}-Dependent Inhibitory Signature in NSCLC Identifies a Lung Multilineage Dedifferentiation

RET^{C634Y}-dependent repressed gene signature in NSCLC (Supplementary Table S2) was validated to effectively stratify NSCLC tumor samples from normal lung tissues through unsupervised clustering (Supplementary Figure S1A) as well as unsupervised PCA (Supplementary Figure S1B). Functional enrichment of these repressed genes, performed on the Gene Ontology Cellular Component (GO-CC) database, revealed their implication mainly in focal adhesion, anchoring junction, and synapse (Figure 2D,E). These results suggest that RET related transcriptional repression occurring in NSCLC could disrupt epithelial cell fate and matrix adhesion.

Functional enrichment performed on Co-expression Lung Atlas through GeneSigDB database confirmed that RET^{C634Y}-dependent repressed gene signature in NSCLC samples was found to be affecting other human lung bulk signatures (red bars, Figure 2F). A comprehensive single-cell atlas of the normal human lung was generated, revealing a distinct gene signature for each lung cell subpopulation [60]. Enrichment based on this atlas reveals that RET-dependent repressed signature in NSCLC may affect several normal lung cell subpopulations such as type I alveolar epithelial cells (AT1s), airway smooth muscle cells, alveolar fibroblasts, pericytes, IGSF21 positive dendritic cells, and vascular smooth muscle cells (green bars, Figure 2F). Moreover, the majority of the repressed genes interact with AT1s (Figure 2G). This suggests that RET^{C634Y}-dependent signature repressed in NSCLC tumor samples may affect several distinct normal lung cell subpopulations through a general lung dedifferentiation program. The observation aligns with the finding that RET fusion-positive lung carcinomas displayed a higher prevalence of poorly differentiated tumors in comparison to those with ALK or EGFR alterations [11].

3.5. RET^{C634Y}-Dependent Signature in NSCLC Is Associated with Poor Prognosis

RET^{C634Y}-dependent activated signature, constituted by the 33 genes found upregulated in NSCLC (Supplementary Table S3), was verified to stratify NSCLC tumor samples from normal lung by unsupervised clustering (Supplementary Figure S1C) but also by unsupervised PCA (Supplementary Figure S1D). Functional enrichment performed on DisGeNET database confirmed that RET^{C634Y}-dependent activated signature is associated with known lung cancer pathogenesis such as carcinoma and malignant neoplasia (Figure 3A). Moreover, this signature can be integrated in a network of genes related to aggressive cancer signature (Figure 3B). These results suggest that RET^{C634Y}-dependent activated signature could be associated with patients with a poor prognosis.

The transcriptome data obtained through RNA-sequencing from a cohort of 510 lung adenocarcinoma patients, compiled by The Cancer Genome Atlas (TCGA), were examined by comparing them to RET^{C634Y}-dependent activated signature. *RET* and a subset of nine genes was found to be overexpressed in more than 4% of tumor samples (Figure 3C). Among these genes, six were already identified in the lung cancer related network of genes associated with RET^{C634Y} signature (*TMEM45B*, *CLDN1*, *TRIM29*, *SMUG1*, *SATB2*, and *EFNA3*) (Figure 3B). The three other genes are *HS3ST1*, *PROM2*, and *C1QTNF6*. Combined overexpression of these nine genes with *RET* in TCGA lung cancer transcriptomes was found to significantly stratify patients according to their overall survival (Figure 3D). Moreover, univariate overall survival analysis of these individual 10 genes overexpressed in adenocarcinoma revealed a dramatic prognosis, the worst being *C1QTNF6* and *PROM2* overexpression (Figure 3E). The expression of *C1QTNF6* and *PROM2* was quantified by qRT-PCR and both genes were found to be upregulated in $iRET^{C634Y}$ LPCs as compared to $iRET^{CTRL}$ LPCs, indicating that RET^{C634Y} is associated with the overexpression of NSCLC poor prognosis markers (Figure 3F).

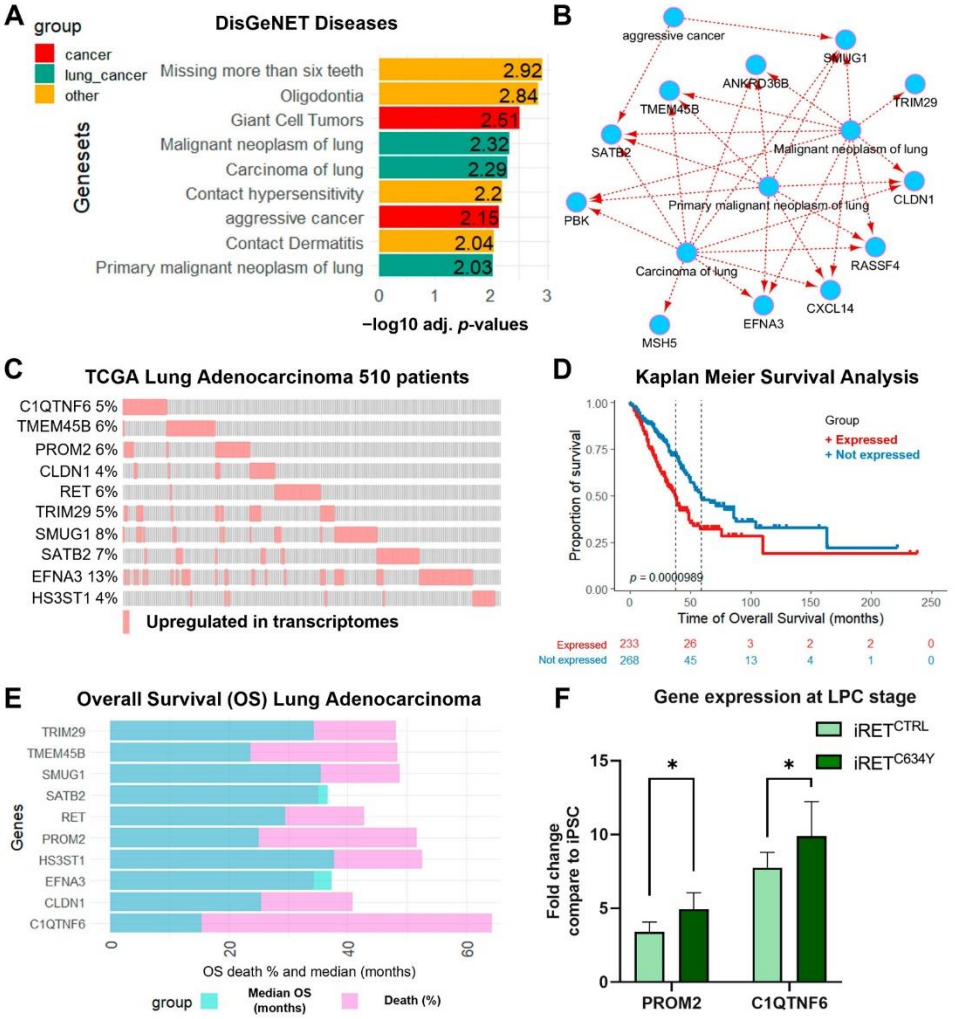

Figure 3. Adverse lung cancer prognosis for patients overexpressing RET^{C634Y}-dependent activated signature. (**A**) Barplot of functional enrichment performed with RET^{C634Y}-dependent activated signature on DisGeNET disease database. (**B**) Lung cancer related networks of genes found upregulated in NSCLC with RET^{C634Y}-dependent activated model integration. (**C**) Oncoprint of the RET 10 genes signature in the transcriptome of the TCGA lung adenocarcinoma cohort (510 patients/510 samples). (**D**) Kaplan–Meier curve and log-rank test analysis assessing the overall survival (OS) of lung adenocarcinoma patients, comparing those with (red) and without (blue) the overexpression of RET 10 genes signature. (**E**) Barplot of univariate overall survival analysis for the individual genes of RET 10 genes signature. The proportion of patient deaths among those exhibiting gene overexpression (purple) and the corresponding median overall survival (blue) are displayed. (**F**) Expression of two cancer markers associated with adverse prognosis quantified by qRT-PCR. Fold changes ($2^{-\Delta\Delta Ct}$) have been normalized to iPSC stage. Experiments were performed three times. *p*-values were calculated using a two-tailed Student's *t*-test. * $p < 0.05$.

The overexpression of this 10 gene signature can be significantly associated with the clinical data of patients (Supplementary Figure S2A). For example, an increase of hypoxia can be computed by three distinct scores (Winter, Ragnum, and Buffa scores) (Supplementary Figure S2B). A significant association was also observed with the increase of genomic alteration scores such as the fraction of genome altered, MSIsensor score, and tumor mutation burden (Supplementary Figure S2C). Other parameters reflecting the genomic instability such as the mutation count and the aneuploidy score were also found

to be significantly increased with this signature (Supplementary Figure S2C). All together, these results confirmed that *RET*^{C634Y}-dependent activated signature is associated with poor prognosis in lung cancer.

3.6. Differentiation of LPCs from RET^{C634Y} *Knock-In iPSCs Results in the Overexpression of FOXA2 and NKX2-1*

To ascertain the impact of the *RET*^{C634Y} mutation on LPC differentiation, a *RET*^{C634Y} knock-in model (PB68-RET^{C634Y}) was generated using a wild-type (WT) iPSC (PB68-WT) [33]. Using the previously described differentiation protocol, both iPSC lines were differentiated into LPCs. *RET* overexpression was confirmed through qRT-PCR analysis, revealing more than a 10-fold increase in expression in LPCs derived from PB68-RET^{C634Y} as compared to PB68-WT (Figure 4A). Activation of the RET pathway through its phosphorylation was assessed using immunofluorescence staining, which displayed a robust phospho-RET signal in LPCs derived from PB68-RET^{C634Y}, whereas LPCs derived from PB68-WT showed minimal signal. (Figure 4B). These results confirmed the successful generation of a *RET*^{C634Y} knock-in model by showing the overexpression and activation of RET in PB68-RET^{C634Y}.

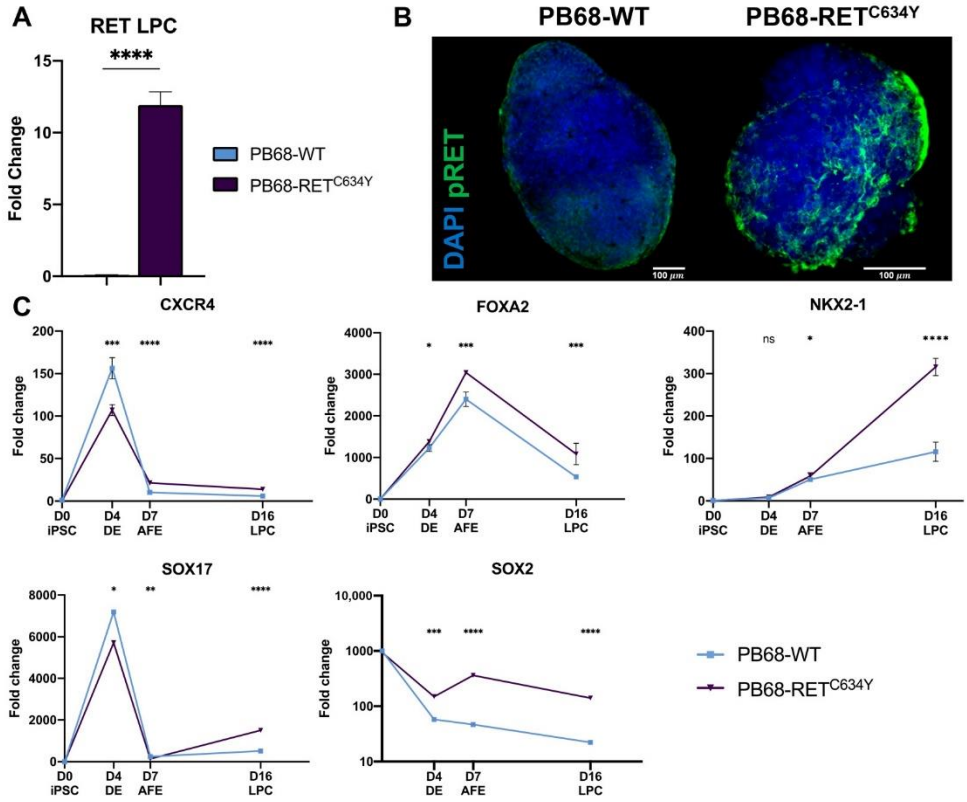

Figure 4. LPCs generated from *RET*^{C634Y} knock-in iPSCs are also associated with an overexpression of FOXA2 and NKX2-1. (**A**) qRT-PCR quantification of RET mRNA in LPCs derived from PB68-WT and PB68-RET^{C634Y} iPSCs. (**B**) Immunostaining of LPCs derived from PB68-WT and PB68-RET^{C634Y} iPSCs showing the expression of pRET (green) and DAPI (blue). (**C**) Expression of the differentiation markers specific to each stage quantified by qRT-PCR. Fold changes ($2^{-\Delta\Delta Ct}$) have been normalized to iPSC stage. Differentiation experiments were performed three times for each condition. *p*-values were calculated at each stage using a two-tailed Student's *t*-test. ns, not significant; ns: non-significant, * $p < 0.05$; ** $p < 0.01$; *** $p < 0.001$; **** $p < 0.0001$.

As described previously, qRT-PCR analysis was performed to assess the expression levels of stage-specific markers at various time points (Figure 4C). Strikingly, the knock-in of RET^{C634Y} mutation exhibited a similar effect on the expression of the differentiation markers when compared to the patient-derived RET^{C634Y} mutation. This effect was evident in the downregulation of *CXCR4* and *SOX17* during the DE stage, as well as the upregulation of *FOXA2* and *NKX2-1* during the AFE and LPC stages, respectively. However, it is noteworthy that the observed results for *SOX2* contrasted with the findings described earlier. Collectively, these findings strongly indicate a significant association between the RET^{C634Y} mutation, and the observed phenotypes associated with NSCLC during LPC differentiation.

3.7. RET^{C634Y} Knock-In Induces a Signature of Fibroblastic and Metastatic Lung Adenocarcinoma in iPSC-Derived LPCs

To validate the impact of RET^{C634Y} knock-in on transcriptional regulation during iPSC-derived LPC differentiation, whole transcriptome sequencing was done in triplicate for PB68-WT and PB68-RET^{C634Y} at both iPSC and LPC stages. The same analysis protocol employed for iRET iPSCs was applied, revealing a set of 1107 genes specifically overexpressed during PB68-RET^{C634Y} LPC differentiation. These genes constitute a specific RET^{C634Y} knock-in (RET-KI) signature (Figure 5A). This specific RET-KI signature was used to perform functional enrichment analysis on a single-cell atlas of metastatic lung adenocarcinoma [61]. This analysis revealed a notable enrichment of these genes within the signature of fibroblastic and metastatic lung adenocarcinoma (Figure 5B). With this enrichment, it was possible to build a lung fibroblast related gene network which shared some markers with other subtypes of tumor microenvironment cells like myofibroblasts and smooth muscle cells (Figure 5C). Among the genes involved in this network, nine of them were found to be overexpressed in more than 1% of lung samples based on the TCGA 510 lung adenocarcinoma patient RNA sequencing (Figure 5D). Moreover, the combinatorial overexpression of these nine markers was found to be associated with unfavorable overall survival of the patients (Figure 5E). Moreover, crossing the RET^{C634Y}-dependent gene signature with the specific RET-KI gene signature revealed 67 commonly regulated genes during these two experiments, including *C1QTNF6* (Supplementary Table S4). The expression of *C1QTNF6* and *PROM2* was also quantified by qRT-PCR and both genes were found to be in PB68-RET^{C634Y} LPCs as compared to PB68-WT LPCs indicating that RET pathway activation is associated with the overexpression of these two NSCLC poor prognosis markers (Figure 5F). Collectively, these data indicate that RET-KI induced a signature of metastatic lung adenocarcinoma during iPSC-derived LPC differentiation. Hence, this knock-in experiment serves to validate the role of the RET^{C634Y} mutation as a driver of NSCLC features in LPCs derived from iPSCs carrying RET mutation.

3.8. RET Inhibitor Treatment Leads to the Downregulation of the Cancer Associated Marker in LPCs Derived from RET^{C634Y} iPSCs

To confirm that the observed phenotypes were specifically induced by the RET^{C634Y} mutation during LPC differentiation, we added into the differentiation media the RET inhibitor pralsetinib (BLU-667) at a daily concentration of 10 nM. Pralsetinib is a drug designed to selectively target oncogenic RET alterations such as KIF5B-RET and CCDC6-RET fusions and RET^{C634Y} mutations [62]. It is currently being tested in phase I/II of the ARROW trial and exhibits promising results [63].

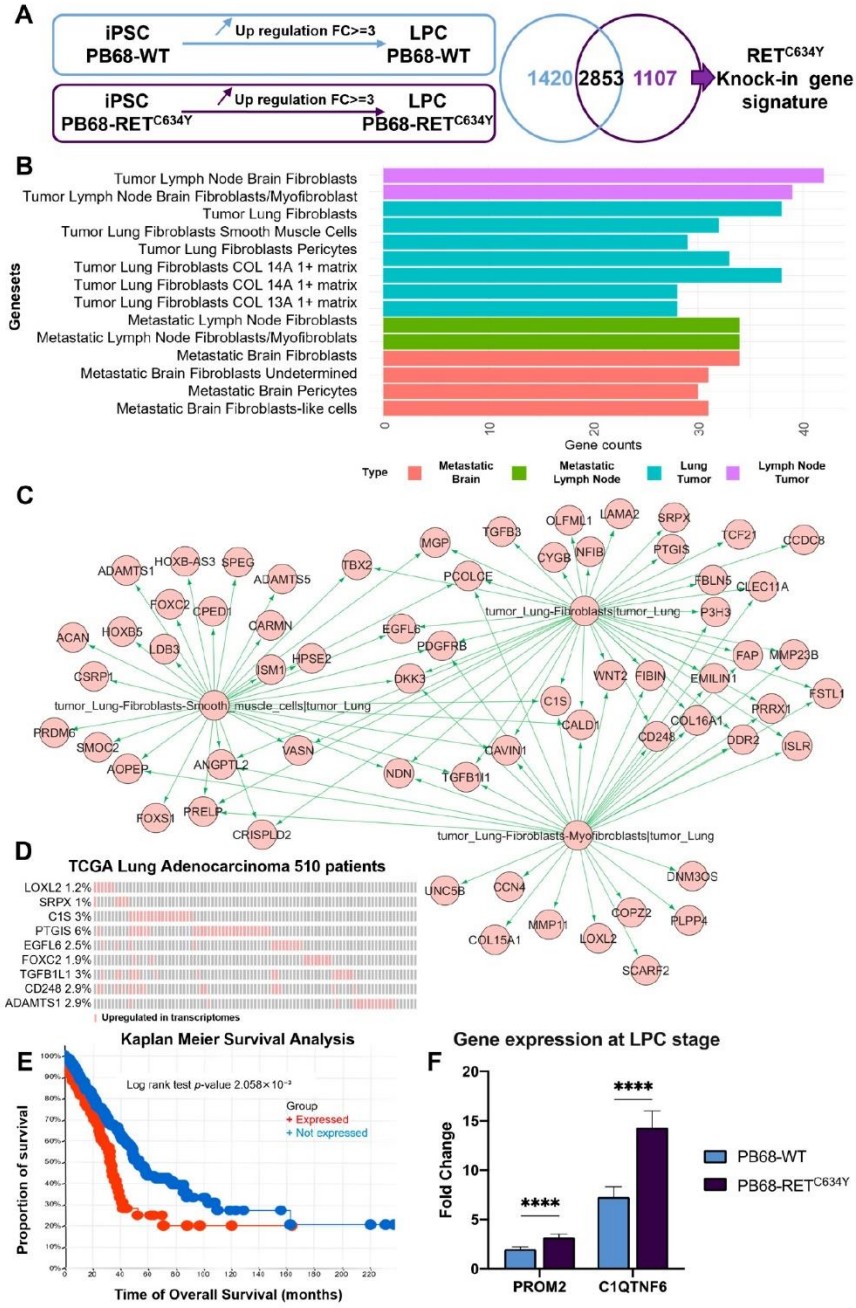

Figure 5. *RET*^{C634Y} knock-in (RET-KI) induced a metastatic and fibroblastic lung adenocarcinoma expression signature in iPSC-derived LPCs. (**A**) Method for analyzing the RET-KI dependent signature during iPSC-derived LPC differentiation. (**B**) Functional enrichment on a single-cell atlas of metastatic lung adenocarcinoma with the genes upregulated specifically during RET-KI LPC differentiation. (**C**) Fibroblastic functional enriched network drawn during RET-KI LPC differentiation. (**D**) Oncoprint of RET-KI markers found overexpressed in the transcriptome of the TCGA lung adenocarcinoma cohort (510 patients/510 samples). (**E**) Kaplan–Meier curve and log-rank test analysis assessing the overall survival (OS) of lung adenocarcinoma patients, comparing those with (red) and without (blue) the overexpression of RET-KI markers. (**F**) Expression of C1QTNF6 and PROM2, two cancers markers associated with adverse prognosis, quantified by qRT-PCR at LPC stage. Fold changes ($2^{-\Delta\Delta Ct}$) were normalized to iPSC stage. Experiments were performed three times. *p*-values were calculated using a two-tailed Student's *t*-test. **** $p < 0.0001$.

Through qRT-PCR analysis, we measured the expression levels of the differentiation markers *FOXA2* and *NKX2-1*, which were found to be regulated by RET^{C634Y} in our models, along with the cancerous markers *C1QTNF6* and *PROM2* previously identified. The gene expressions were measured on cells differentiated with and without pralsetinib. (Figure 6). In the iRET model, the expressions of *NKX2-1*, *C1QTNF6*, and *PROM2* exhibited highly significant levels of interactions between the cell lines and the two conditions (Supplementary Table S5). In all three cases, pairwise comparison analyses revealed that the addition of pralsetinib had no significant effect on LPCs derived from $iRET^{CTRL}$ but led to a significant inhibition in the expression of the genes expressed by $iRET^{C634}$ derived LPCs (Figure 6A). In the PB68 model, only *FOXA2* and *PROM2* genes exhibited significant levels of interactions between the cell lines and the two conditions but all four genes were affected significantly by pralsetinib treatment (Supplementary Table S6). Indeed, the addition of pralsetinib resulted in a significant inhibition of *FOXA2*, *NKX2-1*, and *C1QTNF6* in PB68-RET^{C634Y} cells, whereas no significant changes in expression were observed in PB68-WT cells (Figure 6B). Additionally, pralsetinib treatment led to a very strong inhibition of *PROM2* expression in all the cell lines (Figure 6B). In both models, a positive response to the RET inhibitor pralsetinib was observed as demonstrated by the downregulation of the cancer markers, indicating that their expression is regulated by RET^{C634Y} mutation. Therefore, this validates the suitability of such models as valuable tools for testing potential drugs and for identifying new therapeutic options for RET-driven NSCLC treatment.

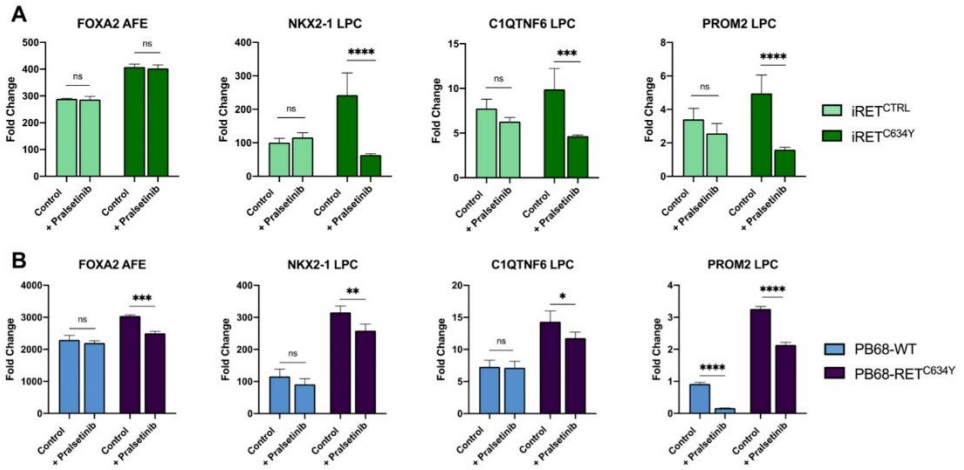

Figure 6. RET inhibitor pralsetinib treatment has a specific inhibitory effect on the genes upregulated by RET^{C634Y} mutation. (**A**,**B**) Expression of *FOXA2*, *NKX2-1*, *C1QTNF6*, *PROM2* quantified by qRT-PCR in iRET model (**A**) and PB68 model (**B**) with and without daily 10 nM pralsetinib treatment. Fold changes ($2^{-\Delta\Delta Ct}$) have been normalized to iPSC stage. Experiments were performed three times. Two-ways ANOVA was performed to test the effect of cell lines and pralsetinib treatment. For each combination of cell lines and genes, a Sidak's multiple comparisons test was performed to test the effect of pralsetinib treatment as compared to WT. ns: non-significant, * $p < 0.05$; ** $p < 0.01$; *** $p < 0.001$; **** $p < 0.0001$.

4. Discussion

RET rearrangements occur in approximately 1–2% of NSCLC, but they tend to affect a younger population of patients, and they are more frequently observed in individuals who have never smoked or have a limited smoking history [7]. *RET* rearrangements generate a novel fusion oncogene that leads to constitutive activation of the RET kinase domain [64]. This activation promotes downstream signaling pathways, such as the MAPK and PI3K-AKT pathways, which are critical for cell proliferation, survival, and other cancer-related processes [8,10]. *RET*-rearranged NSCLC lung cancers are also known to exhibit less differentiated tumors compared to other molecular types of NSCLC [11]. Furthermore, the

RET^{C634Y} mutation is a specific genetic alteration commonly found in medullary thyroid carcinoma (MTC). *RET*^{C634Y} mutation leads to the constitutive activation of RET also resulting in uncontrolled cell growth and proliferation. Consequently, the effects of the *RET*^{C634Y} mutation on the activation of the RET pathway resemble those seen in other *RET* rearrangements observed NSCLC [29–31].

Developing new models of NSCLC, particularly those involving rare oncogenic drivers such as RET, holds significant promise for advancing the development of novel therapies. Furthermore, the use of iPSCs to generate such models offers numerous advantages. They serve as an inexhaustible source of patient-specific cells, allowing researchers to investigate disease mechanisms, accelerate drug discovery, and explore the possibilities of personalized cell-based therapies with unprecedented potential [22,65]. However, the reprogramming of lung differentiated cells poses significant challenges, leading to the absence of NSCLC patient-derived iPSC lines and therefore the lack of NSCLC models derived from patient iPSCs. The objective of this study was to evaluate the viability of using iPSCs derived from patients carrying *RET* inherited mutations as an alternative method for developing RET-driven NSCLC models from iPSCs.

However, iPSCs exhibit unpredictable variability in their ability to differentiate into functional cells of a specific lineage due to their genetic background. This can pose challenges when comparing cells differentiated from patient-specific iPSCs and control iPSCs [66]. To address this issue and isolate the impact of oncogenic driver mutations, isogenic pairs of disease-specific and control iPSCs were generated [23,67]. The widespread adoption of genome editing tools, such as the CRISPR/Cas9 system, allows for the creation of control iPSCs, wherein the oncogenic mutation is corrected [68–70]. By differentiating in parallel patient-derived iPSCs and their CRISPR-corrected isogenic control iPSCs, it is possible to identify the distinct characteristics linked to the mutation. This approach was employed to evaluate the impact of *RET*^{C634Y} mutation on the differentiation of LPCs from iPSCs by comparing patient-derived iPSCs carrying the *RET*^{C634Y} mutation (iRET^{C634Y}) with its CRISPR-corrected isogenic control (iRET^{CTRL}) [34,35]. This strategy was complemented with the generation of a model of *RET*^{C634Y} knock-in in an iPSC derived from a healthy donor (PB68-RET^{C634Y} and PB68-WT, respectively) [33]. The knock-in of a mutated gene in iPSCs has already been shown to successfully generate the NSCLC model. Indeed, Dost and colleagues showed that the introduction of *KRAS*^{G12D} in healthy iPSC induces the development of NSCLC in iPSC-derived lung organoids [24].

Therefore, in this study, we employed these two approaches to successfully generate lung cell progenitors (LPCs) from iPSCs expressing the *RET*^{C634Y} mutation (Figure 1A–C). We demonstrated that these LPCs exhibit several characteristics associated with *RET*-rearranged NSCLC when compared to control iPSCs (Figures 1 and 4). For instance, *FOXA2* was found to be overexpressed at the AFE stage in both models by *RET* mutations, consistent with its upregulation by KIF5B-RET fusion in NSCLC through RET downstream signaling pathways (Figures 1E and 4C) [55]. Furthermore, in both models the *RET*^{C634Y} mutation was found to upregulate *NKX2-1*. NKX2-1 serves as a marker for lung progenitors, but it has also been identified as a tumor biomarker in lung cancer [57] due to its overexpression in adenocarcinoma [58,59].

Transcriptomic analyses performed on LPCs derived from the patient-derived iPSC iRET^{C634Y} and from its CRISPR-corrected control iRET^{CTRL}, revealed a specific RET^{C634Y} signature (Figure 2A–C). We identified a subset of 10 genes, including *C1QTNF6* and *PROM2*, that showed a significant correlation with patients with poor prognosis (Figure 3C–E). *C1QTNF6* or C1q/tumor necrosis factor-related protein 6, is known to promote cell proliferation, migration, and invasion while inhibiting apoptosis in NSCLC, both in vitro and in vivo [71]. Additionally, *PROM2* overexpression is associated with poor overall survival in lung cancer [72]. However, these two cancerous markers have not yet been identified in *RET*-rearranged NSCLC. Studying the expression of these genes in patient samples could be valuable in assessing whether our models can predict adverse prognostic markers linked to *RET*-rearrangements and identify novel therapeutic targets. Particularly, considering

that PROM2 is a membrane receptor, it could hold significant potential as a target for CAR-T cell therapy.

Additionally, a similar transcriptomic analysis was performed with the RET knock-in model to validate the impact of RET^{C634Y} mutation on transcriptional regulation during iPSC-derived LPC differentiation (Figure 5). Whole transcriptome sequencing revealed a specific RET^{C634Y} knock-in (RET-KI) signature associated with unfavorable overall survival in patients (Figure 5B–E). Additionally, 67 genes were commonly regulated in both RET^{C634Y}-dependent and RET-KI signatures, including *C1QTNF6* (Supplementary Table S4). Subsequently, we confirmed the upregulation of *C1QTNF6* and *PROM2* through qRT-PCR analysis in the LPCs derived from the two models of RET^{C634Y}-mutated iPSCs (Figures 3F and 5F). This suggests that RET pathway activation is associated with the overexpression of these poor prognosis markers in both models of RET-driven NSCLC. Overall, this knock-in experiment validated the role of RET^{C634Y} mutation as a driver of NSCLC features in LPCs derived from iPSCs.

RET rearrangements are considered as actionable molecular alteration, meaning they can be specifically targeted with precision medicines such as pralsetinib [63]. In our models of RET-driven NSCLC, LPCs derived from RET mutated iPSCs responded positively to the pralsetinib treatment (Figure 6). They showed a downregulation of *NKX2-1* and *FOXA2* as well as the cancerous markers *C1QTNF6* and *PROM2*, while almost no significant effect was observed on LPCs derived from control iPSCs (Figure 6A,B). These findings are interesting as they verify that the upregulation of these markers is indeed regulated by the RET pathway. Moreover, there is currently a lack of comprehensive investigation into the efficacy of RET inhibitors in preclinical lung cancer models with RET fusions [17]. The reported effectiveness of pralsetinib and other specific RET inhibitors such as cabozantinib or selpercatinib has been limited to only a few patient-derived lung cancer cell lines or PDX models [17,73]. The scarcity of patient-derived disease models is likely responsible for the limited available data in this area. Therefore, our model of patient-derived iPSCs could serve as a solution to this problem. However, while targeted therapies have shown promising results, acquired resistance to RET inhibitors can develop over time. Understanding the mechanisms of resistance is essential to develop strategies to overcome it and prolong the effectiveness of treatment. Our RET-driven NSCLC model derived from patient iPSCs offers the potential to generate iPSC clones resistant to pralsetinib treatment. These resistant clones can then be employed to study the underlying mechanisms of resistance or to identify new drugs that can effectively overcome this resistance.

While LPCs derived from RET^{C634Y} iPSCs may not fully replicate all the characteristics of patients *RET*-rearranged NSCLC due to the involvement of complex processes and interactions between differentiated tissues, our study demonstrates that it serves as an accurate and easily generable model. With a 16-day differentiation protocol, we showed that this model can be used for drug testing and the identification of potential novel cancer biomarkers. At present, our focus is on generating mature 3D organoids from these LPCs, which we believe will enhance the accuracy of the *RET*-rearranged NSCLC modeling. One limitation of our model is that, in primary NSCLC, RET activation occurs through *RET* rearrangements rather than *RET* mutations. However, the consequences of both alterations involve the activation of RET signaling via phosphorylation. This suggests that our model will be of significant interest for further developments. While the expression of some genes identified as overexpressed in RET mutant cell lines has not been observed in NSCLC, our model showed a clear correlation of the expression of genes such as *C1QTNF6* and *PROM2* with primary patient transcriptome and survival.

Overall, these findings suggest that the presence of the RET^{C634Y} mutation alone is enough to induce a phenotype resembling that of *RET*-rearranged NSCLC in LPCs generated from iPSCs. Consequently, this study demonstrates the potential of using iPSCs derived from patients carrying inherited mutations to model diseases in cases where patient iPSCs are not readily available or difficult to generate. This study establishes the first model of RET-driven NSCLC LPCs generated from patient-derived iPSCs.

Supplementary Materials: The following supporting information can be downloaded at: https://www.mdpi.com/article/10.3390/cells12242847/s1, Figure S1: (A) Expression heatmap (GSE44077) of the 97 RET^{C634Y}-dependent repressed genes in NSCLC. (B) Unsupervised principal component analysis based on the 97 repressed RET^{C634Y}-dependent genes in NSCLC tumors (GSE44077). (C) Expression heatmap (GSE44077) of the 33 upregulated RET^{C634Y}-dependent genes in NSCLC tumors. (D) Unsupervised principal component analysis based on the 33 upregulated RET^{C634Y}-dependent genes in NSCLC tumors (GSE44077). Figure S2: Significant clinical associations found with RET 10 gene signature in lung adenocarcinoma tumors from TCGA cohort: (A) Barplot of significant clinical parameters found associated with the over expression of the RET 10 genes signature in TCGA lung adenocarcinoma cohort. (B) Significant associations with three distinct hypoxia scores. (C) Significant associations with sample parameters. Table S1: Primers used for qRT-PCR. Table S2: RET^{C634Y}-dependent repressed gene signature in NSCLC tumor. Table S3: RET^{C634Y}-dependent activated gene signature in NSCLC tumor. Table S4: 67 commonly regulated genes in RET^{C634Y}-dependent gene signature and RET-KI gene signature. Table S5: Two-way ANOVA analyzing the effect of the cells and pralsetinib treatment on the gene expression in iRET model. Percentage of total variation and p-value summary are shown for each gene. ns: non-significant * $p < 0.05$; ** $p < 0.01$; *** $p < 0.001$; **** $p < 0.0001$. Table S6: Two-way ANOVA analyzing the effect of the cells and pralsetinib treatment on the gene expression in PB68 model. Percentage of total variation and p-value summary are shown for each gene. ns: non-significant * $p < 0.05$; ** $p < 0.01$; *** $p < 0.001$; **** $p < 0.0001$.

Author Contributions: Conceptualization, P.M. and A.G.T.; methodology, P.M. and J.W.H.; software, C.D.; validation, P.M., J.W.H. and A.G.T.; formal analysis, P.M., J.W.H. and J.I.; investigation, P.M., J.W.H. and A.G.T.; resources, P.M.; writing—original draft preparation, P.M. and C.D.; writing—review and editing, P.M., J.I. and A.G.T.; visualization, P.M.; supervision, A.G.T. and A.B.-G.; project administration, P.M. and A.G.T.; funding acquisition, A.B.-G. and A.G.T. All authors have read and agreed to the published version of the manuscript.

Funding: This research received no external funding.

Institutional Review Board Statement: This study was conducted in accordance with the Declaration of Helsinki and approved by IRB from INSERM, approval code PP-13-001.

Data Availability Statement: Data is contained within the article and Supplementary Material.

Acknowledgments: We would like to acknowledge Vaincre le Cancer for funding the fellowships of P.M. and J.I. Thanks to GENOM'IC Research facility from Institut Cochin (Paris) for the sequencing (bulk RNA).

Conflicts of Interest: The authors declare no conflict of interest.

References

1. Sung, H.; Ferlay, J.; Siegel, R.L.; Laversanne, M.; Soerjomataram, I.; Jemal, A.; Bray, F. Global Cancer Statistics 2020: GLOBOCAN Estimates of Incidence and Mortality Worldwide for 36 Cancers in 185 Countries. *CA Cancer J. Clin.* **2021**, *71*, 209–249. [CrossRef]
2. Lewis, D.R.; Check, D.P.; Caporaso, N.E.; Travis, W.D.; Devesa, S.S. US Lung Cancer Trends by Histologic Type. *Cancer* **2014**, *120*, 2883–2892. [CrossRef]
3. Nicholson, A.G.; Tsao, M.S.; Beasley, M.B.; Borczuk, A.C.; Brambilla, E.; Cooper, W.A.; Dacic, S.; Jain, D.; Kerr, K.M.; Lantuejoul, S.; et al. The 2021 WHO Classification of Lung Tumors: Impact of Advances Since 2015. *J. Thorac. Oncol.* **2022**, *17*, 362–387. [CrossRef]
4. Cancer Genome Atlas Research Network. Comprehensive Molecular Profiling of Lung Adenocarcinoma. *Nature* **2014**, *511*, 543–550. [CrossRef]
5. Jordan, E.J.; Kim, H.R.; Arcila, M.E.; Barron, D.; Chakravarty, D.; Gao, J.; Chang, M.T.; Ni, A.; Kundra, R.; Jonsson, P.; et al. Prospective Comprehensive Molecular Characterization of Lung Adenocarcinomas for Efficient Patient Matching to Approved and Emerging Therapies. *Cancer Discov.* **2017**, *7*, 596–609. [CrossRef]
6. Tsuta, K.; Kohno, T.; Yoshida, A.; Shimada, Y.; Asamura, H.; Furuta, K.; Kushima, R. RET-Rearranged Non-Small-Cell Lung Carcinoma: A Clinicopathological and Molecular Analysis. *Br. J. Cancer* **2014**, *110*, 1571–1578. [CrossRef]
7. Hess, L.M.; Han, Y.; Zhu, Y.E.; Bhandari, N.R.; Sireci, A. Characteristics and Outcomes of Patients with RET-Fusion Positive Non-Small Lung Cancer in Real-World Practice in the United States. *BMC Cancer* **2021**, *21*, 28. [CrossRef] [PubMed]
8. Qian, Y.; Chai, S.; Liang, Z.; Wang, Y.; Zhou, Y.; Xu, X.; Zhang, C.; Zhang, M.; Si, J.; Huang, F.; et al. KIF5B-RET Fusion Kinase Promotes Cell Growth by Multilevel Activation of STAT3 in Lung Cancer. *Mol. Cancer* **2014**, *13*, 176. [CrossRef] [PubMed]

9. Mizukami, T.; Shiraishi, K.; Shimada, Y.; Ogiwara, H.; Tsuta, K.; Ichikawa, H.; Sakamoto, H.; Kato, M.; Shibata, T.; Nakano, T.; et al. Molecular Mechanisms Underlying Oncogenic RET Fusion in Lung Adenocarcinoma. *J. Thorac. Oncol.* **2014**, *9*, 622–630. [CrossRef] [PubMed]
10. Schubert, L.; Le, A.T.; Estrada-Bernal, A.; Doak, A.E.; Yoo, M.; Ferrara, S.E.; Goodspeed, A.; Kinose, F.; Rix, U.; Tan, A.-C.; et al. Novel Human-Derived RET Fusion NSCLC Cell Lines Have Heterogeneous Responses to RET Inhibitors and Differential Regulation of Downstream Signaling. *Mol. Pharmacol.* **2021**, *99*, 435–447. [CrossRef]
11. Wang, R.; Hu, H.; Pan, Y.; Li, Y.; Ye, T.; Li, C.; Luo, X.; Wang, L.; Li, H.; Zhang, Y.; et al. RET Fusions Define a Unique Molecular and Clinicopathologic Subtype of Non-Small-Cell Lung Cancer. *J. Clin. Oncol.* **2012**, *30*, 4352–4359. [CrossRef] [PubMed]
12. Piotrowska, Z.; Isozaki, H.; Lennerz, J.K.; Gainor, J.F.; Lennes, I.T.; Zhu, V.W.; Marcoux, N.; Banwait, M.K.; Digumarthy, S.R.; Su, W.; et al. Landscape of Acquired Resistance to Osimertinib in EGFR-Mutant NSCLC and Clinical Validation of Combined EGFR and RET Inhibition with Osimertinib and BLU-667 for Acquired RET Fusion. *Cancer Discov.* **2018**, *8*, 1529–1539. [CrossRef] [PubMed]
13. Awad, M.M.; Liu, S.; Rybkin, I.I.; Arbour, K.C.; Dilly, J.; Zhu, V.W.; Johnson, M.L.; Heist, R.S.; Patil, T.; Riely, G.J.; et al. Acquired Resistance to KRASG12C Inhibition in Cancer. *N. Engl. J. Med.* **2021**, *384*, 2382–2393. [CrossRef] [PubMed]
14. Offin, M.; Guo, R.; Wu, S.L.; Sabari, J.; Land, J.D.; Ni, A.; Montecalvo, J.; Halpenny, D.F.; Buie, L.W.; Pak, T.; et al. Immunophenotype and Response to Immunotherapy of RET-Rearranged Lung Cancers. *JCO Precis. Oncol.* **2019**, *3*, PO.18.00386. [CrossRef] [PubMed]
15. Nelson-Taylor, S.K.; Le, A.T.; Yoo, M.; Schubert, L.; Mishall, K.M.; Doak, A.; Varella-Garcia, M.; Tan, A.-C.; Doebele, R.C. Resistance to RET-Inhibition in RET-Rearranged NSCLC Is Mediated By Reactivation of RAS/MAPK Signaling. *Mol. Cancer Ther.* **2017**, *16*, 1623–1633. [CrossRef]
16. Saito, M.; Ishigame, T.; Tsuta, K.; Kumamoto, K.; Imai, T.; Kohno, T. A Mouse Model of KIF5B-RET Fusion-Dependent Lung Tumorigenesis. *Carcinogenesis* **2014**, *35*, 2452–2456. [CrossRef]
17. Hayashi, T.; Odintsov, I.; Smith, R.S.; Ishizawa, K.; Liu, A.J.W.; Delasos, L.; Kurzatkowski, C.; Tai, H.; Gladstone, E.; Vojnic, M.; et al. RET Inhibition in Novel Patient-Derived Models of RET-Fusion Positive Lung Adenocarcinoma Reveals a Role for MYC Upregulation. *Dis. Model. Mech.* **2020**, *14*, 47779. [CrossRef]
18. Papapetrou, E.P. Patient-Derived Induced Pluripotent Stem Cells in Cancer Research and Precision Oncology. *Nat. Med.* **2016**, *22*, 1392–1401. [CrossRef]
19. Kotini, A.G.; Chang, C.-J.; Chow, A.; Yuan, H.; Ho, T.-C.; Wang, T.; Vora, S.; Solovyov, A.; Husser, C.; Olszewska, M.; et al. Stage-Specific Human Induced Pluripotent Stem Cells Map the Progression of Myeloid Transformation to Transplantable Leukemia. *Cell Stem Cell* **2017**, *20*, 315–328.e7. [CrossRef]
20. Imeri, J.; Desterke, C.; Marcoux, P.; Telliam, G.; Sanekli, S.; Barreau, S.; Erbilgin, Y.; Latsis, T.; Hugues, P.; Sorel, N.; et al. Modeling Blast Crisis Using Mutagenized Chronic Myeloid Leukemia-Derived Induced Pluripotent Stem Cells (iPSCs). *Cells* **2023**, *12*, 598. [CrossRef]
21. Lee, D.-F.; Su, J.; Kim, H.S.; Chang, B.; Papatsenko, D.; Zhao, R.; Yuan, Y.; Gingold, J.; Xia, W.; Darr, H.; et al. Modeling Familial Cancer with Induced Pluripotent Stem Cells. *Cell* **2015**, *161*, 240–254. [CrossRef] [PubMed]
22. Turhan, A.G.; Hwang, J.W.; Chaker, D.; Tasteyre, A.; Latsis, T.; Griscelli, F.; Desterke, C.; Bennaceur-Griscelli, A. iPSC-Derived Organoids as Therapeutic Models in Regenerative Medicine and Oncology. *Front Med. Lausanne* **2021**, *8*, 728543. [CrossRef] [PubMed]
23. Tu, J.; Huo, Z.; Yu, Y.; Zhu, D.; Xu, A.; Huang, M.-F.; Hu, R.; Wang, R.; Gingold, J.A.; Chen, Y.-H.; et al. Hereditary Retinoblastoma iPSC Model Reveals Aberrant Spliceosome Function Driving Bone Malignancies. *Proc. Natl. Acad. Sci. USA* **2022**, *119*, e2117857119. [CrossRef] [PubMed]
24. Dost, A.F.M.; Moye, A.L.; Vedaie, M.; Tran, L.M.; Fung, E.; Heinze, D.; Villacorta-Martin, C.; Huang, J.; Hekman, R.; Kwan, J.H.; et al. Organoids Model Transcriptional Hallmarks of Oncogenic KRAS Activation in Lung Epithelial Progenitor Cells. *Cell Stem Cell* **2020**, *27*, 663–678.e8. [CrossRef] [PubMed]
25. Shi, Y.; Inoue, H.; Wu, J.C.; Yamanaka, S. Induced Pluripotent Stem Cell Technology: A Decade of Progress. *Nat. Rev. Drug Discov.* **2017**, *16*, 115–130. [CrossRef]
26. González, F.; Boué, S.; Belmonte, J.C.I. Methods for Making Induced Pluripotent Stem Cells: Reprogramming à La Carte. *Nat. Rev. Genet.* **2011**, *12*, 231–242. [CrossRef]
27. Rao, M.S.; Malik, N. Assessing iPSC Reprogramming Methods for Their Suitability in Translational Medicine. *J. Cell Biochem.* **2012**, *113*, 3061–3068. [CrossRef]
28. Xu, A.; Liu, M.; Huang, M.-F.; Zhang, Y.; Hu, R.; Gingold, J.A.; Liu, Y.; Zhu, D.; Chien, C.-S.; Wang, W.-C.; et al. Rewired m6A Epitranscriptomic Networks Link Mutant P53 to Neoplastic Transformation. *Nat. Commun.* **2023**, *14*, 1694. [CrossRef]
29. Plaza-Menacho, I.; Mologni, L.; McDonald, N.Q. Mechanisms of RET Signaling in Cancer: Current and Future Implications for Targeted Therapy. *Cell. Signal.* **2014**, *26*, 1743–1752. [CrossRef] [PubMed]
30. Kouvaraki, M.A.; Shapiro, S.E.; Perrier, N.D.; Cote, G.J.; Gagel, R.F.; Hoff, A.O.; Sherman, S.I.; Lee, J.E.; Evans, D.B. RET Proto-Oncogene: A Review and Update of Genotype-Phenotype Correlations in Hereditary Medullary Thyroid Cancer and Associated Endocrine Tumors. *Thyroid* **2005**, *15*, 531–544. [CrossRef] [PubMed]
31. Wells, S.A.; Pacini, F.; Robinson, B.G.; Santoro, M. Multiple Endocrine Neoplasia Type 2 and Familial Medullary Thyroid Carcinoma: An Update. *J. Clin. Endocrinol. Metab.* **2013**, *98*, 3149–3164. [CrossRef] [PubMed]

32. Leibel, S.L.; McVicar, R.N.; Winquist, A.M.; Niles, W.D.; Snyder, E.Y. Generation of Complete Multi−Cell Type Lung Organoids From Human Embryonic and Patient-Specific Induced Pluripotent Stem Cells for Infectious Disease Modeling and Therapeutics Validation. *Curr. Protoc. Stem Cell Biol.* **2020**, *54*, e118. [CrossRef] [PubMed]
33. Marcoux, P.; Imeri, J.; Desterke, C.; Latsis, T.; Chaker, D.; Hugues, P.; Griscelli, A.B.; Turhan, A.G. Impact of the Overexpression of the Tyrosine Kinase Receptor (RET) in the Hematopoietic Potential of Induced Pluripotent Stem Cells (iPSCs). *Cytotherapy* **2023**. [CrossRef] [PubMed]
34. Hadoux, J.; Féraud, O.; Griscelli, F.; Opolon, P.; Divers, D.; Gobbo, E.; Schlumberger, M.; Bennaceur-Griscelli, A.; Turhan, A.G. Generation of an Induced Pluripotent Stem Cell Line from a Patient with Hereditary Multiple Endocrine Neoplasia 2A (MEN2A) Syndrome with RET Mutation. *Stem Cell Res.* **2016**, *17*, 154–157. [CrossRef] [PubMed]
35. Hadoux, J.; Desterke, C.; Féraud, O.; Guibert, M.; De Rose, R.F.; Opolon, P.; Divers, D.; Gobbo, E.; Griscelli, F.; Schlumberger, M.; et al. Transcriptional Landscape of a RETC634Y-Mutated iPSC and Its CRISPR-Corrected Isogenic Control Reveals the Putative Role of EGR1 Transcriptional Program in the Development of Multiple Endocrine Neoplasia Type 2A-Associated Cancers. *Stem Cell Res.* **2018**, *26*, 8–16. [CrossRef] [PubMed]
36. Dobin, A.; Davis, C.A.; Schlesinger, F.; Drenkow, J.; Zaleski, C.; Jha, S.; Batut, P.; Chaisson, M.; Gingeras, T.R. STAR: Ultrafast Universal RNA-Seq Aligner. *Bioinformatics* **2013**, *29*, 15–21. [CrossRef] [PubMed]
37. Li, B.; Dewey, C.N. RSEM: Accurate Transcript Quantification from RNA-Seq Data with or without a Reference Genome. *BMC Bioinform.* **2011**, *12*, 323. [CrossRef]
38. Love, M.I.; Huber, W.; Anders, S. Moderated Estimation of Fold Change and Dispersion for RNA-Seq Data with DESeq2. *Genome Biol.* **2014**, *15*, 550. [CrossRef]
39. Kadara, H.; Fujimoto, J.; Yoo, S.-Y.; Maki, Y.; Gower, A.C.; Kabbout, M.; Garcia, M.M.; Chow, C.-W.; Chu, Z.; Mendoza, G.; et al. Transcriptomic Architecture of the Adjacent Airway Field Cancerization in Non–Small Cell Lung Cancer. *JNCI J. Natl. Cancer Inst.* **2014**, *106*, dju004. [CrossRef]
40. Liu, J.; Lichtenberg, T.; Hoadley, K.A.; Poisson, L.M.; Lazar, A.J.; Cherniack, A.D.; Kovatich, A.J.; Benz, C.C.; Levine, D.A.; Lee, A.V.; et al. An Integrated TCGA Pan-Cancer Clinical Data Resource to Drive High-Quality Survival Outcome Analytics. *Cell* **2018**, *173*, 400–416.e11. [CrossRef]
41. Gao, J.; Aksoy, B.A.; Dogrusoz, U.; Dresdner, G.; Gross, B.; Sumer, S.O.; Sun, Y.; Jacobsen, A.; Sinha, R.; Larsson, E.; et al. Integrative Analysis of Complex Cancer Genomics and Clinical Profiles Using the cBioPortal. *Sci. Signal.* **2013**, *6*, pl1. [CrossRef]
42. Kuleshov, M.V.; Jones, M.R.; Rouillard, A.D.; Fernandez, N.F.; Duan, Q.; Wang, Z.; Koplev, S.; Jenkins, S.L.; Jagodnik, K.M.; Lachmann, A.; et al. Enrichr: A Comprehensive Gene Set Enrichment Analysis Web Server 2016 Update. *Nucleic Acids Res.* **2016**, *44*, W90–W97. [CrossRef] [PubMed]
43. Chen, J.; Bardes, E.E.; Aronow, B.J.; Jegga, A.G. ToppGene Suite for Gene List Enrichment Analysis and Candidate Gene Prioritization. *Nucleic Acids Res.* **2009**, *37*, W305–W311. [CrossRef] [PubMed]
44. Ashburner, M.; Ball, C.A.; Blake, J.A.; Botstein, D.; Butler, H.; Cherry, J.M.; Davis, A.P.; Dolinski, K.; Dwight, S.S.; Eppig, J.T.; et al. Gene Ontology: Tool for the Unification of Biology. *Nat. Genet.* **2000**, *25*, 25–29. [CrossRef]
45. Piñero, J.; Ramírez-Anguita, J.M.; Saüch-Pitarch, J.; Ronzano, F.; Centeno, E.; Sanz, F.; Furlong, L.I. The DisGeNET Knowledge Platform for Disease Genomics: 2019 Update. *Nucleic Acids Res.* **2020**, *48*, D845–D855. [CrossRef] [PubMed]
46. Culhane, A.C.; Schröder, M.S.; Sultana, R.; Picard, S.C.; Martinelli, E.N.; Kelly, C.; Haibe-Kains, B.; Kapushesky, M.; St Pierre, A.-A.; Flahive, W.; et al. GeneSigDB: A Manually Curated Database and Resource for Analysis of Gene Expression Signatures. *Nucleic Acids Res.* **2012**, *40*, D1060–D1066. [CrossRef] [PubMed]
47. Liberzon, A.; Birger, C.; Thorvaldsdóttir, H.; Ghandi, M.; Mesirov, J.P.; Tamayo, P. The Molecular Signatures Database Hallmark Gene Set Collection. *Cels* **2015**, *1*, 417–425. [CrossRef]
48. Cline, M.S.; Smoot, M.; Cerami, E.; Kuchinsky, A.; Landys, N.; Workman, C.; Christmas, R.; Avila-Campilo, I.; Creech, M.; Gross, B.; et al. Integration of Biological Networks and Gene Expression Data Using Cytoscape. *Nat. Protoc.* **2007**, *2*, 2366–2382. [CrossRef]
49. Wickham, H. *Ggplot2: Elegant Graphics for Data Analysis*; Springer: New York, NY, USA, 2009; ISBN 978-0-387-98140-6.
50. D'Amour, K.A.; Agulnick, A.D.; Eliazer, S.; Kelly, O.G.; Kroon, E.; Baetge, E.E. Efficient Differentiation of Human Embryonic Stem Cells to Definitive Endoderm. *Nat. Biotechnol.* **2005**, *23*, 1534–1541. [CrossRef]
51. Green, M.D.; Chen, A.; Nostro, M.-C.; d'Souza, S.L.; Schaniel, C.; Lemischka, I.R.; Gouon-Evans, V.; Keller, G.; Snoeck, H.-W. Generation of Anterior Foregut Endoderm from Human Embryonic and Induced Pluripotent Stem Cells. *Nat. Biotechnol.* **2011**, *29*, 267–272. [CrossRef]
52. Minoo, P.; Hu, L.; Xing, Y.; Zhu, N.L.; Chen, H.; Li, M.; Borok, Z.; Li, C. Physical and Functional Interactions between Homeodomain NKX2.1 and Winged Helix/Forkhead FOXA1 in Lung Epithelial Cells. *Mol. Cell. Biol.* **2007**, *27*, 2155–2165. [CrossRef]
53. Huang, S.X.L.; Islam, M.N.; O'Neill, J.; Hu, Z.; Yang, Y.-G.; Chen, Y.-W.; Mumau, M.; Green, M.D.; Vunjak-Novakovic, G.; Bhattacharya, J.; et al. Efficient Generation of Lung and Airway Epithelial Cells from Human Pluripotent Stem Cells. *Nat. Biotechnol.* **2014**, *32*, 84–91. [CrossRef]
54. Rock, J.R.; Onaitis, M.W.; Rawlins, E.L.; Lu, Y.; Clark, C.P.; Xue, Y.; Randell, S.H.; Hogan, B.L.M. Basal Cells as Stem Cells of the Mouse Trachea and Human Airway Epithelium. *Proc. Natl. Acad. Sci. USA* **2009**, *106*, 12771–12775. [CrossRef] [PubMed]

55. Lee, M.-R.; Shin, J.-Y.; Kim, M.-Y.; Kim, J.-O.; Jung, C.K.; Kang, J. FOXA2 and STAT5A Regulate Oncogenic Activity of KIF5B-RET Fusion. *Am. J. Cancer Res.* **2023**, *13*, 638–653. [PubMed]
56. Ochieng, J.K.; Schilders, K.; Kool, H.; Boerema-De Munck, A.; Buscop-Van Kempen, M.; Gontan, C.; Smits, R.; Grosveld, F.G.; Wijnen, R.M.H.; Tibboel, D.; et al. Sox2 Regulates the Emergence of Lung Basal Cells by Directly Activating the Transcription of Trp63. *Am. J. Respir. Cell Mol. Biol.* **2014**, *51*, 311–322. [CrossRef] [PubMed]
57. Yang, L.; Lin, M.; Ruan, W.; Dong, L.; Chen, E.; Wu, X.; Ying, K. Nkx2-1: A Novel Tumor Biomarker of Lung Cancer. *J. Zhejiang Univ. Sci. B* **2012**, *13*, 855–866. [CrossRef]
58. Tan, D.; Li, Q.; Deeb, G.; Ramnath, N.; Slocum, H.K.; Brooks, J.; Cheney, R.; Wiseman, S.; Anderson, T.; Loewen, G. Thyroid Transcription Factor-1 Expression Prevalence and Its Clinical Implications in Non-Small Cell Lung Cancer: A High-Throughput Tissue Microarray and Immunohistochemistry Study. *Hum. Pathol.* **2003**, *34*, 597–604. [CrossRef]
59. Myong, N.-H. Thyroid Transcription Factor-1 (TTF-1) Expression in Human Lung Carcinomas: Its Prognostic Implication and Relationship with Wxpressions of P53 and Ki-67 Proteins. *J. Korean Med. Sci.* **2003**, *18*, 494–500. [CrossRef]
60. Travaglini, K.J.; Nabhan, A.N.; Penland, L.; Sinha, R.; Gillich, A.; Sit, R.V.; Chang, S.; Conley, S.D.; Mori, Y.; Seita, J.; et al. A Molecular Cell Atlas of the Human Lung from Single-Cell RNA Sequencing. *Nature* **2020**, *587*, 619–625. [CrossRef]
61. Kim, N.; Kim, H.K.; Lee, K.; Hong, Y.; Cho, J.H.; Choi, J.W.; Lee, J.-I.; Suh, Y.-L.; Ku, B.M.; Eum, H.H.; et al. Single-Cell RNA Sequencing Demonstrates the Molecular and Cellular Reprogramming of Metastatic Lung Adenocarcinoma. *Nat. Commun.* **2020**, *11*, 2285. [CrossRef]
62. Subbiah, V.; Gainor, J.F.; Rahal, R.; Brubaker, J.D.; Kim, J.L.; Maynard, M.; Hu, W.; Cao, Q.; Sheets, M.P.; Wilson, D.; et al. Precision Targeted Therapy with BLU-667 for RET-Driven Cancers. *Cancer Discov.* **2018**, *8*, 836–849. [CrossRef] [PubMed]
63. Gainor, J.F.; Curigliano, G.; Kim, D.-W.; Lee, D.H.; Besse, B.; Baik, C.S.; Doebele, R.C.; Cassier, P.A.; Lopes, G.; Tan, D.S.W.; et al. Pralsetinib for RET Fusion-Positive Non-Small-Cell Lung Cancer (ARROW): A Multi-Cohort, Open-Label, Phase 1/2 Study. *Lancet Oncol.* **2021**, *22*, 959–969. [CrossRef] [PubMed]
64. Ferrara, R.; Auger, N.; Auclin, E.; Besse, B. Clinical and Translational Implications of RET Rearrangements in Non–Small Cell Lung Cancer. *J. Thorac. Oncol.* **2018**, *13*, 27–45. [CrossRef] [PubMed]
65. Stadtfeld, M.; Hochedlinger, K. Induced Pluripotency: History, Mechanisms, and Applications. *Genes. Dev.* **2010**, *24*, 2239–2263. [CrossRef]
66. Soldner, F.; Jaenisch, R. iPSC Disease Modeling. *Science* **2012**, *338*, 1155–1156. [CrossRef]
67. Soldner, F.; Laganière, J.; Cheng, A.W.; Hockemeyer, D.; Gao, Q.; Alagappan, R.; Khurana, V.; Golbe, L.I.; Myers, R.H.; Lindquist, S.; et al. Generation of Isogenic Pluripotent Stem Cells Differing Exclusively at Two Early Onset Parkinson Point Mutations. *Cell* **2011**, *146*, 318–331. [CrossRef] [PubMed]
68. Byrne, S.M.; Church, G.M. Crispr-Mediated Gene Targeting of Human Induced Pluripotent Stem Cells. *Curr. Protoc. Stem Cell Biol.* **2015**, *35*, 5A.8.1–5A.8.22. [CrossRef]
69. Johnson, J.Z.; Hockemeyer, D. Human Stem Cell-Based Disease Modeling: Prospects and Challenges. *Curr. Opin. Cell Biol.* **2015**, *37*, 84–90. [CrossRef]
70. Li, X.-F.; Zhou, Y.-W.; Cai, P.-F.; Fu, W.-C.; Wang, J.-H.; Chen, J.-Y.; Yang, Q.-N. CRISPR/Cas9 Facilitates Genomic Editing for Large-Scale Functional Studies in Pluripotent Stem Cell Cultures. *Hum. Genet.* **2019**, *138*, 1217–1225. [CrossRef]
71. Zhang, W.; Feng, G. C1QTNF6 Regulates Cell Proliferation and Apoptosis of NSCLC In Vitro and In Vivo. *Biosci. Rep.* **2021**, *41*, BSR20201541. [CrossRef]
72. Saha, S.K.; Islam, S.M.R.; Kwak, K.-S.; Rahman, M.S.; Cho, S.-G. PROM1 and PROM2 Expression Differentially Modulates Clinical Prognosis of Cancer: A Multiomics Analysis. *Cancer Gene Ther.* **2020**, *27*, 147–167. [CrossRef] [PubMed]
73. Li, G.G.; Somwar, R.; Joseph, J.; Smith, R.S.; Hayashi, T.; Martin, L.; Franovic, A.; Schairer, A.; Martin, E.; Riely, G.J.; et al. Antitumor Activity of RXDX-105 in Multiple Cancer Types with RET Rearrangements or Mutations. *Clin. Cancer Res.* **2017**, *23*, 2981–2990. [CrossRef] [PubMed]

Disclaimer/Publisher's Note: The statements, opinions and data contained in all publications are solely those of the individual author(s) and contributor(s) and not of MDPI and/or the editor(s). MDPI and/or the editor(s) disclaim responsibility for any injury to people or property resulting from any ideas, methods, instructions or products referred to in the content.

Supplementary material

Supplementary figures

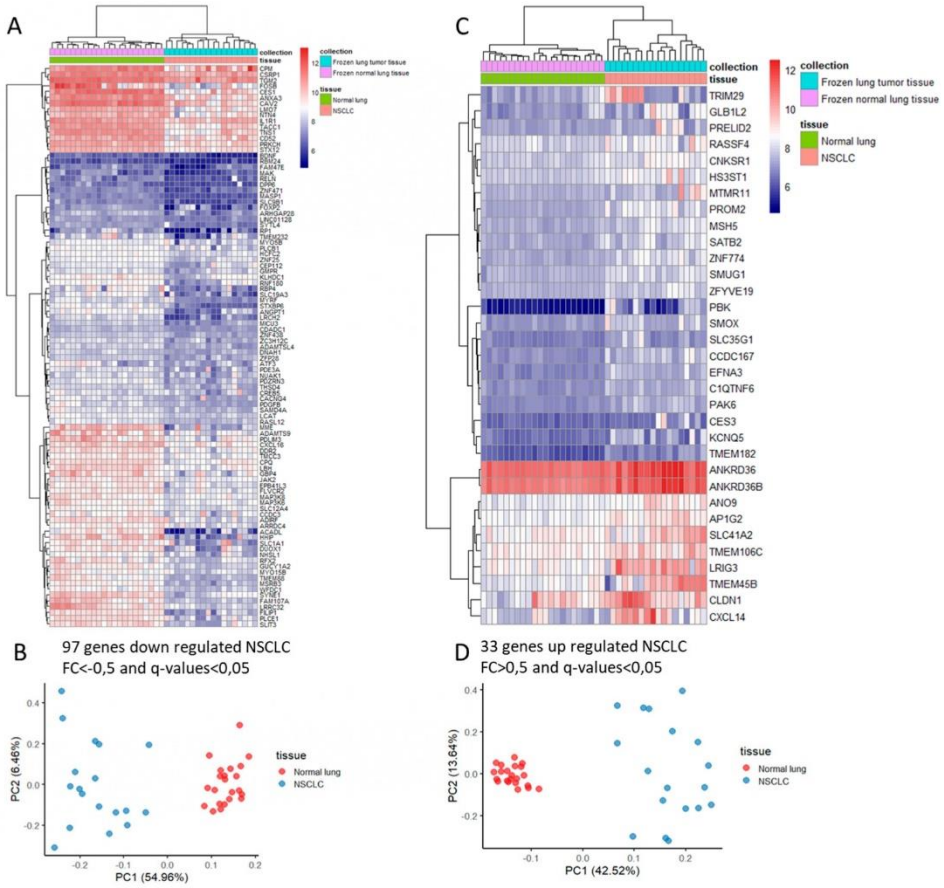

Supplemental Figure S1: (A) Expression heatmap (GSE44077) of the 97 RET^{C634Y}-dependent repressed genes in NSCLC tumors. **(B)** Unsupervised principal component analysis based on the 97 repressed RET^{C634Y}-dependent genes in NSCLC tumors (GSE44077). **(C)** Expression heatmap (GSE44077) of the 33 upregulated RET^{C634Y}-dependent genes in NSCLC tumors. **(D)** Unsupervised principal component analysis based on the 33 upregulated RET^{C634Y}-dependent genes in NSCLC tumors (GSE44077).

1

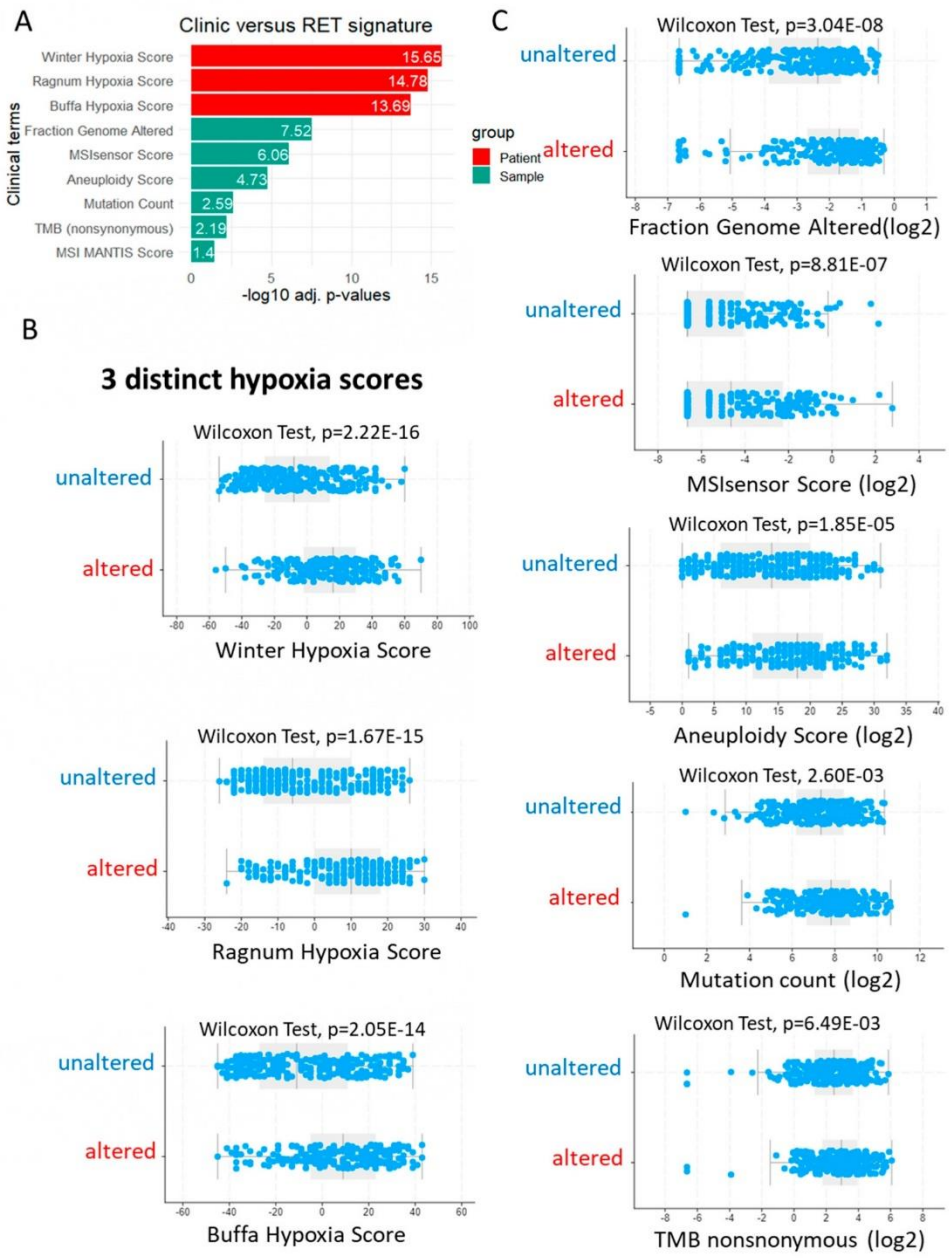

Supplemental Figure S2: Significant clinical associations found with RET 10 genes signature in lung adenocarcinoma tumors from TCGA cohort: (A) Barplot of significant clinical parameters found associated with the over expression of the RET 10 genes signature in TCGA lung adenocarcinoma cohort. **(B)** Significant associations with 3 distinct hypoxia score. **(C)** Significant associations with sample parameters.

Supplementary tables

Supplementary Table S1: Primers used for qRT-PCR

Primers	Sequence
ACTIN_FW	CACCATTGGCAATGAGCGGTTC
ACTIN_RV	AGGTCTTTGCGGATGTCCACGT
C1QTNF6_FW	GGTCAAGGGTTCTGTGAGGAG
C1QTNF6_RV	TCAGATGACTTTGGTGGAAGG

CXCR4_FW	CCCATCCTCTATGCTTTCCTTG
CXCR4_RV	GTCCACCTCGCTTTCCTTTG
FOXA2_FW	GCCGCAGATACCTCCTACTACC
FOXA2_RV	CCACTTGCTCTCTCACTTGTCC
NKX2-1_FW	CTCGCTCATTTGTTGGCGAC
NKX2-1_RV	CGTGTGCTTTGGACTCATCG
PROM2_FW	AGGCTGGAGAAGGATGTATGG
PROM2_RV	CAACTCTGAAGGGAAAGGATTG
RET_FW	CATCAGCAAAGACCTGGAGAAG
RET_RV	AATCAGGGAGTCAGATGGAGTG
SOX17_FW	CTGCAACTATCCTGACGTGTG
SOX17_RV	ACCCAGGAGTCTGAGGATTTC
SOX2_FW	CGAACCATCTCTGTGGTCTTG
SOX2_RV	ATTACCAACGGTGTCAACCTG

Supplementary Table S2: RET^{C634Y}-dependent repressed gene signature in NSCLC tumor

Gene	logFC	AveExpr	P.Value	adj.P.Val
ACADL	-2.799	8.126	7.87E-12	2.33E-10
HHIP	-2.608	8.820	5.85E-12	1.84E-10
MME	-2.442	9.065	1.24E-11	3.46E-10
FOSB	-2.250	9.783	7.15E-07	4.93E-06
CES1	-2.109	10.597	1.49E-13	8.32E-12
STXBP6	-2.023	7.788	1.28E-16	3.21E-14
FILIP1	-1.912	8.713	1.97E-12	7.07E-11
FAM107A	-1.875	8.948	1.05E-15	1.06E-13
ANGPT1	-1.748	8.079	5.36E-11	1.22E-09
LRRC32	-1.746	9.229	1.85E-11	4.90E-10
DUOX1	-1.741	8.731	4.89E-08	4.92E-07
SYNE1	-1.733	9.235	1.78E-14	1.12E-12
SLC19A3	-1.700	7.872	1.67E-08	1.78E-07
SLIT3	-1.668	8.911	3.78E-12	1.27E-10
CAV2	-1.642	10.792	6.66E-13	3.35E-11
LRCH2	-1.605	7.519	4.85E-11	1.16E-09
TNS1	-1.604	10.258	1.39E-12	5.81E-11
RBP4	-1.571	7.981	3.33E-06	1.78E-05
RP1	-1.566	6.732	2.33E-06	1.33E-05
SLC1A1	-1.559	8.681	1.11E-05	5.43E-05
MSRB3	-1.554	8.535	3.01E-18	1.52E-15
ANXA3	-1.490	10.456	1.03E-10	2.16E-09
TMEM88	-1.485	8.495	1.60E-12	6.18E-11
PLCE1	-1.447	8.952	2.44E-09	3.50E-08
LMO7	-1.385	9.901	3.35E-09	4.56E-08
GUCY1A2	-1.339	8.808	5.65E-16	9.48E-14
GBP4	-1.315	9.199	1.48E-06	8.96E-06
TACC1	-1.310	10.264	1.11E-14	7.96E-13
ADIRF	-1.261	9.117	2.16E-10	4.17E-09
ADAMTS9	-1.222	9.277	8.72E-06	4.34E-05
NTN4	-1.212	9.852	1.21E-07	1.15E-06
TMEM232	-1.189	7.778	8.61E-04	2.85E-03
PDLIM3	-1.175	9.387	1.28E-06	8.04E-06

RNF180	-1.129	8.480	3.46E-07	2.76E-06
RFX2	-1.108	8.774	8.04E-07	5.46E-06
WFDC1	-1.084	8.523	8.22E-11	1.80E-09
DDR2	-1.011	9.172	5.58E-09	6.52E-08
CD52	-1.008	10.210	8.76E-07	5.84E-06
EPB41L3	-1.007	8.948	4.70E-09	6.07E-08
MYRF	-1.006	7.804	1.34E-07	1.25E-06
NHSL1	-0.970	8.481	5.28E-06	2.77E-05
PDGFB	-0.952	8.020	1.13E-08	1.27E-07
LBH	-0.944	9.366	1.95E-09	2.98E-08
PRKCH	-0.943	10.184	3.35E-10	6.01E-09
PDZRN3	-0.913	8.164	1.45E-08	1.59E-07
KLHDC1	-0.902	8.846	2.79E-06	1.51E-05
MAK	-0.888	6.507	1.38E-05	6.60E-05
FLVCR2	-0.881	9.048	2.74E-07	2.22E-06
CPM	-0.869	10.868	1.84E-03	5.76E-03
SLC9B1	-0.860	6.647	5.21E-09	6.52E-08
MICU3	-0.853	7.697	2.41E-08	2.53E-07
MYO15B	-0.843	8.697	4.98E-07	3.48E-06
STX12	-0.823	9.987	5.43E-15	4.55E-13
MASP1	-0.817	6.646	9.41E-16	1.06E-13
ARRDC4	-0.794	8.844	8.82E-07	5.84E-06
PDE3A	-0.790	8.053	3.63E-04	1.30E-03
CPQ	-0.782	9.333	4.37E-07	3.21E-06
ARHGAP28	-0.770	7.450	1.68E-05	7.97E-05
ATF3	-0.759	8.029	3.96E-03	1.08E-02
CSRP1	-0.759	10.916	3.61E-10	6.27E-09
SAMD4A	-0.753	8.162	4.09E-07	3.07E-06
ZC3H12C	-0.751	7.988	9.82E-07	6.33E-06
FOXP2	-0.744	7.001	4.37E-03	1.16E-02
ADAMTSL4	-0.743	7.892	7.05E-09	8.06E-08
SLC12A4	-0.725	8.781	8.96E-13	4.10E-11
CACNG4	-0.725	8.033	1.82E-04	7.06E-04
CXCL16	-0.723	9.608	2.75E-06	1.51E-05
JAK2	-0.711	9.095	1.53E-07	1.33E-06
BDNF	-0.692	6.159	1.65E-06	9.88E-06
MAP3K8	-0.681	9.071	1.26E-06	8.04E-06
RASL12	-0.672	8.154	1.64E-10	3.31E-09
MAP3K6	-0.667	8.945	1.91E-06	1.12E-05
CCDC3	-0.655	8.783	4.08E-03	1.10E-02
FAM47E	-0.654	6.579	5.24E-03	1.34E-02
TGM2	-0.638	11.307	4.76E-07	3.39E-06
TMCC3	-0.636	9.015	1.41E-06	8.63E-06
LCAT	-0.629	8.397	7.96E-10	1.33E-08
PLCB1	-0.624	8.574	9.27E-04	3.03E-03
ZNF471	-0.595	6.774	7.83E-06	4.02E-05
CDADC1	-0.590	7.533	2.48E-10	4.61E-09
ZNF25	-0.590	8.482	1.89E-07	1.60E-06
SYTL4	-0.581	7.178	2.54E-05	1.16E-04
GMPR	-0.576	8.185	1.04E-04	4.23E-04
CREB5	-0.573	8.168	8.26E-03	1.98E-02
RELN	-0.559	6.735	3.58E-03	9.95E-03

CEP112	-0.550	8.285	3.92E-03	1.08E-02
DNAH1	-0.541	7.823	1.94E-06	1.12E-05
NUAK1	-0.533	8.024	2.60E-03	7.65E-03
HCFC2	-0.532	8.572	5.17E-08	5.10E-07
IL1R1	-0.520	10.581	8.56E-05	3.51E-04
ZNF438	-0.520	7.784	1.91E-07	1.60E-06
ZFP28	-0.518	7.814	8.09E-06	4.07E-05
RBM24	-0.514	5.990	2.35E-06	1.33E-05
LINC01128	-0.512	7.158	3.61E-07	2.83E-06
MYO5B	-0.511	8.388	6.60E-03	1.63E-02
DPP6	-0.509	6.565	3.43E-03	9.70E-03
THSD4	-0.509	8.041	3.56E-04	1.29E-03

Supplementary Table S3: RET^{C634Y}-dependent activated gene signature in NSCLC tumor

Gene	logFC	AveExpr	P.Value	adj.P.Val
PBK	1.666	5.811	2.51E-07	2.07E-06
CXCL14	1.559	8.459	3.22E-05	1.43E-04
LRIG3	1.327	9.242	4.04E-07	3.07E-06
CLDN1	1.140	9.410	5.31E-04	1.83E-03
TMEM45B	1.099	8.852	1.54E-03	4.87E-03
TRIM29	1.091	7.748	5.64E-03	1.43E-02
PROM2	0.845	7.650	1.51E-09	2.37E-08
CCDC167	0.843	7.215	4.41E-09	5.83E-08
KCNQ5	0.793	6.747	8.52E-05	3.51E-04
EFNA3	0.777	7.043	4.74E-11	1.16E-09
TMEM182	0.763	6.377	9.26E-10	1.50E-08
ZNF774	0.743	7.610	3.08E-09	4.30E-08
HS3ST1	0.701	8.090	6.98E-06	3.62E-05
AP1G2	0.685	8.693	5.44E-09	6.52E-08
SMOX	0.659	7.314	3.77E-05	1.64E-04
ANKRD36B	0.657	11.221	2.53E-06	1.41E-05
GLB1L2	0.654	7.373	1.12E-02	2.50E-02
MSH5	0.614	7.594	7.21E-08	6.97E-07
SLC41A2	0.585	9.029	6.35E-03	1.58E-02
ANO9	0.584	8.540	7.92E-06	4.02E-05
ANKRD36	0.583	11.413	1.93E-05	9.00E-05
PAK6	0.579	7.061	5.38E-09	6.52E-08
CES3	0.579	6.554	5.20E-03	1.34E-02
SMUG1	0.574	7.654	2.30E-09	3.41E-08
CNKSR1	0.573	8.019	4.78E-07	3.39E-06
MTMR11	0.570	7.669	8.80E-03	2.09E-02
TMEM106C	0.560	9.067	1.51E-04	6.04E-04
PRELID2	0.557	7.385	7.27E-03	1.77E-02
C1QTNF6	0.536	7.101	3.90E-08	4.01E-07
RASSF4	0.534	8.120	7.02E-04	2.37E-03
SLC35G1	0.531	6.861	2.95E-04	1.10E-03
SATB2	0.514	7.550	7.68E-05	3.24E-04
ZFYVE19	0.506	7.611	1.41E-07	1.25E-06

Supplementary Table S4: 67 commonly regulated genes in RET^{C634Y}-dependent gene signature and RET-KI gene signature

Gene symbol	Gene ID	Description
ACOX1	51	acyl-CoA oxidase 1
APBB3	10307	amyloid beta precursor protein binding family B member 3
ARHGAP5-AS1	84837	ARHGAP5 antisense RNA 1
ARPIN	348110	actin related protein 2/3 complex inhibitor
BTBD9	114781	BTB domain containing 9
C1QTNF6	114904	C1q and TNF related 6
C1S	716	complement C1s
CDC42EP1	11135	CDC42 effector protein 1
CEP112	201134	centrosomal protein 112
CHST3	9469	carbohydrate sulfotransferase 3
CPM	1368	carboxypeptidase M
CSRP1	1465	cysteine and glycine rich protein 1
CXCL1	2919	C-X-C motif chemokine ligand 1
DDR2	4921	discoidin domain receptor tyrosine kinase 2
EEF1AKMT3	25895	EEF1A lysine methyltransferase 3
ELK3	2004	ETS transcription factor ELK3
FILIP1	27145	filamin A interacting protein 1
GOLGA8O	728047	golgin A8 family member O
HCFC2	29915	host cell factor C2
HMGB1P31	100873894	high mobility group box 1 pseudogene 31
HS3ST1	9957	heparan sulfate-glucosamine 3-sulfotransferase 1
IL1R1	3554	interleukin 1 receptor type 1
IPP	3652	intracisternal A particle-promoted polypeptide
IRF9	10379	interferon regulatory factor 9
KANTR	102723508	KANTR integral membrane protein
KCNAB3	9196	potassium voltage-gated channel subfamily A regulatory beta subunit 3
KCTD21-AS1	100289388	KCTD21 antisense RNA 1
KIAA1841	NA	NA
LGALS8	3964	galectin 8
LINC00324	284029	long intergenic non-protein coding RNA 324
LINC01948	102467147	long intergenic non-protein coding RNA 1948
LRIG3	121227	leucine rich repeats and immunoglobulin like domains 3
LRRC32	2615	leucine rich repeat containing 32
LRTOMT	220074	leucine rich transmembrane and O-methyltransferase domain containing
LTBP3	4054	latent transforming growth factor beta binding protein 3
MAPK8IP2	23542	mitogen-activated protein kinase 8 interacting protein 2
MEGF6	1953	multiple EGF like domains 6
MICU3	286097	mitochondrial calcium uptake family member 3
MMP25-AS1	100507419	MMP25 antisense RNA 1
MTMR11	10903	myotubularin related protein 11
NCR3LG1	374383	natural killer cell cytotoxicity receptor 3 ligand 1
PDZRN3	23024	PDZ domain containing ring finger 3
PIGQ	9091	phosphatidylinositol glycan anchor biosynthesis class Q
RN7SL574P	106481079	RNA, 7SL, cytoplasmic 574, pseudogene
RNPEPL1	57140	arginyl aminopeptidase like 1
SCNN1D	6339	sodium channel epithelial 1 subunit delta
SEPTIN5	5413	septin 5

RNPEPL1	57140	arginyl aminopeptidase like 1
SCNN1D	6339	sodium channel epithelial 1 subunit delta
SEPTIN5	5413	septin 5
SLC35D1	23169	solute carrier family 35 member D1
SMPD3	55512	sphingomyelin phosphodiesterase 3
SOCAR	105373557	serous ovarian cancer associated RNA
SREBF1	6720	sterol regulatory element binding transcription factor 1
ST3GAL5	8869	ST3 beta-galactoside alpha-2,3-sialyltransferase 5
SUN2	25777	Sad1 and UNC84 domain containing 2
SYT17	51760	synaptotagmin 17
THNSL2	55258	threonine synthase like 2
THSD4	79875	thrombospondin type 1 domain containing 4
TMEM88	92162	transmembrane protein 88
TNS1	7145	tensin 1
TRAM2-AS1	401264	TRAM2 antisense RNA 1
TSPOAP1	9256	TSPO associated protein 1
USP47	55031	ubiquitin specific peptidase 47
ZBTB42	100128927	zinc finger and BTB domain containing 42
ZC3H12C	85463	zinc finger CCCH-type containing 12C
ZNF230	7773	zinc finger protein 230
ZNF292	23036	zinc finger protein 292
ZNF584	201514	zinc finger protein 584
ZNF688	146542	zinc finger protein 688

Supplementary Table 5: Two-way ANOVA analyzing the effect of the cells and Pralsetinib treatment on the gene expression in iRET model. Percentage of total variation and P-value summary are shown for each gene. ns: non-significant *, P<0.05; **, P< 0.01; ***, P<0.001; ****, P<0.0001.

iRET		Anova results		
Gene	Stade	Cell lines	Pralsetinib	Interraction
FOXA2	AFE	97,74% ****	0,52% ns	0,01% ns
NKX2-1	LPC	6,97% *	23,49% **	32,89% ***
C1QTNF6	LPC	0,28% ns	48,26% ***	15,15% *
PROM2	LPC	1,12% ns	59,01% ****	21,38% **

Supplementary Table 6: Two-way ANOVA analyzing the effect of the cells and Pralsetinib treatment on the gene expression in PB68 model. Percentage of total variation and P-value summary are shown for each gene. ns: non-significant *, P<0.05; **, P< 0.01; ***, P<0.001; ****, P<0.0001.

PB68		Anova results		
Gene	Stade	Cell lines	Pralsetinib	Interraction
FOXA2	AFE	62,30% ****	22,40% ****	10,86% **
NKX2-1	LPC	91,58% ****	4,50% **	0,68% ns
C1QTNF6	LPC	67,55% ****	3,64% ***	2,90% ns
PROM2	LPC	88,95% ****	16,93% ****	0,66% ***

3. Perspectives: Generation of 3D lung organoids from patient-derived iPSCs carrying *RET*^{C634Y} mutation as a model of RET-driven NSCLC

In this section of the results, I will present the ongoing experiment that follows the second article of this manuscript (**Article 2,** Marcoux, Hwang, et al. 2023). As mentioned in the discussion of the preceding article, our current focus is on generating mature organoids from the previously described lung cell progenitors (LPCs). Indeed, organoids have emerged as a prominent model for studying lung cancer due to their three-dimensional structure derived from stem cells and their ability to exhibit self-organization, closely resembling the architectural complexity and diverse cell lineages observed *in vivo*. Consequently, several models of lung organoids have been established in recent years (Rock et al. 2009; McQualter et al. 2010; Chapman et al. 2011). Models of lung cancer organoids derived from patient samples have also been developed to investigate various processes associated with lung cancer (Di Liello et al. 2019; Zhang et al. 2018; Kim et al. 2019). In addition, there has been growing interest in iPSC-derived organoids, which combine the self-organizing potential of iPSCs with the ability to differentiate into organ-specific cell types (Garreta et al. 2021). For example, various protocols have been described for generating iPSC-derived lung organoids (Dye et al. 2015; Leibel et al. 2020). The integration of patient-derived iPSCs and organoid modeling holds great potential for disease modeling, high-throughput drug screening, and target discovery, paving the way for significant advancements in these areas (Turhan et al. 2021).

In the preceding article, we have shown that LPCs derived from iPSCs carrying the *RET*^{C634Y} somatic mutation exhibit distinct features resembling RET-driven NSCLC. In order to generate a potentially more precise model, we have pursued the differentiation of LPCs into mature 3D organoids and study their characteristics. For now, 3D organoids have only been generated using the knock-in model (PB68-WT and PB68-RET^{C634Y}). Additionally, a RET^{WT} knock-in model was differentiated (PB68-RET^{WT}) and is expected to exhibit an intermediate level of RET activation as shown in the first article of this manuscript (**Article 1**, Marcoux, Imeri, et al. 2023). Morphological and phenotypical analyses have been conducted on the organoids generated from these iPSCs, but RNA single-cell analysis is still pending to investigate the impact of RET activation on the diversity of the cell population within the organoids.

MATERIALS AND METHODS

This section of the manuscript will be focused on explaining the methodologies and procedures specifically related to the novel experiments presented here. For additional details on other aspects, please refer to the Materials and Methods of the **Article 2** (Marcoux, Hwang, et al. 2023)**.**

3D lung organoid formation and branching.

The protocol was adapted from Leibel et al. 2020. The LPCs (16-25 days old) were embedded in matrigel in either 6-well or 24-well transwell inserts and allowed to incubate in the incubator until the matrigel solidified. After solidification, 3D organoid induction media were added to the wells, and the transwell inserts were placed. Media were changed daily for the first 6 days. Subsequently, branching media were introduced to the wells, and media changes were performed every other day for 6-12 days. Recipes for the media are presented in the following table:

Media	***Cat. No.***	***Concentration***
Serum-free basal medium		
Iscove's Modi!ed Dulbecco's Medium	*31980030; Gibco*	*72,50%*
Ham's F12	*11765054; Gibco*	*25,00%*
Glutamax	*35050061; Gibco*	*1,00%*
B27 without retinoic acid	*12587010; ThermoFisher*	*1,00%*
N2	*17502048; ThermoFisher*	*0,50%*
Pen/Strep	*15140-122; Gibco*	*10 U*
L-Ascorbic acid 2-phosphate (AA2P)	*A8960; Sigma-Aldrich*	*50 µg/mL*
Monothioglycerol	*M6145; Sigma-Aldrich*	*20 µM*
Bovine serum albumin (BSA) Fraction V, 7.5% solution	*15260-037; Gibco*	*0,75%*
3D organoid induction medium (day 17-22)		
Serum-free basal medium		
FGF7	*251-KG-010/CF; Bio Techne*	*10 ng/mL*
FGF10	*345-FG-025/CF; Bio Techne*	*10 ng/mL*
CHIR99021 (CHIR) solution	*72054; Stemcell Technology*	*3 µM*
EGF	*236-EG-200; Bio Techne*	*10 ng/mL*
3D organoid branching medium (day 23-28)		
Serum-free basal medium		
FGF7	*251-KG-010/CF; Bio Techne*	*10 ng/mL*
FGF10	*345-FG-025/CF; Bio Techne*	*10 ng/mL*
CHIR99021 (CHIR) solution	*72054; Stemcell Technology*	*3 µM*
EGF	*236-EG-200; Bio Techne*	*10 ng/mL*
All-trans retinoic acid	*72262; Stemcell Technology*	*0,1 µM*
VEGF/PIGF	*297-VP; Bio Techne*	*10 ng/mL*

3D organoid maturation medium (day 29-34)		
Serum-free basal medium		
FGF7	*251-KG-010/CF; Bio Techne*	*10 ng/mL*
FGF10	*345-FG-025/CF; Bio Techne*	*10 ng/mL*
CHIR99021 (CHIR) solution	*72054; Stemcell Technology*	*3 µM*
EGF	*236-EG-200; Bio Techne*	*10 ng/mL*
All-trans retinoic acid	*72262; Stemcell Technology*	*0,1 µM*
VEGF/PIGF	*297-VP; Bio Techne*	*10 ng/mL*
Dexamethasone	*D4902-25MG; Sigma Aldrich*	*50 nM*
cAMP	*20-198; Sigma Aldrich*	*10 nM*
IBMX	*I5879-100MG; SigmaAldrich*	*100 µM*

In vivo mice transplantation

Six- to eight-week-old mice (male and female) were anaesthetized with isofluorane (2%). Day-17 LPCs were collected and embedded in Matrigel. This suspension was either injected subcutaneous into the loose skin over the neck or transplanted into a pocket in the subcutaneous space above the leg. The mice were palpated every week to monitor the potential tumor growth. Experiment is still ongoing.

Single cell RNA sequencing

PB68-WT, PB68-RET^{WT} and PB68-RET^{C634Y} organoids were dissociated using a TrypLE 20-minute treatment, followed by mechanical dissociation. Debris was then filtered through a cell strainer, and cell viability was assessed using Trypan Blue staining. Single cells were counted and further processed using Chromium10x Genomics protocol (V3.1). Single-cell Gel Bead-In-EMulsions (GEMs) were generated using a Chromium Controller instrument (10x Genomics). Sequencing libraries were prepared using Chromium Single Cell 3' Reagent Kits (10x Genomics), according to the manufacturer's instructions. Briefly, GEM-RT was performed in a thermal cycler using a protocol including incubation at 53°C for 45 min and 85°C for 5 min. Post GEM-RT Cleanup using DynaBeads MyOne Silane Beads was followed by cDNA am-plification (98°C for 3 min, cycled 12 x 98°C for 15 s, 67°C for 20s, 72°C for1 min, and 72°C 1 min). After a cleanup with SPRIselect Reagent Kit and fragment size estimation with High Sensitivity™ HS DNA kit run on 2100 Bioanalyzer (Agilent), the libraries were constructed by performing the following steps: fragmentation, end-repair, A-tailing, SPRIselect cleanup, adaptor ligation, SPRIselect cleanup, sample index PCR, and SPRIselect size selection.

The fragment size estimation of the resulting libraries was assessed with High Sensitivity™ HS DNA kit runned on 2100 Bioanalyzer (Agilent) and quantified using the Qubit™ dsDNA High Sensitivity HS assay (ThermoFisher Scientific). Libraries were then sequenced by pair with a HighOutput flowcel using an Illumina Nextseq 500 with the following mode: 26 bp (10X Index + UMI), 8 bp (i7 Index) and 57 bp (Read 2).

The sequencing data was processed into transcript count tables with the Cell Ranger Single Cell Software Suite 1.3.1 by 10X Genomics (http://10xgenomics.com/). Raw base call files from the Nextseq 500 were demultiplexed with the cellranger mkfastq pipeline into library-specific FASTQ files. The FASTQ files for each library were then processed independently with the cellranger count pipeline. This pipeline used STAR21 to align cDNA reads to the Mus musculus transcriptome (Sequence: GRCm38, Annotation: Gencode v25). Once aligned, barcodes associated with these reads – cell identifiers and Unique Molecular Identifiers (UMIs), underwent filtering and correction. Reads associated with retained barcodes were quantified and used to build a transcript count table. Resulting data for each sample were then aggregated using the cellranger aggr pipeline, which performed a between-sample normalization step and concatenated the two tran-script count tables.

RESULTS

RET^{WT} knock-in model shows intermediate level of RET pathway activation

For this project, we introduced a third model of RET activation using a RET^{WT} knock-in iPSC model. This approach was designed to activate the RET pathway at an intermediate level between the PB68-WT and PB68-RET^{C634Y} models. Results supporting this hypothesis have already been demonstrated in the **Article 1** (Marcoux, Imeri, et al. 2023)**.**

PB68-RET^{WT} iPSCs were differentiated into LPC following the protocol presented in the article 2. qRT-PCR analyses at LPC stage confirmed that RET mRNA level is found between PB68-WT and PB68-RET^{C634} (**Figure 1A**). Immunofluorescence staining targeting phospho RET confirmed the activation of the protein in LPC derived from PB68-RETWT iPSCs (**Figure 1B**). As described in the article 2, qRT-PCR analysis was performed to assess the expression levels of the differentiation markers *FOXA2* and *NKX2-1*, which were found to be regulated by *RET^{C634Y}* in the article 2, along with the cancerous markers *C1QTNF6* and *PROM2* previously identified (**Figure 1C**). The expression level of these differentiation and cancer-related markers in the RET^{WT} knock-in model were intermediate between those observed in PB68-WT and PB68-RET^{C634Y} without Pralsetinib treatment. When treated with Pralsetinib, a significant reduction of *FOXA2*, *C1QTNF6* and *PROM2* expression level was observed as compared to untreated condition (**Figure 1C**). This shows that the PB68-RET^{WT} model positively responds to RET inhibitor Pralsetinib and therefore that the knock-in of RET^{WT} model induces the activation of RET pathway. These results confirm the successful generation of a RET^{WT} knock-in model that displays an intermediary level of RET activation.

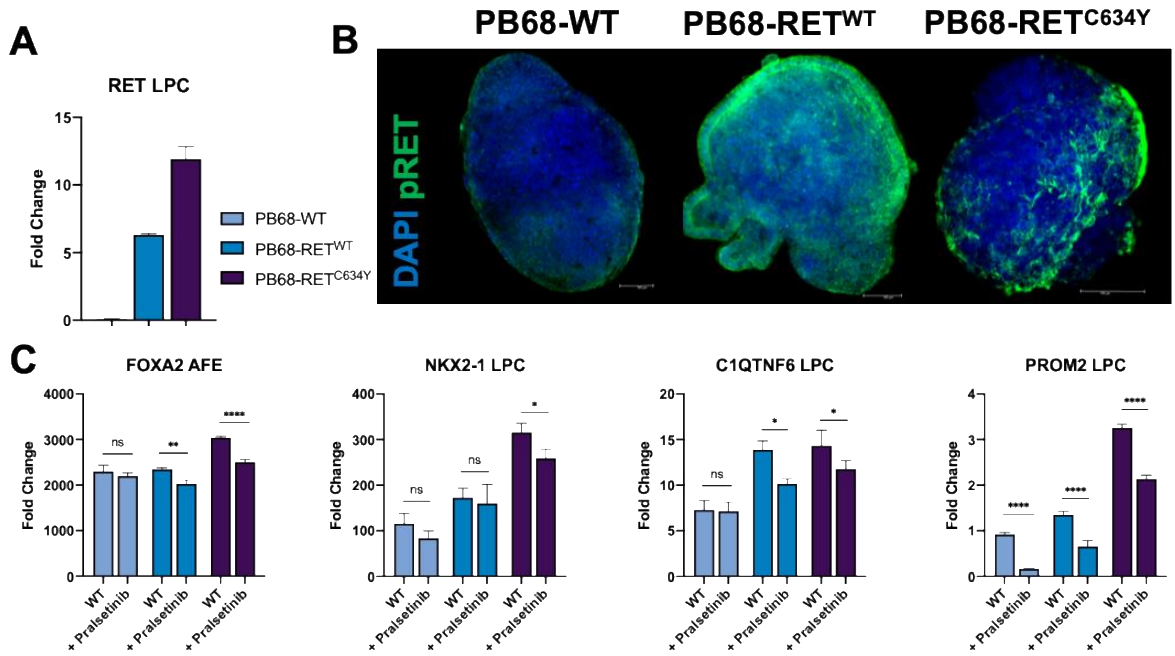

Figure 1: LPCs generated from RET^{WT} knock-in iPSCs display an intermediary level of RET but they still respond to Pralsetinib treatment. (A) *qRT-PCR quantification of RET mRNA in LPCs derived from PB68-WT, PB68-RET^{WT}*

PB68-RET^{C634Y} iPSCs. ***(B)*** *Immunostaining of LPCs derived from PB68-WT, PB68-RET^{WT} PB68-RET^{C634Y} iPSCs showing the expression of pRET (green) and DAPI (blue).* ***(C)*** *Expression of FOXA2, NKX2-1, C1QTNF6, PROM2 quantified by qRT-PCR in PB68 model with and without daily 10 nM Pralsetinib treatment. Fold change ($2^{-\Delta\Delta Ct}$) have been normalized to iPSC stage. Experiments have been performed three times. Two-ways ANOVA were performed to test the effect of cell lines and Pralsetinib treatment. For each combination of cell lines and genes, a Sidak's multiple comparisons test was performed to test the effect of Pralsetinib treatment as compared to untreated. ns: non-significant, *, P<0.05; **, P< 0.01; ***, P<0.001; ****, P<0.0001.*

Generation of 3D mature lung organoids from RET knock-in iPSCs

Subsequently, the three iPSC lines were differentiated into mature 3D organoids using the provided protocol (**Figure 2A**) (Leibel et al. 2020). Morphological analysis reveals that organoids derived from all three iPSC lines exhibit the typical classical shape (**Figure 2B**). To further confirm the phenotype of the organoid, an immunostaining for the Surfactant protein C (SFTPC) was performed. SFTPC is an alveolar lineage marker expressed by alveolar type II cells (AT2). Immunofluorescence staining revealed that SFTPC was overexpressed in organoids derived from PB68-RETWT and PB68-RET^{C634Y} in comparison to PB68-WT. Additionally, SFTPC is highly expressed in PB68-RET^{C634Y} organoids than in PB68-RET^{WT} organoids. Additional immunostainings with different markers are on their way to have a better phenotypic characterization of the generated organoids. We are also planning to analyze the expression of the cancerous markers found upregulated by RET^{C634Y} mutation in the LPC model, namely PROM2 and C1QTNF6.

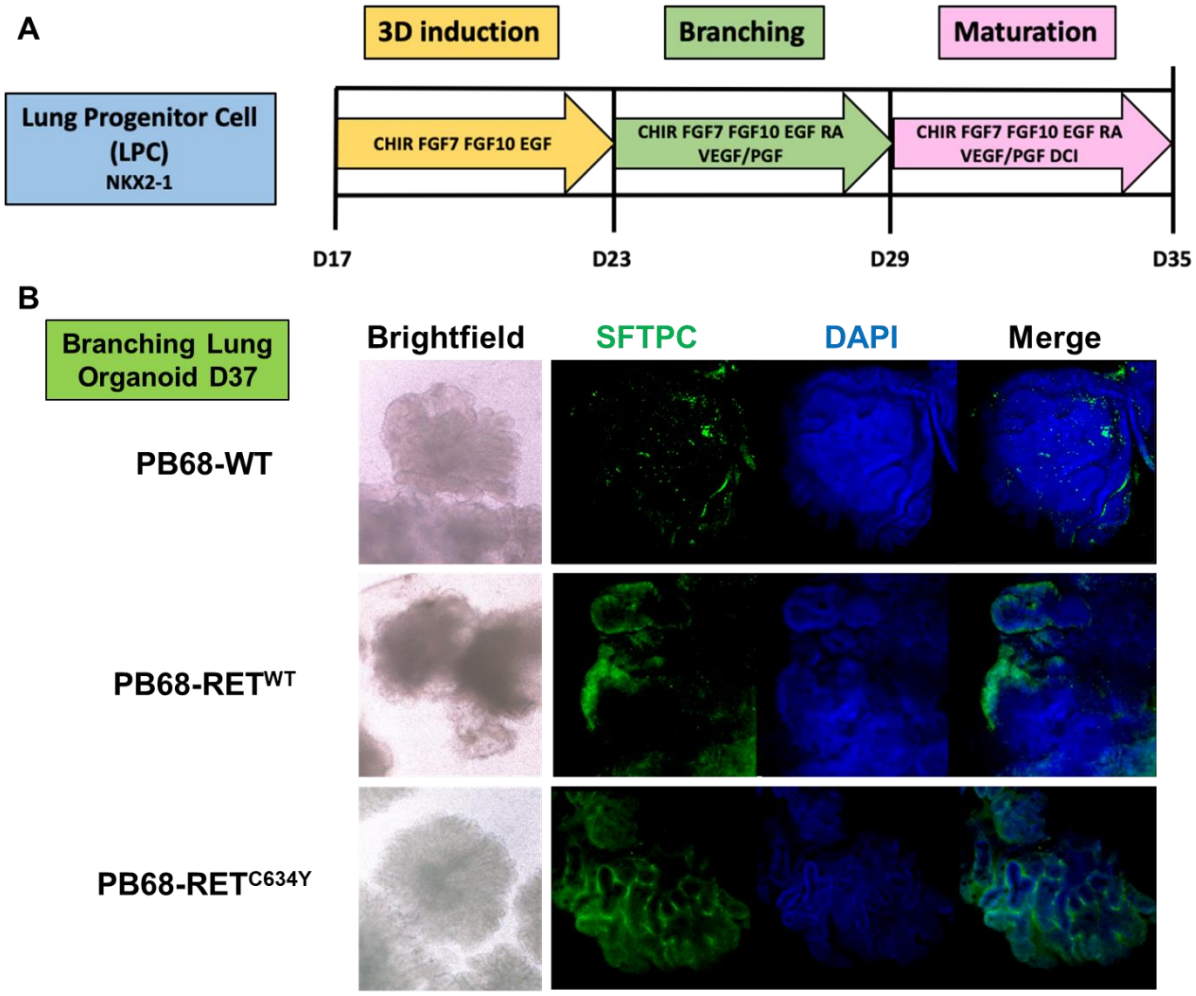

Figure 2: Generation of lung progenitor cells (LPCs) from iRET^{C634Y} is associated with the overexpression of FOXA2 and NKX2-1. (A) *Schematic representation of the differentiation protocol from LPC to mature 3D lung organoids* ***(B)*** *Immunostaining of D37 branching lung organoids derived from PB68-WT, PB68-RET^{WT} and PB68-RET^{C634Y} iPSCs showing the expression of SFTPC (green), DAPI (blue) or merged.*

Single cell RNA sequencing for identification of distinct cell populations affected by RET mutation during organoid differentiation

If there is a delay in the differentiation process or even dedifferentiation, and we observe the overexpression of cancerous markers in the iPSC-derived organoids carrying the RET^{C634Y} mutation, it suggests that there might be distinct cell populations with varying gene expression profiles within the samples. To investigate this further, we plan to utilize single-cell RNA sequencing (scRNA-Seq) technology. ScRNA-Seq allows us to analyze gene expression at the individual cell level, providing a comprehensive view of the cellular heterogeneity within a population. By performing scRNA-Seq on the iPSC-derived LPCs, we can identify and characterize different cell clusters based on their unique gene expression profiles. This will help us understand the diverse cellular states present within the cultures, such as undifferentiated cells, partially differentiated cells, and those exhibiting features similar to RET-driven NSCLC. Additionally, scRNA-Seq can uncover rare cell subpopulations that might be important for the disease development but would be challenging to detect using traditional bulk

RNA sequencing. The data obtained from scRNA-Seq analysis will enable us to identify specific gene expression patterns associated with RET activation and its effects on the differentiation process. This information will be important in understanding the molecular mechanisms underlying the observed phenotypic changes in the iPSC-derived organoids. It will also provide insights into how RET mutations impact the differentiation potential and behavior of these iPSCs.

Furthermore, we also assessed the oncogenic potential of the RET knock-in models *in vivo.* 6-week mice were either injected or transplanted with LPCs derived from PB68-WT, PB68-RET^{WT} or PB68-RET^{C634Y} iPSCs. Unfortunately, this preliminary experiment did not yield the anticipated results, as we did not observe any LPC engraftment, and consequently, no tumor development was detected. We are planning to do this experiment again and transplant cells for mature organoids as well. If these experiments give interesting results, it would be valuable to conduct a similar analysis using a patient-derived iPSC model ($iRET^{C634Y}$ and $iRET^{CTRL}$).

DISCUSSION

In summary, this chapter delves into an ongoing experiment that follows the trajectory set by the second article of this manuscript. As discussed in the preceding article, our primary focus resides in generating mature organoids from the previously generated lung cell progenitors (LPCs). Organoids are important model for comprehending lung cancer because they closely mimic the intricate architectural complexities and diverse cell lineages observed *in vivo*.

To date, 3D organoids have exclusively been generated using the knock-in models (PB68-WT and PB68-RET^{C634Y}). In addition, a RET^{WT} knock-in model (PB68-RET^{WT}) has been differentiated, with an intermediate level of RET activation. Phenotypic and morphological analyses of organoids derived from these iPSCs have been undertaken. However, a comprehensive RNA single-cell analysis is required, this analysis is pending, which aims to explore the impact of RET activation on the diversity of cell populations within these organoids.

DISCUSSION & CONCLUSIONS

DISCUSSION & CONCLUSIONS

The breakthrough discovery of iPSCs by Yamanaka in 2006, initially in mice, and its application to human in 2007, has marked the beginning of a revolutionary era in the field of stem cell biology as it challenged the previously established dogma about the impossibility of de-differentiation of a cell towards an embryonic state (Takahashi & Yamanaka 2006; Takahashi et al. 2007). It also created an unprecedented hope for the therapy of several diseases as it became theoretically possible to generate embryonic like cells with the potential of regenerating organs and tissues (Shi et al. 2017). iPSCs also opened a novel field of disease modeling to study the cellular and molecular mechanisms underlying various diseases. By generating iPSCs from patients with specific genetic disorders or diseases it is possible to create patient-specific disease models. In these models the abnormal gene can be corrected and serve to understand the progression and the mechanisms of the diseases or to test potential drugs in a more relevant cellular context. However, generating patient-derived iPSCs presents several challenges.

The generation of iPSCs is a complex and time-consuming process with relatively low efficiency, posing significant limitations on the ability to reprogram all types of cells. Most reprogramming protocols are optimized for cells that are readily available and easily reprogrammed, such as PBMCs, mesenchymal stem cells, and fibroblasts, which exhibit high proliferation rates and chromatin accessibility (González et al. 2011). The reprogramming of cancer cells with specific mutations of interest is complicated for several reasons. The high genotypic variability of these tissues makes challenging the generation of iPSCs harboring all the mutations present within a tumor (Rao & Malik 2012). Moreover, the tumor microenvironment can influence the reprogramming process, and the presence of oncogenic factors, such as *TP53* mutations or invalidations, may interfere with iPSC generation (Papapetrou 2016). Additionally, epigenetic memory in cancer cells can pose obstacles during reprogramming, potentially affecting iPSCs stability and functionality. Despite these challenges, generating iPSCs carrying somatic mutations from patients suffering from hereditary cancers is a more feasible goal, as these mutations are present in each somatic cell. This characteristic allows researchers to use classic reprogramming protocols to generate iPSC from readily available non-cancerous cell types carrying the mutation.

Furthermore, iPSCs display inherent variability in their ability to differentiate into specialized functional cells of a specific lineage due to their genetic background (Kilpinen et al. 2017). This variability can pose challenges when comparing cells derived from patient-specific iPSCs with those from control iPSCs (Soldner & Jaenisch 2012). To overcome this issue and isolate the impact of oncogenic driver mutations, isogenic pairs of disease-specific and control iPSCs have been generated

(Soldner et al. 2011). Isogenic pairs are identical except for a specific genetic difference, the presence or absence of the oncogenic mutation. The development and widespread adoption of genome editing tools, particularly the CRISPR/Cas9 system, have enabled researchers to precisely engineer control iPSCs in which the oncogenic mutation is corrected (Byrne & Church 2015; Johnson & Hockemeyer 2015; Li, Zhou, et al. 2019). This approach allows for a more controlled and direct comparison between disease-specific and control cells, helping to understand the specific effects of the mutation on cell behavior, differentiation potential, and disease-related processes.

The knock-in technique is another technical approach that can be used to investigate the impact of a gene of interest while minimizing the influence of unrelated genetic variations in iPSCs (Banan 2020). The knock-in of a specific gene or mutation into an iPSCs create a distinct cell line expressing the gene or mutation of interest and sharing the same genetic background as the wild type iPSCs allowing a direct comparison of their characteristics and behaviors during differentiation. In the case of oncogenic mutation, the mutation induced at the pluripotent state can be propagated with generation of "transformed tissues". For instance, after the introducing of $KRAS^{G21D}$ oncogene into WT iPSCs, it is possible to differentiate alveolar type 2 cells where genomic pathways similar to lung adenocarcinoma are induced (Dost et al. 2020). This approach facilitates the study of the effect of the gene on various cellular processes, including differentiation, proliferation, and responses to drugs or treatments.

Throughout the work during my PhD, I employed both approaches to investigate the impact of RET pathway activation in two different projects: one focused on the role of RET during iPSC-derived hematopoiesis, and the other one aimed on the modeling of RET-driven Non-Small Cell Lung Cancer (NSCLC). I have used an iPSC line derived from a patient carrying the RET^{C634Y} somatic mutation ($iRET^{C634Y}$) along with its isogenic CRISPR-corrected control ($iRET^{CTRL}$) which were generated previously in our laboratory (Hadoux et al. 2016; Hadoux et al. 2018). In parallel, I have generated via lentiviral mediated gene transfer, the overexpression of RET^{WT} or RET^{C634Y} in iPSCs derived from healthy donors (PB33-WT and PB68-WT). These iPSCs (PB33-RET^{WT}, PB33-RET^{C634Y}, PB68-RET^{WT}, PB68-RET^{C634Y}) serve as models of RET pathway activation as demonstrated in the results section of this manuscript.

The generation of HSCs with long-term repopulation potential from iPSCs is a key research goal to address the need for new sources in hematopoietic stem cell transplantation (HSCT). However, iPSC-derived hematopoiesis currently produces mature blood cells but lacks long-term engraftable HSCs (Kaufman et al. 2001; Chadwick et al. 2003; Zambidis et al. 2005). Various studies have explored the possibility of generating iPSC-derived engraftable HSCs, but significant challenges remain. One approach involves generating iPSC-derived HSCs from human teratomas, which can migrate and

repopulate the bone marrow (Amabile et al. 2013; Suzuki et al. 2013). Another method involves ectopically expressing specific transcription factors, such as HOXA9, ERG, RORA, SOX4, and MYB, to produce short-term engraftable HSCs (Doulatov et al. 2013). However, these two approaches remain unsuitable for clinical uses and the generation of fully engraftable HSCs necessitates further optimization of hematopoietic differentiation protocols or a deeper understanding of differentiation mechanisms. The RET pathway has been identified as crucial for HSC development and expansion in mice and umbilical cord blood, with RET neurotrophic factor partners promoting HSC survival, expansion, and function (Fonseca-Pereira et al. 2014; Grey et al. 2020). However, the impact of RET activation during iPSC-derived hematopoiesis is still not characterized.

In our first study (**Article 1**, Marcoux, Imeri, et al. 2023) the overexpression of RET^{WT} and RET^{C634Y} by knock-in in iPSCs revealed that RET activation reduces the number of HSC-like cells and hematopoietic progenitors, affecting their potential to form colonies (Marcoux, Imeri, et al. 2023). Moreover, the use of patient-derived iPSCs with an endogenous RET^{C634Y} mutation also showed inhibitory effects similar to knock-in models. Transcriptomic analysis further revealed that RET activation led to the upregulation of genes associated with the MAPKs, immune system, and hematopoietic regulation. Notably, genes like DLK1 and NR4A3, involved in restricting HSC proliferation and hematopoiesis (Mirshekar-Syahkal et al. 2013; Freire & Conneely 2018), were upregulated in response to RET activation. Overall, this study highlights the complexity of RET activation effects during iPSC-derived hematopoiesis and suggests potential regulatory pathways responsible for this inhibition such as DLK1 and the MAPK pathway. At present, it remains unclear whether manipulation of these inhibitory genes could restore this phenotype. Understanding the mechanisms behind RET impact on HSC differentiation is important for optimizing iPSC-based hematopoietic strategies. Future experiments will shed light on the potential for reversing this inhibitory effect.

The second part of my work (**Article 2,** Marcoux, Hwang, et al. 2023) focused on evaluating the possibility of using patient-derived iPSCs with *RET* somatic mutations to develop RET-driven NSCLC models. Various models of *RET*-rearranged lung cancer have been established over the years, including those using cancer cell lines (Nelson-Taylor et al. 2017), genetically engineered mouse models expressing KIF5B-RET fusion protein (Saito et al. 2014b), and PDX-derived lung adenocarcinoma cells harboring KIF5B-RET fusion (Hayashi et al. 2020). However, there is currently a lack of RET-driven NSCLC models based on patient-derived iPSCs, which could offer valuable insights into this disease. Patient-derived iPSC models allow the capture of the unique genetic characteristics of individual patients, providing a more precise representation of the disease biology as compared to the use of cancer cell lines. These iPSC models facilitate disease modeling, patient-specific organoid creation, and

investigations in cancer development, high-throughput drug screening, and target discovery, offering significant potential for advancements in these critical areas of research.

In our second study (**Article 2,** Marcoux, Hwang, et al. 2023), we successfully generated lung cell progenitor cells (LPCs) from iPSCs expressing the *RET*^{C634Y} mutation. The LPCs derived from these iPSCs exhibited characteristics associated with *RET*-rearranged NSCLC when compared to control iPSCs. The qRT-PCR analysis revealed the overexpression of *FOXA2* during AFE stage in both models, consistent with its upregulation in KIF5B-RET fusion NSCLC (Lee et al. 2023). Moreover, the *RET*^{C634Y} mutation led to the upregulation of *NKX2-1,* which serves as a marker for lung progenitors and has been identified as a tumor biomarker in lung cancer (Myong 2003; Tan et al. 2003). Transcriptomic analyses were performed to identify specific signatures associated with the *RET* mutation in iPSC-derived LPC. The *RET*^{C634Y} mutation was found to influence transcriptional regulation, leading to lung dedifferentiation and upregulation of cancerous markers associated with poor prognosis. Finally, RET-mutated LPCs exhibited a favorable response to the RET-specific inhibitor treatment, Pralsetinib, resulting in the downregulation of the previously identified cancerous marker. This study demonstrates that patient-derived iPSCs carrying *RET*^{C634Y} somatic mutations could be utilized as a valuable model for studying RET-driven NSCLC, drug testing, and identifying potential cancer biomarkers. The generated LPCs provide an accurate and easily generable model for studying NSCLC and its response to targeted therapies. This study represents an important step towards understanding RET-driven NSCLC and developing new treatments.

To create a more precise model, we have continued to differentiate LPCs into mature 3D organoids to study their properties (**Perspectives**). So far, 3D organoids have been successfully generated using the knock-in model (PB68-WT and PB68-RET^{C634Y}). Additionally, the RET^{WT} knock-in model (PB68-RET^{WT}) has also been differentiated, which is expected to show an intermediate level of RET activation based on the findings from the first article of this manuscript (**Article 1**, Marcoux, Imeri, et al. 2023).Morphological and phenotypical analyses have been performed on the organoids derived from these iPSCs, but further investigations using single-cell RNA sequencing are still underway to explore the impact of RET activation on the cell population diversity within the organoids.

If the *RET*^{C634Y} mutation causes a delay in the differentiation process or even dedifferentiation, as suggested in the literature (Wang et al. 2012), it is expected to observe some heterogeneity among the cell populations when comparing the organoids derived from the different iPSCs. To thoroughly explore this cellular heterogeneity, it is possible to use single-cell RNA sequencing (scRNA-Seq). By analyzing gene expression at the individual cell level, scRNA-Seq provides a comprehensive understanding of the various cell clusters present within the organoids, including those that may

exhibit features similar to RET-driven NSCLC. Through scRNA-Seq, it becomes possible to identify and characterize these distinct cell clusters based on their unique gene expression profiles. Additionally, scRNA-Seq will provide deeper insights into how *RET* mutations influence the differentiation potential and behavior of these cells, and their potential role in the development and progression of RET-driven NSCLC. Moreover, scRNA-Seq data can reveal potential key regulators or therapeutic targets that play important roles in the context of RET-driven NSCLC. This knowledge holds the potential to pave the way for the discovery of novel strategies for targeted therapies and precision medicine approaches, ultimately benefiting patients with RET-driven NSCLC.

Interestingly, RET^{M918T}, another *RET* single point mutation, has been found as an oncogenic driver in Small Cell Lung Cancer (SCLC) (Dabir et al. 2014). RET^{M918T} mutation is one of the most potent transforming *RET* mutations in medullary thyroid carcinoma (MTC) and is associated with a more severe clinical phenotype due potentially to its increased TK activity (Jasim et al. 2011). In a precedent study, my colleagues have generated an iPSC from a patient with this RET^{M918T} mutation, who developed both pheochromocytoma and MTC (Bennaceur-Griscelli et al. 2017). During my PhD, we attempted to generate a CRISPR-corrected isogenic control iPSC but we encountered technical challenges that prevented us from achieving this objective. Indeed, the Cas9 employed to correct the RET^{C634Y} mutation proved inapplicable to the RET^{M918T} mutation due to the absence of an appropriate PAM sequence in proximity to the mutation site. This challenge could have been addressed by designing a novel protocol utilizing alternative Cas9 or novel base editing technology. Unfortunately, time constraints during my PhD prevented us from pursuing this project. Nevertheless, with this tool, we could conduct a similar study as presented in article 2, aiming to develop a model of SCLC using patient-derived iPSCs. This model could serve as a valuable resource for comprehending RET-mutant SCLC and exploring the identification and testing of novel therapies. However, *RET* mutations in SCLC are very rare as several studies have reported only a limited number of cases with such mutations (Mulligan et al. 1998; Rudin et al. 2012; Peifer et al. 2012). Nevertheless, the rarity of these mutations does not diminish the significance of identifying a targetable driver for patients with specific cancers. Treating a patient with a RET-mutant SCLC using a targeted inhibitor of RET would be of great interest, illustrating the potential for personalized and effective therapies in rare cases.

Patient-derived iPSCs carrying somatic mutation are important tools for the study of hereditary cancers. For example, a study used patient-specific iPSCs derived from a family affected by Li-Fraumeni Syndrome (LFS) and investigated the impact of mutant p53 on the development of osteosarcoma (OS). By utilizing these LFS iPSCs, they were able to generate osteoblasts (OBs) that mirrored the characteristics of OS, including impaired osteoblastic differentiation and tumorigenic properties (Lee et al. 2015). Another study demonstrated the feasibility of generating iPSC lines from *BRCA1* mutant

fibroblasts to provide a platform to investigate the influence of the mutation on gene expression and genome stability (Soyombo et al. 2013). Moreover, in our research group, we have also successfully generated an iPSC from a patient carrying a *c-MET* mutation and diagnosed with hereditary papillary renal cell carcinoma (PRCC) (Hwang et al. 2019). Through our study, we demonstrated that *in vitro* kidney organoids derived from these iPSCs accurately replicate the transcriptomic characteristics of primary PRCC across a significant patient cohort. Finally, the presence of particular oncogenic mutations in an iPSC enables the modeling of diverse cancers based on the chosen differentiation pathway. Therefore, our team have also explored the potential of c-MET-mutated iPSCs to serve as a model for glioblastoma (GBM), a malignancy where c-MET overexpression has been reported in about 10% of cases (Kwak et al. 2015). Our investigation revealed that neural structures derived from these iPSCs exhibited transcriptomic profiles closely resembling those observed in human GBM (Hwang et al. 2020). These studies show the potential of iPSC carrying somatic mutation for modeling oncogenic tissues.

Overall, the work presented in this manuscript illustrates the importance of iPSC CRISPR isogenic models for studying gene functions in specific cellular differentiation contexts. The ability to generate diverse models from the same iPSC line, depending on the goal of the study and the protocol of differentiation, allows the possibility to explore how a particular mutation can exhibit distinct effects in a specific cellular environment.

Nonetheless, our studies involving unique iPSC lines carrying the RET^{C634Y} somatic mutation do present certain limitations that necessitate further investigations. In the context of hematopoiesis, we have used global hematopoiesis induction techniques which do not allow generation of true HSCs. The inhibitory impact observed at the clonogenic cell level has allowed us to pinpoint the involvement of inhibitory mechanisms very early in the differentiation process of RET-expressing iPSCs. It would be of interest to explore the potential effect of RET expression in a DOX-inducible system after the induction of mesoderm stage during differentiation. These experiments could be coupled with iPSC lines in which the identified inhibitory pathways have been disrupted.

Similarly, the characterization of the molecular patterns of NSCLC identified in the LPCs generated from RET-overexpressing iPSC needs to be pursued in the mature lung cells. We have initiated these experiments, and the ongoing molecular analysis of these cells is currently in progress.

To conclude, throughout my work, I used unique iPSC lines available in the laboratory to demonstrate the potential to investigate the influence of the tyrosine kinase receptor RET in two distinct contexts. These experiments showed the complexity of iPSC models which represent a unique experimental tool for disease modeling and drug discovery.

APPENDICES

APPENDICES

Throughout my PhD, I had the opportunity to work on various projects alongside my main thesis. This section presents abstracts summarizing the different papers I contributed to:

- **Article 1**: Modeling Chimeric Antigen-Receptor (CAR)-Engineered Natural Killer (NK) Cells Targeting Chronic Myeloid Leukemia (CML) Blast Crisis
- **Article 2**: Comparative Transcriptome Analyses in Mantle Cell Lymphoma (MCL): Evidence of E2F1 As a Major Target in Aggressive Blastoid MCL Model
- **Article 3**: Modeling Blast Crisis Using Mutagenized Chronic Myeloid Leukemia-Derived Induced Pluripotent Stem Cells (iPSCs)
- **Article 4**: Case report: Long-term voluntary Tyrosine Kinase Inhibitor (TKI) discontinuation in chronic myeloid leukemia (CML): Molecular evidence of an immune surveillance
- **Article 5**: Molecular investigation of adequate sources of mesenchymal stem cells for cell therapy of COVID-19-associated organ failure

1. Article 1: Chimeric Antigen-Receptor (CAR)- Engineered Natural Killer (NK) Cells Targeting Chronic Myeloid Leukemia (CML) Blast Crisis

Article submitted in Frontiers in Immunology

Chimeric Antigen-Receptor (CAR)- Engineered Natural Killer (NK) Cells Targeting Chronic Myeloid Leukemia (CML) Blast Crisis

Jusuf Imeri[1], **Paul Marcoux**[1], Matthias Huyghe[1], Christophe Desterke[1], Daianne Maciely Carvalho Fantacini[2], Frank Griscelli[1,3,4,5], Dimas Tadeu Covas[6,7], Lucas Edouardo Botelho de Souza[6,7], Annelise Bennaceur Griscelli[1,3,4,8], Ali G Turhan[1,2,3,4,8] *

[1] INSERM UMR-S-1310, Université Paris Saclay, 94800 Villejuif, Université Paris Saclay, 94800 Villejuif, France.
[2] Blood Center of Ribeirão Preto/Ribeirão Preto School of Medicine/University of São Paulo - Ribeirão Preto/SP, Brazil
[3] INGESTEM National iPSC Infrastructure, 94800 Villejuif, France
[4] CITHERA, Centre for IPSC Therapies, INSERM UMS-45, Genopole Campus, 91100 Evry, France
[5] Université Paris Descartes, Faculté Sorbonne Paris Cité, Faculté des Sciences Pharmaceutiques et Biologiques, Paris, France
[6] Blood Center of Ribeirão Preto/Ribeirão Preto School of Medicine/University of São Paulo - Ribeirão Preto/SP, Brazil
[7] Biotechnology Nucleus of Ribeirão Preto/Butantan Institute - Ribeirão Preto/SP, Brazil
[8] APHP Paris Saclay, Department of Hematology, Hopital Bicetre & Paul Brousse, Villejuif 94800, France
* Correspondence: turviv33@gmail.com

ABSTRACT

Background: The use of tyrosine kinase inhibitors (TKIs) has dramatically modified the therapy of chronic myeloid leukemia (CML), generating durable remissions and prolonging survival in TKI-responders. However, progression to blast crisis (BC) still occurs especially in TKI-resistant patients and represents a clinical challenge. We and others have identified IL2RA/CD25 as a typical cell surface marker of BC-CML and reported that its overexpression is correlated with the progression of CML from CP-CML to BC-CML (Imeri et al, Cells 2023). Here we show the experimental development of a third-generation CAR-NK therapy strategy against the CD25 based on the scFV of the clinically approved monoclonal humanized antibody, Basiliximab.

Methods: As NK cell model, we have used the NK92 cell line which has a well-established and clinically demonstrated NK cell activity. We have lentivirally transduced NK92 cells with the CAR construct containing a selectable gene (GFP). After FACS-sorting of GFP-positive cells, phenotypical characterization was performed by FACS. The expression of the CAR-CD25 at the surface of the cells was demonstrated an anti-Fab antibody and double-positive (Fab/GFP) cells were further purified. The functionality of the cells was evaluated using CD107a degranulation assay after 3h co-culture and ELISA for IFN-gamma release. We have in parallel engineered K562 cells expressing CD25 by lentiviral transduction (K562- CD25) as well as also a second target cell line (RAJI) using the same strategy.

Annexin V staining of target K562 cells was used for *in vitro* cytotoxicity assessments. For *in vivo* assays, NSG mice were intraperitoneally (IP) injected with K562-CD25 cells expressing Luciferase at Day-3 (3.106 cells/mouse, n = 13). At Days 0, 3, and 7, mice were treated by IP injection of either irradiated CD25 CAR-NK92 cells (10 .106/mouse n=6) or irradiated Wild-type (WT)-NK92 cells (n=5). The clinical evolution of mice transplanted mice was followed weekly by luminescence (IVIS 200).

Results: After cell sorting, we obtained more than 90% of double-positive NK92 CAR^+/GFP^+ cells. Lentiviral transduction did not affect the activatory or inhibitory signals of NK92 cells. No statistical differences were observed between CD25 CAR-NK92 and WT- NK92 cells for the expression of NKp30, NKp46, KirDl2-3, TIGIT, and DNAM. However, we observed a strong increase in the Granzyme B and Perforin in CD25 CAR-NK92 cells after co-culture with K562-CD25 as compared to WT NK92 cells ($p<0.001$). Importantly, we have found increased levels of degranulation after co-culture of target K562-CD25 with CD25-CAR-NK92 cells (40%) as compared to cells co- cultured with WT NK92 alone (20%) suggesting strongly the occurrence of an additional specific effect due to CAR-CD25. IFN-gamma levels after co- culture of CAR CD25 NK92 cells were also found to be significantly increased (400 pg/mL) in as compared to co-cultures of target cells with WT-NK92 (200 pg/mL)($p<0.0001$). Similarly, *in vitro* cytotoxicity assays showed induction of higher levels of apoptosis in target cells (K562-CD25 and Raji-CD25) when co-cultured with CD25 CAR-NK92 as compared to NK92 WT ($p<0.0001$). In *in vivo* experiments, we have analyzed K562-CD25 leukemia-bearing mice treated with CAR-NK92 cells (n=6) or WT-NK92 cells (n=5). These experiments analyzed at day +30 post-transplant showed stronger anti-leukemia effect of CAR-NK therapy by IVIS imaging with a survival rate of 84% for mice treated with CD25 CAR-NK92 versus 40% for those treated with WT-NK92. All control mice transplanted with K562-CD25 cells and left untreated died by day +20.

Conclusion: We show here for the first time the potential use of an NK cell- mediated CAR therapy strategy targeting CD25 which has been shown to be upregulated in CML blast crisis. The experimental data show a significantly increased and selective *in vitro* and *in vivo* cytotoxicity of CD25 CAR-NK92 cells against CD25-expressing leukemia cells as compared to WT-NK92 cells. These results suggest that targeting CD25 by a CD25 CAR based on Basilixiamb's scFV might be an interesting tool in BC-CML and in all acute leukemias overexpressing CD25. In order to translate these findings to NK cells derived from induced pluripotent stem cells (iPSCs), we have produced iPSCs expressing CAR-CD25 constructs and experiments are underway to evaluate the therapeutic potential of iPSC-derived CD25 CAR- NK cells in CML blast crisis or AML models.

2. Article 2: Comparative Transcriptome Analyses in Mantle Cell Lymphoma (MCL): Evidence of E2F1 As a Major Target in Aggressive Blastoid MCL Model

Article submitted in Leukemia and Lymphoma

Comparative Transcriptome Analyses in Mantle Cell Lymphoma (MCL): Evidence of E2F1 As a Major Target in Aggressive Blastoid MCL Model

Jusuf Imeri[1, 2], **Paul Marcoux**[1,2], Christophe Desterke[1,2], Amen Allah Nasr[3], Radhia M'kscher[4], Annelise Bennaceur Griscelli[1,2,3,5,6], Ali G. Turhan[1,2,3,5,6] *

[1] INSERM UMR-S-1310, Université Paris Saclay, 94800 Villejuif, France
[2] Université Paris-Saclay, Faculté de Médecine, 94270 Le Kremlin Bicetre, France
[3] APHP Paris Saclay, Department of Hematology, Hôpital Bicetre, 94270 Le Kremlin Bicetre, France
[4] Service OncoHematologie et Cytogenetique, 94800 Villejuif, France
[5] CITHERA, Centre for iPSC Therapies, INSERM UMS-45, Genopole Campus, 91100 Evry, France
[6] APHP Paris Saclay, Department of Hematology, Hôpital Paul Brousse, 94800 Villejuif, France
* Correspondence: turviv33@gmail.com

ABSTRACT

Background: Mantle cell lymphoma (MCL) is a highly aggressive B-cell lymphoma characterized by the translocation t(11;14)(q13;q32) which triggers the dysregulation of the cyclin D1 by placing its coding gene *CC1ND1* under the control of an immunoglobulin promoter. One of the major consequences of this molecular event is the disturbance of the cyclin D/Rb pathway leading to Rb inactivation and activation the elongation factor E2F1 mainly implicated in cell cycle progression. The mainstay of MCL therapies remains the chemo-immunotherapy followed by autologous transplantation but recently several novel therapies have been developed such as BTK inhibitors, Venetoclax, CDK4/6 inhibitors and more recently CAR-T therapies. However, patients with aggressive forms of MCL exhibit low response rates, requiring the identification of novel therapeutic targets.

Materials and Methods: We have previously generated an MCL cell line (UPN-1) from a patient with a blastoid variant of MCL presenting unique morphological and cytogenetics characteristics (M'kacher et al, Oncogene 2003). This cell line has been shown to harbor a *TP53* mutation and a highly increased sensitivity to radiation despite the absence of functional p53. The molecular basis of this phenomenon has not been explored. In this work, we further characterized UPN-1 cell line using the Clarium S human microarray which has been compared to the gene expression profile of other existing MCL cell lines (GRANTA-519, JEKO-1, JVM-2, MAVEK-1, MINO, REC-1, SP-49, SP53, Z-138). After mathematical correction, a supervised analysis was performed between triplicate samples of UPN-1

and a group constituted with all other MCL cell lines. We have then set up *in vitro* assays to determine the effect of a direct E2F1 inhibitor on the proliferative potential of UPN-1.

Results: The comparative transcriptome analyses revealed a list of 47 genes specially upregulated in UPN-1. Unsupervised classification allowed to discriminate UPN-1 samples from other MCL cell lines based on the expression of these 47 genes. These data suggested a specific expression profile of UPN-1 as compared to other cell lines. Among the upregulated genes, E2F1 elongation factor was found to be highly upregulated in UPN-1 as compared to other MCL cell lines along with positive enrichment of E2F targets which are mainly implicated in cell cycle progression. Interestingly, UPN-1 has a low level of BCL-2 as compared to other MCL lines that could explain its radio sensitivity. However, other signaling pathways involved in the inhibition of apoptosis were found to be present in UPN-1 by geneset enrichment analysis. The expression of *CDKN1A* (p21), major cell cycle regulator and known as a marker of aggressive MCL, was found to be low in UPN-1. A repression of immune response pathway such as NFKB with low expression of NFKBIA was identified. Finally, the expression of PIK3CD which encodes for a therapeutic target in MCL (such as PI3KDelta inhibitor Idelalisib) was also significantly repressed in UPN-1 as compared to nine other MCL cell lines. To evaluate the effect of the direct inhibition of E2F1, we treated UPN-1 cells with a targeted E2F1 inhibitor 5'-Deoxy-5'-(methylthio)adenosine (MTA) which is a protein methylation inhibitor. MTT assays revealed a 50% reduction of proliferation at +4 hours in comparison to the vehicle-treated conditions ($P<0.0001$). Annexin assays showed an increase in early apoptosis (36.6 %) at +8 hours with subsequent rise in late apoptotic cells (64.5 %) observed after 24 hours of treatment. Interestingly, qRT-PCR analyses of MTA-treated cells exhibited a decrease in the expression of downstream factors associated with E2F1, such as *RAD51, BRCA1, CDK2, CCNB2, RANBP1.*

Conclusions: We report here for the first time the comparative transcriptome analysis of the unique aggressive blastoid MCL line UPN-1 as compared to other MCL lines described. This cell line exhibited a major upregulation of E2F1 expression and a down regulation of the cell cycle inhibitor *CDKN1A* (p21). The potential effects of the direct inhibition of E2F1 using the targeted inhibitor MTA demonstrated a reduction in cell proliferation and induction of apoptosis, suggesting the possibility of associating clinically acceptable E2F1 inhibition strategies to other current therapies.

3. Article 3: Modeling Blast Crisis Using Mutagenized Chronic Myeloid Leukemia-Derived Induced Pluripotent Stem Cells (iPSCs)

Cells. 2023 Feb 12;12(4):598.
doi: 10.3390/cells12040598.

Modeling Blast Crisis Using Mutagenized Chronic Myeloid Leukemia-Derived Induced Pluripotent Stem Cells (iPSCs)

Jusuf Imeri[1], Christophe Desterke[1], **Paul Marcoux[1]**, Gladys Telliam[1], Safa Sanekli[1,2], Sylvain Barreau[1,2], Yucel Erbilgin[1,3], Theodoros Latsis[1], Patricia Hugues[1], Nathalie Sorel[1,4], Emilie Cayssials[5], Jean-Claude Chomel[1,4], Annelise Bennaceur-Griscelli[1,2,6,7], Ali G Turhan[1,2,6,7]

[1]INSERM UMR-S-1310, Université Paris Saclay, 94800 Villejuif, France and ESTeam Paris Sud, Université Paris Saclay, 94800 Villejuif, France.
[2]APHP Paris Saclay, Department of Hematology, Hôpital Bicêtre & Paul Brousse, 94800 Villejuif, France.
[3]Aziz Sancar Institute of Experimental Medicine, Istanbul University, 34093 Istanbul, Turkey.
[4]Service de Cancérologie Biologique, CHU de Poitiers, 86000 Poitiers, France.
[5]Service d'Oncologie Hématologique et Thérapie Cellulaire, CHU de Poitiers, 86021 Poitiers, France.
[6]INGESTEM National iPSC Infrastructure, 94800 Villejuif, France.
[7]CITHERA, Centre for iPSC Therapies, INSERM UMS-45, Genopole Campus, 91100 Evry, France.

PMID: 36831265 PMCID: PMC9953961 DOI: 10.3390/cells12040598

Abstract

Purpose: To model CML progression *in vitro* and generate a blast crisis (BC-CML) model *in vitro* in order to identify new targets.

Methods: Three different CML-derived iPSC lines were mutagenized with the alkylating agent ENU on a daily basis for 60 days. Cells were analyzed at D12 of hematopoietic differentiation for their phenotype, clonogenicity, and transcriptomic profile. Single-cell RNA-Seq analysis has been performed at three different time points during hematopoietic differentiation in ENU-treated and untreated cells.

Results: One of the CML-iPSCs, compared to its non-mutagenized counterpart, generated myeloid blasts after hematopoietic differentiation, exhibiting monoblastic patterns and expression of cMPO, CD45, CD34, CD33, and CD13. Single-cell transcriptomics revealed a delay of differentiation in the mutated condition as compared to the control with increased levels of *MSX1* (mesodermal marker) and a decrease in *CD45* and *CD41*. Bulk transcriptomics analyzed along with the GSE4170 GEO dataset reveal a significant overlap between ENU-treated cells and primary BC cells. Among overexpressed genes, *CD25* was identified, and its relevance was confirmed in a cohort of CML patients.

Conclusions: iPSCs are a valuable tool to model CML progression and to identify new targets. Here, we show the relevance of CD25 identified in the iPSC model as a marker of CML progression.

Keywords: CD25; CML modeling; blast crisis CML; iPSC; single-cell transcriptomics.

4. Article 4: Case report: Long-term voluntary Tyrosine Kinase Inhibitor (TKI) discontinuation in chronic myeloid leukemia (CML): Molecular evidence of an immune surveillance

Front Oncol. 2023 Mar 16;13:1117781.
doi: 10.3389/fonc.2023.1117781. eCollection 2023.

Case report: Long-term voluntary Tyrosine Kinase Inhibitor (TKI) discontinuation in chronic myeloid leukemia (CML): Molecular evidence of an immune surveillance

Jusuf Imeri[1], Christophe Desterke[1,2], **Paul Marcoux[1]**, Diana Chaker[1,3], Noufissa Oudrhiri[1,2,3,4], Xavier Fund[1,4], Jamila Faivre[4,5], Annelise Bennaceur-Griscelli [1,2,4,5], Ali G Turhan[1,2,4,5]

[1]INSERM Unité Mixte de Recherche (UMR)_S_1310, Université Paris Saclay, Villejuif, France.
[2]INGESTEM National IPSC Infrastructure, Villejuif, France.
[3]CITHERA, Center for iPSC Therapies, Evry, France.
[4]APHP Paris Saclay, Division of Hematology, Paris Saclay University Hospitals, Le Kremlin Bicêtre, and Villejuif, France.
[5]Inserm Unité Mixte de Recherche (UMR) 1193 Centre-Hepato Biliaire, Paul Brousse, Villejuif, France

PMID: 37007090 PMCID: PMC10062417 DOI: 10.3389/fonc.2023.1117781

Abstract

The classical natural history of chronic myeloid leukemia (CML) has been drastically modified by the introduction of tyrosine kinase inhibitor (TKI) therapies. TKI discontinuation is currently possible in patients in deep molecular responses, using strict recommendations of molecular follow-up due to risk of molecular relapse, especially during the first 6 months. We report here the case of a patient who voluntarily interrupted her TKI therapy. She remained in deep molecular remission (MR4) for 18 months followed by detection of a molecular relapse at +20 months. Despite this relapse, she declined therapy until the occurrence of the hematological relapse (+4 years and 10 months). Retrospective sequential transcriptome experiments and a single-cell transcriptome RNA-seq analysis were performed. They revealed a molecular network focusing on several genes involved in both activation and inhibition of NK-T cell activity. Interestingly, the single-cell transcriptome analysis showed the presence of cells expressing NKG7, a gene involved in granule exocytosis and highly involved in anti-tumor immunity. Single cells expressing as granzyme H, cathepsin-W, and granulysin were also identified. The study of this case suggests that CML was controlled for a long period of time, potentially *via* an immune surveillance phenomenon. The role of NKG7 expression in the occurrence of treatment-free remissions (TFR) should be evaluated in future studies.

Keywords: CML; NKG7; TFR; chronic myelogenous leukemia; natural killer cells.

5. Article 5: Molecular investigation of adequate sources of mesenchymal stem cells for cell therapy of COVID-19-associated organ failure

Stem Cells Transl Med. 2021 Apr;10(4):568-571.
doi: 10.1002/sctm.20-0189. Epub 2020 Nov 25.

Molecular investigation of adequate sources of mesenchymal stem cells for cell therapy of COVID-19-associated organ failure

Christophe Desterke[1,2], Frank Griscelli[1,2,3], Jusuf Imeri[1], **Paul Marcoux[1]**, Thomas Lemonnier[1], Theodoros Latsis[1,2], Ali G Turhan[1,2,4], Annelise Bennaceur-Griscelli[1,2,4]

[1]INSERM UMR-S 935 and University Paris Saclay, Villejuif, France.
[2]INGESTEM National IPSC Infrastructure, Villejuif, France.
[3]Gustave Roussy Institute, Villejuif and Faculty of Pharmacy, Paris Descartes University, Paris, France.
[4]APHP Paris Saclay Division of Hematology and University Paris Saclay Faculty of Medicine, Villejuif, France.

PMID: 33237619 PMCID: PMC7753753 DOI: 10.1002/sctm.20-0189

Abstract

The use of mesenchymal stem cells (MSC) derived from several sources has been suggested as a major anti-inflammation strategy during the recent outbreak of coronavirus-19 (COVID-19). As the virus enters the target cells through the receptor ACE2, it is important to determine if the MSC population transfused to patients could also be a target for the virus entry. We report here that ACE2 is highly expressed in adult bone marrow, adipose tissue, or umbilical cord-derived MSC. On the other hand, placenta-derived MSC express low levels of ACE2 but only in early passages of cultures. MSC derived from human embryonic stem cell or human induced pluripotent stem cells express also very low levels of ACE2. The transcriptome analysis of the MSCs with lowest expression of ACE2 in fetal-like MSCs is found to be associated in particularly with an anti-inflammatory signature. These results are of major interest for designing future clinical MSC-based stem cell therapies for severe COVID-19 infections.

Keywords: adult human bone marrow; embryonic stem cells; induced pluripotent stem cells; lymphocytes; mesenchymal stem cells.

REFERENCES

REFERENCES

Abu-Remaileh M, Gerson A, Farago M, Nathan G, Alkalay I, Zins Rousso S, Gur M, Fainsod A & Bergman Y (2010) Oct-3/4 regulates stem cell identity and cell fate decisions by modulating Wnt/β-catenin signalling. *EMBO J* 29, 3236–3248.

Alanis DM, Chang DR, Akiyama H, Krasnow MA & Chen J (2014) Two nested developmental waves demarcate a compartment boundary in the mouse lung. *Nat Commun* 5, 3923.

Alberg AJ, Brock MV, Ford JG, Samet JM & Spivack SD (2013) Epidemiology of Lung Cancer: Diagnosis and Management of Lung Cancer, 3rd ed: American College of Chest Physicians Evidence-Based Clinical Practice Guidelines. *CHEST* 143, e1S-e29S.

Amabile G, Welner RS, Nombela-Arrieta C, D'Alise AM, Di Ruscio A, Ebralidze AK, Kraytsberg Y, Ye M, Kocher O, Neuberg DS, Khrapko K, Silberstein LE & Tenen DG (2013) In vivo generation of transplantable human hematopoietic cells from induced pluripotent stem cells. *Blood* 121, 1255–1264.

Amit M, Carpenter MK, Inokuma MS, Chiu CP, Harris CP, Waknitz MA, Itskovitz-Eldor J & Thomson JA (2000a) Clonally derived human embryonic stem cell lines maintain pluripotency and proliferative potential for prolonged periods of culture. *Dev Biol* 227, 271–278.

Amit M, Carpenter MK, Inokuma MS, Chiu CP, Harris CP, Waknitz MA, Itskovitz-Eldor J & Thomson JA (2000b) Clonally derived human embryonic stem cell lines maintain pluripotency and proliferative potential for prolonged periods of culture. *Dev Biol* 227, 271–278.

Amit M, Shariki C, Margulets V & Itskovitz-Eldor J (2004) Feeder layer- and serum-free culture of human embryonic stem cells. *Biol Reprod* 70, 837–845.

Anders J, Kjar S & Ibáñez CF (2001) Molecular modeling of the extracellular domain of the RET receptor tyrosine kinase reveals multiple cadherin-like domains and a calcium-binding site. *J Biol Chem* 276, 35808–35817.

Anjos-Afonso F, Buettner F, Mian SA, Rhys H, Perez-Lloret J, Garcia-Albornoz M, Rastogi N, Ariza-McNaughton L & Bonnet D (2022) Single cell analyses identify a highly regenerative and homogenous human CD34+ hematopoietic stem cell population. *Nat Commun* 13, 2048.

Ara T, Tokoyoda K, Sugiyama T, Egawa T, Kawabata K & Nagasawa T (2003) Long-term hematopoietic stem cells require stromal cell-derived factor-1 for colonizing bone marrow during ontogeny. *Immunity* 19, 257–267.

Arai F, Hirao A, Ohmura M, Sato H, Matsuoka S, Takubo K, Ito K, Koh GY & Suda T (2004) Tie2/angiopoietin-1 signaling regulates hematopoietic stem cell quiescence in the bone marrow niche. *Cell* 118, 149–161.

Arai Y, Totoki Y, Takahashi H, Nakamura H, Hama N, Kohno T, Tsuta K, Yoshida A, Asamura H, Mutoh M, Hosoda F, Tsuda H & Shibata T (2013) Mouse Model for ROS1-Rearranged Lung Cancer. *PLOS ONE* 8, e56010.

Araki R, Uda M, Hoki Y, Sunayama M, Nakamura M, Ando S, Sugiura M, Ideno H, Shimada A, Nifuji A & Abe M (2013) Negligible immunogenicity of terminally differentiated cells derived from induced pluripotent or embryonic stem cells. *Nature* 494, 100–104.

Arcila ME, Chaft JE, Nafa K, Roy-Chowdhuri S, Lau C, Zaidinski M, Paik PK, Zakowski MF, Kris MG & Ladanyi M (2012) Prevalence, clinicopathologic associations, and molecular spectrum of ERBB2 (HER2) tyrosine kinase mutations in lung adenocarcinomas. *Clin Cancer Res* 18, 4910–4918.

Avigdor A, Goichberg P, Shivtiel S, Dar A, Peled A, Samira S, Kollet O, Hershkoviz R, Alon R, Hardan I, Ben-Hur H, Naor D, Nagler A & Lapidot T (2004) CD44 and hyaluronic acid cooperate with SDF-1 in the trafficking of human CD34+ stem/progenitor cells to bone marrow. *Blood* 103, 2981–2989.

Avior Y, Sagi I & Benvenisty N (2016) Pluripotent stem cells in disease modelling and drug discovery. *Nat Rev Mol Cell Biol* 17, 170–182.

Awad MM, Liu S, Rybkin II, Arbour KC, Dilly J, Zhu VW, Johnson ML, Heist RS, Patil T, Riely GJ, Jacobson JO, Yang X, Persky NS, Root DE, Lowder KE, Feng H, Zhang SS, Haigis KM, Hung YP, Sholl LM, Wolpin BM, Wiese J, Christiansen J, Lee J, Schrock AB, Lim LP, Garg K, Li M, Engstrom LD, Waters L, Lawson JD, Olson P, Lito P, Ou S-HI, Christensen JG, Jänne PA & Aguirre AJ (2021) Acquired Resistance to KRASG12C Inhibition in Cancer. *N Engl J Med* 384, 2382–2393.

Awad MM, Oxnard GR, Jackman DM, Savukoski DO, Hall D, Shivdasani P, Heng JC, Dahlberg SE, Jänne PA, Verma S, Christensen J, Hammerman PS & Sholl LM (2016) MET Exon 14 Mutations in Non-Small-Cell Lung Cancer Are Associated With Advanced Age and Stage-Dependent MET Genomic Amplification and c-Met Overexpression. *J Clin Oncol* 34, 721–730.

Bahcall M, Awad MM, Sholl LM, Wilson FH, Xu M, Wang S, Palakurthi S, Choi J, Ivanova EV, Leonardi GC, Ulrich BC, Paweletz CP, Kirschmeier PT, Watanabe M, Baba H, Nishino M, Nagy RJ, Lanman RB, Capelletti M, Chambers ES, Redig AJ, VanderLaan PA, Costa DB, Imamura Y & Jänne PA (2018) Amplification of Wild-type KRAS Imparts Resistance to Crizotinib in MET Exon 14 Mutant Non-Small Cell Lung Cancer. *Clin Cancer Res* 24, 5963–5976.

Bai T, Li J, Sinclair A, Imren S, Merriam F, Sun F, O'Kelly MB, Nourigat C, Jain P, Delrow JJ, Basom RS, Hung H-C, Zhang P, Li B, Heimfeld S, Jiang S & Delaney C (2019) Expansion of primitive human hematopoietic stem cells by culture in a zwitterionic hydrogel. *Nat Med* 25, 1566–1575.

Ballerini P, Struski S, Cresson C, Prade N, Toujani S, Deswarte C, Dobbelstein S, Petit A, Lapillonne H, Gautier E-F, Demur C, Lippert E, Pages P, Mansat-De Mas V, Donadieu J, Huguet F, Dastugue N, Broccardo C, Perot C & Delabesse E (2012) RET fusion genes are associated with chronic myelomonocytic leukemia and enhance monocytic differentiation. *Leukemia* 26, 2384–2389.

Baloh RH, Tansey MG, Lampe PA, Fahrner TJ, Enomoto H, Simburger KS, Leitner ML, Araki T, Johnson EM & Milbrandt J (1998) Artemin, a Novel Member of the GDNF Ligand Family, Supports Peripheral and Central Neurons and Signals through the GFRα3–RET Receptor Complex. *Neuron* 21, 1291–1302.

Ban H, Nishishita N, Fusaki N, Tabata T, Saeki K, Shikamura M, Takada N, Inoue M, Hasegawa M, Kawamata S & Nishikawa S-I (2011) Efficient generation of transgene-free human induced pluripotent stem cells (iPSCs) by temperature-sensitive Sendai virus vectors. *Proc Natl Acad Sci U S A* 108, 14234–14239.

Banan M (2020) Recent advances in CRISPR/Cas9-mediated knock-ins in mammalian cells. *Journal of Biotechnology* 308, 1–9.

Barkauskas CE, Cronce MJ, Rackley CR, Bowie EJ, Keene DR, Stripp BR, Randell SH, Noble PW & Hogan BLM (2013) Type 2 alveolar cells are stem cells in adult lung. *J Clin Invest* 123, 3025–3036.

Barrera-Rodríguez R & Fuentes JM (2015) Multidrug resistance characterization in multicellular tumour spheroids from two human lung cancer cell lines. *Cancer Cell Int* 15, 47.

Baum CM, Weissman IL, Tsukamoto AS, Buckle AM & Peault B (1992) Isolation of a candidate human hematopoietic stem-cell population. *Proc Natl Acad Sci U S A* 89, 2804–2808.

Baumheter S, Singer MS, Henzel W, Hemmerich S, Renz M, Rosen SD & Lasky LA (1993) Binding of L-selectin to the vascular sialomucin CD34. *Science* 262, 436–438.

Bazinet A & Popradi G (2019) A general practitioner's guide to hematopoietic stem-cell transplantation. *Curr Oncol* 26, 187–191.

Becker AJ, McCulloch EA & Till JE (1963) Cytological Demonstration of the Clonal Nature of Spleen Colonies Derived from Transplanted Mouse Marrow Cells. *Nature* 197, 452–454.

Becker KA, Ghule PN, Therrien JA, Lian JB, Stein JL, van Wijnen AJ & Stein GS (2006) Self-renewal of human embryonic stem cells is supported by a shortened G1 cell cycle phase. *J Cell Physiol* 209, 883–893.

Bellusci S, Henderson R, Winnier G, Oikawa T & Hogan BL (1996) Evidence from normal expression and targeted misexpression that bone morphogenetic protein (Bmp-4) plays a role in mouse embryonic lung morphogenesis. *Development* 122, 1693–1702.

Bennaceur-Griscelli A, Hadoux J, Féraud O, Opolon P, Divers D, Gobbo E, Schlumberger M, Griscelli F & Turhan AG (2017) Generation of an induced pluripotent stem cell line from a patient with hereditary multiple endocrine neoplasia 2B (MEN2B) syndrome with "highest risk" RET mutation. *Stem Cell Res* 23, 154–157.

Bergethon K, Shaw AT, Ou S-HI, Katayama R, Lovly CM, McDonald NT, Massion PP, Siwak-Tapp C, Gonzalez A, Fang R, Mark EJ, Batten JM, Chen H, Wilner KD, Kwak EL, Clark JW, Carbone DP, Ji H, Engelman JA, Mino-Kenudson M, Pao W & Iafrate AJ (2012) ROS1 rearrangements define a unique molecular class of lung cancers. *J Clin Oncol* 30, 863–870.

Besancenot R, Roos-Weil D, Tonetti C, Abdelouahab H, Lacout C, Pasquier F, Willekens C, Rameau P, Lecluse Y, Micol J-B, Constantinescu SN, Vainchenker W, Solary E & Giraudier S (2014) JAK2 and MPL protein levels determine TPO-induced megakaryocyte proliferation vs differentiation. *Blood* 124, 2104–2115.

Bhatia M, Bonnet D, Kapp U, Wang JC, Murdoch B & Dick JE (1997) Quantitative analysis reveals expansion of human hematopoietic repopulating cells after short-term ex vivo culture. *J Exp Med* 186, 619–624.

Bhatia M, Bonnet D, Murdoch B, Gan OI & Dick JE (1998) A newly discovered class of human hematopoietic cells with SCID-repopulating activity. *Nat Med* 4, 1038–1045.

Bhattacharya J & Westphalen K (2016) Macrophage-epithelial interactions in pulmonary alveoli. *Semin Immunopathol* 38, 461–469.

Blank U & Karlsson S (2015) TGF-β signaling in the control of hematopoietic stem cells. *Blood* 125, 3542–3550.

Boitano AE, Wang J, Romeo R, Bouchez LC, Parker AE, Sutton SE, Walker JR, Flaveny CA, Perdew GH, Denison MS, Schultz PG & Cooke MP (2010) Aryl hydrocarbon receptor antagonists promote the expansion of human hematopoietic stem cells. *Science* 329, 1345–1348.

Borrello MG, Alberti L, Arighi E, Bongarzone I, Battistini C, Bardelli A, Pasini B, Piutti C, Rizzetti MG, Mondellini P, Radice MT & Pierotti MA (1996) The full oncogenic activity of Ret/ptc2 depends on tyrosine 539, a docking site for phospholipase Cgamma. *Mol Cell Biol* 16, 2151–2163.

Bowles DW, Kessler ER & Jimeno A (2011) Multi-targeted tyrosine kinase inhibitors in clinical development: focus on XL-184 (cabozantinib). *Drugs Today (Barc)* 47, 857–868.

Bradley A, Evans M, Kaufman MH & Robertson E (1984) Formation of germ-line chimaeras from embryo-derived teratocarcinoma cell lines. *Nature* 309, 255–256.

Bresciani E, Carrington B, Yu K, Kim EM, Zhen T, Guzman VS, Broadbridge E, Bishop K, Kirby M, Harper U, Wincovitch S, Dell'Orso S, Sartorelli V, Sood R & Liu P (2021) Redundant mechanisms driven independently by RUNX1 and GATA2 for hematopoietic development. *Blood Adv* 5, 4949–4962.

Brons IGM, Smithers LE, Trotter MWB, Rugg-Gunn P, Sun B, Chuva de Sousa Lopes SM, Howlett SK, Clarkson A, Ahrlund-Richter L, Pedersen RA & Vallier L (2007) Derivation of pluripotent epiblast stem cells from mammalian embryos. *Nature* 448, 191–195.

Brooks A, Oostra B & Hofstra R (2005) Studying the genetics of Hirschsprung's disease: unraveling an oligogenic disorder. *Clinical Genetics* 67, 6–14.

Brosh R, Assia-Alroy Y, Molchadsky A, Bornstein C, Dekel E, Madar S, Shetzer Y, Rivlin N, Goldfinger N, Sarig R & Rotter V (2013) p53 Counteracts reprogramming by inhibiting mesenchymal-to-epithelial transition. *Cell Death Differ* 20, 312–320.

Broudy VC (1997) Stem cell factor and hematopoiesis. *Blood* 90, 1345–1364.

Buitenhuis M (2011) The role of PI3K/protein kinase B (PKB/c-akt) in migration and homing of hematopoietic stem and progenitor cells. *Curr Opin Hematol* 18, 226–230.

Burns CE, Traver D, Mayhall E, Shepard JL & Zon LI (2005) Hematopoietic stem cell fate is established by the Notch-Runx pathway. *Genes Dev* 19, 2331–2342.

Burri PH (1984) Fetal and postnatal development of the lung. *Annu Rev Physiol* 46, 617–628.

Buta C, David R, Dressel R, Emgård M, Fuchs C, Gross U, Healy L, Hescheler J, Kolar R, Martin U, Mikkers H, Müller F-J, Schneider RK, Seiler AEM, Spielmann H & Weitzer G (2013) Reconsidering pluripotency tests: Do we still need teratoma assays? *Stem Cell Research* 11, 552–562.

Butler JM, Nolan DJ, Vertes EL, Varnum-Finney B, Kobayashi H, Hooper AT, Seandel M, Shido K, White IA, Kobayashi M, Witte L, May C, Shawber C, Kimura Y, Kitajewski J, Rosenwaks Z, Bernstein ID & Rafii S (2010) Endothelial cells are essential for the self-renewal and repopulation of Notch-dependent hematopoietic stem cells. *Cell Stem Cell* 6, 251–264.

Byrne AT, Alférez DG, Amant F, Annibali D, Arribas J, Biankin AV, Bruna A, Budinská E, Caldas C, Chang DK, Clarke RB, Clevers H, Coukos G, Dangles-Marie V, Eckhardt SG, Gonzalez-Suarez E, Hermans E, Hidalgo M, Jarzabek MA, de Jong S, Jonkers J, Kemper K, Lanfrancone L, Mælandsmo GM, Marangoni E, Marine J-C, Medico E, Norum JH, Palmer HG, Peeper DS, Pelicci PG, Piris-Gimenez A, Roman-Roman S, Rueda OM, Seoane J, Serra V, Soucek L, Vanhecke D, Villanueva A, Vinolo E, Bertotti A & Trusolino L (2017) Interrogating open issues in cancer precision medicine with patient-derived xenografts. *Nat Rev Cancer* 17, 254–268.

Byrne SM & Church GM (2015) Crispr-mediated Gene Targeting of Human Induced Pluripotent Stem Cells. *Curr Protoc Stem Cell Biol* 35, 5A.8.1-5A.8.22.

Cacalano G, Fariñas I, Wang LC, Hagler K, Forgie A, Moore M, Armanini M, Phillips H, Ryan AM, Reichardt LF, Hynes M, Davies A & Rosenthal A (1998) GFRalpha1 is an essential receptor component for GDNF in the developing nervous system and kidney. *Neuron* 21, 53–62.

Cairoli R, Grillo G, Beghini A, Tedeschi A, Ripamonti CB, Larizza L & Morra E (2003) C-Kit point mutations in core binding factor leukemias: correlation with white blood cell count and the white blood cell index. *Leukemia* 17, 471–472.

Calvi LM & Link DC (2015) The hematopoietic stem cell niche in homeostasis and disease. *Blood* 126, 2443–2451.

Cancer Genome Atlas Research Network (2014) Comprehensive molecular profiling of lung adenocarcinoma. *Nature* 511, 543–550.

Cardoso WV & Lü J (2006) Regulation of early lung morphogenesis: questions, facts and controversies. *Development* 133, 1611–1624.

Carlomagno F, Guida T, Anaganti S, Vecchio G, Fusco A, Ryan AJ, Billaud M & Santoro M (2004) Disease associated mutations at valine 804 in the RET receptor tyrosine kinase confer resistance to selective kinase inhibitors. *Oncogene* 23, 6056–6063.

Carlson KM, Dou S, Chi D, Scavarda N, Toshima K, Jackson CE, Wells SA, Goodfellow PJ & Donis-Keller H (1994) Single missense mutation in the tyrosine kinase catalytic domain of the RET protooncogene is associated with multiple endocrine neoplasia type 2B. *Proc Natl Acad Sci U S A* 91, 1579–1583.

Carver-Moore K, Broxmeyer HE, Luoh SM, Cooper S, Peng J, Burstein SA, Moore MW & de Sauvage FJ (1996) Low levels of erythroid and myeloid progenitors in thrombopoietin-and c-mpl-deficient mice. *Blood* 88, 803–808.

Cau F, Pisu E, Gerosa C, Senes G, Ronchi F, Botta C, Felice ED, Uda F, Marinelli V, Faa G, Fanos V, Moretti C & Fanni D (2016) Interindividual variability in the expression of surfactant protein A and B in the human lung during development. *European Journal of Histochemistry* 60. Available at: https://www.ejh.it/index.php/ejh/article/view/2678 [Accessed August 8, 2023].

Chadwick K, Wang L, Li L, Menendez P, Murdoch B, Rouleau A & Bhatia M (2003) Cytokines and BMP-4 promote hematopoietic differentiation of human embryonic stem cells. *Blood* 102, 906–915.

Chagraoui J, Lehnertz B, Girard S, Spinella JF, Fares I, Tomellini E, Mayotte N, Corneau S, MacRae T, Simon L & Sauvageau G (2019) UM171 induces a homeostatic inflammatory-detoxification response supporting human HSC self-renewal. *PLoS One* 14, e0224900.

Challen GA, Boles NC, Chambers SM & Goodell MA (2010) Distinct hematopoietic stem cell subtypes are differentially regulated by TGF-beta1. *Cell Stem Cell* 6, 265–278.

Chapman HA, Li X, Alexander JP, Brumwell A, Lorizio W, Tan K, Sonnenberg A, Wei Y & Vu TH (2011) Integrin α6β4 identifies an adult distal lung epithelial population with regenerative potential in mice. *J Clin Invest* 121, 2855–2862.

Chen G, Gulbranson DR, Hou Z, Bolin JM, Ruotti V, Probasco MD, Smuga-Otto K, Howden SE, Diol NR, Propson NE, Wagner R, Lee GO, Antosiewicz-Bourget J, Teng JMC & Thomson JA (2011) Chemically defined conditions for human iPS cell derivation and culture. *Nat Methods* 8, 424–429.

Chen J-R, Tang Z-H, Zheng J, Shi H-S, Ding J, Qian X-D, Zhang C, Chen J-L, Wang C-C, Li L, Chen J-Z, Yin S-K, Shao J-Z, Huang T-S, Chen P, Guan M-X & Wang J-F (2016) Effects of genetic correction on the differentiation of hair cell-like cells from iPSCs with MYO15A mutation. *Cell Death Differ* 23, 1347–1357.

Chen MJ, Yokomizo T, Zeigler BM, Dzierzak E & Speck NA (2009) Runx1 is required for the endothelial to haematopoietic cell transition but not thereafter. *Nature* 457, 887–891.

Cheng T, Rodrigues N, Shen H, Yang Y, Dombkowski D, Sykes M & Scadden DT (2000) Hematopoietic stem cell quiescence maintained by p21cip1/waf1. *Science* 287, 1804–1808.

Choi K (2002) The hemangioblast: a common progenitor of hematopoietic and endothelial cells. *J Hematother Stem Cell Res* 11, 91–101.

Chow A, Lucas D, Hidalgo A, Méndez-Ferrer S, Hashimoto D, Scheiermann C, Battista M, Leboeuf M, Prophete C, van Rooijen N, Tanaka M, Merad M & Frenette PS (2011) Bone marrow CD169+ macrophages promote the retention of hematopoietic stem and progenitor cells in the mesenchymal stem cell niche. *J Exp Med* 208, 261–271.

Christensen JL, Wright DE, Wagers AJ & Weissman IL (2004) Circulation and Chemotaxis of Fetal Hematopoietic Stem Cells. *PLOS Biology* 2, e75.

Civin CI, Strauss LC, Brovall C, Fackler MJ, Schwartz JF & Shaper JH (1984) Antigenic analysis of hematopoiesis. III. A hematopoietic progenitor cell surface antigen defined by a monoclonal antibody raised against KG-1a cells. *J Immunol* 133, 157–165.

Cook MM, Futrega K, Osiecki M, Kabiri M, Kul B, Rice A, Atkinson K, Brooke G & Doran M (2012) Micromarrows—Three-Dimensional Coculture of Hematopoietic Stem Cells and Mesenchymal Stromal Cells. *Tissue Engineering Part C: Methods* 18, 319–328.

Cosma MP, Cardone M, Carlomagno F & Colantuoni V (1998) Mutations in the extracellular domain cause RET loss of function by a dominant negative mechanism. *Mol Cell Biol* 18, 3321–3329.

Coulpier M, Anders J & Ibáñez CF (2002) Coordinated activation of autophosphorylation sites in the RET receptor tyrosine kinase: importance of tyrosine 1062 for GDNF mediated neuronal differentiation and survival. *J Biol Chem* 277, 1991–1999.

Cowan AJ, Green DJ, Kwok M, Lee S, Coffey DG, Holmberg LA, Tuazon S, Gopal AK & Libby EN (2022) Diagnosis and Management of Multiple Myeloma: A Review. *JAMA* 327, 464–477.

Cowan CA, Atienza J, Melton DA & Eggan K (2005) Nuclear Reprogramming of Somatic Cells After Fusion with Human Embryonic Stem Cells. *Science* 309, 1369–1373.

Crapo JD, Barry BE, Gehr P, Bachofen M & Weibel ER (1982) Cell number and cell characteristics of the normal human lung. *Am Rev Respir Dis* 126, 332–337.

Crisan M & Dzierzak E (2016) The many faces of hematopoietic stem cell heterogeneity. *Development* 143, 4571–4581.

Cutz J-C, Guan J, Bayani J, Yoshimoto M, Xue H, Sutcliffe M, English J, Flint J, LeRiche J, Yee J, Squire JA, Gout PW, Lam S & Wang Y-Z (2006) Establishment in severe combined immunodeficiency mice of subrenal capsule xenografts and transplantable tumor lines from a variety of primary human lung cancers: potential models for studying tumor progression-related changes. *Clin Cancer Res* 12, 4043–4054.

Cyganek L, Tiburcy M, Sekeres K, Gerstenberg K, Bohnenberger H, Lenz C, Henze S, Stauske M, Salinas G, Zimmermann W-H, Hasenfuss G & Guan K (2018) Deep phenotyping of human induced pluripotent stem cell-derived atrial and ventricular cardiomyocytes. *JCI Insight* 3, e99941, 99941.

Dabir S, Babakoohi S, Kluge A, Morrow JJ, Kresak A, Yang M, MacPherson D, Wildey G & Dowlati A (2014) RET mutation and expression in small-cell lung cancer. *J Thorac Oncol* 9, 1316–1323.

Dagogo-Jack I, Stevens SE, Lin JJ, Nagy R, Ferris L, Shaw AT & Gainor JF (2018) Emergence of a RET V804M Gatekeeper Mutation During Treatment With Vandetanib in RET-Rearranged NSCLC. *Journal of Thoracic Oncology* 13, e226–e227.

Dahéron L, Opitz SL, Zaehres H, Lensch MW, Andrews PW, Itskovitz-Eldor J & Daley GQ (2004) LIF/STAT3 signaling fails to maintain self-renewal of human embryonic stem cells. *Stem Cells* 22, 770–778.

DAI L, LU C, YU X, DAI L-J & ZHOU JX (2015) Construction of orthotopic xenograft mouse models for human pancreatic cancer. *Exp Ther Med* 10, 1033–1038.

D'Amour KA, Agulnick AD, Eliazer S, Kelly OG, Kroon E & Baetge EE (2005) Efficient differentiation of human embryonic stem cells to definitive endoderm. *Nat Biotechnol* 23, 1534–1541.

Danopoulos S, Alonso I, Thornton ME, Grubbs BH, Bellusci S, Warburton D & Al Alam D (2018) Human lung branching morphogenesis is orchestrated by the spatiotemporal distribution of ACTA2, SOX2, and SOX9. *American Journal of Physiology-Lung Cellular and Molecular Physiology* 314, L144–L149.

Danto SI, Shannon JM, Borok Z, Zabski SM & Crandall ED (1995) Reversible transdifferentiation of alveolar epithelial cells. *Am J Respir Cell Mol Biol* 12, 497–502.

Defossez G, Le Guyader-Peyrou S, Grosclaude P, Colonna M, Dantony E, & Uhry Z (2019) *Estimations nationales de l'incidence et de la mortalité par cancer en France métropolitaine entre 1990 et 2018. Synthèse., 2019. 20 p*, Saint-Maurice : Santé publique France.

Dela Cruz CS, Tanoue LT & Matthay RA (2011) Lung Cancer: Epidemiology, Etiology, and Prevention. *Clin Chest Med* 32, 10.1016/j.ccm.2011.09.001.

deMello DE & Reid LM (2000) Embryonic and early fetal development of human lung vasculature and its functional implications. *Pediatr Dev Pathol* 3, 439–449.

Demirci S, Leonard A & Tisdale JF (2020) Hematopoietic stem cells from pluripotent stem cells: Clinical potential, challenges, and future perspectives. *STEM CELLS Translational Medicine* 9, 1549–1557.

Desai TJ, Brownfield DG & Krasnow MA (2014a) Alveolar progenitor and stem cells in lung development, renewal and cancer. *Nature* 507, 190–194.

Desai TJ, Brownfield DG & Krasnow MA (2014b) Alveolar progenitor and stem cells in lung development, renewal and cancer. *Nature* 507, 190–194.

Devriendt K, Vanhole C, Matthijs G & de Zegher F (1998) Deletion of thyroid transcription factor-1 gene in an infant with neonatal thyroid dysfunction and respiratory failure. *N Engl J Med* 338, 1317–1318.

Di Liello R, Ciaramella V, Barra G, Venditti M, Della Corte CM, Papaccio F, Sparano F, Viscardi G, Iacovino ML, Minucci S, Fasano M, Ciardiello F & Morgillo F (2019) Ex vivo lung cancer spheroids resemble treatment response of a patient with NSCLC to chemotherapy and immunotherapy: case report and translational study. *ESMO Open* 4, e000536.

DiGiusto D, Chen S, Combs J, Webb S, Namikawa R, Tsukamoto A, Chen BP & Galy AH (1994) Human fetal bone marrow early progenitors for T, B, and myeloid cells are found exclusively in the population expressing high levels of CD34. *Blood* 84, 421–432.

Ding L, Saunders TL, Enikolopov G & Morrison SJ (2012) Endothelial and perivascular cells maintain haematopoietic stem cells. *Nature* 481, 457–462.

Dobbs LG, Gonzalez RF, Allen L & Froh DK (1999) HTI56, an Integral Membrane Protein Specific to Human Alveolar Type I Cells. *J Histochem Cytochem.* 47, 129–137.

Doss MX & Sachinidis A (2019) Current Challenges of iPSC-Based Disease Modeling and Therapeutic Implications. *Cells* 8, 403.

Dost AFM, Moye AL, Vedaie M, Tran LM, Fung E, Heinze D, Villacorta-Martin C, Huang J, Hekman R, Kwan JH, Blum BC, Louie SM, Rowbotham SP, de Aja JS, Piper ME, Bhetariya PJ, Bronson RT, Emili A, Mostoslavsky G, Fishbein GA, Wallace WD, Krysan K, Dubinett SM, Yanagawa J, Kotton DN & Kim CF (2020) Organoids model transcriptional hallmarks of oncogenic KRAS activation in lung epithelial progenitor cells. *Cell Stem Cell* 27, 663-678.e8.

Doulatov S, Vo LT, Chou SS, Kim PG, Arora N, Li H, Hadland BK, Bernstein ID, Collins JJ, Zon LI & Daley GQ (2013) Induction of multipotential hematopoietic progenitors from human pluripotent stem cells via respecification of lineage-restricted precursors. *Cell Stem Cell* 13, 459–470.

Drilon A, Oxnard GR, Tan DSW, Loong HHF, Johnson M, Gainor J, McCoach CE, Gautschi O, Besse B, Cho BC, Peled N, Weiss J, Kim Y-J, Ohe Y, Nishio M, Park K, Patel J, Seto T, Sakamoto T, Rosen E, Shah MH, Barlesi F, Cassier PA, Bazhenova L, De Braud F, Garralda E, Velcheti V, Satouchi M, Ohashi K, Pennell NA, Reckamp KL, Dy GK, Wolf J, Solomon B, Falchook G, Ebata K, Nguyen M, Nair B, Zhu EY, Yang L, Huang X, Olek E, Rothenberg SM, Goto K & Subbiah V (2020) Efficacy of Selpercatinib in RET Fusion-Positive Non-Small-Cell Lung Cancer. *N Engl J Med* 383, 813–824.

Drilon A, Rekhtman N, Arcila M, Wang L, Ni A, Albano M, Van Voorthuysen M, Somwar R, Smith RS, Montecalvo J, Plodkowski A, Ginsberg MS, Riely GJ, Rudin CM, Ladanyi M & Kris MG (2016) Cabozantinib in patients with advanced RET-rearranged non-small-cell lung cancer: an open-label, single-centre, phase 2, single-arm trial. *The Lancet Oncology* 17, 1653–1660.

Drilon A, Rogers E, Zhai D, Deng W, Zhang X, Lee D, Ung J, Whitten J, Zhang H, Liu J, Hu T, Zhuang H, Lu Y, Huang Z, Graber A, Zimmerman Z, Xin R, Cui JJ & Subbiah V (2019) 506P - TPX-0046 is a novel and potent RET/SRC inhibitor for RET-driven cancers. *Annals of Oncology* 30, v190–v191.

Du WW, Yang W, Liu E, Yang Z, Dhaliwal P & Yang BB (2016) Foxo3 circular RNA retards cell cycle progression via forming ternary complexes with p21 and CDK2. *Nucleic Acids Res* 44, 2846–2858.

Du X, Shao Y, Qin H-F, Tai Y-H & Gao H-J (2018) ALK-rearrangement in non-small-cell lung cancer (NSCLC). *Thorac Cancer* 9, 423–430.

Duncan AW, Rattis FM, DiMascio LN, Congdon KL, Pazianos G, Zhao C, Yoon K, Cook JM, Willert K, Gaiano N & Reya T (2005) Integration of Notch and Wnt signaling in hematopoietic stem cell maintenance. *Nat Immunol* 6, 314–322.

DuPage M, Dooley AL & Jacks T (2009) Conditional mouse lung cancer models using adenoviral or lentiviral delivery of Cre recombinase. *Nat Protoc* 4, 1064–1072.

Durbec P, Marcos-Gutierrez CV, Kilkenny C, Grigoriou M, Wartiowaara K, Suvanto P, Smith D, Ponder B, Costantini F, Saarma M, Sariola H & Pachnis V (1996) GDNF signalling through the Ret receptor tyrosine kinase. *Nature* 381, 789–793.

Dye BR, Dedhia PH, Miller AJ, Nagy MS, White ES, Shea LD & Spence JR (2016) A bioengineered niche promotes in vivo engraftment and maturation of pluripotent stem cell derived human lung organoids J. Rossant, ed. *eLife* 5, e19732.

Dye BR, Hill DR, Ferguson MA, Tsai Y-H, Nagy MS, Dyal R, Wells JM, Mayhew CN, Nattiv R, Klein OD, White ES, Deutsch GH & Spence JR (2015) In vitro generation of human pluripotent stem cell derived lung organoids J. Rossant, ed. *eLife* 4, e05098.

Ebert AD, Yu J, Rose FF, Mattis VB, Lorson CL, Thomson JA & Svendsen CN (2009) Induced pluripotent stem cells from a spinal muscular atrophy patient. *Nature* 457, 277–280.

Edery P, Lyonnet S, Mulligan LM, Pelet A, Dow E, Abel L, Holder S, Nihoul-Fékété C, Ponder BA & Munnich A (1994) Mutations of the RET proto-oncogene in Hirschsprung's disease. *Nature* 367, 378–380.

Encinas M, Crowder RJ, Milbrandt J & Johnson EM (2004) Tyrosine 981, a Novel Ret Autophosphorylation Site, Binds c-Src to Mediate Neuronal Survival *. *Journal of Biological Chemistry* 279, 18262–18269.

Eng C, Smith DP, Mulligan LM, Nagai MA, Healey CS, Ponder MA, Gardner E, Scheumann GF, Jackson CE & Tunnacliffe A (1994) Point mutation within the tyrosine kinase domain of the RET proto-oncogene in multiple endocrine neoplasia type 2B and related sporadic tumours. *Hum Mol Genet* 3, 237–241.

Engelman JA, Zejnullahu K, Mitsudomi T, Song Y, Hyland C, Park JO, Lindeman N, Gale C-M, Zhao X, Christensen J, Kosaka T, Holmes AJ, Rogers AM, Cappuzzo F, Mok T, Lee C, Johnson BE, Cantley LC & Jänne PA (2007a) MET amplification leads to gefitinib resistance in lung cancer by activating ERBB3 signaling. *Science* 316, 1039–1043.

Engelman JA, Zejnullahu K, Mitsudomi T, Song Y, Hyland C, Park JO, Lindeman N, Gale C-M, Zhao X, Christensen J, Kosaka T, Holmes AJ, Rogers AM, Cappuzzo F, Mok T, Lee C, Johnson BE, Cantley LC & Jänne PA (2007b) MET amplification leads to gefitinib resistance in lung cancer by activating ERBB3 signaling. *Science* 316, 1039–1043.

Evans MJ & Kaufman MH (1981) Establishment in culture of pluripotential cells from mouse embryos. *Nature* 292, 154–156.

Fares I, Calvanese V & Mikkola HKA (2022) Decoding Human Hematopoietic Stem Cell Self-Renewal. *Curr Stem Cell Rep* 8, 93–106.

Fares I, Chagraoui J, Gareau Y, Gingras S, Ruel R, Mayotte N, Csaszar E, Knapp DJHF, Miller P, Ngom M, Imren S, Roy D-C, Watts KL, Kiem H-P, Herrington R, Iscove NN, Humphries RK, Eaves CJ, Cohen S, Marinier A, Zandstra PW & Sauvageau G (2014) Cord blood expansion. Pyrimidoindole derivatives are agonists of human hematopoietic stem cell self-renewal. *Science* 345, 1509–1512.

Federation AJ, Bradner JE & Meissner A (2014) The use of small molecules in somatic-cell reprogramming. *Trends Cell Biol* 24, 179–187.

Ferkowicz MJ, Starr M, Xie X, Li W, Johnson SA, Shelley WC, Morrison PR & Yoder MC (2003) CD41 expression defines the onset of primitive and definitive hematopoiesis in the murine embryo. *Development* 130, 4393–4403.

Ferrara R, Auger N, Auclin E & Besse B (2018) Clinical and Translational Implications of RET Rearrangements in Non–Small Cell Lung Cancer. *Journal of Thoracic Oncology* 13, 27–45.

Fialkow PJ, Gartler SM & Yoshida A (1967) Clonal origin of chronic myelocytic leukemia in man. *Proc Natl Acad Sci U S A* 58, 1468–1471.

Fidler-Benaoudia MM, Torre LA, Bray F, Ferlay J & Jemal A (2020) Lung cancer incidence in young women vs. young men: A systematic analysis in 40 countries. *Int J Cancer* 147, 811–819.

Fleming HE, Janzen V, Lo Celso C, Guo J, Leahy KM, Kronenberg HM & Scadden DT (2008) Wnt signaling in the niche enforces hematopoietic stem cell quiescence and is necessary to preserve self-renewal in vivo. *Cell Stem Cell* 2, 274–283.

Fonseca-Pereira D, Arroz-Madeira S, Rodrigues-Campos M, Barbosa IAM, Domingues RG, Bento T, Almeida ARM, Ribeiro H, Potocnik AJ, Enomoto H & Veiga-Fernandes H (2014) The neurotrophic factor receptor RET drives haematopoietic stem cell survival and function. *Nature* 514, 98–101.

Forristal CE, Wright KL, Hanley NA, Oreffo ROC & Houghton FD (2010) Hypoxia inducible factors regulate pluripotency and proliferation in human embryonic stem cells cultured at reduced oxygen tensions. *Reproduction* 139, 85–97.

Frame JM, McGrath KE & Palis J (2013) Erythro-myeloid progenitors: “definitive” hematopoiesis in the conceptus prior to the emergence of hematopoietic stem cells. *Blood Cells Mol Dis* 51, 220–225.

Freire PR & Conneely OM (2018) NR4A1 and NR4A3 restrict HSC proliferation via reciprocal regulation of C/EBPα and inflammatory signaling. *Blood* 131, 1081–1093.

Fujino N, Kubo H, Ota C, Suzuki T, Suzuki S, Yamada M, Takahashi T, He M, Suzuki T, Kondo T & Yamaya M (2012) A Novel Method for Isolating Individual Cellular Components from the Adult Human Distal Lung. *Am J Respir Cell Mol Biol* 46, 422–430.

Fusaki N, Ban H, Nishiyama A, Saeki K & Hasegawa M (2009) Efficient induction of transgene-free human pluripotent stem cells using a vector based on Sendai virus, an RNA virus that does not integrate into the host genome. *Proc Jpn Acad Ser B Phys Biol Sci* 85, 348–362.

Gainor JF, Curigliano G, Kim D-W, Lee DH, Besse B, Baik CS, Doebele RC, Cassier PA, Lopes G, Tan DSW, Garralda E, Paz-Ares LG, Cho BC, Gadgeel SM, Thomas M, Liu SV, Taylor MH, Mansfield AS, Zhu VW, Clifford C, Zhang H, Palmer M, Green J, Turner CD & Subbiah V (2021) Pralsetinib for RET fusion-positive non-small-cell lung cancer (ARROW): a multi-cohort, open-label, phase 1/2 study. *The Lancet Oncology* 22, 959–969.

Gandhi J, Zhang J, Xie Y, Soh J, Shigematsu H, Zhang W, Yamamoto H, Peyton M, Girard L, Lockwood WW, Lam WL, Varella-Garcia M, Minna JD & Gazdar AF (2009) Alterations in Genes of the EGFR Signaling Pathway and Their Relationship to EGFR Tyrosine Kinase Inhibitor Sensitivity in Lung Cancer Cell Lines. *PLOS ONE* 4, e4576.

Gao J, Yan X-L, Li R, Liu Y, He W, Sun S, Zhang Y, Liu B, Xiong J & Mao N (2010) Characterization of OP9 as authentic mesenchymal stem cell line. *J Genet Genomics* 37, 475–482.

Gao X, Bali AS, Randell SH & Hogan BLM (2015) GRHL2 coordinates regeneration of a polarized mucociliary epithelium from basal stem cells. *Journal of Cell Biology* 211, 669–682.

Gari M, Goodeve A, Wilson G, Winship P, Langabeer S, Linch D, Vandenberghe E, Peake I & Reilly J (1999) c-kit proto-oncogene exon 8 in-frame deletion plus insertion mutations in acute myeloid leukaemia. *British Journal of Haematology* 105, 894–900.

Garreta E, Kamm RD, Chuva de Sousa Lopes SM, Lancaster MA, Weiss R, Trepat X, Hyun I & Montserrat N (2021) Rethinking organoid technology through bioengineering. *Nat Mater* 20, 145–155.

Gattei V, Celetti A, Cerrato A, Degan M, De Iuliis A, Rossi FM, Chiappetta G, Consales C, Improta S, Zagonel V, Aldinucci D, Agosti V, Santoro M, Vecchio G, Pinto A & Grieco M (1997) Expression of the RET receptor tyrosine kinase and GDNFR-alpha in normal and leukemic human hematopoietic cells and stromal cells of the bone marrow microenvironment. *Blood* 89, 2925–2937.

Gazdar AF, Bunn PA & Minna JD (2017) Small-cell lung cancer: what we know, what we need to know and the path forward. *Nat Rev Cancer* 17, 725–737.

Gazdar AF, Gao B & Minna JD (2010) Lung cancer cell lines: Useless artifacts or invaluable tools for medical science? *Lung Cancer* 68, 309–318.

Geneste O, Bidaud C, De Vita G, Hofstra RM, Tartare-Deckert S, Buys CH, Lenoir GM, Santoro M & Billaud M (1999) Two distinct mutations of the RET receptor causing Hirschsprung's disease impair the binding of signalling effectors to a multifunctional docking site. *Hum Mol Genet* 8, 1989–1999.

Gerber H-P, Malik AK, Solar GP, Sherman D, Liang XH, Meng G, Hong K, Marsters JC & Ferrara N (2002) VEGF regulates haematopoietic stem cell survival by an internal autocrine loop mechanism. *Nature* 417, 954–958.

Giandomenico SL, Sutcliffe M & Lancaster MA (2021) Generation and long-term culture of advanced cerebral organoids for studying later stages of neural development. *Nat Protoc* 16, 579–602.

Goldman DC, Bailey AS, Pfaffle DL, Al Masri A, Christian JL & Fleming WH (2009) BMP4 regulates the hematopoietic stem cell niche. *Blood* 114, 4393–4401.

González F, Boué S & Belmonte JCI (2011) Methods for making induced pluripotent stem cells: reprogramming à la carte. *Nat Rev Genet* 12, 231–242.

Gonzalez RF, Allen L, Gonzales L, Ballard PL & Dobbs LG (2010) HTII-280, a biomarker specific to the apical plasma membrane of human lung alveolar type II cells. *J Histochem Cytochem* 58, 891–901.

Gotoh S, Ito I, Nagasaki T, Yamamoto Y, Konishi S, Korogi Y, Matsumoto H, Muro S, Hirai T, Funato M, Mae S-I, Toyoda T, Sato-Otsubo A, Ogawa S, Osafune K & Mishima M (2014) Generation of Alveolar Epithelial Spheroids via Isolated Progenitor Cells from Human Pluripotent Stem Cells. *Stem Cell Reports* 3, 394–403.

Green MD, Chen A, Nostro M-C, d'Souza SL, Schaniel C, Lemischka IR, Gouon-Evans V, Keller G & Snoeck H-W (2011) Generation of anterior foregut endoderm from human embryonic and induced pluripotent stem cells. *Nat Biotechnol* 29, 267–272.

Greenbaum A, Hsu Y-MS, Day RB, Schuettpelz LG, Christopher MJ, Borgerding JN, Nagasawa T & Link DC (2013) CXCL12 in early mesenchymal progenitors is required for haematopoietic stem-cell maintenance. *Nature* 495, 227–230.

Grey W, Chauhan R, Piganeau M, Huerga Encabo H, Garcia-Albornoz M, McDonald NQ & Bonnet D (2020) Activation of the receptor tyrosine kinase RET improves long-term hematopoietic stem cell outgrowth and potency. *Blood* 136, 2535–2547.

Grieco M, Santoro M, Berlingieri MT, Melillo RM, Donghi R, Bongarzone I, Pierotti MA, Della Porta G, Fusco A & Vecchio G (1990) PTC is a novel rearranged form of the ret proto-oncogene and is frequently detected in vivo in human thyroid papillary carcinomas. *Cell* 60, 557–563.

Grigorova M, Lyman RC, Caldas C & Edwards PAW (2005) Chromosome abnormalities in 10 lung cancer cell lines of the NCI-H series analyzed with spectral karyotyping. *Cancer Genetics and Cytogenetics* 162, 1–9.

Guan J, Wang G, Wang J, Zhang Z, Fu Y, Cheng L, Meng G, Lyu Y, Zhu J, Li Y, Wang Y, Liuyang S, Liu B, Yang Z, He H, Zhong X, Chen Q, Zhang X, Sun S, Lai W, Shi Y, Liu L, Wang L, Li C, Lu S & Deng H (2022) Chemical reprogramming of human somatic cells to pluripotent stem cells. *Nature* 605, 325–331.

Guha P, Morgan JW, Mostoslavsky G, Rodrigues NP & Boyd AS (2013) Lack of immune response to differentiated cells derived from syngeneic induced pluripotent stem cells. *Cell Stem Cell* 12, 407–412.

Gujral TS, Singh VK, Jia Z & Mulligan LM (2006) Molecular mechanisms of RET receptor-mediated oncogenesis in multiple endocrine neoplasia 2B. *Cancer Res* 66, 10741–10749.

Guo R, Schreyer M, Chang JC, Rothenberg SM, Henry D, Cotzia P, Kris MG, Rekhtman N, Young RJ, Hyman DM & Drilon A (2019) Response to Selective RET Inhibition With LOXO-292 in a Patient With RET Fusion-Positive Lung Cancer With Leptomeningeal Metastases. *JCO Precis Oncol* 3, PO.19.00021.

Gurdon JB (2006) From nuclear transfer to nuclear reprogramming: the reversal of cell differentiation. *Annu Rev Cell Dev Biol* 22, 1–22.

Gurdon JB (1962) The developmental capacity of nuclei taken from intestinal epithelium cells of feeding tadpoles. *J Embryol Exp Morphol* 10, 622–640.

Gutman JA, Riddell SR, McGoldrick S & Delaney C (2010) Double unit cord blood transplantation. *Chimerism* 1, 21–22.

Haar JL & Ackerman GA (1971) A phase and electron microscopic study of vasculogenesis and erythropoiesis in the yolk sac of the mouse. *Anat Rec* 170, 199–223.

Haas S, Hansson J, Klimmeck D, Loeffler D, Velten L, Uckelmann H, Wurzer S, Prendergast ÁM, Schnell A, Hexel K, Santarella-Mellwig R, Blaszkiewicz S, Kuck A, Geiger H, Milsom MD, Steinmetz LM, Schroeder T, Trumpp A, Krijgsveld J & Essers MAG (2015) Inflammation-Induced Emergency Megakaryopoiesis Driven by Hematopoietic Stem Cell-like Megakaryocyte Progenitors. *Cell Stem Cell* 17, 422–434.

Hackett NR, Shaykhiev R, Walters MS, Wang R, Zwick RK, Ferris B, Witover B, Salit J & Crystal RG (2011) The Human Airway Epithelial Basal Cell Transcriptome. *PLOS ONE* 6, e18378.

Hadoux J, Desterke C, Féraud O, Guibert M, De Rose RF, Opolon P, Divers D, Gobbo E, Griscelli F, Schlumberger M, Bennaceur-Griscelli A & Turhan AG (2018) Transcriptional landscape of a RETC634Y-mutated iPSC and its CRISPR-corrected isogenic control reveals the putative role of EGR1 transcriptional program in the development of multiple endocrine neoplasia type 2A-associated cancers. *Stem Cell Res* 26, 8–16.

Hadoux J, Féraud O, Griscelli F, Opolon P, Divers D, Gobbo E, Schlumberger M, Bennaceur-Griscelli A & Turhan AG (2016) Generation of an induced pluripotent stem cell line from a patient with hereditary multiple endocrine neoplasia 2A (MEN2A) syndrome with RET mutation. *Stem Cell Res* 17, 154–157.

Hamatani K, Eguchi H, Ito R, Mukai M, Takahashi K, Taga M, Imai K, Cologne J, Soda M, Arihiro K, Fujihara M, Abe K, Hayashi T, Nakashima M, Sekine I, Yasui W, Hayashi Y & Nakachi K (2008) RET/PTC rearrangements preferentially occurred in papillary thyroid cancer among atomic bomb survivors exposed to high radiation dose. *Cancer Res* 68, 7176–7182.

Hamidi S & Sheng G (2018) Epithelial-mesenchymal transition in haematopoietic stem cell development and homeostasis. *The Journal of Biochemistry* 164, 265–275.

Hanna J, Cheng AW, Saha K, Kim J, Lengner CJ, Soldner F, Cassady JP, Muffat J, Carey BW & Jaenisch R (2010) Human embryonic stem cells with biological and epigenetic characteristics similar to those of mouse ESCs. *Proc Natl Acad Sci U S A* 107, 9222–9227.

Hanna J, Saha K, Pando B, van Zon J, Lengner CJ, Creyghton MP, van Oudenaarden A & Jaenisch R (2009) Direct cell reprogramming is a stochastic process amenable to acceleration. *Nature* 462, 595–601.

Hanna J, Wernig M, Markoulaki S, Sun C-W, Meissner A, Cassady JP, Beard C, Brambrink T, Wu L-C, Townes TM & Jaenisch R (2007) Treatment of sickle cell anemia mouse model with iPS cells generated from autologous skin. *Science* 318, 1920–1923.

Hao Q, Shah A, Thiemann F, Smogorzewska E & Crooks G (1995) A functional comparison of CD34 + CD38- cells in cord blood and bone marrow. *Blood* 86, 3745–3753.

Hawkins F, Kramer P, Jacob A, Driver I, Thomas DC, McCauley KB, Skvir N, Crane AM, Kurmann AA, Hollenberg AN, Nguyen S, Wong BG, Khalil AS, Huang SXL, Guttentag S, Rock JR, Shannon JM, Davis BR & Kotton DN (2017) Prospective isolation of NKX2-1–expressing human lung progenitors derived from pluripotent stem cells. *J Clin Invest* 127, 2277–2294.

Hayashi T, Odintsov I, Smith RS, Ishizawa K, Liu AJW, Delasos L, Kurzatkowski C, Tai H, Gladstone E, Vojnic M, Kohsaka S, Suzawa K, Liu Z, Kunte S, Mattar MS, Khodos I, Davare MA, Drilon A, Cheng E, Stanchina E de, Ladanyi M & Somwar R (2020) RET inhibition in novel patient-derived models of RET-fusion positive lung adenocarcinoma reveals a role for MYC upregulation. *Dis Model Mech* 14, dmm047779, dmm.047779.

Hecht SS (1999) Tobacco smoke carcinogens and lung cancer. *J Natl Cancer Inst* 91, 1194–1210.

Hérault A, Binnewies M, Leong S, Calero-Nieto FJ, Zhang SY, Kang Y-A, Wang X, Pietras EM, Chu SH, Barry-Holson K, Armstrong S, Göttgens B & Passegué E (2017) Myeloid progenitor cluster formation drives emergency and leukaemic myelopoiesis. *Nature* 544, 53–58.

Hess LM, Han Y, Zhu YE, Bhandari NR & Sireci A (2021) Characteristics and outcomes of patients with RET-fusion positive non-small lung cancer in real-world practice in the United States. *BMC Cancer* 21, 28.

Hida T, Velcheti V, Reckamp KL, Nokihara H, Sachdev P, Kubota T, Nakada T, Dutcus CE, Ren M & Tamura T (2019) A phase 2 study of lenvatinib in patients with RET fusion-positive lung adenocarcinoma. *Lung Cancer* 138, 124–130.

Hockemeyer D & Jaenisch R (2016) Induced pluripotent stem cells meet genome editing. *Cell Stem Cell* 18, 573–586.

Hoeffel G & Ginhoux F (2015) Ontogeny of Tissue-Resident Macrophages. *Front Immunol* 6, 486.

Hoffman RM (2015) Patient-derived orthotopic xenografts: better mimic of metastasis than subcutaneous xenografts. *Nat Rev Cancer* 15, 451–452.

Hogan BLM, Barkauskas CE, Chapman HA, Epstein JA, Jain R, Hsia CCW, Niklason L, Calle E, Le A, Randell SH, Rock J, Snitow M, Krummel M, Stripp BR, Vu T, White ES, Whitsett JA & Morrisey EE (2014) Repair and Regeneration of the Respiratory System: Complexity, Plasticity, and Mechanisms of Lung Stem Cell Function. *Cell Stem Cell* 15, 123–138.

Höpfl G, Gassmann M & Desbaillets I (2004) Differentiating embryonic stem cells into embryoid bodies. *Methods Mol Biol* 254, 79–98.

Hovatta O, Mikkola M, Gertow K, Strömberg A-M, Inzunza J, Hreinsson J, Rozell B, Blennow E, Andäng M & Ahrlund-Richter L (2003) A culture system using human foreskin fibroblasts as feeder cells allows production of human embryonic stem cells. *Hum Reprod* 18, 1404–1409.

Howington JA, Blum MG, Chang AC, Balekian AA & Murthy SC (2013) Treatment of stage I and II non-small cell lung cancer: Diagnosis and management of lung cancer, 3rd ed: American College of Chest Physicians evidence-based clinical practice guidelines. *Chest* 143, e278S-e313S.

Howlader N, Forjaz G, Mooradian MJ, Meza R, Kong CY, Cronin KA, Mariotto AB, Lowy DR & Feuer EJ (2020) The Effect of Advances in Lung-Cancer Treatment on Population Mortality. *N Engl J Med* 383, 640–649.

Hrustanovic G, Olivas V, Pazarentzos E, Tulpule A, Asthana S, Blakely CM, Okimoto RA, Lin L, Neel DS, Sabnis A, Flanagan J, Chan E, Varella-Garcia M, Aisner DL, Vaishnavi A, Ou S-HI, Collisson EA, Ichihara E, Mack PC, Lovly CM, Karachaliou N, Rosell R, Riess JW, Doebele RC & Bivona TG (2015) RAS-MAPK dependence underlies a rational polytherapy strategy in EML4-ALK-positive lung cancer. *Nat Med* 21, 1038–1047.

Hrvatin S, O'Donnell CW, Deng F, Millman JR, Pagliuca FW, DiIorio P, Rezania A, Gifford DK & Melton DA (2014) Differentiated human stem cells resemble fetal, not adult, β cells. *Proc Natl Acad Sci U S A* 111, 3038–3043.

Huang Q, Schneeberger VE, Luetteke N, Jin C, Afzal R, Budzevich MM, Makanji RJ, Martinez GV, Shen T, Zhao L, Fung K-M, Haura EB, Coppola D & Wu J (2016) Preclinical Modeling of KIF5B–RET Fusion Lung Adenocarcinoma. *Molecular Cancer Therapeutics* 15, 2521–2529.

Huang S & Terstappen LW (1994) Lymphoid and myeloid differentiation of single human CD34+, HLA-DR+, CD38- hematopoietic stem cells. *Blood* 83, 1515–1526.

Huang Z, Su W, Lu T, Wang Y, Dong Y, Qin Y, Liu D, Sun L & Jiao W (2020) First-Line Immune-Checkpoint Inhibitors in Non-Small Cell Lung Cancer: Current Landscape and Future Progress. *Front Pharmacol* 11, 578091.

Hwang JW, Desterke C, Féraud O, Richard S, Ferlicot S, Verkarre V, Patard JJ, Loisel-Duwattez J, Foudi A, Griscelli F, Bennaceur-Griscelli A & Turhan AG (2019) iPSC-Derived Embryoid Bodies as Models of c-Met-Mutated Hereditary Papillary Renal Cell Carcinoma. *Int J Mol Sci* 20, 4867.

Hwang JW, Loisel-Duwattez J, Desterke C, Latsis T, Pagliaro S, Griscelli F, Bennaceur-Griscelli A & Turhan AG (2020) A novel neuronal organoid model mimicking glioblastoma (GBM) features from induced pluripotent stem cells (iPSC). *Biochim Biophys Acta Gen Subj* 1864, 129540.

Ikeda K, Clark JC, Shaw-White JR, Stahlman MT, Boutell CJ & Whitsett JA (1995) Gene Structure and Expression of Human Thyroid Transcription Factor-1 in Respiratory Epithelial Cells (∗). *Journal of Biological Chemistry* 270, 8108–8114.

International Stem Cell Initiative, Adewumi O, Aflatoonian B, Ahrlund-Richter L, Amit M, Andrews PW, Beighton G, Bello PA, Benvenisty N, Berry LS, Bevan S, Blum B, Brooking J, Chen KG, Choo ABH, Churchill GA, Corbel M, Damjanov I, Draper JS, Dvorak P, Emanuelsson K, Fleck RA, Ford A, Gertow K, Gertsenstein M, Gokhale PJ, Hamilton RS, Hampl A, Healy LE, Hovatta O, Hyllner J, Imreh MP, Itskovitz-Eldor J, Jackson J, Johnson JL, Jones M, Kee K, King BL, Knowles BB, Lako M, Lebrin F, Mallon BS, Manning D, Mayshar Y, McKay RDG, Michalska AE, Mikkola M, Mileikovsky M, Minger SL, Moore HD, Mummery CL, Nagy A, Nakatsuji N, O'Brien CM, Oh SKW, Olsson C, Otonkoski T, Park K-Y, Passier R, Patel H, Patel M, Pedersen R, Pera MF, Piekarczyk MS, Pera RAR, Reubinoff BE, Robins AJ, Rossant J, Rugg-Gunn P, Schulz TC, Semb H, Sherrer ES, Siemen H, Stacey GN, Stojkovic M, Suemori H, Szatkiewicz J, Turetsky T, Tuuri T, van den Brink S, Vintersten K, Vuoristo S, Ward D, Weaver TA, Young LA & Zhang W (2007) Characterization of human embryonic stem cell lines by the International Stem Cell Initiative. *Nat Biotechnol* 25, 803–816.

Iscove NN & Nawa K (1997) Hematopoietic stem cells expand during serial transplantation in vivo without apparent exhaustion. *Curr Biol* 7, 805–808.

Ivanovs A, Rybtsov S, Anderson RA, Turner ML & Medvinsky A (2014) Identification of the Niche and Phenotype of the First Human Hematopoietic Stem Cells. *Stem Cell Reports* 2, 449–456.

Iwashita T, Asai N, Murakami H, Matsuyama M & Takahashi M (1996) Identification of tyrosine residues that are essential for transforming activity of the ret proto-oncogene with MEN2A or MEN2B mutation. *Oncogene* 12, 481–487.

Iwashita T, Murakami H, Asai N & Takahashi M (1996) Mechanism of ret dysfunction by Hirschsprung mutations affecting its extracellular domain. *Hum Mol Genet* 5, 1577–1580.

Jacków J, Guo Z, Hansen C, Abaci HE, Doucet YS, Shin JU, Hayashi R, DeLorenzo D, Kabata Y, Shinkuma S, Salas-Alanis JC & Christiano AM (2019) CRISPR/Cas9-based targeted genome editing for correction of recessive dystrophic epidermolysis bullosa using iPS cells. *Proceedings of the National Academy of Sciences* 116, 26846–26852.

Jackson EL, Willis N, Mercer K, Bronson RT, Crowley D, Montoya R, Jacks T & Tuveson DA (2001) Analysis of lung tumor initiation and progression using conditional expression of oncogenic K-ras. *Genes Dev.* 15, 3243–3248.

Jain S, Naughton CK, Yang M, Strickland A, Vij K, Encinas M, Golden J, Gupta A, Heuckeroth R, Johnson EM & Milbrandt J (2004) Mice expressing a dominant-negative Ret mutation phenocopy human Hirschsprung disease and delineate a direct role of Ret in spermatogenesis. *Development* 131, 5503–5513.

Jasim S, Ying AK, Waguespack SG, Rich TA, Grubbs EG, Jimenez C, Hu MI, Cote G & Habra MA (2011) Multiple endocrine neoplasia type 2B with a RET proto-oncogene A883F mutation displays a more indolent form of medullary thyroid carcinoma compared with a RET M918T mutation. *Thyroid* 21, 189–192.

Jemal A, Miller KD, Ma J, Siegel RL, Fedewa SA, Islami F, Devesa SS & Thun MJ (2018) Higher Lung Cancer Incidence in Young Women Than Young Men in the United States. *N Engl J Med* 378, 1999–2009.

Jha P (2009) Avoidable global cancer deaths and total deaths from smoking. *Nat Rev Cancer* 9, 655–664.

Ji H, Li D, Chen L, Shimamura T, Kobayashi S, McNamara K, Mahmood U, Mitchell A, Sun Y, Al-Hashem R, Chirieac LR, Padera R, Bronson RT, Kim W, Jänne PA, Shapiro GI, Tenen D, Johnson BE, Weissleder R, Sharpless NE & Wong K-K (2006) The impact of human EGFR kinase domain mutations on lung tumorigenesis and in vivo sensitivity to EGFR-targeted therapies. *Cancer Cell* 9, 485–495.

Johnson JZ & Hockemeyer D (2015) Human stem cell-based disease modeling: prospects and challenges. *Curr Opin Cell Biol* 37, 84–90.

Jordan EJ, Kim HR, Arcila ME, Barron D, Chakravarty D, Gao J, Chang MT, Ni A, Kundra R, Jonsson P, Jayakumaran G, Gao SP, Johnsen HC, Hanrahan AJ, Zehir A, Rekhtman N, Ginsberg MS, Li BT, Yu HA, Paik PK, Drilon A, Hellmann MD, Reales DN, Benayed R, Rusch VW, Kris MG, Chaft JE, Baselga J, Taylor BS, Schultz N, Rudin CM, Hyman DM, Berger MF, Solit DB, Ladanyi M & Riely GJ (2017) Prospective Comprehensive Molecular Characterization of Lung Adenocarcinomas for Efficient Patient Matching to Approved and Emerging Therapies. *Cancer Discov* 7, 596–609.

Juntilla MM, Patil VD, Calamito M, Joshi RP, Birnbaum MJ & Koretzky GA (2010) AKT1 and AKT2 maintain hematopoietic stem cell function by regulating reactive oxygen species. *Blood* 115, 4030–4038.

Kanakry CG, Fuchs EJ & Luznik L (2016) Modern approaches to HLA-haploidentical blood or marrow transplantation. *Nat Rev Clin Oncol* 13, 132.

Kato S, Subbiah V, Marchlik E, Elkin SK, Carter JL & Kurzrock R (2017) RET Aberrations in Diverse Cancers: Next-Generation Sequencing of 4,871 Patients. *Clin Cancer Res* 23, 1988–1997.

Kaufman DS, Hanson ET, Lewis RL, Auerbach R & Thomson JA (2001) Hematopoietic colony-forming cells derived from human embryonic stem cells. *Proc Natl Acad Sci U S A* 98, 10716–10721.

Kaushansky K (2006) Hematopoietic growth factors, signaling and the chronic myeloproliferative disorders. *Cytokine Growth Factor Rev* 17, 423–430.

Kawamoto Y, Takeda K, Okuno Y, Yamakawa Y, Ito Y, Taguchi R, Kato M, Suzuki H, Takahashi M & Nakashima I (2004) Identification of RET autophosphorylation sites by mass spectrometry. *J Biol Chem* 279, 14213–14224.

Kemper K, Krijgsman O, Cornelissen-Steijger P, Shahrabi A, Weeber F, Song J-Y, Kuilman T, Vis DJ, Wessels LF, Voest EE, Schumacher TN, Blank CU, Adams DJ, Haanen JB & Peeper DS (2015) Intra- and inter-tumor heterogeneity in a vemurafenib-resistant melanoma patient and derived xenografts. *EMBO Mol Med* 7, 1104–1118.

Kennedy M, D'Souza SL, Lynch-Kattman M, Schwantz S & Keller G (2007) Development of the hemangioblast defines the onset of hematopoiesis in human ES cell differentiation cultures. *Blood* 109, 2679–2687.

Kho AT, Chhabra D, Sharma S, Qiu W, Carey VJ, Gaedigk R, Vyhlidal CA, Leeder JS, Tantisira KG & Weiss ST (2016) Age, Sexual Dimorphism, and Disease Associations in the Developing Human Fetal Lung Transcriptome. *Am J Respir Cell Mol Biol* 54, 814–821.

Khoor A, Gray ME, Singh G & Stahlman MT (1996) Ontogeny of Clara cell-specific protein and its mRNA: their association with neuroepithelial bodies in human fetal lung and in bronchopulmonary dysplasia. *J Histochem Cytochem.* 44, 1429–1438.

Khoor A, Stahlman MT, Gray ME & Whitsett JA (1994) Temporal-spatial distribution of SP-B and SP-C proteins and mRNAs in developing respiratory epithelium of human lung. *J Histochem Cytochem.* 42, 1187–1199.

Kilpinen H, Goncalves A, Leha A, Afzal V, Alasoo K, Ashford S, Bala S, Bensaddek D, Casale FP, Culley OJ, Danecek P, Faulconbridge A, Harrison PW, Kathuria A, McCarthy D, McCarthy SA, Meleckyte R, Memari Y, Moens N, Soares F, Mann A, Streeter I, Agu CA, Alderton A, Nelson R, Harper S, Patel M, White A, Patel SR, Clarke L, Halai R, Kirton CM, Kolb-Kokocinski A, Beales P, Birney E, Danovi D, Lamond AI, Ouwehand WH, Vallier L, Watt FM, Durbin R, Stegle O & Gaffney DJ (2017) Common genetic variation drives molecular heterogeneity in human iPSCs. *Nature* 546, 370–375.

Kim M, Mun H, Sung CO, Cho EJ, Jeon H-J, Chun S-M, Jung DJ, Shin TH, Jeong GS, Kim DK, Choi EK, Jeong S-Y, Taylor AM, Jain S, Meyerson M & Jang SJ (2019) Patient-derived lung cancer organoids as in vitro cancer models for therapeutic screening. *Nat Commun* 10, 3991.

Kim PG, Albacker CE, Lu Y, Jang I, Lim Y, Heffner GC, Arora N, Bowman TV, Lin MI, Lensch MW, De Los Angeles A, Zon LI, Loewer S & Daley GQ (2013) Signaling axis involving Hedgehog, Notch, and Scl promotes the embryonic endothelial-to-hematopoietic transition. *Proceedings of the National Academy of Sciences* 110, E141–E150.

Kimura ET, Nikiforova MN, Zhu Z, Knauf JA, Nikiforov YE & Fagin JA (2003) High prevalence of BRAF mutations in thyroid cancer: genetic evidence for constitutive activation of the RET/PTC-RAS-BRAF signaling pathway in papillary thyroid carcinoma. *Cancer Res* 63, 1454–1457.

Kingsley PD, Malik J, Fantauzzo KA & Palis J (2004) Yolk sac–derived primitive erythroblasts enucleate during mammalian embryogenesis. *Blood* 104, 19–25.

Kitaoka H, Burri PH & Weibel ER (1996) Development of the human fetal airway tree: Analysis of the numerical density of airway endtips. *The Anatomical Record* 244, 207–213.

Kjaer S & Ibáñez CF (2003) Intrinsic susceptibility to misfolding of a hot-spot for Hirschsprung disease mutations in the ectodomain of RET. *Hum Mol Genet* 12, 2133–2144.

Knowles PP, Murray-Rust J, Kjær S, Scott RP, Hanrahan S, Santoro M, Ibáñez CF & McDonald NQ (2006) Structure and Chemical Inhibition of the RET Tyrosine Kinase Domain *. *Journal of Biological Chemistry* 281, 33577–33587.

Kobari L, Yates F, Oudrhiri N, Francina A, Kiger L, Mazurier C, Rouzbeh S, El-Nemer W, Hebert N, Giarratana M-C, François S, Chapel A, Lapillonne H, Luton D, Bennaceur-Griscelli A & Douay L (2012) Human induced pluripotent stem cells can reach complete terminal maturation: in vivo and in vitro evidence in the erythropoietic differentiation model. *Haematologica* 97, 1795–1803.

Kohno T, Ichikawa H, Totoki Y, Yasuda K, Hiramoto M, Nammo T, Sakamoto H, Tsuta K, Furuta K, Shimada Y, Iwakawa R, Ogiwara H, Oike T, Enari M, Schetter AJ, Okayama H, Haugen A, Skaug V, Chiku S, Yamanaka I, Arai Y, Watanabe S, Sekine I, Ogawa S, Harris CC, Tsuda H, Yoshida T, Yokota J & Shibata T (2012) KIF5B-RET fusions in lung adenocarcinoma. *Nat Med* 18, 375–377.

Konishi S, Gotoh S, Tateishi K, Yamamoto Y, Korogi Y, Nagasaki T, Matsumoto H, Muro S, Hirai T, Ito I, Tsukita S & Mishima M (2016) Directed Induction of Functional Multi-ciliated Cells in Proximal Airway Epithelial Spheroids from Human Pluripotent Stem Cells. *Stem Cell Reports* 6, 18–25.

Kool H, Mous D, Tibboel D, de Klein A & Rottier RJ (2014) Pulmonary vascular development goes awry in congenital lung abnormalities. *Birth Defects Research Part C: Embryo Today: Reviews* 102, 343–358.

Kosaka T, Yatabe Y, Endoh H, Kuwano H, Takahashi T & Mitsudomi T (2004) Mutations of the Epidermal Growth Factor Receptor Gene in Lung Cancer: Biological and Clinical Implications. *Cancer Research* 64, 8919–8923.

Kotzbauer PT, Lampe PA, Heuckeroth RO, Golden JP, Creedon DJ, Johnson Jr EM & Milbrandt J (1996) Neurturin, a relative of glial-cell-line-derived neurotrophic factor. *Nature* 384, 467–470.

Kouvaraki MA, Shapiro SE, Perrier ND, Cote GJ, Gagel RF, Hoff AO, Sherman SI, Lee JE & Evans DB (2005) RET proto-oncogene: a review and update of genotype-phenotype correlations in hereditary medullary thyroid cancer and associated endocrine tumors. *Thyroid* 15, 531–544.

Kramer ER, Aron L, Ramakers GMJ, Seitz S, Zhuang X, Beyer K, Smidt MP & Klein R (2007) Absence of Ret signaling in mice causes progressive and late degeneration of the nigrostriatal system. *PLoS Biol* 5, e39.

Ku C-J, Hosoya T, Maillard I & Engel JD (2012) GATA-3 regulates hematopoietic stem cell maintenance and cell-cycle entry. *Blood* 119, 2242–2251.

Kubota H, Avarbock MR & Brinster RL (2004) Growth factors essential for self-renewal and expansion of mouse spermatogonial stem cells. *Proc Natl Acad Sci U S A* 101, 16489–16494.

Kung P, Goldstein G, Reinherz EL & Schlossman SF (1979) Monoclonal antibodies defining distinctive human T cell surface antigens. *Science* 206, 347–349.

Kurzrock R, Sherman SI, Ball DW, Forastiere AA, Cohen RB, Mehra R, Pfister DG, Cohen EEW, Janisch L, Nauling F, Hong DS, Ng CS, Ye L, Gagel RF, Frye J, Müller T, Ratain MJ & Salgia R (2011) Activity of XL184 (Cabozantinib), an Oral Tyrosine Kinase Inhibitor, in Patients With Medullary Thyroid Cancer. *J Clin Oncol* 29, 2660–2666.

Kwak Y, Kim S-I, Park C-K, Paek SH, Lee S-T & Park S-H (2015) C-MET overexpression and amplification in gliomas. *Int J Clin Exp Pathol* 8, 14932–14938.

Lake JI & Heuckeroth RO (2013) Enteric nervous system development: migration, differentiation, and disease. *Am J Physiol Gastrointest Liver Physiol* 305, G1-24.

Lamm N, Ben-David U, Golan-Lev T, Storchová Z, Benvenisty N & Kerem B (2016) Genomic Instability in Human Pluripotent Stem Cells Arises from Replicative Stress and Chromosome Condensation Defects. *Cell Stem Cell* 18, 253–261.

Lampreia FP, Carmelo JG & Anjos-Afonso F (2017) Notch Signaling in the Regulation of Hematopoietic Stem Cell. *Curr Stem Cell Rep* 3, 202–209.

Lancaster MA, Renner M, Martin C-A, Wenzel D, Bicknell LS, Hurles ME, Homfray T, Penninger JM, Jackson AP & Knoblich JA (2013) Cerebral organoids model human brain development and microcephaly. *Nature* 501, 373–379.

Larbi A, Gombert J-M, Auvray C, l'Homme B, Magniez A, Féraud O, Coulombel L, Chapel A, Mitjavila-Garcia MT, Turhan AG, Haddad R & Bennaceur-Griscelli A (2012) The HOXB4 homeoprotein promotes the ex vivo enrichment of functional human embryonic stem cell-derived NK cells. *PLoS One* 7, e39514.

Laresgoiti U, Nikolić MZ, Rao C, Brady JL, Richardson RV, Batchen EJ, Chapman KE & Rawlins EL (2016) Lung epithelial tip progenitors integrate glucocorticoid- and STAT3-mediated signals to control progeny fate. *Development* 143, 3686–3699.

Laurenti E & Göttgens B (2018) From haematopoietic stem cells to complex differentiation landscapes. *Nature* 553, 418–426.

Lazzaro D, Price M, de Felice M & Di Lauro R (1991) The transcription factor TTF-1 is expressed at the onset of thyroid and lung morphogenesis and in restricted regions of the foetal brain. *Development* 113, 1093–1104.

Le Rolle A-F, Klempner SJ, Garrett CR, Seery T, Sanford EM, Balasubramanian S, Ross JS, Stephens PJ, Miller VA, Ali SM & Chiu VK (2015) Identification and characterization of RET fusions in advanced colorectal cancer. *Oncotarget* 6, 28929–28937.

Lee D-F, Su J, Kim HS, Chang B, Papatsenko D, Zhao R, Yuan Y, Gingold J, Xia W, Darr H, Mirzayans R, Hung M-C, Schaniel C & Lemischka IR (2015) Modeling Familial Cancer with Induced Pluripotent Stem Cells. *Cell* 161, 240–254.

Lee M-R, Shin J-Y, Kim M-Y, Kim J-O, Jung CK & Kang J (2023) FOXA2 and STAT5A regulate oncogenic activity of KIF5B-RET fusion. *Am J Cancer Res* 13, 638–653.

Lee S-H, Lee J-K, Ahn M-J, Kim D-W, Sun J-M, Keam B, Kim TM, Heo DS, Ahn JS, Choi Y-L, Min H-S, Jeon YK & Park K (2017) Vandetanib in pretreated patients with advanced non-small cell lung cancer-harboring RET rearrangement: a phase II clinical trial. *Annals of Oncology* 28, 292–297.

Lee-Thedieck C & Spatz JP (2014) Biophysical regulation of hematopoietic stem cells. *Biomater Sci* 2, 1548–1561.

Leibel SL, McVicar RN, Winquist AM, Niles WD & Snyder EY (2020) Generation of Complete Multi−Cell Type Lung Organoids From Human Embryonic and Patient-Specific Induced Pluripotent Stem Cells for Infectious Disease Modeling and Therapeutics Validation. *Curr Protoc Stem Cell Biol* 54, e118.

Leisten I, Kramann R, Ventura Ferreira MS, Bovi M, Neuss S, Ziegler P, Wagner W, Knüchel R & Schneider RK (2012) 3D co-culture of hematopoietic stem and progenitor cells and mesenchymal stem cells in collagen scaffolds as a model of the hematopoietic niche. *Biomaterials* 33, 1736–1747.

Levinson S & Cagan RL (2016) Drosophila Cancer Models Identify Functional Differences between Ret Fusions. *Cell Reports* 16, 3052–3061.

Lewis DR, Check DP, Caporaso NE, Travis WD & Devesa SS (2014) US lung cancer trends by histologic type. *Cancer* 120, 2883–2892.

Li D, Liu J, Yang X, Zhou C, Guo J, Wu C, Qin Y, Guo L, He J, Yu S, Liu H, Wang X, Wu F, Kuang J, Hutchins AP, Chen J & Pei D (2017) Chromatin Accessibility Dynamics during iPSC Reprogramming. *Cell Stem Cell* 21, 819-833.e6.

Li HL, Fujimoto N, Sasakawa N, Shirai S, Ohkame T, Sakuma T, Tanaka M, Amano N, Watanabe A, Sakurai H, Yamamoto T, Yamanaka S & Hotta A (2015) Precise correction of the dystrophin gene in duchenne muscular dystrophy patient induced pluripotent stem cells by TALEN and CRISPR-Cas9. *Stem Cell Reports* 4, 143–154.

Li J, Shang G, Chen Y-J, Brautigam CA, Liou J, Zhang X & Bai X (2019) Cryo-EM analyses reveal the common mechanism and diversification in the activation of RET by different ligands M. Lemmon, C. Wolberger, D. J. Leahy, & A. Whitty, eds. *eLife* 8, e47650.

Li R, Liang J, Ni S, Zhou T, Qing X, Li H, He W, Chen J, Li F, Zhuang Q, Qin B, Xu J, Li W, Yang J, Gan Y, Qin D, Feng S, Song H, Yang D, Zhang B, Zeng L, Lai L, Esteban MA & Pei D (2010) A mesenchymal-to-epithelial transition initiates and is required for the nuclear reprogramming of mouse fibroblasts. *Cell Stem Cell* 7, 51–63.

Li S, Liu S, Deng J, Akbay EA, Hai J, Ambrogio C, Zhang L, Zhou F, Jenkins RW, Adeegbe DO, Gao P, Wang X, Paweletz CP, Herter-Sprie GS, Chen T, Gutiérrez-Quiceno L, Zhang Y, Merlino AA, Quinn MM, Zeng Y, Yu X, Liu Y, Fan L, Aguirre AJ, Barbie DA, Yi X & Wong K-K (2018) Assessing Therapeutic Efficacy of MEK Inhibition in a KRASG12C-Driven Mouse Model of Lung Cancer. *Clinical Cancer Research* 24, 4854–4864.

Li X-F, Zhou Y-W, Cai P-F, Fu W-C, Wang J-H, Chen J-Y & Yang Q-N (2019) CRISPR/Cas9 facilitates genomic editing for large-scale functional studies in pluripotent stem cell cultures. *Hum Genet* 138, 1217–1225.

Li X-L, Xue Y, Yang Y-J, Zhang C-X, Wang Y, Duan Y-Y, Meng Y-N & Fu J (2015) Hematopoietic stem cells: cancer involvement and myeloid leukemia. *Eur Rev Med Pharmacol Sci* 19, 1829–1836.

Lichtinger M, Ingram R, Hannah R, Müller D, Clarke D, Assi SA, Lie-A-Ling M, Noailles L, Vijayabaskar MS, Wu M, Tenen DG, Westhead DR, Kouskoff V, Lacaud G, Göttgens B & Bonifer C (2012) RUNX1 reshapes the epigenetic landscape at the onset of haematopoiesis. *EMBO J* 31, 4318–4333.

Lim W, Ridge CA, Nicholson AG & Mirsadraee S (2018) The 8th lung cancer TNM classification and clinical staging system: review of the changes and clinical implications. *Quant Imaging Med Surg* 8, 709–718.

Lim WF, Inoue-Yokoo T, Tan KS, Lai MI & Sugiyama D (2013) Hematopoietic cell differentiation from embryonic and induced pluripotent stem cells. *Stem Cell Res Ther* 4, 71.

Lim ZR, Vassilev S, Leong YW, Hang JW, Rénia L, Malleret B & Oh SK-W (2021) Industrially Compatible Transfusable iPSC-Derived RBCs: Progress, Challenges and Prospective Solutions. *International Journal of Molecular Sciences* 22, 9808.

Lin C, Wang S, Xie W, Zheng R, Gan Y & Chang J (2016) Apatinib inhibits cellular invasion and migration by fusion kinase KIF5B-RET via suppressing RET/Src signaling pathway. *Oncotarget* 7, 59236–59244.

Lin JJ, Kennedy E, Sequist LV, Brastianos PK, Goodwin KE, Stevens S, Wanat AC, Stober LL, Digumarthy SR, Engelman JA, Shaw AT & Gainor JF (2016) Clinical Activity of Alectinib in Advanced RET-Rearranged Non–Small Cell Lung Cancer. *Journal of Thoracic Oncology* 11, 2027–2032.

Lin JJ, Liu SV, McCoach CE, Zhu VW, Tan AC, Yoda S, Peterson J, Do A, Prutisto-Chang K, Dagogo-Jack I, Sequist LV, Wirth LJ, Lennerz JK, Hata AN, Mino-Kenudson M, Nardi V, Ou S-HI, Tan DS-W & Gainor JF (2020) Mechanisms of resistance to selective RET tyrosine kinase inhibitors in RET fusion-positive non-small-cell lung cancer. *Annals of Oncology* 31, 1725–1733.

Linnekin D (1999) Early signaling pathways activated by c-Kit in hematopoietic cells p. *The International Journal of Biochemistry*.

Liu F, Poursine-Laurent J, Wu HY & Link DC (1997) Interleukin-6 and the Granulocyte Colony-Stimulating Factor Receptor Are Major Independent Regulators of Granulopoiesis In Vivo But Are Not Required for Lineage Commitment or Terminal Differentiation. *Blood* 90, 2583–2590.

Liu X, Driskell RR & Engelhardt JF (2004) Airway Glandular Development and Stem Cells. In *Current Topics in Developmental Biology*. Academic Press, pp.33–56. Available at: https://www.sciencedirect.com/science/article/pii/S0070215304640038 [Accessed August 7, 2023].

Liu X, Li C, Zheng K, Zhao X, Xu X, Yang A, Yi M, Tao H, Xie B, Qiu M & Yang J (2020) Chromosomal aberration arises during somatic reprogramming to pluripotent stem cells. *Cell Division* 15, 12.

Liu X, Vega QC, Decker RA, Pandey A, Worby CA & Dixon JE (1996) Oncogenic RET Receptors Display Different Autophosphorylation Sites and Substrate Binding Specificities (∗). *Journal of Biological Chemistry* 271, 5309–5312.

Liuyang S, Wang G, Wang Y, He H, Lyu Y, Cheng L, Yang Z, Guan J, Fu Y, Zhu J, Zhong X, Sun S, Li C, Wang J & Deng H (2023) Highly efficient and rapid generation of human pluripotent stem cells by chemical reprogramming. *Cell Stem Cell* 30, 450-459.e9.

Look DC, Walter MJ, Williamson MR, Pang L, You Y, Sreshta JN, Johnson JE, Zander DS & Brody SL (2001) Effects of Paramyxoviral Infection on Airway Epithelial Cell Foxj1 Expression, Ciliogenesis, and Mucociliary Function. *The American Journal of Pathology* 159, 2055–2069.

Lu P, Weaver VM & Werb Z (2012) The extracellular matrix: a dynamic niche in cancer progression. *J Cell Biol* 196, 395–406.

Lu Z, Hong CC, Kong G, Assumpção ALFV, Ong IM, Bresnick EH, Zhang J & Pan X (2018) Polycomb Group Protein YY1 Is an Essential Regulator of Hematopoietic Stem Cell Quiescence. *Cell Rep* 22, 1545–1559.

Ludwig TE, Bergendahl V, Levenstein ME, Yu J, Probasco MD & Thomson JA (2006) Feeder-independent culture of human embryonic stem cells. *Nat Methods* 3, 637–646.

Luo J, Emanuele MJ, Li D, Creighton CJ, Schlabach MR, Westbrook TF, Wong K-K & Elledge SJ (2009) A Genome-wide RNAi Screen Identifies Multiple Synthetic Lethal Interactions with the Ras Oncogene. *Cell* 137, 835–848.

Lynch TJ, Bell DW, Sordella R, Gurubhagavatula S, Okimoto RA, Brannigan BW, Harris PL, Haserlat SM, Supko JG, Haluska FG, Louis DN, Christiani DC, Settleman J & Haber DA (2004) Activating Mutations in the Epidermal Growth Factor Receptor Underlying Responsiveness of Non–Small-Cell Lung Cancer to Gefitinib. *New England Journal of Medicine* 350, 2129–2139.

Ma F, Ebihara Y, Umeda K, Sakai H, Hanada S, Zhang H, Zaike Y, Tsuchida E, Nakahata T, Nakauchi H & Tsuji K (2008) Generation of functional erythrocytes from human embryonic stem cell-derived definitive hematopoiesis. *Proceedings of the National Academy of Sciences* 105, 13087–13092.

Ma Q, Jones D, Borghesani PR, Segal RA, Nagasawa T, Kishimoto T, Bronson RT & Springer TA (1998) Impaired B-lymphopoiesis, myelopoiesis, and derailed cerebellar neuron migration in CXCR4- and SDF-1-deficient mice. *Proceedings of the National Academy of Sciences* 95, 9448–9453.

Maherali N, Sridharan R, Xie W, Utikal J, Eminli S, Arnold K, Stadtfeld M, Yachechko R, Tchieu J, Jaenisch R, Plath K & Hochedlinger K (2007) Directly reprogrammed fibroblasts show global epigenetic remodeling and widespread tissue contribution. *Cell Stem Cell* 1, 55–70.

Majeti R, Park CY & Weissman IL (2007) Identification of a hierarchy of multipotent hematopoietic progenitors in human cord blood. *Cell Stem Cell* 1, 635–645.

Marchetti A, Martella C, Felicioni L, Barassi F, Salvatore S, Chella A, Camplese PP, Iarussi T, Mucilli F, Mezzetti A, Cuccurullo F, Sacco R & Buttitta F (2005) EGFR Mutations in Non–Small-Cell Lung Cancer: Analysis of a Large Series of Cases and Development of a Rapid and Sensitive Method for Diagnostic Screening With Potential Implications on Pharmacologic Treatment. *JCO* 23, 857–865.

Marcoux P, Hwang JW, Desterke C, Imeri J, Bennaceur-Griscelli A & Turhan AG (2023) Modeling RET-Rearranged Non-Small Cell Lung Cancer (NSCLC): Generation of Lung Progenitor Cells (LPCs) from Patient-Derived Induced Pluripotent Stem Cells (iPSCs). *Cells* 12, 2847.

Marcoux P, Imeri J, Desterke C, Latsis T, Chaker D, Hugues P, Griscelli AB & Turhan AG (2023) Impact of the overexpression of the tyrosine kinase receptor (RET) in the hematopoietic potential of induced pluripotent stem cells (iPSCs). *Cytotherapy*. Available at: https://www.sciencedirect.com/science/article/pii/S146532492301054X [Accessed November 2, 2023].

Marión RM, Strati K, Li H, Murga M, Blanco R, Ortega S, Fernandez-Capetillo O, Serrano M & Blasco MA (2009) A p53-mediated DNA damage response limits reprogramming to ensure iPS cell genomic integrity. *Nature* 460, 1149–1153.

Marjanovic ND, Hofree M, Chan JE, Canner D, Wu K, Trakala M, Hartmann GG, Smith OC, Kim JY, Evans KV, Hudson A, Ashenberg O, Porter CBM, Bejnood A, Subramanian A, Pitter K, Yan Y, Delorey T, Phillips DR, Shah N, Chaudhary O, Tsankov A, Hollmann T, Rekhtman N, Massion PP, Poirier JT, Mazutis L, Li R, Lee J-H, Amon A, Rudin CM, Jacks T, Regev A & Tammela T (2020) Emergence of a High-Plasticity Cell State during Lung Cancer Evolution. *Cancer Cell* 38, 229-246.e13.

Martin GR (1981) Isolation of a pluripotent cell line from early mouse embryos cultured in medium conditioned by teratocarcinoma stem cells. *Proc Natl Acad Sci U S A* 78, 7634–7638.

Maswabi BCL, Molinsky J, Savvulidi F, Zikmund T, Prukova D, Tuskova D, Klanova M, Vockova P, Lateckova L, Sefc L, Zivny J, Trneny M & Klener P (2017) Hematopoiesis in patients with mature B-cell malignancies is deregulated even in patients with undetectable bone marrow involvement. *Haematologica* 102, e152–e155.

Maxwell KG & Millman JR (2021) Applications of iPSC-derived beta cells from patients with diabetes. *CR Med* 2. Available at: https://www.cell.com/cell-reports-medicine/abstract/S2666-3791(21)00054-9 [Accessed April 28, 2023].

Mayani H & Lansdorp PM (1994) Thy-1 expression is linked to functional properties of primitive hematopoietic progenitor cells from human umbilical cord blood. *Blood* 83, 2410–2417.

Mayer IM, Hoelbl-Kovacic A, Sexl V & Doma E (2022) Isolation, Maintenance and Expansion of Adult Hematopoietic Stem/Progenitor Cells and Leukemic Stem Cells. *Cancers* 14, 1723.

McCune JM, Namikawa R, Kaneshima H, Shultz LD, Lieberman M & Weissman IL (1988) The SCID-hu mouse: murine model for the analysis of human hematolymphoid differentiation and function. *Science* 241, 1632–1639.

McGrath KE, Frame JM, Fegan KH, Bowen JR, Conway SJ, Catherman SC, Kingsley PD, Koniski AD & Palis J (2015) Distinct Sources of Hematopoietic Progenitors Emerge before HSCs and Provide Functional Blood Cells in the Mammalian Embryo. *Cell Reports* 11, 1892–1904.

McQualter JL, Yuen K, Williams B & Bertoncello I (2010) Evidence of an epithelial stem/progenitor cell hierarchy in the adult mouse lung. *Proceedings of the National Academy of Sciences* 107, 1414–1419.

Mendelson A & Frenette PS (2014) Hematopoietic stem cell niche maintenance during homeostasis and regeneration. *Nat Med* 20, 833–846.

Méndez-Ferrer S, Michurina TV, Ferraro F, Mazloom AR, Macarthur BD, Lira SA, Scadden DT, Ma'ayan A, Enikolopov GN & Frenette PS (2010) Mesenchymal and haematopoietic stem cells form a unique bone marrow niche. *Nature* 466, 829–834.

Meng X, Lindahl M, Hyvönen ME, Parvinen M, de Rooij DG, Hess MW, Raatikainen-Ahokas A, Sainio K, Rauvala H, Lakso M, Pichel JG, Westphal H, Saarma M & Sariola H (2000) Regulation of cell fate decision of undifferentiated spermatogonia by GDNF. *Science* 287, 1489–1493.

Meyrick B, Sturgess JM & Reid L (1969) A reconstruction of the duct system and secretory tubules of the human bronchial submucosal gland. *Thorax* 24, 729–736.

Milbrandt J, Sauvage FJ de, Fahrner TJ, Baloh RH, Leitner ML, Tansey MG, Lampe PA, Heuckeroth RO, Kotzbauer PT, Simburger KS, Golden JP, Davies JA, Vejsada R, Kato AC, Hynes M, Sherman D, Nishimura M, Wang L-C, Vandlen R, Moffat B, Klein RD, Poulsen K, Gray C, Garces A, Henderson CE, Phillips HS & Johnson EM (1998) Persephin, a Novel Neurotrophic Factor Related to GDNF and Neurturin. *Neuron* 20, 245–253.

Miller AJ, Hill DR, Nagy MS, Aoki Y, Dye BR, Chin AM, Huang S, Zhu F, White ES, Lama V & Spence JR (2018) In Vitro Induction and In Vivo Engraftment of Lung Bud Tip Progenitor Cells Derived from Human Pluripotent Stem Cells. *Stem Cell Reports* 10, 101–119.

Miller CL & Eaves CJ (1997) Expansion in vitro of adult murine hematopoietic stem cells with transplantable lympho-myeloid reconstituting ability. *Proc Natl Acad Sci U S A* 94, 13648–13653.

Miller JS, McCullar V, Punzel M, Lemischka IR & Moore KA (1999) Single adult human CD34(+)/Lin-/CD38(-) progenitors give rise to natural killer cells, B-lineage cells, dendritic cells, and myeloid cells. *Blood* 93, 96–106.

Miller RA & Ruddle FH (1976) Pluripotent teratocarcinoma-thymus somatic cell hybrids. *Cell* 9, 45–55.

Minoo P, Hu L, Xing Y, Zhu NL, Chen H, Li M, Borok Z & Li C (2007) Physical and functional interactions between homeodomain NKX2.1 and winged helix/forkhead FOXA1 in lung epithelial cells. *Mol Cell Biol* 27, 2155–2165.

Minoo P, Su G, Drum H, Bringas P & Kimura S (1999) Defects in Tracheoesophageal and Lung Morphogenesis inNkx2.1(−/−) Mouse Embryos. *Developmental Biology* 209, 60–71.

Mirshekar-Syahkal B, Haak E, Kimber GM, Leusden K van, Harvey K, O'Rourke J, Laborda J, Bauer SR, Bruijn MFTR de, Ferguson-Smith AC, Dzierzak E & Ottersbach K (2013) Dlk1 is a negative regulator of emerging hematopoietic stem and progenitor cells. *Haematologica* 98, 163–171.

Miyakawa Y, Rojnuckarin P, Habib T & Kaushansky K (2001) Thrombopoietin Induces Phosphoinositol 3-Kinase Activation through SHP2, Gab, and Insulin Receptor Substrate Proteins in BAF3 Cells and Primary Murine Megakaryocytes. *Journal of Biological Chemistry* 276, 2494–2502.

Miyamoto K, Araki KY, Naka K, Arai F, Takubo K, Yamazaki S, Matsuoka S, Miyamoto T, Ito K, Ohmura M, Chen C, Hosokawa K, Nakauchi H, Nakayama K, Nakayama KI, Harada M, Motoyama N, Suda T & Hirao A (2007) Foxo3a is essential for maintenance of the hematopoietic stem cell pool. *Cell Stem Cell* 1, 101–112.

Mizukami T, Shiraishi K, Shimada Y, Ogiwara H, Tsuta K, Ichikawa H, Sakamoto H, Kato M, Shibata T, Nakano T & Kohno T (2014) Molecular mechanisms underlying oncogenic RET fusion in lung adenocarcinoma. *J Thorac Oncol* 9, 622–630.

Mohr JC, de Pablo JJ & Palecek SP (2006) 3-D microwell culture of human embryonic stem cells. *Biomaterials* 27, 6032–6042.

Mohtashami M, Shah DK, Nakase H, Kianizad K, Petrie HT & Zúñiga-Pflücker JC (2010) Direct comparison of Dll1- and Dll4-mediated Notch activation levels shows differential lymphomyeloid lineage commitment outcomes. *J Immunol* 185, 867–876.

Moore MW, Klein RD, Fariñas I, Sauer H, Armanini M, Phillips H, Reichardt LF, Ryan AM, Carver-Moore K & Rosenthal A (1996) Renal and neuronal abnormalities in mice lacking GDNF. *Nature* 382, 76–79.

Morabito A, Piccirillo MC, Falasconi F, De Feo G, Del Giudice A, Bryce J, Di Maio M, De Maio E, Normanno N & Perrone F (2009) Vandetanib (ZD6474), a Dual Inhibitor of Vascular Endothelial Growth Factor Receptor (VEGFR) and Epidermal Growth Factor Receptor (EGFR) Tyrosine Kinases: Current Status and Future Directions. *The Oncologist* 14, 378–390.

Mora-Roldan GA, Ramirez-Ramirez D, Pelayo R & Gazarian K (2021) Assessment of the Hematopoietic Differentiation Potential of Human Pluripotent Stem Cells in 2D and 3D Culture Systems. *Cells* 10, 2858.

Morgan KM, Riedlinger GM, Rosenfeld J, Ganesan S & Pine SR (2017) Patient-Derived Xenograft Models of Non-Small Cell Lung Cancer and Their Potential Utility in Personalized Medicine. *Front Oncol* 7, 2.

Morganti C, Cabezas-Wallscheid N & Ito K (2022) Metabolic Regulation of Hematopoietic Stem Cells. *Hemasphere* 6, e740.

Morita Y, Ema H & Nakauchi H (2010) Heterogeneity and hierarchy within the most primitive hematopoietic stem cell compartment. *J Exp Med* 207, 1173–1182.

Morrison SJ & Kimble J (2006) Asymmetric and symmetric stem-cell divisions in development and cancer. *Nature* 441, 1068–1074.

Morrison SJ & Weissman IL (1994) The long-term repopulating subset of hematopoietic stem cells is deterministic and isolatable by phenotype. *Immunity* 1, 661–673.

Mossadegh-Keller N, Sarrazin S, Kandalla PK, Espinosa L, Stanley ER, Nutt SL, Moore J & Sieweke MH (2013) M-CSF instructs myeloid lineage fate in single haematopoietic stem cells. *Nature* 497, 239–243.

Muller-Sieburg CE, Cho RH, Karlsson L, Huang J-F & Sieburg HB (2004) Myeloid-biased hematopoietic stem cells have extensive self-renewal capacity but generate diminished lymphoid progeny with impaired IL-7 responsiveness. *Blood* 103, 4111–4118.

Müller-Sieburg CE, Cho RH, Thoman M, Adkins B & Sieburg HB (2002) Deterministic regulation of hematopoietic stem cell self-renewal and differentiation. *Blood* 100, 1302–1309.

Muller-Sieburg CE, Whitlock CA & Weissman IL (1986) Isolation of two early B lymphocyte progenitors from mouse marrow: a committed pre-pre-B cell and a clonogenic Thy-1-lo hematopoietic stem cell. *Cell* 44, 653–662.

Mulligan LM (2014) RET revisited: expanding the oncogenic portfolio. *Nat Rev Cancer* 14, 173–186.

Mulligan LM, Timmer T, Ivanchuk SM, Campling BG, Young LC, Rabbitts PH, Sundaresan V, Hofstra RM & Eng C (1998) Investigation of the genes for RET and its ligand complex, GDNF/GFR alpha-I, in small cell lung carcinoma. *Genes Chromosomes Cancer* 21, 326–332.

Myong N-H (2003) Thyroid transcription factor-1 (TTF-1) expression in human lung carcinomas: its prognostic implication and relationship with wxpressions of p53 and Ki-67 proteins. *J Korean Med Sci* 18, 494–500.

Naik SH, Perié L, Swart E, Gerlach C, van Rooij N, de Boer RJ & Schumacher TN (2013) Diverse and heritable lineage imprinting of early haematopoietic progenitors. *Nature* 496, 229–232.

Nakahara F, Borger DK, Wei Q, Pinho S, Maryanovich M, Zahalka AH, Suzuki M, Cruz CD, Wang Z, Xu C, Boulais PE, Ma'ayan A, Greally JM & Frenette PS (2019) Engineering a haematopoietic stem cell niche by revitalizing mesenchymal stromal cells. *Nat Cell Biol* 21, 560–567.

Nakano T, Kodama H & Honjo T (1994) Generation of lymphohematopoietic cells from embryonic stem cells in culture. *Science* 265, 1098–1101.

Nakaoku T, Kohno T, Araki M, Niho S, Chauhan R, Knowles PP, Tsuchihara K, Matsumoto S, Shimada Y, Mimaki S, Ishii G, Ichikawa H, Nagatoishi S, Tsumoto K, Okuno Y, Yoh K, McDonald NQ & Goto K (2018) A secondary RET mutation in the activation loop conferring resistance to vandetanib. *Nat Commun* 9, 625.

Nakayama S, Iida K, Tsuzuki T, Iwashita T, Murakami H, Asai N, Iwata Y, Ichihara M, Ito S, Kawai K, Asai M, Kurokawa K & Takahashi M (1999) Implication of expression of GDNF/Ret signalling components in differentiation of bone marrow haemopoietic cells. *British Journal of Haematology* 105, 50–57.

Narayanan M, Owers-Bradley J, Beardsmore CS, Mada M, Ball I, Garipov R, Panesar KS, Kuehni CE, Spycher BD, Williams SE & Silverman M (2012) Alveolarization continues during childhood and adolescence: new evidence from helium-3 magnetic resonance. *Am J Respir Crit Care Med* 185, 186–191.

Naughton CK, Jain S, Strickland AM, Gupta A & Milbrandt J (2006) Glial cell-line derived neurotrophic factor-mediated RET signaling regulates spermatogonial stem cell fate. *Biol Reprod* 74, 314–321.

Nelson-Taylor SK, Le AT, Yoo M, Schubert L, Mishall KM, Doak A, Varella-Garcia M, Tan A-C & Doebele RC (2017) Resistance to RET-Inhibition in RET-Rearranged NSCLC Is Mediated By Reactivation of RAS/MAPK Signaling. *Molecular Cancer Therapeutics* 16, 1623–1633.

Nestorowa S, Hamey FK, Pijuan Sala B, Diamanti E, Shepherd M, Laurenti E, Wilson NK, Kent DG & Göttgens B (2016) A single-cell resolution map of mouse hematopoietic stem and progenitor cell differentiation. *Blood* 128, e20–e31.

Nicholson AG, Tsao MS, Beasley MB, Borczuk AC, Brambilla E, Cooper WA, Dacic S, Jain D, Kerr KM, Lantuejoul S, Noguchi M, Papotti M, Rekhtman N, Scagliotti G, van Schil P, Sholl L, Yatabe Y, Yoshida A & Travis WD (2022) The 2021 WHO Classification of Lung Tumors: Impact of Advances Since 2015. *J Thorac Oncol* 17, 362–387.

Nie Y, Han Y-C & Zou Y-R (2008) CXCR4 is required for the quiescence of primitive hematopoietic cells. *J Exp Med* 205, 777–783.

Nikolić MZ, Caritg O, Jeng Q, Johnson J-A, Sun D, Howell KJ, Brady JL, Laresgoiti U, Allen G, Butler R, Zilbauer M, Giangreco A & Rawlins EL (2017) Human embryonic lung epithelial tips are multipotent progenitors that can be expanded in vitro as long-term self-renewing organoids. *Elife* 6, e26575.

Nikolić MZ, Sun D & Rawlins EL (2018) Human lung development: recent progress and new challenges. *Development* 145, dev163485.

Nokihara H, Nishio M, Yamamoto N, Fujiwara Y, Horinouchi H, Kanda S, Horiike A, Ohyanagi F, Yanagitani N, Nguyen L, Yaron Y, Borgman A & Tamura T (2019) Phase 1 Study of Cabozantinib in Japanese Patients With Expansion Cohorts in Non–Small-Cell Lung Cancer. *Clinical Lung Cancer* 20, e317–e328.

Notta F, Doulatov S, Laurenti E, Poeppl A, Jurisica I & Dick JE (2011) Isolation of Single Human Hematopoietic Stem Cells Capable of Long-Term Multilineage Engraftment. *Science* 333, 218–221.

Nottingham WT, Jarratt A, Burgess M, Speck CL, Cheng J-F, Prabhakar S, Rubin EM, Li P-S, Sloane-Stanley J, Kong-a-San J & de Bruijn MFTR (2007) Runx1-mediated hematopoietic stem-cell emergence is controlled by a Gata/Ets/SCL-regulated enhancer. *Blood* 110, 4188–4197.

Ntanasis-Stathopoulos I, Gavriatopoulou M, Kastritis E, Terpos E & Dimopoulos MA (2020) Multiple myeloma: Role of autologous transplantation. *Cancer Treat Rev* 82, 101929.

Oberg M, Jaakkola MS, Woodward A, Peruga A & Prüss-Ustün A (2011) Worldwide burden of disease from exposure to second-hand smoke: a retrospective analysis of data from 192 countries. *Lancet* 377, 139–146.

Offin M, Guo R, Wu SL, Sabari J, Land JD, Ni A, Montecalvo J, Halpenny DF, Buie LW, Pak T, Liu D, Riely GJ, Hellmann MD, Benayed R, Arcila M, Kris MG, Rudin CM, Li BT, Ladanyi M, Rekhtman N & Drilon A (2019) Immunophenotype and Response to Immunotherapy of RET-Rearranged Lung Cancers. *JCO Precis Oncol* 3, PO.18.00386.

Ogawa M (1993) Differentiation and Proliferation of Hematopoietic Stem Cells. *Blood* 81, 2844–2853.

Ohlsson E, Schuster MB, Hasemann M & Porse BT (2016) The multifaceted functions of C/EBPα in normal and malignant haematopoiesis. *Leukemia* 30, 767–775.

Okita K, Ichisaka T & Yamanaka S (2007) Generation of germline-competent induced pluripotent stem cells. *Nature* 448, 313–317.

Olson OC, Kang Y-A & Passegué E (2020) Normal Hematopoiesis Is a Balancing Act of Self-Renewal and Regeneration. *Cold Spring Harb Perspect Med* 10, a035519.

Onder TT, Kara N, Cherry A, Sinha AU, Zhu N, Bernt KM, Cahan P, Marcarci BO, Unternaehrer J, Gupta PB, Lander ES, Armstrong SA & Daley GQ (2012) Chromatin-modifying enzymes as modulators of reprogramming. *Nature* 483, 598–602.

Osawa M, Hanada K, Hamada H & Nakauchi H (1996) Long-term lymphohematopoietic reconstitution by a single CD34-low/negative hematopoietic stem cell. *Science* 273, 242–245.

Ou S-HI & Zhu VW (2020) Catalog of 5′ fusion partners in RET+ NSCLC Circa 2020. *JTO Clin Res Rep* 1, 100037.

Paez JG, Jänne PA, Lee JC, Tracy S, Greulich H, Gabriel S, Herman P, Kaye FJ, Lindeman N, Boggon TJ, Naoki K, Sasaki H, Fujii Y, Eck MJ, Sellers WR, Johnson BE & Meyerson M (2004) EGFR Mutations in Lung Cancer: Correlation with Clinical Response to Gefitinib Therapy. *Science* 304, 1497–1500.

Pakkala S & Ramalingam SS (2018) Personalized therapy for lung cancer: striking a moving target. *JCI Insight* 3. Available at: https://insight.jci.org/articles/view/120858 [Accessed May 22, 2023].

Palis J (2016) Hematopoietic stem cell-independent hematopoiesis: emergence of erythroid, megakaryocyte, and myeloid potential in the mammalian embryo. *FEBS Letters* 590, 3965–3974.

Palis J, Malik J, Mcgrath KE & Kingsley PD (2010) Primitive erythropoiesis in the mammalian embryo. *Int. J. Dev. Biol.* 54, 1011–1018.

Pao W, Miller VA, Politi KA, Riely GJ, Somwar R, Zakowski MF, Kris MG & Varmus H (2005) Acquired Resistance of Lung Adenocarcinomas to Gefitinib or Erlotinib Is Associated with a Second Mutation in the EGFR Kinase Domain. *PLOS Medicine* 2, e73.

Pao W, Wang TY, Riely GJ, Miller VA, Pan Q, Ladanyi M, Zakowski MF, Heelan RT, Kris MG & Varmus HE (2005) KRAS mutations and primary resistance of lung adenocarcinomas to gefitinib or erlotinib. *PLoS Med* 2, e17.

Papapetrou EP (2016) Patient-derived induced pluripotent stem cells in cancer research and precision oncology. *Nat Med* 22, 1392–1401.

Paratala BS, Chung JH, Williams CB, Yilmazel B, Petrosky W, Williams K, Schrock AB, Gay LM, Lee E, Dolfi SC, Pham K, Lin S, Yao M, Kulkarni A, DiClemente F, Liu C, Rodriguez-Rodriguez L, Ganesan S, Ross JS, Ali SM, Leyland-Jones B & Hirshfield KM (2018) RET rearrangements are actionable alterations in breast cancer. *Nat Commun* 9, 4821.

Parimi V, Tolba K, Danziger N, Kuang Z, Sun D, Lin DI, Hiemenz MC, Schrock AB, Ross JS, Oxnard GR & Huang RSP (2023) Genomic landscape of 891 RET fusions detected across diverse solid tumor types. *NPJ Precis Oncol* 7, 10.

Passegué E, Wagers AJ, Giuriato S, Anderson WC & Weissman IL (2005) Global analysis of proliferation and cell cycle gene expression in the regulation of hematopoietic stem and progenitor cell fates. *J Exp Med* 202, 1599–1611.

de Pater E, Kaimakis P, Vink CS, Yokomizo T, Yamada-Inagawa T, van der Linden R, Kartalaei PS, Camper SA, Speck N & Dzierzak E (2013) Gata2 is required for HSC generation and survival. *J Exp Med* 210, 2843–2850.

Pearson AT, Finkel KA, Warner KA, Nör F, Tice D, Martins MD, Jackson TL & Nör JE (2016) Patient-derived xenograft (PDX) tumors increase growth rate with time. *Oncotarget* 7, 7993–8005.

Peifer M, Fernández-Cuesta L, Sos ML, George J, Seidel D, Kasper LH, Plenker D, Leenders F, Sun R, Zander T, Menon R, Koker M, Dahmen I, Müller C, Di Cerbo V, Schildhaus H-U, Altmüller J, Baessmann I, Becker C, de Wilde B, Vandesompele J, Böhm D, Ansén S, Gabler F, Wilkening I, Heynck S, Heuckmann JM, Lu X, Carter SL, Cibulskis K, Banerji S, Getz G, Park K-S, Rauh D, Grütter C, Fischer M, Pasqualucci L, Wright G, Wainer Z, Russell P, Petersen I, Chen Y, Stoelben E, Ludwig C, Schnabel P, Hoffmann H, Muley T, Brockmann M, Engel-Riedel W, Muscarella LA, Fazio VM, Groen H, Timens W, Sietsma H, Thunnissen E, Smit E, Heideman DA, Snijders PJ, Cappuzzo F, Ligorio C, Damiani S, Field J, Solberg S, Brustugun OT, Lund-Iversen M, Sänger J, Clement JH, Soltermann A, Moch H, Weder W, Solomon B, Soria J-C, Validire P, Besse B, Brambilla E, Brambilla C, Lantuejoul S, Lorimier P, Schneider PM, Hallek M, Pao W, Meyerson M, Sage J, Shendure J, Schneider R, Büttner R, Wolf J, Nürnberg P, Perner S, Heukamp LC, Brindle PK, Haas S & Thomas RK (2012) Integrative genome analyses identify key somatic driver mutations of small cell lung cancer. *Nat Genet* 44, 1104–1110.

Perrinjaquet M, Vilar M & Ibáñez CF (2010) Protein-tyrosine phosphatase SHP2 contributes to GDNF neurotrophic activity through direct binding to phospho-Tyr687 in the RET receptor tyrosine kinase. *J Biol Chem* 285, 31867–31875.

Petrelli A, Gilestro GF, Lanzardo S, Comoglio PM, Migone N & Giordano S (2002) The endophilin-CIN85-Cbl complex mediates ligand-dependent downregulation of c-Met. *Nature* 416, 187–190.

Phelps DS & Floros J (1988) Localization of surfactant protein synthesis in human lung by in situ hybridization. *Am Rev Respir Dis* 137, 939–942.

Piccolo FM, Pereira CF, Cantone I, Brown K, Tsubouchi T, Soza-Ried J, Merkenschlager M & Fisher AG (2011) Using heterokaryons to understand pluripotency and reprogramming. *Philosophical Transactions of the Royal Society B: Biological Sciences* 366, 2260–2265.

Pichel JG, Shen L, Sheng HZ, Granholm AC, Drago J, Grinberg A, Lee EJ, Huang SP, Saarma M, Hoffer BJ, Sariola H & Westphal H (1996) Defects in enteric innervation and kidney development in mice lacking GDNF. *Nature* 382, 73–76.

Pietras EM, Mirantes-Barbeito C, Fong S, Loeffler D, Kovtonyuk LV, Zhang S, Lakshminarasimhan R, Chin CP, Techner J-M, Will B, Nerlov C, Steidl U, Manz MG, Schroeder T & Passegué E (2016) Chronic interleukin-1 exposure drives haematopoietic stem cells towards precocious myeloid differentiation at the expense of self-renewal. *Nat Cell Biol* 18, 607–618.

Pietras EM, Warr MR & Passegué E (2011) Cell cycle regulation in hematopoietic stem cells. *Journal of Cell Biology* 195, 709–720.

Piotrowska Z, Isozaki H, Lennerz JK, Gainor JF, Lennes IT, Zhu VW, Marcoux N, Banwait MK, Digumarthy SR, Su W, Yoda S, Riley AK, Nangia V, Lin JJ, Nagy RJ, Lanman RB, Dias-Santagata D, Mino-Kenudson M, Iafrate AJ, Heist RS, Shaw AT, Evans EK, Clifford C, Ou S-HI, Wolf B, Hata AN & Sequist LV (2018) Landscape of Acquired Resistance to Osimertinib in EGFR-Mutant NSCLC and Clinical Validation of Combined EGFR and RET Inhibition with Osimertinib and BLU-667 for Acquired RET Fusion. *Cancer Discovery* 8, 1529–1539.

Plaza-Menacho I, Mologni L & McDonald NQ (2014) Mechanisms of RET signaling in cancer: Current and future implications for targeted therapy. *Cellular Signalling* 26, 1743–1752.

Politi K, Zakowski MF, Fan P-D, Schonfeld EA, Pao W & Varmus HE (2006) Lung adenocarcinomas induced in mice by mutant EGF receptors foundin human lung cancers respondto a tyrosine kinase inhibitor orto down-regulation of the receptors. *Genes Dev.* 20, 1496–1510.

Poulos MG, Guo P, Kofler NM, Pinho S, Gutkin MC, Tikhonova A, Aifantis I, Frenette PS, Kitajewski J, Rafii S & Butler JM (2013) Endothelial Jagged-1 is necessary for homeostatic and regenerative hematopoiesis. *Cell Rep* 4, 1022–1034.

Pyo KH, Lim SM, Kim HR, Sung YH, Yun MR, Kim S-M, Kim H, Kang HN, Lee JM, Kim SG, Park CW, Chang H, Shim HS, Lee H-W & Cho BC (2017) Establishment of a Conditional Transgenic Mouse Model Recapitulating EML4-ALK–Positive Human Non–Small Cell Lung Cancer. *Journal of Thoracic Oncology* 12, 491–500.

Qian H, Buza-Vidas N, Hyland CD, Jensen CT, Antonchuk J, Månsson R, Thoren LA, Ekblom M, Alexander WS & Jacobsen SEW (2007) Critical role of thrombopoietin in maintaining adult quiescent hematopoietic stem cells. *Cell Stem Cell* 1, 671–684.

Qian Y, Chai S, Liang Z, Wang Y, Zhou Y, Xu X, Zhang C, Zhang M, Si J, Huang F, Huang Z, Hong W & Wang K (2014) KIF5B-RET fusion kinase promotes cell growth by multilevel activation of STAT3 in lung cancer. *Mol Cancer* 13, 176.

Qiu C, Ma Y, Wang J, Peng S & Huang Y (2010) Lin28-mediated post-transcriptional regulation of Oct4 expression in human embryonic stem cells. *Nucleic Acids Research* 38, 1240–1248.

Rackley CR & Stripp BR (2012) Building and maintaining the epithelium of the lung. *J Clin Invest* 122, 2724–2730.

Rafii S, Butler JM & Ding B-S (2016) Angiocrine functions of organ-specific endothelial cells. *Nature* 529, 316–325.

Raic A, Naolou T, Mohra A, Chatterjee C & Lee-Thedieck C (2019) 3D models of the bone marrow in health and disease: yesterday, today and tomorrow. *MRS Commun* 9, 37–52.

Raic A, Rödling L, Kalbacher H & Lee-Thedieck C (2014) Biomimetic macroporous PEG hydrogels as 3D scaffolds for the multiplication of human hematopoietic stem and progenitor cells. *Biomaterials* 35, 929–940.

Ramalingam S & Belani C (2008) Systemic chemotherapy for advanced non-small cell lung cancer: recent advances and future directions. *Oncologist* 13 Suppl 1, 5–13.

Rankin SA & Zorn AM (2014) Gene Regulatory Networks governing lung specification. *J Cell Biochem* 115, 1343–1350.

Rao I, Crisafulli L, Paulis M & Ficara F (2022) Hematopoietic Cells from Pluripotent Stem Cells: Hope and Promise for the Treatment of Inherited Blood Disorders. *Cells* 11, 557.

Rao MS & Malik N (2012) Assessing iPSC Reprogramming Methods for Their Suitability in Translational Medicine. *J Cell Biochem* 113, 3061–3068.

Rawlins EL, Clark CP, Xue Y & Hogan BLM (2009) The Id2+ distal tip lung epithelium contains individual multipotent embryonic progenitor cells. *Development* 136, 3741–3745.

Regua AT, Najjar M & Lo H-W (2022) RET signaling pathway and RET inhibitors in human cancer. *Frontiers in Oncology* 12. Available at: https://www.frontiersin.org/articles/10.3389/fonc.2022.932353 [Accessed May 18, 2023].

Reilly JT (2003) Receptor tyrosine kinases in normal and malignant haematopoiesis. *Blood Reviews* 17, 241–248.

Renner M, Lancaster MA, Bian S, Choi H, Ku T, Peer A, Chung K & Knoblich JA (2017) Self-organized developmental patterning and differentiation in cerebral organoids. *EMBO J* 36, 1316–1329.

Reya T, Duncan AW, Ailles L, Domen J, Scherer DC, Willert K, Hintz L, Nusse R & Weissman IL (2003) A role for Wnt signalling in self-renewal of haematopoietic stem cells. *Nature* 423, 409–414.

Ribeiro-Filho AC, Levy D, Ruiz JLM, Mantovani M da C & Bydlowski SP (2019) Traditional and Advanced Cell Cultures in Hematopoietic Stem Cell Studies. *Cells* 8, 1628.

Ricarte-Filho JC, Li S, Garcia-Rendueles MER, Montero-Conde C, Voza F, Knauf JA, Heguy A, Viale A, Bogdanova T, Thomas GA, Mason CE & Fagin JA (2013) Identification of kinase fusion oncogenes in post-Chernobyl radiation-induced thyroid cancers. *J Clin Invest* 123, 4935–4944.

Riddell J, Gazit R, Garrison BS, Guo G, Saadatpour A, Mandal PK, Ebina W, Volchkov P, Yuan G-C, Orkin SH & Rossi DJ (2014) Reprogramming committed murine blood cells to induced hematopoietic stem cells with defined factors. *Cell* 157, 549–564.

Robert-Moreno À, Espinosa L, de la Pompa JL & Bigas A (2005) RBPjκ-dependent Notch function regulates Gata2 and is essential for the formation of intra-embryonic hematopoietic cells. *Development* 132, 1117–1126.

Robichaux JP, Elamin YY, Tan Z, Carter BW, Zhang S, Liu S, Li S, Chen T, Poteete A, Estrada-Bernal A, Le AT, Truini A, Nilsson MB, Sun H, Roarty E, Goldberg SB, Brahmer JR, Altan M, Lu C, Papadimitrakopoulou V, Politi K, Doebele RC, Wong K-K & Heymach JV (2018) Mechanisms and clinical activity of an EGFR and HER2 exon 20-selective kinase inhibitor in non-small cell lung cancer. *Nat Med* 24, 638–646.

Robinton DA & Daley GQ (2012) The promise of induced pluripotent stem cells in research and therapy. *Nature* 481, 295–305.

Rock JR, Onaitis MW, Rawlins EL, Lu Y, Clark CP, Xue Y, Randell SH & Hogan BLM (2009) Basal cells as stem cells of the mouse trachea and human airway epithelium. *Proceedings of the National Academy of Sciences* 106, 12771–12775.

Rödling L, Schwedhelm I, Kraus S, Bieback K, Hansmann J & Lee-Thedieck C (2017) 3D models of the hematopoietic stem cell niche under steady-state and active conditions. *Sci Rep* 7, 4625.

Rodriguez-Fraticelli AE, Wolock SL, Weinreb CS, Panero R, Patel SH, Jankovic M, Sun J, Calogero RA, Klein AM & Camargo FD (2018) Clonal analysis of lineage fate in native hematopoiesis. *Nature* 553, 212–216.

Romeo G, Ronchetto P, Luo Y, Barone V, Seri M, Ceccherini I, Pasini B, Bocciardi R, Lerone M & Kääriäinen H (1994) Point mutations affecting the tyrosine kinase domain of the RET proto-oncogene in Hirschsprung's disease. *Nature* 367, 377–378.

Rosfjord E, Lucas J, Li G & Gerber H-P (2014) Advances in patient-derived tumor xenografts: from target identification to predicting clinical response rates in oncology. *Biochem Pharmacol* 91, 135–143.

Rosnet O, Schiff C, Pébusque M-J, Marchetto S, Tonnelle C, Toiron Y, Birg F & Birnbaum D (1993) Human FLT3/FLK2 Gene: cDNA Cloning and Expression in Hematopoietic Cells. *Blood* 82, 1110–1119.

Rowe RG & Daley GQ (2019) Induced pluripotent stem cells in disease modelling and drug discovery. *Nat Rev Genet* 20, 377–388.

Ruano-Raviña A, Provencio M, Calvo de Juan V, Carcereny E, Moran T, Rodriguez-Abreu D, López-Castro R, Cuadrado Albite E, Guirado M, Gómez González L, Massutí B, Ortega Granados AL, Blasco A, Cobo M, Garcia-Campelo R, Bosch J, Trigo J, Juan Ó, Aguado de la Rosa C, Dómine M, Sala M, Oramas J, Casal-Rubio J & Cerezo S (2020) Lung cancer symptoms at diagnosis: results of a nationwide registry study. *ESMO Open* 5, e001021.

Rudin CM, Durinck S, Stawiski EW, Poirier JT, Modrusan Z, Shames DS, Bergbower EA, Guan Y, Shin J, Guillory J, Rivers CS, Foo CK, Bhatt D, Stinson J, Gnad F, Haverty PM, Gentleman R, Chaudhuri S, Janakiraman V, Jaiswal BS, Parikh C, Yuan W, Zhang Z, Koeppen H, Wu TD, Stern HM, Yauch RL, Huffman KE, Paskulin DD, Illei PB, Varella-Garcia M, Gazdar AF, de Sauvage FJ, Bourgon R, Minna JD, Brock MV & Seshagiri S (2012) Comprehensive genomic analysis identifies SOX2 as a frequently amplified gene in small-cell lung cancer. *Nat Genet* 44, 1111–1116.

Rumman M, Dhawan J & Kassem M (2015) Concise Review: Quiescence in Adult Stem Cells: Biological Significance and Relevance to Tissue Regeneration. *STEM CELLS* 33, 2903–2912.

Rybtsov S, Sobiesiak M, Taoudi S, Souilhol C, Senserrich J, Liakhovitskaia A, Ivanovs A, Frampton J, Zhao S & Medvinsky A (2011) Hierarchical organization and early hematopoietic specification of the developing HSC lineage in the AGM region. *J Exp Med* 208, 1305–1315.

Saarma M (2000) GDNF - a stranger in the TGF-beta superfamily? *Eur J Biochem* 267, 6968–6971.

Sachs N, Papaspyropoulos A, Zomer-van Ommen DD, Heo I, Böttinger L, Klay D, Weeber F, Huelsz-Prince G, Iakobachvili N, Amatngalim GD, de Ligt J, van Hoeck A, Proost N, Viveen MC, Lyubimova A, Teeven L, Derakhshan S, Korving J, Begthel H, Dekkers JF, Kumawat K, Ramos E, van Oosterhout MF, Offerhaus GJ, Wiener DJ, Olimpio EP, Dijkstra KK, Smit EF, van der Linden M, Jaksani S, van de Ven M, Jonkers J, Rios AC, Voest EE, van Moorsel CH, van der Ent CK, Cuppen E, van Oudenaarden A, Coenjaerts FE, Meyaard L, Bont LJ, Peters PJ, Tans SJ, van Zon JS, Boj SF, Vries RG, Beekman JM & Clevers H (2019) Long-term expanding human airway organoids for disease modeling. *The EMBO Journal* 38, e100300.

Saito M, Ishigame T, Tsuta K, Kumamoto K, Imai T & Kohno T (2014a) A mouse model of KIF5B-RET fusion-dependent lung tumorigenesis. *Carcinogenesis* 35, 2452–2456.

Saito M, Ishigame T, Tsuta K, Kumamoto K, Imai T & Kohno T (2014b) A mouse model of KIF5B-RET fusion-dependent lung tumorigenesis. *Carcinogenesis* 35, 2452–2456.

Sánchez MP, Silos-Santiago I, Frisén J, He B, Lira SA & Barbacid M (1996) Renal agenesis and the absence of enteric neurons in mice lacking GDNF. *Nature* 382, 70–73.

Sanjuan-Pla A, Macaulay IC, Jensen CT, Woll PS, Luis TC, Mead A, Moore S, Carella C, Matsuoka S, Bouriez Jones T, Chowdhury O, Stenson L, Lutteropp M, Green JCA, Facchini R, Boukarabila H, Grover A, Gambardella A, Thongjuea S, Carrelha J, Tarrant P, Atkinson D, Clark S-A, Nerlov C & Jacobsen SEW (2013) Platelet-biased stem cells reside at the apex of the haematopoietic stem-cell hierarchy. *Nature* 502, 232–236.

Sato T, Vries RG, Snippert HJ, van de Wetering M, Barker N, Stange DE, van Es JH, Abo A, Kujala P, Peters PJ & Clevers H (2009) Single Lgr5 stem cells build crypt-villus structures in vitro without a mesenchymal niche. *Nature* 459, 262–265.

Sawyers CL (2002) Rational therapeutic intervention in cancer: kinases as drug targets. *Curr Opin Genet Dev* 12, 111–115.

Scandura JM, Boccuni P, Massagué J & Nimer SD (2004) Transforming growth factor β-induced cell cycle arrest of human hematopoietic cells requires p57KIP2 up-regulation. *Proceedings of the National Academy of Sciences* 101, 15231–15236.

Schaffer BE, Park K-S, Yiu G, Conklin JF, Lin C, Burkhart DL, Karnezis AN, Sweet-Cordero EA & Sage J (2010) Loss of p130 Accelerates Tumor Development in a Mouse Model for Human Small-Cell Lung Carcinoma. *Cancer Research* 70, 3877–3883.

Scheiner ZS, Talib S & Feigal EG (2014) The Potential for Immunogenicity of Autologous Induced Pluripotent Stem Cell-derived Therapies. *J Biol Chem* 289, 4571–4577.

Schittny JC (2017) Development of the lung. *Cell Tissue Res* 367, 427–444.

Schlumberger M, Elisei R, Müller S, Schöffski P, Brose M, Shah M, Licitra L, Krajewska J, Kreissl MC, Niederle B, Cohen EEW, Wirth L, Ali H, Clary DO, Yaron Y, Mangeshkar M, Ball D, Nelkin B & Sherman S (2017) Overall survival analysis of EXAM, a phase III trial of cabozantinib in patients with radiographically progressive medullary thyroid carcinoma. *Annals of Oncology* 28, 2813–2819.

Schoffski P, Aftimos PG, Massard C, Italiano A, Jungels C, Andreas K, Keegan M & Ho PTC (2019) A phase I study of BOS172738 in patients with advanced solid tumors with RET gene alterations including non-small cell lung cancer and medullary thyroid cancer. *JCO* 37, TPS3162–TPS3162.

Schöffski P, Gordon M, Smith DC, Kurzrock R, Daud A, Vogelzang NJ, Lee Y, Scheffold C & Shapiro GI (2017) Phase II randomised discontinuation trial of cabozantinib in patients with advanced solid tumours. *European Journal of Cancer* 86, 296–304.

Schofield R (1978) The relationship between the spleen colony-forming cell and the haemopoietic stem cell. *Blood Cells* 4, 7–25.

Schubert L, Le AT, Estrada-Bernal A, Doak AE, Yoo M, Ferrara SE, Goodspeed A, Kinose F, Rix U, Tan A-C & Doebele RC (2021) Novel Human-Derived RET Fusion NSCLC Cell Lines Have Heterogeneous Responses to RET Inhibitors and Differential Regulation of Downstream Signaling. *Mol Pharmacol* 99, 435–447.

Schuchardt A, D'Agati V, Larsson-Blomberg L, Costantini F & Pachnis V (1994) Defects in the kidney and enteric nervous system of mice lacking the tyrosine kinase receptor Ret. *Nature* 367, 380–383.

Schuringa JJ, Wojtachnio K, Hagens W, Vellenga E, Buys CH, Hofstra R & Kruijer W (2001) MEN2A-RET-induced cellular transformation by activation of STAT3. *Oncogene* 20, 5350–5358.

Sequist LV, Han J-Y, Ahn M-J, Cho BC, Yu H, Kim S-W, Yang JC-H, Lee JS, Su W-C, Kowalski D, Orlov S, Cantarini M, Verheijen RB, Mellemgaard A, Ottesen L, Frewer P, Ou X & Oxnard G (2020) Osimertinib plus savolitinib in patients with EGFR mutation-positive, MET-amplified, non-small-cell lung cancer after progression on EGFR tyrosine kinase inhibitors: interim results from a multicentre, open-label, phase 1b study. *The Lancet Oncology* 21, 373–386.

Shaw AT, Friboulet L, Leshchiner I, Gainor JF, Bergqvist S, Brooun A, Burke BJ, Deng Y-L, Liu W, Dardaei L, Frias RL, Schultz KR, Logan J, James LP, Smeal T, Timofeevski S, Katayama R, Iafrate AJ, Le L, McTigue M, Getz G, Johnson TW & Engelman JA (2016) Resensitization to Crizotinib by the Lorlatinib ALK Resistance Mutation L1198F. *New England Journal of Medicine* 374, 54–61.

Sherr CJ & Roberts JM (1999) CDK inhibitors: positive and negative regulators of G1-phase progression. *Genes Dev* 13, 1501–1512.

Shi Y, Inoue H, Wu JC & Yamanaka S (2017) Induced pluripotent stem cell technology: a decade of progress. *Nat Rev Drug Discov* 16, 115–130.

Shigematsu H & Gazdar AF (2006) Somatic mutations of epidermal growth factor receptor signaling pathway in lung cancers. *Int J Cancer* 118, 257–262.

Shirasawa M, Fujiwara N, Hirabayashi S, Ohno H, Iida J, Makita K & Hata Y (2004) Receptor for advanced glycation end-products is a marker of type I lung alveolar cells. *Genes to Cells* 9, 165–174.

Shivdasani RA, Mayer EL & Orkin SH (1995) Absence of blood formation in mice lacking the T-cell leukaemia oncoprotein tal-1/SCL. *Nature* 373, 432–434.

Shultz LD, Lyons BL, Burzenski LM, Gott B, Chen X, Chaleff S, Kotb M, Gillies SD, King M, Mangada J, Greiner DL & Handgretinger R (2005) Human lymphoid and myeloid cell development in NOD/LtSz-scid IL2R gamma null mice engrafted with mobilized human hemopoietic stem cells. *J Immunol* 174, 6477–6489.

Sidney LE, Branch MJ, Dunphy SE, Dua HS & Hopkinson A (2014) Concise review: evidence for CD34 as a common marker for diverse progenitors. *Stem Cells* 32, 1380–1389.

Siegel RL, Miller KD, Fuchs HE & Jemal A (2022) Cancer statistics, 2022. *CA: A Cancer Journal for Clinicians* 72, 7–33.

Siminovitch L, McCulloch EA & Till JE (1963) The distribution of colony-forming cells among spleen colonies. *Journal of Cellular and Comparative Physiology* 62, 327–336.

Simonato L, Agudo A, Ahrens W, Benhamou E, Benhamou S, Boffetta P, Brennan P, Darby SC, Forastiere F, Fortes C, Gaborieau V, Gerken M, Gonzales CA, Jöckel KH, Kreuzer M, Merletti F, Nyberg F, Pershagen G, Pohlabeln H, Rösch F, Whitley E, Wichmann HE & Zambon P (2001) Lung cancer and cigarette smoking in Europe: an update of risk estimates and an assessment of inter-country heterogeneity. *Int J Cancer* 91, 876–887.

Singh KP, Casado FL, Opanashuk LA & Gasiewicz TA (2009) The aryl hydrocarbon receptor has a normal function in the regulation of hematopoietic and other stem/progenitor cell populations. *Biochemical Pharmacology* 77, 577–587.

Sipple JH (1961) The association of pheochromocytoma with carcinoma of the thyroid gland. *The American Journal of Medicine* 31, 163–166.

Skálová A, Ptáková N, Santana T, Agaimy A, Ihrler S, Uro-Coste E, Thompson LDR, Bishop JA, Baněčkova M, Rupp NJ, Morbini P, de Sanctis S, Schiavo-Lena M, Vanecek T, Michal M & Leivo I (2019) NCOA4-RET and TRIM27-RET Are Characteristic Gene Fusions in Salivary Intraductal Carcinoma, Including Invasive and Metastatic Tumors: Is "Intraductal" Correct? *Am J Surg Pathol* 43, 1303–1313.

Skálová A, Vanecek T, Uro-Coste E, Bishop JA, Weinreb I, Thompson LDR, de Sanctis S, Schiavo-Lena M, Laco J, Badoual C, Santana Conceiçao T, Ptáková N, Baněčkova M, Miesbauerová M & Michal M (2018) Molecular Profiling of Salivary Gland Intraductal Carcinoma Revealed a Subset of Tumors Harboring NCOA4-RET and Novel TRIM27-RET Fusions: A Report of 17 cases. *Am J Surg Pathol* 42, 1445–1455.

Skoulidis F & Heymach JV (2019) Co-occurring genomic alterations in non-small-cell lung cancer biology and therapy. *Nat Rev Cancer* 19, 495–509.

Smith AG, Heath JK, Donaldson DD, Wong GG, Moreau J, Stahl M & Rogers D (1988) Inhibition of pluripotential embryonic stem cell differentiation by purified polypeptides. *Nature* 336, 688–690.

Soldner F & Jaenisch R (2012) iPSC Disease Modeling. *Science* 338, 1155–1156.

Soldner F, Laganière J, Cheng AW, Hockemeyer D, Gao Q, Alagappan R, Khurana V, Golbe LI, Myers RH, Lindquist S, Zhang L, Guschin D, Fong LK, Vu BJ, Meng X, Urnov FD, Rebar EJ, Gregory PD, Zhang HS & Jaenisch R (2011) Generation of isogenic pluripotent stem cells differing exclusively at two early onset Parkinson point mutations. *Cell* 146, 318–331.

Solomon BJ, Tan L, Lin JJ, Wong SQ, Hollizeck S, Ebata K, Tuch BB, Yoda S, Gainor JF, Sequist LV, Oxnard GR, Gautschi O, Drilon A, Subbiah V, Khoo C, Zhu EY, Nguyen M, Henry D, Condroski KR, Kolakowski GR, Gomez E, Ballard J, Metcalf AT, Blake JF, Dawson S-J, Blosser W, Stancato LF, Brandhuber BJ, Andrews S, Robinson BG & Rothenberg SM (2020) RET Solvent Front Mutations Mediate Acquired Resistance to Selective RET Inhibition in RET-Driven Malignancies. *J Thorac Oncol* 15, 541–549.

Solomon BJ, Zhou CC, Drilon A, Park K, Wolf J, Elamin Y, Davis HM, Soldatenkova V, Sashegyi A, Lin AB, Lin BK, F Loong HH, Novello S, Arriola E, Pérol M, Goto K & Santini FC (2021) Phase III study of selpercatinib versus chemotherapy ± pembrolizumab in untreated RET positive non-small-cell lung cancer. *Future Oncology* 17, 763–773.

Somwar R, Smith R, Hayashi T, Ishizawa K, Snyder Charen A, Khodos I, Mattar M, He J, Balasubramanian S, Stephens P, Lipson D, de Stanchina E, Davare M, Miller VA, Riely GJ, Rudin CM, Kris MG, Cheng E, Ladanyi M & Drilon AE (2016) MDM2 amplification (Amp) to mediate cabozantinib resistance in patients (Pts) with advanced RET-rearranged lung cancers. *JCO* 34, 9068–9068.

Soria J-C, Ohe Y, Vansteenkiste J, Reungwetwattana T, Chewaskulyong B, Lee KH, Dechaphunkul A, Imamura F, Nogami N, Kurata T, Okamoto I, Zhou C, Cho BC, Cheng Y, Cho EK, Voon PJ, Planchard D, Su W-C, Gray JE, Lee S-M, Hodge R, Marotti M, Rukazenkov Y & Ramalingam SS (2018) Osimertinib in Untreated EGFR-Mutated Advanced Non–Small-Cell Lung Cancer. *New England Journal of Medicine* 378, 113–125.

Soyombo AA, Wu Y, Kolski L, Rios JJ, Rakheja D, Chen A, Kehler J, Hampel H, Coughran A & Ross TS (2013) Analysis of Induced Pluripotent Stem Cells from a BRCA1 Mutant Family. *Stem Cell Reports* 1, 336–349.

Spangrude GJ, Heimfeld S & Weissman IL (1988) Purification and characterization of mouse hematopoietic stem cells. *Science* 241, 58–62.

Spence JR, Mayhew CN, Rankin SA, Kuhar MF, Vallance JE, Tolle K, Hoskins EE, Kalinichenko VV, Wells SI, Zorn AM, Shroyer NF & Wells JM (2011) Directed differentiation of human pluripotent stem cells into intestinal tissue in vitro. *Nature* 470, 105–109.

Stadtfeld M & Hochedlinger K (2010) Induced pluripotency: history, mechanisms, and applications. *Genes Dev* 24, 2239–2263.

Stahlman MT, Besnard V, Wert SE, Weaver TE, Dingle S, Xu Y, von Zychlin K, Olson SJ & Whitsett JA (2007) Expression of ABCA3 in developing lung and other tissues. *J Histochem Cytochem* 55, 71–83.

Stanulović VS, Cauchy P, Assi SA & Hoogenkamp M (2017) LMO2 is required for TAL1 DNA binding activity and initiation of definitive haematopoiesis at the haemangioblast stage. *Nucleic Acids Research* 45, 9874–9888.

Stenhouse G, Fyfe N, King G, Chapman A & Kerr KM (2004) Thyroid transcription factor 1 in pulmonary adenocarcinoma. *J Clin Pathol* 57, 383–387.

Stevens LC (1970) The development of transplantable teratocarcinomas from intratesticular grafts of pre- and postimplantation mouse embryos. *Developmental Biology* 21, 364–382.

Stier S, Ko Y, Forkert R, Lutz C, Neuhaus T, Grünewald E, Cheng T, Dombkowski D, Calvi LM, Rittling SR & Scadden DT (2005) Osteopontin is a hematopoietic stem cell niche component that negatively regulates stem cell pool size. *J Exp Med* 201, 1781–1791.

Subbiah V, Gainor JF, Rahal R, Brubaker JD, Kim JL, Maynard M, Hu W, Cao Q, Sheets MP, Wilson D, Wilson KJ, DiPietro L, Fleming P, Palmer M, Hu MI, Wirth L, Brose MS, Ou S-HI, Taylor M, Garralda E, Miller S, Wolf B, Lengauer C, Guzi T & Evans EK (2018) Precision Targeted Therapy with BLU-667 for RET-Driven Cancers. *Cancer Discovery* 8, 836–849.

Subbiah V, Velcheti V, Tuch BB, Ebata K, Busaidy NL, Cabanillas ME, Wirth LJ, Stock S, Smith S, Lauriault V, Corsi-Travali S, Henry D, Burkard M, Hamor R, Bouhana K, Winski S, Wallace RD, Hartley D, Rhodes S, Reddy M, Brandhuber BJ, Andrews S, Rothenberg SM & Drilon A (2018) Selective RET kinase inhibition for patients with RET-altered cancers. *Annals of Oncology* 29, 1869–1876.

Subbiah V, Yang D, Velcheti V, Drilon A & Meric-Bernstam F (2020) State-of-the-Art Strategies for Targeting RET-Dependent Cancers. *J Clin Oncol* 38, 1209–1221.

Suda T & Dexter TM (1981) Effect of hydrocortisone on long-term human marrow cultures. *Br J Haematol* 48, 661–664.

Sugiyama T, Kohara H, Noda M & Nagasawa T (2006) Maintenance of the hematopoietic stem cell pool by CXCL12-CXCR4 chemokine signaling in bone marrow stromal cell niches. *Immunity* 25, 977–988.

Sun J, Ramos A, Chapman B, Johnnidis JB, Le L, Ho Y-J, Klein A, Hofmann O & Camargo FD (2014) Clonal dynamics of native haematopoiesis. *Nature* 514, 322–327.

Sung H, Ferlay J, Siegel RL, Laversanne M, Soerjomataram I, Jemal A & Bray F (2021) Global Cancer Statistics 2020: GLOBOCAN Estimates of Incidence and Mortality Worldwide for 36 Cancers in 185 Countries. *CA: A Cancer Journal for Clinicians* 71, 209–249.

Sutherland HJ, Eaves CJ, Eaves AC, Dragowska W & Lansdorp PM (1989) Characterization and partial purification of human marrow cells capable of initiating long-term hematopoiesis in vitro. *Blood* 74, 1563–1570.

Suzuki N, Yamazaki S, Yamaguchi T, Okabe M, Masaki H, Takaki S, Otsu M & Nakauchi H (2013) Generation of Engraftable Hematopoietic Stem Cells From Induced Pluripotent Stem Cells by Way of Teratoma Formation. *Molecular Therapy* 21, 1424–1431.

Swarr DT & Morrisey EE (2015) Lung Endoderm Morphogenesis: Gasping for Form and Function. *Annu Rev Cell Dev Biol* 31, 553–573.

Szilvassy SJ, Humphries RK, Lansdorp PM, Eaves AC & Eaves CJ (1990) Quantitative assay for totipotent reconstituting hematopoietic stem cells by a competitive repopulation strategy. *Proc Natl Acad Sci U S A* 87, 8736–8740.

Tacha D, Yu C, Bremer R, Qi W & Haas T (2012) A 6-antibody panel for the classification of lung adenocarcinoma versus squamous cell carcinoma. *Appl Immunohistochem Mol Morphol* 20, 201–207.

Takahashi K, Tanabe K, Ohnuki M, Narita M, Ichisaka T, Tomoda K & Yamanaka S (2007) Induction of pluripotent stem cells from adult human fibroblasts by defined factors. *Cell* 131, 861–872.

Takahashi K & Yamanaka S (2006) Induction of pluripotent stem cells from mouse embryonic and adult fibroblast cultures by defined factors. *Cell* 126, 663–676.

Takahashi M, Ritz J & Cooper GM (1985) Activation of a novel human transforming gene, ret, by DNA rearrangement. *Cell* 42, 581–588.

Takasato M, Er PX, Chiu HS, Maier B, Baillie GJ, Ferguson C, Parton RG, Wolvetang EJ, Roost MS, Chuva de Sousa Lopes SM & Little MH (2015) Kidney organoids from human iPS cells contain multiple lineages and model human nephrogenesis. *Nature* 526, 564–568.

Takebe T, Sekine K, Enomura M, Koike H, Kimura M, Ogaeri T, Zhang R-R, Ueno Y, Zheng Y-W, Koike N, Aoyama S, Adachi Y & Taniguchi H (2013) Vascularized and functional human liver from an iPSC-derived organ bud transplant. *Nature* 499, 481–484.

Tan D, Li Q, Deeb G, Ramnath N, Slocum HK, Brooks J, Cheney R, Wiseman S, Anderson T & Loewen G (2003) Thyroid transcription factor-1 expression prevalence and its clinical implications in non-small cell lung cancer: a high-throughput tissue microarray and immunohistochemistry study. *Hum Pathol* 34, 597–604.

Tanabe K, Nakamura M, Narita M, Takahashi K & Yamanaka S (2013) Maturation, not initiation, is the major roadblock during reprogramming toward pluripotency from human fibroblasts. *Proceedings of the National Academy of Sciences* 110, 12172–12179.

Taoudi S, Gonneau C, Moore K, Sheridan JM, Blackburn CC, Taylor E & Medvinsky A (2008) Extensive hematopoietic stem cell generation in the AGM region via maturation of VE-cadherin+CD45+ pre-definitive HSCs. *Cell Stem Cell* 3, 99–108.

Tavian M, Coulombel L, Luton D, Clemente HS, Dieterlen-Lièvre F & Péault B (1996) Aorta-associated CD34+ hematopoietic cells in the early human embryo. *Blood* 87, 67–72.

Teixeira VH, Nadarajan P, Graham TA, Pipinikas CP, Brown JM, Falzon M, Nye E, Poulsom R, Lawrence D, Wright NA, McDonald S, Giangreco A, Simons BD & Janes SM (2013) Stochastic homeostasis in human airway epithelium is achieved by neutral competition of basal cell progenitors B. Hogan, ed. *eLife* 2, e00966.

Teshigawara R, Cho J, Kameda M & Tada T (2017) Mechanism of human somatic reprogramming to iPS cell. *Lab Invest* 97, 1152–1157.

Thomson JA, Itskovitz-Eldor J, Shapiro SS, Waknitz MA, Swiergiel JJ, Marshall VS & Jones JM (1998) Embryonic Stem Cell Lines Derived from Human Blastocysts. *Science* 282, 1145–1147.

Thun M, Peto R, Boreham J & Lopez AD (2012) Stages of the cigarette epidemic on entering its second century. *Tob Control* 21, 96–101.

Tosca L, Feraud O, Magniez A, Bas C, Griscelli F, Bennaceur-Griscelli A & Tachdjian G (2015) Genomic instability of human embryonic stem cell lines using different passaging culture methods. *Mol Cytogenet* 8, 30.

Toscani D, Bolzoni M, Accardi F, Aversa F & Giuliani N (2015) The osteoblastic niche in the context of multiple myeloma. *Ann N Y Acad Sci* 1335, 45–62.

Tothova Z, Kollipara R, Huntly BJ, Lee BH, Castrillon DH, Cullen DE, McDowell EP, Lazo-Kallanian S, Williams IR, Sears C, Armstrong SA, Passegué E, DePinho RA & Gilliland DG (2007) FoxOs Are Critical Mediators of Hematopoietic Stem Cell Resistance to Physiologic Oxidative Stress. *Cell* 128, 325–339.

Treutlein B, Brownfield DG, Wu AR, Neff NF, Mantalas GL, Espinoza FH, Desai TJ, Krasnow MA & Quake SR (2014) Reconstructing lineage hierarchies of the distal lung epithelium using single-cell RNA-seq. *Nature* 509, 371–375.

Tsim S, O'Dowd CA, Milroy R & Davidson S (2010) Staging of non-small cell lung cancer (NSCLC): A review. *Respiratory Medicine* 104, 1767–1774.

Tsui DCC, Kavanagh BD, Honce JM, Rossi C, Patil T & Camidge DR (2022) Central Nervous System Response to Selpercartinib in Patient With RET-rearranged Non-small Cell Lung Cancer After Developing Leptomeningeal Disease on Pralsetinib. *Clinical Lung Cancer* 23, e5–e8.

Tsuta K, Kohno T, Yoshida A, Shimada Y, Asamura H, Furuta K & Kushima R (2014) RET-rearranged non-small-cell lung carcinoma: a clinicopathological and molecular analysis. *Br J Cancer* 110, 1571–1578.

Turhan AG, Hwang JW, Chaker D, Tasteyre A, Latsis T, Griscelli F, Desterke C & Bennaceur-Griscelli A (2021) iPSC-Derived Organoids as Therapeutic Models in Regenerative Medicine and Oncology. *Front Med (Lausanne)* 8, 728543.

Tursky ML, Loi TH, Artuz CM, Alateeq S, Wolvetang EJ, Tao H, Ma DD & Molloy TJ (2020) Direct Comparison of Four Hematopoietic Differentiation Methods from Human Induced Pluripotent Stem Cells. *Stem Cell Reports* 15, 735–748.

Vagapova ER, Spirin PV, Lebedev TD & Prassolov VS (2018) The Role of TAL1 in Hematopoiesis and Leukemogenesis. *Acta Naturae* 10, 15–23.

Vanuytsel K, Villacorta-Martin C, Lindstrom-Vautrin J, Wang Z, Garcia-Beltran WF, Vrbanac V, Parsons D, Lam EC, Matte TM, Dowrey TW, Kumar SS, Li M, Wang F, Yeung AK, Mostoslavsky G, Dries R, Campbell JD, Belkina AC, Balazs AB & Murphy GJ (2022) Multi-modal profiling of human fetal liver hematopoietic stem cells reveals the molecular signature of engraftment. *Nat Commun* 13, 1103.

Varnum-Finney B, Brashem-Stein C & Bernstein ID (2003) Combined effects of Notch signaling and cytokines induce a multiple log increase in precursors with lymphoid and myeloid reconstituting ability. *Blood* 101, 1784–1789.

Varum S, Rodrigues AS, Moura MB, Momcilovic O, Easley CA, Ramalho-Santos J, Van Houten B & Schatten G (2011) Energy metabolism in human pluripotent stem cells and their differentiated counterparts. *PLoS One* 6, e20914.

Velten L, Haas SF, Raffel S, Blaszkiewicz S, Islam S, Hennig BP, Hirche C, Lutz C, Buss EC, Nowak D, Boch T, Hofmann W-K, Ho AD, Huber W, Trumpp A, Essers MAG & Steinmetz LM (2017) Human haematopoietic stem cell lineage commitment is a continuous process. *Nat Cell Biol* 19, 271–281.

Verfaillie CM & Miller JS (1995) A novel single-cell proliferation assay shows that long-term culture-initiating cell (LTC-IC) maintenance over time results from the extensive proliferation of a small fraction of LTC-IC. *Blood* 86, 2137–2145.

Wagner JE, Barker JN, DeFor TE, Baker KS, Blazar BR, Eide C, Goldman A, Kersey J, Krivit W, MacMillan ML, Orchard PJ, Peters C, Weisdorf DJ, Ramsay NKC & Davies SM (2002) Transplantation of unrelated donor umbilical cord blood in 102 patients with malignant and nonmalignant diseases: influence of CD34 cell dose and HLA disparity on treatment-related mortality and survival. *Blood* 100, 1611–1618.

Walasek MA, van Os R & de Haan G (2012) Hematopoietic stem cell expansion: challenges and opportunities. *Ann N Y Acad Sci* 1266, 138–150.

Walser T, Cui X, Yanagawa J, Lee JM, Heinrich E, Lee G, Sharma S & Dubinett SM (2008) Smoking and Lung Cancer. *Proc Am Thorac Soc* 5, 811–815.

Wang R, Hu H, Pan Y, Li Y, Ye T, Li C, Luo X, Wang L, Li H, Zhang Y, Li F, Lu Y, Lu Q, Xu J, Garfield D, Shen L, Ji H, Pao W, Sun Y & Chen H (2012) RET fusions define a unique molecular and clinicopathologic subtype of non-small-cell lung cancer. *J Clin Oncol* 30, 4352–4359.

Wang Y, Jiang T, Qin Z, Jiang J, Wang Q, Yang S, Rivard C, Gao G, Ng TL, Tu MM, Yu H, Ji H, Zhou C, Ren S, Zhang J, Bunn P, Doebele RC, Camidge DR & Hirsch FR (2019) HER2 exon 20 insertions in non-small-cell lung cancer are sensitive to the irreversible pan-HER receptor tyrosine kinase inhibitor pyrotinib. *Annals of Oncology* 30, 447–455.

Warren L, Manos PD, Ahfeldt T, Loh Y-H, Li H, Lau F, Ebina W, Mandal PK, Smith ZD, Meissner A, Daley GQ, Brack AS, Collins JJ, Cowan C, Schlaeger TM & Rossi DJ (2010) Highly efficient reprogramming to pluripotency and directed differentiation of human cells with synthetic modified mRNA. *Cell Stem Cell* 7, 618–630.

Weibel ER (1963) *Morphometry of the Human Lung*, Berlin, Heidelberg: Springer. Available at: http://link.springer.com/10.1007/978-3-642-87553-3 [Accessed August 7, 2023].

Weibel ER (2015) On the Tricks Alveolar Epithelial Cells Play to Make a Good Lung. *Am J Respir Crit Care Med* 191, 504–513.

Weissferdt A (2014) Large cell carcinoma of lung: On the verge of extinction? *Seminars in Diagnostic Pathology* 31, 278–288.

Weissman IL (2000) Stem Cells: Units of Development, Units of Regeneration, and Units in Evolution. *Cell* 100, 157–168.

Weissman IL & Shizuru JA (2008) The origins of the identification and isolation of hematopoietic stem cells, and their capability to induce donor-specific transplantation tolerance and treat autoimmune diseases. *Blood* 112, 3543–3553.

Wells SA (2018) Advances in the management of MEN2: from improved surgical and medical treatment to novel kinase inhibitors. *Endocrine-Related Cancer* 25, T1–T13.

Wells SA, Pacini F, Robinson BG & Santoro M (2013) Multiple endocrine neoplasia type 2 and familial medullary thyroid carcinoma: an update. *J Clin Endocrinol Metab* 98, 3149–3164.

Wesselschmidt RL (2011) The teratoma assay: an in vivo assessment of pluripotency. *Methods Mol Biol* 767, 231–241.

Wilkinson AC, Ishida R, Kikuchi M, Sudo K, Morita M, Crisostomo RV, Yamamoto R, Loh KM, Nakamura Y, Watanabe M, Nakauchi H & Yamazaki S (2019) Long-term ex vivo hematopoietic stem cell expansion affords nonconditioned transplantation. *Nature* 571, 117–121.

Williams ED (1965) A review of 17 cases of carcinoma of the thyroid and phaeochromocytoma. *J Clin Pathol* 18, 288–292.

Williams MC (2003) Alveolar Type I Cells: Molecular Phenotype and Development. *Annu. Rev. Physiol.* 65, 669–695.

Winkler IG, Sims NA, Pettit AR, Barbier V, Nowlan B, Helwani F, Poulton IJ, van Rooijen N, Alexander KA, Raggatt LJ & Lévesque J-P (2010) Bone marrow macrophages maintain hematopoietic stem cell (HSC) niches and their depletion mobilizes HSCs. *Blood* 116, 4815–4828.

Wistuba II, Bryant D, Behrens C, Milchgrub S, Virmani AK, Ashfaq R, Minna JD & Gazdar AF (1999) Comparison of Features of Human Lung Cancer Cell Lines and Their Corresponding Tumors1. *Clinical Cancer Research* 5, 991–1000.

Wu AM, Till JE, Siminovitch L & McCulloch EA (1968) CYTOLOGICAL EVIDENCE FOR A RELATIONSHIP BETWEEN NORMAL HEMATOPOIETIC COLONY-FORMING CELLS AND CELLS OF THE LYMPHOID SYSTEM. *J Exp Med* 127, 455–464.

Xiao Z, Jiang Q, Willette-Brown J, Xi S, Zhu F, Burkett S, Back T, Song N-Y, Datla M, Sun Z, Goldszmid R, Lin F, Cohoon T, Pike K, Wu X, Schrump DS, Wong K-K, Young HA, Trinchieri G, Wiltrout RH & Hu Y (2013) The Pivotal Role of IKKα in the Development of Spontaneous Lung Squamous Cell Carcinomas. *Cancer Cell* 23, 527–540.

Xie F, Ye L, Chang JC, Beyer AI, Wang J, Muench MO & Kan YW (2014) Seamless gene correction of β-thalassemia mutations in patient-specific iPSCs using CRISPR/Cas9 and piggyBac. *Genome Res* 24, 1526–1533.

Xu A-N, Liu D, Dai Y-T, Zhang F, Shen J, Hu C-L, Xu C-H, Zhang Y-L, Xie Y-Y, Huang Q-H, Xu P-F, Wang L, Cheng L, Huang J, Chen Z, Chen S-J & Sun X-J (2019) Differential Expression of CD49f Discriminates the Independently Emerged Hematopoietic Stem Cells and Erythroid-Biased Progenitors. *Blood* 134, 3700.

Xu H, Lyu X, Yi M, Zhao W, Song Y & Wu K (2018) Organoid technology and applications in cancer research. *Journal of Hematology & Oncology* 11, 116.

Yagi M, Ritchie KA, Sitnicka E, Storey C, Roth GJ & Bartelmez S (1999) Sustained ex vivo expansion of hematopoietic stem cells mediated by thrombopoietin. *Proceedings of the National Academy of Sciences* 96, 8126–8131.

Yakes FM, Chen J, Tan J, Yamaguchi K, Shi Y, Yu P, Qian F, Chu F, Bentzien F, Cancilla B, Orf J, You A, Laird AD, Engst S, Lee L, Lesch J, Chou Y-C & Joly AH (2011) Cabozantinib (XL184), a Novel MET and VEGFR2 Inhibitor, Simultaneously Suppresses Metastasis, Angiogenesis, and Tumor Growth. *Molecular Cancer Therapeutics* 10, 2298–2308.

Yakubov E, Rechavi G, Rozenblatt S & Givol D (2010) Reprogramming of human fibroblasts to pluripotent stem cells using mRNA of four transcription factors. *Biochem Biophys Res Commun* 394, 189–193.

Yamamoto R, Morita Y, Ooehara J, Hamanaka S, Onodera M, Rudolph KL, Ema H & Nakauchi H (2013) Clonal analysis unveils self-renewing lineage-restricted progenitors generated directly from hematopoietic stem cells. *Cell* 154, 1112–1126.

Yamamoto Y, Gotoh S, Korogi Y, Seki M, Konishi S, Ikeo S, Sone N, Nagasaki T, Matsumoto H, Muro S, Ito I, Hirai T, Kohno T, Suzuki Y & Mishima M (2017) Long-term expansion of alveolar stem cells derived from human iPS cells in organoids. *Nat Methods* 14, 1097–1106.

Yamanaka S (2020) Pluripotent Stem Cell-Based Cell Therapy—Promise and Challenges. *Cell Stem Cell* 27, 523–531.

Yamashita A, Morioka M, Kishi H, Kimura T, Yahara Y, Okada M, Fujita K, Sawai H, Ikegawa S & Tsumaki N (2014) Statin treatment rescues FGFR3 skeletal dysplasia phenotypes. *Nature* 513, 507–511.

Yamazaki S, Ema H, Karlsson G, Yamaguchi T, Miyoshi H, Shioda S, Taketo MM, Karlsson S, Iwama A & Nakauchi H (2011) Nonmyelinating Schwann cells maintain hematopoietic stem cell hibernation in the bone marrow niche. *Cell* 147, 1146–1158.

Yao S, Chen S, Clark J, Hao E, Beattie GM, Hayek A & Ding S (2006) Long-term self-renewal and directed differentiation of human embryonic stem cells in chemically defined conditions. *Proc Natl Acad Sci U S A* 103, 6907–6912.

Yarden Y, Kuang WJ, Yang-Feng T, Coussens L, Munemitsu S, Dull TJ, Chen E, Schlessinger J, Francke U & Ullrich A (1987) Human proto-oncogene c-kit: a new cell surface receptor tyrosine kinase for an unidentified ligand. *The EMBO Journal* 6, 3341–3351.

Ye M, Zhang H, Amabile G, Yang H, Staber PB, Zhang P, Levantini E, Alberich-Jordà M, Zhang J, Kawasaki A & Tenen DG (2013) C/EBPa controls acquisition and maintenance of adult haematopoietic stem cell quiescence. *Nat Cell Biol* 15, 385–394.

Yoh K, Seto T, Satouchi M, Nishio M, Yamamoto N, Murakami H, Nogami N, Nosaki K, Kohno T, Tsuta K, Nomura S, Ikeno T, Wakabayashi M, Sato A, Matsumoto S & Goto K (2021) Final survival results for the LURET phase II study of vandetanib in previously treated patients with RET-rearranged advanced non-small cell lung cancer. *Lung Cancer* 155, 40–45.

Yonemura Y, Ku H, Lyman SD & Ogawa M (1997) In Vitro Expansion of Hematopoietic Progenitors and Maintenance of Stem Cells: Comparison Between FLT3/FLK-2 Ligand and KIT Ligand. *Blood* 89, 1915–1921.

Yoshida Y, Takahashi K, Okita K, Ichisaka T & Yamanaka S (2009) Hypoxia enhances the generation of induced pluripotent stem cells. *Cell Stem Cell* 5, 237–241.

Yoshihara H, Arai F, Hosokawa K, Hagiwara T, Takubo K, Nakamura Y, Gomei Y, Iwasaki H, Matsuoka S, Miyamoto K, Miyazaki H, Takahashi T & Suda T (2007) Thrombopoietin/MPL signaling regulates hematopoietic stem cell quiescence and interaction with the osteoblastic niche. *Cell Stem Cell* 1, 685–697.

Yu H, Li Q, Kolosov VP, Perelman JM & Zhou X (2010) Interleukin-13 induces mucin 5AC production involving STAT6/SPDEF in human airway epithelial cells. *Cell Commun Adhes* 17, 83–92.

Yu J, Chau KF, Vodyanik MA, Jiang J & Jiang Y (2011) Efficient feeder-free episomal reprogramming with small molecules. *PLoS One* 6, e17557.

Yzaguirre AD, de Bruijn MFTR & Speck NA (2017) The role of Runx1 in embryonic blood cell formation. *Adv Exp Med Biol* 962, 47–64.

Zahid U, Akbar F, Amaraneni A, Husnain M, Chan O, Riaz IB, McBride A, Iftikhar A & Anwer F (2017) A Review of Autologous Stem Cell Transplantation in Lymphoma. *Curr Hematol Malig Rep* 12, 217–226.

Zambidis ET, Peault B, Park TS, Bunz F & Civin CI (2005) Hematopoietic differentiation of human embryonic stem cells progresses through sequential hematoendothelial, primitive, and definitive stages resembling human yolk sac development. *Blood* 106, 860–870.

Zappa C & Mousa SA (2016) Non-small cell lung cancer: current treatment and future advances. *Transl Lung Cancer Res* 5, 288–300.

Zhan B, Wen S, Lu J, Shen G, Lin X, Feng J & Huang H (2017) Identification and causes of metabonomic difference between orthotopic and subcutaneous xenograft of pancreatic cancer. *Oncotarget* 8, 61264–61281.

Zhang J, Ratanasirintrawoot S, Chandrasekaran S, Wu Z, Ficarro SB, Yu C, Ross CA, Cacchiarelli D, Xia Q, Seligson M, Shinoda G, Xie W, Cahan P, Wang L, Ng S-C, Tintara S, Trapnell C, Onder T, Loh Y-H, Mikkelsen T, Sliz P, Teitell MA, Asara JM, Marto JA, Li H, Collins JJ & Daley GQ (2016) LIN28 Regulates Stem Cell Metabolism and Conversion to Primed Pluripotency. *Cell Stem Cell* 19, 66–80.

Zhang P, Zhang C, Li J, Han J, Liu X & Yang H (2019) The physical microenvironment of hematopoietic stem cells and its emerging roles in engineering applications. *Stem Cell Res Ther* 10, 327.

Zhang Z, Wang H, Ding Q, Xing Y, Xu Z, Lu C, Luo D, Xu L, Xia W, Zhou C & Shi M (2018) Establishment of patient-derived tumor spheroids for non-small cell lung cancer. *PLOS ONE* 13, e0194016.

Zhou H, Wu S, Joo JY, Zhu S, Han DW, Lin T, Trauger S, Bien G, Yao S, Zhu Y, Siuzdak G, Schöler HR, Duan L & Ding S (2009) Generation of induced pluripotent stem cells using recombinant proteins. *Cell Stem Cell* 4, 381–384.

Zou P, Yoshihara H, Hosokawa K, Tai I, Shinmyozu K, Tsukahara F, Maru Y, Nakayama K, Nakayama KI & Suda T (2011) p57(Kip2) and p27(Kip1) cooperate to maintain hematopoietic stem cell quiescence through interactions with Hsc70. *Cell Stem Cell* 9, 247–261.